

SYNTHESIS AND CHARACTERIZATION OF  
CYCLODEXTRIN BASED POLYMERS FOR  
NOVEL APPLICATIONS

Thesis Submitted To  
THE MAHARAJA SAYAJIRAO UNIVERSITY OF BARODA

For The Degree of  
Doctor of Philosophy  
In  
Applied Chemistry

Submitted  
By  
Vinod I. Bhoi



Applied Chemistry Department  
Faculty of Technology & Engineering  
The M. S. University of Baroda  
Vadodara- 390 001  
Gujarat, India

April 2012

Tel: 2434188 extn. 415, 212



**APPLIED CHEMISTRY DEPARTMENT**  
Faculty of Technology & Engineering  
The Maharaja Sayajirao University of Baroda  
Post Box No: 51, Kalabhavan  
Vadodara-390 001, Gujarat (INDIA)

## DST-FIST Sponsored Department

Ref. No. App Ch./

Date: 13/04/2012

### CERTIFICATE

This is to certify that the thesis entitled “**Synthesis and characterization of cyclodextrin based polymers for novel applications**” submitted by Mr. Vinod I. Bhoi to The M. S. University of Baroda, Vadodara for the award of Ph.D degree in Applied Chemistry incorporates the original research work carried out by him under my supervision.

Prof. C. N. Murthy  
Research Guide  
Applied Chemistry Department  
Faculty of Technology & Engineering

Head  
Applied Chemistry Department  
Faculty of Technology & Engineering

Dean  
Faculty of Technology & Engineering  
The M. S. University of Baroda

## DECLARATION

I state that the work presented in this thesis entitled “**Synthesis and characterization of cyclodextrin based polymers for novel applications**” comprises independent investigations carried out by me under the guidance of Prof. C. N. Murthy. Wherever references have been made to the work of others, it has been clearly indicated with the source of information under the references section. The matter presented in this thesis has not been submitted elsewhere for the award of any other degree. Any errors in fact or interpretation in the thesis are purely the fault of the researcher.

Signature of the Candidate  
(Vinod I. Bhoi)

Certified and forwarded through:

Prof. C. N. Murthy  
Research Guide  
Applied Chemistry Department  
Faculty of Technology & Engineering  
The M. S. University of Baroda

## Acknowledgements

My path to Doctorate in Applied Chemistry has been neither easy nor straightforward, but underway; I have met many interesting people and gained a lot of scientific and life experience. Those years would have been much more difficult without the assistance of those who gave their support in different ways.

I am immensely pleased to place on record my profound gratitude and heartfelt thanks to my guide Prof. C. N. Murthy for his guidance during my research, who suggested the problems, gave the expert suggestions, extended all facilities, provided inspiring guidance and encouragement for the successful completion of my research work. I deem it as my privilege to work under his able guidance. I consider it a great opportunity to have been his student, and I will ever remain grateful to him.

This work would not be possible without financial support. I deeply thank University Grants Commission (UGC) and The Maharaja Sayajirao University of Baroda for providing me financial support, first under UGC major research project and second UGC sanctioned scheme of “Research fellowship in science for the meritorious students” (RFSMS).

I would take this opportunity to thank Dr. Saurabh K. Patel, Associate Professor, Department of Chemistry, Veer Narmad South Gujarat University, Surat to introduce me to the Applied Chemistry Department and for her continuous encouragement during my research work.

I thank Dr. C. T. Rao, Sun Pharma Advance Research Centre (SPARC), Vadodara for providing help in freeze drying facility.

I thank Dr. K. V. R. Murthy, Applied Physics Department for his valuable guidance, support and help in the fluorescence studies and some XRD analysis.

I certainly would not be able to produce so many results and data without the help of my senior Dr. Santosh Kumar. I was very lucky, during my peak time of experimental work, Dr. Santosh Kumar was working at GIST, South Korea as a Research Scientist and he could help me by providing all the analysis facilities of GIST and helpful discussions.

Further, I would like to thank my fellow research colleagues R. Murali, Mayur Patel, Parimal Patel, Indrajit Shown, Renu Singh, Prachi Shah, Gangadhar, Vaishali Suthar, Srushti Deshmukh, Gautum Patel, Deepak Singh, Purvang Patel, Vishal Modi, Seema Patel, Umesh Chaudhari, Brijesh Shah, Tarun Parangi and Shrinivas Ghodke for their discussions and comments during the group meetings, Lunch and Tea breaks.

I wish to express my heartfelt thanks to Prof. Toyoko Imae, Prof. Ujihara Masaki, Dr. Prashanthi and other members of the Prof. Toyoko Imae's laboratory of Graduate Institute of Applied Science and Technology, National Taiwan University of Science and Technology, Taipei, Taiwan for their kind support and guidance during my visit to Taiwan.

I am thankful to all the teachers and non-teaching staff of the Applied Chemistry Department for supporting me throughout the research work. Especially, I am thankful to Dr. Rakesh Sharma and Dr. D. P. Bharambe for their friendly and moral support.

Also outside of science, there were people whose help and support was very important. I would like to thank my friends Neel Sheth, Tejash Parmar, Pravin Patil, Deepak Chaudhari and Anil Mistry for their moral support.

I am thankful to my friends from Dr. V. S. Hall, Rajesh SV, Thomson Alex, Hemant Mande, Jaimin Ray, Gopal Bhatt, Harish Talele, Rahul Ghildiyal, Mahesh Patel, Deenakaran, Sunil Shah, Deepak Adhikari, Ashok, Sanjay, and so on for their support and nice company.

My deepest heartfelt gratitude and indebtedness belong to my father Ishwarbhai, mother Babyben and three younger brothers Sandeep, Rohit and Sajan for their moral support and making me pass through the difficult situations with great ease during my prolonged years of my research work.

Finally, I would like to thank my beautiful wife Hetal V. Bhoi for her moral support and sacrifice during the last stage of research work especially when I was writing the thesis.

**Vinod I. Bhoi**

## **DEDICATION**

*This Thesis is dedicated to my beloved Mother Babyben*

## TABLE OF CONTENTS

<b>Contents</b>	<b>vii-xii</b>
<b>List of Figures</b>	<b>xiii-xix</b>
<b>List of Schemes</b>	<b>xx</b>
<b>List of Tables</b>	<b>xxi</b>
<b>Abbreviations</b>	<b>xxii-xxiii</b>

### Contents

	<b>Page No.</b>
<b>Chapter 1 Introduction</b>	<b>1-38</b>
1.1 Brief History of Cyclodextrins	1
1.2 Structural Features of Cyclodextrins	2
1.3 Shape and Size of Cyclodextrins	5
1.4 Solubility of Cyclodextrins	6
1.5 Viscosity and Stability of Cyclodextrins	9
1.6 Host-Guest Inclusion Complex of Cyclodextrins	9
1.7 Synthesis of Cyclodextrins	11
1.8 Chemical Modification of Cyclodextrins	13
1.9 Methods for Modification of Cyclodextrins	13
1.10 Mono-, di- and tri-substituted Cyclodextrins	16
1.11 Cyclodextrin Polymers	18
1.12 Applications of Cyclodextrins and Cyclodextrin based Polymers	25
1.13 Aim of the Thesis	29
References	31-38
<b>Chapter 2 Synthesis of Difunctionalized <math>\beta</math>-Cyclodextrin Monomers</b>	<b>39-66</b>
2.1 Introduction	39
2.2 Experimental	41

2.2.1	Materials	41
2.2.2	Measurements	41
2.2.3	Synthesis of 6 <sup>A</sup> ,6 <sup>D</sup> -biphenyl bridged β-Cyclodextrin	41
2.2.4	Synthesis of 6 <sup>A</sup> ,6 <sup>D</sup> -diiodo 6 <sup>A</sup> ,6 <sup>D</sup> -dideoxy β-Cyclodextrin	42
2.2.5	Synthesis of 6 <sup>A</sup> ,6 <sup>D</sup> -diazido 6 <sup>A</sup> ,6 <sup>D</sup> -dideoxy β-Cyclodextrin	42
2.2.6	Synthesis of 6 <sup>A</sup> ,6 <sup>D</sup> -diamino 6 <sup>A</sup> ,6 <sup>D</sup> -dideoxy β-Cyclodextrin	43
2.3	Characterization of Difunctionalized β-Cyclodextrin Monomers	45
2.3.1	6 <sup>A</sup> ,6 <sup>D</sup> -biphenyl bridged β-Cyclodextrin (2)	45
2.3.2	6 <sup>A</sup> ,6 <sup>D</sup> -diiodo 6 <sup>A</sup> ,6 <sup>D</sup> -dideoxy β-Cyclodextrin (3)	53
2.3.3	6 <sup>A</sup> ,6 <sup>D</sup> -diazido 6 <sup>A</sup> ,6 <sup>D</sup> -dideoxy β-Cyclodextrin (4)	56
2.3.4	6 <sup>A</sup> ,6 <sup>D</sup> -diamino 6 <sup>A</sup> ,6 <sup>D</sup> -dideoxy β-Cyclodextrin (5)	59
2.4	Conclusions	65
	References	66
<b>Chapter 3</b>	<b>Synthesis of Cyclodextrin based Polymers</b>	<b>67-89</b>
3.1	Introduction	67
3.2	Experimental	69
	3.2.1 Materials	69
	3.2.2 Measurements	69
	3.2.3 Synthesis of β-Cyclodextrin and Cyanuric chloride as Linker based Polymers	69
	3.2.4 Synthesis of β-Cyclodextrin and Urea or Thiourea as Linker based Polymers	71
	3.2.5 Determination of Aqueous Solubility of Polymers	71
3.3	Results and Discussion	73
	3.3.1 Aqueous Solubility of β-CD Polymers	73
	3.3.2 Characterization of β-Cyclodextrin and Cyanuric chloride as Linker based Polymers	75
	3.3.2.1 Fourier Transform Infrared Spectroscopy (FTIR)	75

3.3.2.2	Nuclear Magnetic Resonance Spectroscopy (NMR)	76
3.3.2.3	Thermogravimetric Analysis (TGA)	78
3.3.2.4	X-ray Diffraction (XRD)	79
3.3.2.5	Molecular Weight (Mw)	80
3.3.3	Characterization of $\beta$ -cyclodextrin and Urea or Thiourea as Linker based Polymers	82
3.3.3.1	Fourier Transform Infrared Spectroscopy (FTIR)	82
3.3.3.2	Nuclear Magnetic Resonance Spectroscopy (NMR)	83
3.3.3.3	Thermogravimetric Analysis (TGA)	84
3.3.3.4	X-ray Diffraction (XRD)	85
3.3.3.5	Molecular Weight (Mw)	86
3.4	Conclusions	87
	References	88-89
<b>Chapter 4</b>	<b>Applications of Cyclodextrin based Polymers</b>	<b>90-121</b>
<b>4.1</b>	<b>Aqueous Solubilization of Carbamazepine by Cyclodextrin based Polymers</b>	<b>90</b>
4.1.1	Introduction	90
4.1.2	Experimental	92
	4.1.2.1 Materials	92
	4.1.2.2 Measurements	92
	4.1.2.3 Synthesis of $\beta$ -CD-P-CBZ Inclusion Complex	92
	4.1.2.4 Phase Solubility	93
	4.1.2.5 Dissolution Studies	94
4.1.3	Results and Discussion	95
	4.1.3.1 Molecular Modeling	95
	4.1.3.2 Fourier Transform Infrared Spectroscopy (FTIR)	96
	4.1.3.3 UV-Visible Spectroscopy (UV-Vis)	97
	4.1.3.4 Nuclear Magnetic Resonance Spectroscopy (NMR)	98
	4.1.3.5 Thermogravimetric Analysis (TGA)	99

4.1.3.6	Phase Solubility Diagrams of the $\beta$ -CD-P/CBZ Inclusion Complex	101
4.1.3.7	Dissolution Studies	102
4.1.4	Conclusions	104
<b>4.2</b>	<b>Fluorescence Sensitizing of Pyrene by Cyclodextrin based Polymer</b>	<b>105</b>
4.2.1	Introduction	105
4.2.2	Experimental	107
4.2.2.1	Materials	107
4.2.2.2	Measurements	107
4.2.2.3	Procedure of binary pyrene- $\beta$ -CD or $\beta$ -CD polymer inclusion complex	107
4.2.2.4	Procedure of ternary pyrene-adamantol- $\beta$ -CD or pyrene-adamantol- $\beta$ -CD polymer inclusion complex	108
4.2.3	Results and Discussion	110
4.2.3.1	Molecular Modeling	110
4.2.3.2	UV-Visible Spectroscopy (UV-Vis)	111
4.2.3.3	Fluorescence Emission Spectra	111
4.2.4	Conclusions	118
	References	119-121
<b>Chapter 5</b>	<b>Solubilization of Fullerenes</b>	<b>122-164</b>
<b>5.1</b>	<b>Solubilization of [60]Fullerene by Modified <math>\beta</math>-Cyclodextrin</b>	<b>122</b>
5.1.1	Introduction	122
5.1.2	Experimental	124
5.1.2.1	Materials	124
5.1.2.2	Measurements	124
5.1.2.3	Synthesis of $\beta$ -Cyclodextrin-[60]Fullerene Adduct	125
5.1.3	Results and Discussion	127
5.1.3.1	Fourier Transform Infrared Spectroscopy (FTIR)	129

5.1.3.2	UV-Visible Spectroscopy (UV-Vis)	130
5.1.3.3	Nuclear Magnetic Resonance Spectroscopy (NMR)	131
5.1.3.4	Thermogravimetric Analysis (TGA)	134
5.1.3.5	X-ray Diffraction (XRD)	135
5.1.3.6	Transmission Electron Micrograph (TEM) and Field Emission Scanning Electron Microscopy (FE-SEM)	136
5.1.3.7	Atomic Force Microscopy (AFM)	139
5.1.4	Conclusions	140
<b>5.2</b>	<b>Solubilization of [60]Fullerene and [70]Fullerene by Disaccharides</b>	<b>141</b>
5.2.1	Introduction	141
5.2.2	Experimental	143
5.2.2.1	Materials	143
5.2.2.2	Measurements	143
5.2.2.3	Synthesis of the [60]fullerene-disaccharide complex	144
5.2.2.4	Determination of Aqueous Solubility of Complex and Quantification of [60]Fullerene	145
5.2.2.5	Radical Scavenging	145
5.2.3	Results and Discussion	147
5.2.3.1	Aqueous Solubility of Complexes	149
5.2.3.2	Fourier Transform Infrared Spectroscopy (FTIR)	149
5.2.3.3	UV-Visible Spectroscopy (UV-Vis)	150
5.2.3.4	Thermogravimetric Analysis (TGA)	152
5.2.3.5	Nuclear Magnetic Resonance Spectroscopy (NMR)	153
5.2.3.6	X-ray Diffraction (XRD)	154
5.2.3.7	Transmission Electron Micrograph (TEM) and Static Light Scattering (SLS)	155
5.2.3.8	Molecular Modeling	157

	5.2.3.9 Radical Scavenging	157
	5.2.3.10 Kinetics of Radical Scavenging Reaction	158
5.2.4	Conclusions	160
	References	161-164
<b>Chapter 6</b>	<b>Surface Immobilization of Carbon Nanotubes by <math>\beta</math>-Cyclodextrins and Their Inclusion Ability</b>	<b>165-186</b>
6.1	Introduction	165
6.2	Experimental	168
	6.2.1 Materials	168
	6.2.2 Measurements	168
	6.2.3 Carboxylic acid Functionalization of MWCNTs	169
	6.2.4 Surface Immobilization of MWCNTs with $\beta$ -Cyclodextrins	169
	6.2.5 Sample Preparation for Fluorescence Measurement	170
6.3	Results and Discussion	171
	6.3.1 Characterization of $\beta$ -Cyclodextrins Immobilized on MWCNTs	171
	6.3.1.1 Fourier Transform Infrared Spectroscopy (FTIR)	171
	6.3.1.2 Dispersibility	172
	6.3.1.3 Thermogravimetric Analysis (TGA)	173
	6.3.1.4 Energy Dispersive Spectroscopy (EDS)	174
	6.3.1.5 Transmission Electron Micrograph (TEM)	175
	6.3.2 Inclusion Ability of $\beta$ -Cyclodextrins Immobilized on MWCNTs	177
	6.3.2.1 Fluorescence Spectroscopy	177
6.4	Conclusions	183
	References	184-186
	<b>Summary of the Thesis</b>	<b>187-190</b>
	<b>List of Publications</b>	<b>191</b>
	<b>List of Presentations</b>	<b>192-193</b>

## List of Figures

Figure No.	Title	Page No.
<b>Chapter 1</b>	<b>Introduction</b>	
1.1	Cyclodextrins papers and patents in Last 5 decades	2
1.2	Schematic structures of native $\alpha$ -, $\beta$ - and $\gamma$ -cyclodextrins	3
1.3	(a) 3D Molecular structure of $\beta$ -CD, (b) Torus (Bucket) shape of CD and (c) Common Structure of CDs	5
1.4	Molecular Dimensions of $\alpha$ -, $\beta$ - and $\gamma$ -Cyclodextrins	6
1.5	(a) Solubility of $\beta$ -CD as a function of different cosolvent in water mixture and (b) Solubility of $\beta$ -CD as a function of DMSO in water-DMSO mixture	8
1.6	Host-Guest Inclusion Complexation	9
1.7	Synthesis of cyclodextrins from starch by enzymatic digestion	12
1.8	Overview of the methods for modification of cyclodextrins	14
1.9	Possible positional isomers of mono, di and tri-modified $\alpha$ -CD and $\beta$ -CD	16
1.10	Specific introductions of mono-, di- and tri- substituents to cyclodextrins	18
1.11	Structural classification of cyclodextrin polymers	19
1.12	Synthetic scheme of linear pendent-cyclodextrin polymer	20
1.13	Synthetic scheme of CD-CM-Chitosan polymer	21
1.14	Synthesis of novel linear water-soluble polymer	21
1.15	Synthesis of linear cationic cyclodextrin main-chain polymer	22
1.16	Synthesis of supramolecular polymers constructed by cyclodextrins with cinnamide	22
1.17	Synthesis of $\beta$ -cyclodextrin-epichlorohydrin polymer	23
1.18	Synthesis of $\beta$ -cyclodextrin-hexamethylene diisocyanate polymer	23
1.19	Physical immobilization of CDs on polymer by mixing	24
1.20	Synthesis of Necklace Type CD polymers (Polyrotaxane)	25

1.21	Theoretical phase-solubility diagram	27
1.22	Trends of cyclodextrins science and technology	28
<b>Chapter 2 Synthesis of Difunctionalized <math>\beta</math>-Cyclodextrin Monomers</b>		
2.1	Structural dimension of the $\beta$ -cyclodextrin and biphenyl-4,4'-disulfonyl chloride	40
2.2	FTIR spectrum of 6 <sup>A</sup> ,6 <sup>D</sup> -biphenyl bridged $\beta$ -cyclodextrin	48
2.3	UV-Vis spectra of biphenyl-4,4'-disulfonyl chloride in chloroform, $\beta$ -cyclodextrin in water and biphenyl bridged $\beta$ -cyclodextrin in water	48
2.4	<sup>1</sup> H NMR spectrum of $\beta$ -cyclodextrin in DMSO-d <sub>6</sub>	49
2.5	<sup>1</sup> H NMR spectrum of biphenyl bridged $\beta$ -cyclodextrin in DMSO-d <sub>6</sub>	49
2.6	<sup>1</sup> H NMR spectrum of $\beta$ -cyclodextrin in D <sub>2</sub> O	50
2.7	<sup>1</sup> H NMR spectrum of biphenyl bridged $\beta$ -cyclodextrin in D <sub>2</sub> O	50
2.8	<sup>13</sup> C NMR spectrum of $\beta$ -cyclodextrin in D <sub>2</sub> O	51
2.9	<sup>13</sup> C NMR spectrum of $\beta$ -cyclodextrin in DMSO-d <sub>6</sub>	51
2.10	<sup>13</sup> C NMR spectrum of biphenyl bridged $\beta$ -cyclodextrin in DMSO-d <sub>6</sub>	52
2.11	FTIR spectrum of 6 <sup>A</sup> ,6 <sup>D</sup> -diiodo 6 <sup>A</sup> ,6 <sup>D</sup> -dideoxy $\beta$ -cyclodextrin	54
2.12	<sup>1</sup> H NMR of 6 <sup>A</sup> ,6 <sup>D</sup> -diiodo 6 <sup>A</sup> ,6 <sup>D</sup> -dideoxy $\beta$ -cyclodextrin in D <sub>2</sub> O	54
2.13	<sup>13</sup> C NMR spectrum of 6 <sup>A</sup> ,6 <sup>D</sup> -diiodo 6 <sup>A</sup> ,6 <sup>D</sup> -dideoxy $\beta$ -cyclodextrin in D <sub>2</sub> O	55
2.14	FTIR spectrum of 6 <sup>A</sup> ,6 <sup>D</sup> -diazido 6 <sup>A</sup> ,6 <sup>D</sup> -dideoxy $\beta$ -cyclodextrin	57
2.15	<sup>1</sup> H NMR spectrum of 6 <sup>A</sup> ,6 <sup>D</sup> -diazido 6 <sup>A</sup> ,6 <sup>D</sup> -dideoxy $\beta$ -cyclodextrin D <sub>2</sub> O	57
2.16	<sup>13</sup> C NMR spectrum of 6 <sup>A</sup> ,6 <sup>D</sup> -diazido 6 <sup>A</sup> ,6 <sup>D</sup> -dideoxy $\beta$ -cyclodextrin in D <sub>2</sub> O	58
2.17	FTIR spectrum of 6 <sup>A</sup> ,6 <sup>D</sup> -diamino 6 <sup>A</sup> ,6 <sup>D</sup> -dideoxy	61

	$\beta$ -cyclodextrin	
2.18	$^1\text{H}$ NMR spectrum of $6^{\text{A}},6^{\text{D}}$ -diamino $6^{\text{A}},6^{\text{D}}$ -dideoxy $\beta$ -cyclodextrin in $\text{D}_2\text{O}$	61
2.19	$^1\text{H}$ NMR spectrum of $6^{\text{A}},6^{\text{D}}$ -diamino $6^{\text{A}},6^{\text{D}}$ -dideoxy $\beta$ -cyclodextrin in $\text{DMSO-d}_6$	62
2.20	$^{13}\text{C}$ NMR spectrum of $6^{\text{A}},6^{\text{D}}$ -diamino $6^{\text{A}},6^{\text{D}}$ -dideoxy $\beta$ -cyclodextrin in $\text{D}_2\text{O}$	62
<b>Chapter 3 Synthesis of Cyclodextrin based Polymers</b>		
3.1	FTIR spectra of (a) $\beta$ -CD, (b) $\beta$ -CD-CC polymer and (c) $\beta$ -CD-CC-DEG polymer	75
3.2	$^1\text{H}$ NMR spectra of (a) $\beta$ -CD, (b) $\beta$ -CD-CC polymer and (c) $\beta$ -CD-CC-DEG polymer in $\text{D}_2\text{O}$	76
3.3	$^{13}\text{C}$ NMR spectra of (a) $\beta$ -CD, (b) $\beta$ -CD-CC polymer and (c) $\beta$ -CD-CC-DEG polymer in $\text{D}_2\text{O}$	77
3.4	TGA curves of $\beta$ -CD, $\beta$ -CD-CC polymer and $\beta$ -CD-CC-DEG polymer	78
3.5	XRD patterns of (a) $\beta$ -CD, (b) $\beta$ -CD-CC polymer and (c) $\beta$ -CD-CC-DEG polymer	79
3.6	Debye plot of $\beta$ -CD-CC polymer	80
3.7	FTIR spectra of (a) diiodo $\beta$ -CD, (b) Urea and (c) $\beta$ -CD-Urea polymer	82
3.8	$^1\text{H}$ NMR spectra of (a) diiodo $\beta$ -CD and (b) $\beta$ -CD-Urea polymer in $\text{D}_2\text{O}$	83
3.9	$^{13}\text{C}$ NMR spectra of (a) diiodo $\beta$ -CD and (b) $\beta$ -CD-Urea polymer in $\text{D}_2\text{O}$	84
3.10	TGA curves of diiodo $\beta$ -CD and $\beta$ -CD-Urea polymer	85
3.11	XRD curves of (a) diiodo $\beta$ -CD and (b) $\beta$ -CD-Urea polymer	86
<b>Chapter 4 Applications of Cyclodextrin based Polymers</b>		
<b>4.1 Aqueous Solubilization of Carbamazepine by Cyclodextrin based Polymers</b>		
4.1.1	Energy-minimized space-filling molecular model of	95

	inclusion complex	
4.1.2	FTIR spectra of (a) $\beta$ -CD-CC-P, (b) $\beta$ -CD-Urea-P, (c) CBZ, (d) CBZ encapsulated $\beta$ -CD-CC-P and (e) CBZ encapsulated $\beta$ -CD-Urea	97
4.1.3	UV-Vis spectra of CBZ in ethanol, $\beta$ -CD polymer in water and CBZ encapsulated $\beta$ -CD polymer in water	98
4.1.4	$^1\text{H}$ NMR spectra of (a) $\beta$ -CD-CC-P, (b) $\beta$ -CD-Urea-P, (c) CBZ, (d) CBZ encapsulated $\beta$ -CD-CC-P and (e) CBZ encapsulated $\beta$ -CD-Urea	99
4.1.5	TGA curves of (a) $\beta$ -CD, (b) CBZ and (c) CBZ encapsulated $\beta$ -CD. Inset TGA curves of (a) $\beta$ -CD-CC-P, (b) CBZ and (c) CBZ encapsulated $\beta$ -CD-CC-P	100
4.1.6	Phase solubility diagrams of CBZ in $\beta$ -CD and $\beta$ -CD polymers.	102
4.1.7	Dissolution curves of CBZ with $\beta$ -CD and $\beta$ -CD polymers	103
<b>4.2</b>	<b>Fluorescence Sensitizing of Pyrene by Cyclodextrin based Polymers</b>	
4.2.1	Energy-minimized space-filling molecular model of inclusion complex	110
4.2.2	UV-Vis spectra of pyrene ( $1.66 \times 10^{-6}\text{M}$ ) in aqueous solution of (A) $\beta$ -CD and (B) $\beta$ -CD-polymer at different concentrations: (a) 0.00 %, (b) 0.166 %, (c) 0.333 %, (d) 0.500 %, (e) 0.666 %, (f) 0.833 %	111
4.2.3	Fluorescence spectra (excited at 340 nm) of pyrene ( $1.66 \times 10^{-6}\text{M}$ ) in aqueous solution of (A) $\beta$ -CD and (B) $\beta$ -CD-polymer at different concentrations: (a) 0.00 %, (b) 0.166 %, (c) 0.333 %, (d) 0.500 %, (e) 0.666 %, (f) 0.833 %	112
4.2.4	Benesi-Hildebrand plot of $[\text{Py}]/I$ Vs $1/[\beta\text{-CD}]$ and $[\text{Py}]/I$ Vs $1/[\beta\text{-CD Polymer}]$	114
4.2.5	Fluorescence spectra (excited at 340 nm) of pyrene ( $1.25 \times 10^{-6}\text{M}$ ) in presence (0.166 %) of (A) $\beta$ -CD and (B) $\beta$ -CD-	115

	polymer at different concentration of adamantol: (a) $1.25 \times 10^{-6}$ M, (b) $2.50 \times 10^{-6}$ M, (c) $3.75 \times 10^{-6}$ M (d) $5.00 \times 10^{-6}$ M, (e) $6.25 \times 10^{-6}$ M, (f) $7.50 \times 10^{-6}$ M	
4.2.6	Energy-minimized space-filling molecular model of ternary inclusion complex	116
4.2.7	Stern-Volmer plots of $I_0/I$ Vs [Adamantol] for $\beta$ -CD and $\beta$ -CD polymer	117
<b>Chapter 5</b>	<b>Solubilization of Fullerenes</b>	
<b>5.1</b>	<b>Solubilization of [60]Fullerene by Modified <math>\beta</math>-cyclodextrin</b>	
5.1.1	Photograph of [A] $C_{60}$ in toluene, [B] Diazido $\beta$ -CD in DMSO, [C] $\beta$ -CD- $C_{60}$ adduct in water, [D] $\beta$ -CD- $C_{60}$ adduct in toluene and [E] $\beta$ -CD- $C_{60}$ adduct in water + toluene	128
5.1.2	Photograph of [A] $C_{60}$ in toluene, [B] $\beta$ -CD in DMSO, [C] $\beta$ -CD- $C_{60}$ inclusion complex in water, [D] $\beta$ -CD- $C_{60}$ inclusion complex in toluene and [E] $\beta$ -CD- $C_{60}$ inclusion complex in water + toluene	128
5.1.3	FTIR spectra of (a) diazido $\beta$ -CD, (b) $C_{60}$ , (c) $\beta$ -CD- $C_{60}$ adduct	129
5.1.4	UV-Vis spectra of $C_{60}$ in toluene, diazido $\beta$ -CD in water and $\beta$ -CD- $C_{60}$ adduct in toluene	130
5.1.5	UV-Vis spectra of $C_{60}$ in toluene, $\beta$ -CD- $C_{60}$ 2:1 inclusion complex in water and $\beta$ -CD- $C_{60}$ 2:1 inclusion complex in toluene	131
5.1.6	$^1\text{H}$ NMR spectra of diazido $\beta$ -CD and $\beta$ -CD- $C_{60}$ adduct in $\text{DMSO-d}_6$	132
5.1.7	$^1\text{H}$ -NMR spectra of diazido $\beta$ -CD and $\beta$ -CD- $C_{60}$ adduct in $\text{D}_2\text{O}$	133
5.1.8	$^{13}\text{C}$ -NMR spectrum of $\beta$ -CD- $C_{60}$ adduct in $\text{D}_2\text{O}$ and $\text{DMSO-d}_6$	134
5.1.9	TGA curves of (a) $\beta$ -CD, (b) diazido $\beta$ -CD, (c) $C_{60}$ and (d) $\beta$ -CD- $C_{60}$ adduct	135

5.1.10	X-ray diffractogram of (a) C <sub>60</sub> , (b) diazido β-CD and (c) β-CD-C <sub>60</sub> adduct	136
5.1.11	(a) TEM image (b) SEM image and (c) Schematic illustration of the proposed supramolecular self-assembly of β-CD-C <sub>60</sub> adduct	137
5.1.12	TEM image of self-assembly of 2:1 inclusion complex of β-CD and [60]fullerene.	138
5.1.13	AFM images of β-CD-[60]fullerene adduct	139
<b>5.2</b>	<b>Solubilization of [60]Fullerene and [70]Fullerene by Disaccharides</b>	
5.2.1	Photograph of [A] C <sub>60</sub> in toluene, [B] lactose in DMSO, [C] lactose-C <sub>60</sub> complex in water, [D] lactose-C <sub>60</sub> complex in toluene and [E] lactose-C <sub>60</sub> complex in water + toluene	148
5.2.2	Photograph of [A] C <sub>70</sub> in toluene, [B] lactose in DMSO, [C] lactose-C <sub>70</sub> complex in water, [D] lactose-C <sub>70</sub> complex in toluene and [E] lactose-C <sub>70</sub> complex in water + toluene	148
5.2.3	FTIR absorption spectra of (a) C <sub>60</sub> , (b) lactose and (c) lactose-C <sub>60</sub> complex	150
5.2.4	UV-Vis spectra of lactose, C <sub>60</sub> , lactose-C <sub>60</sub> complex and inset C <sub>60</sub> extracted from complex by toluene	151
5.2.5	TGA curves of lactose, C <sub>60</sub> and lactose-C <sub>60</sub> complex	152
5.2.6	<sup>1</sup> H NMR spectra of lactose and lactose-C <sub>60</sub> complex in D <sub>2</sub> O	153
5.2.7	<sup>13</sup> C NMR spectra of lactose and lactose-C <sub>60</sub> complex in D <sub>2</sub> O	154
5.2.8	X-ray diffractogram of (a) C <sub>60</sub> , (b) lactose and (c) lactose-C <sub>60</sub> complex	155
5.2.9	(a) TEM micrograph of lactose-C <sub>60</sub> complex; inset: HRTEM image of C <sub>60</sub> lattice (b) spherical self-assembly of lactose-C <sub>60</sub> complex (c) histogram of lattice spacing	156
5.2.10	Particle size of lactose-C <sub>60</sub> complex by static light scattering	156
5.2.11	Space-filling energy-minimized (MM2) molecular models showing different views of lactose-C <sub>60</sub> complex	157
5.2.12	Color bleaching UV-Vis spectra of radical scavenging of	158

	most stable free radical DPPH with lactose-C <sub>60</sub> complex	
5.2.13	Pseudo-first-order rate correlations for DPPH in of reaction between DPPH and lactose-C <sub>60</sub> complex	159
<b>Chapter 6</b>	<b>Surface Immobilization of Carbon Nanotubes by <math>\beta</math>-Cyclodextrins and Their Inclusion Ability</b>	
6.1	FTIR spectra of (a) oxidized MWCNTs, (b) diamino $\beta$ -cyclodextrin and (c) $\beta$ -cyclodextrin-modified MWCNTs	172
6.2	Dispersibility of (a) pristine MWCNTs, (b) oxidized MWCNTs and (c) $\beta$ -cyclodextrin-modified MWCNTs.	173
6.3	TGA curves of (a) oxidized MWCNTs, (b) diamino $\beta$ -cyclodextrin and (c) $\beta$ -cyclodextrin-modified MWCNTs	174
6.4	FE-SEM combined EDS of (a) pristine MWCNTs, (b) oxidized MWCNTs and (c) $\beta$ -cyclodextrin-modified MWCNTs	175
6.5	TEM images of (a) pristine MWCNTs, (b) oxidized MWCNTs, (c) $\beta$ -cyclodextrin-modified MWCNTs without staining and (d) $\beta$ -cyclodextrin-modified MWCNTs staining with phosphotungstic acid	176
6.6	Fluorescence spectra (excited at 480 nm) of rhodamine 6G ( $5 \times 10^{-6}$ M) in aqueous solutions of (A) diamino $\beta$ -cyclodextrin, (B) pristine MWCNTs, (C) oxidized MWCNTs and (D) $\beta$ -cyclodextrin-modified MWCNTs at different concentrations: (a) 0, (b) 2.5, (c) 5.0, (d) 7.5, (e) 10.0, (f) 12.5, (g) 15.0, (h) 17.5, (i) 20.0 and (j) 22.5 $\mu\text{g/mL}$	177
6.7	Change in fluorescence intensity at 554 nm of rhodamine 6G ( $5 \times 10^{-6}$ M) as a function of concentration of (a) pristine MWCNTs, (b) diamino $\beta$ -cyclodextrin, (c) oxidized MWCNTs and (d) $\beta$ -cyclodextrin-modified MWCNTs in water	180
6.8	Stern-Volmer plots for (a) pristine MWCNTs, (b) oxidized MWCNTs and (c) $\beta$ -cyclodextrin-modified MWCNTs	181

## List of Schemes

<b>Scheme No.</b>	<b>Title</b>	<b>Page No.</b>
2.1	Synthetic scheme for the synthesis of selectively difunctionalized $\beta$ -cyclodextrins	44
3.1	Synthesis of $\beta$ -cyclodextrin-cyanuric chloride and PEG based polymers	70
3.2	Reaction scheme for the synthesis of $\beta$ -cyclodextrin polymer with short linker Urea	71
4.1.1	Scheme shows the formation of inclusion complex of drug CBZ with $\beta$ -CD-CC-P in mixed solvents system	93
4.2.1	Scheme for the formation of binary pyrene- $\beta$ -CD inclusion complex in mixed solvent system	107
4.2.2	Scheme for the formation of binary pyrene- $\beta$ -CD-P inclusion complex in mixed solvent system	108
4.2.3	Scheme for the formation of ternary pyrene-adamantol- $\beta$ -CD inclusion complex in mixed solvent system	109
4.2.4	Scheme for the formation of ternary pyrene-adamantol- $\beta$ -CD-P inclusion complex in mixed solvent system	109
5.1.1	Covalent and Non-covalent interaction of modified $\beta$ -CD and [60]fullerene	126
5.1.2	Non-covalent 2:1 inclusion complex of $\beta$ -CD and [60]fullerene	126
5.2.1	Complexation of lactose- $C_{60}$ in mixed solvent system	144
5.2.2	Reaction scheme for radical scavenging of most-stable free radical DPPH with lactose- $C_{60}$ complex	146
6.1	Synthetic scheme of chemical immobilization of $\beta$ -cyclodextrins on MWCNTs	169
6.2	Mechanism for the reaction of diamino $\beta$ -cyclodextrin with oxidized MWCNT by an activated ester intermediate	170
6.3	Schematic illustrations of the formation of $\beta$ -cyclodextrin-dye inclusion complex and the adsorption of dyes on MWCNTs	179

## List of Tables

Table No.	Title	Page No.
1.1	Physical properties of the three major cyclodextrins	4
1.2	Solubility of cyclodextrins in water as a function of temperature	7
1.3	Thermodynamics parameter of three major cyclodextrins	8
2.1	$^1\text{H}$ NMR chemical shifts, $\delta(\text{ppm})$ , of C-H protons in unsubstituted $\beta$ -CD and substituted $\beta$ -CD in $\text{D}_2\text{O}$	63
2.2	$^1\text{H}$ NMR chemical shifts, $\delta(\text{ppm})$ , of C-H protons in unsubstituted $\beta$ -CD and substituted $\beta$ -CD in $\text{DMSO-d}_6$	63
2.3	$^{13}\text{C}$ NMR chemical shifts, $\delta(\text{ppm})$ , of unsubstituted $\beta$ -CDs and substituted $\beta$ -CD	64
3.1	Aqueous solubility of $\beta$ -CD polymers at $25^\circ\text{C}$	74
3.2	Molecular Weight of $\beta$ -CD-CC-PEG polymers at $25^\circ\text{C}$ by SLS	81
3.3	Molecular Weight of $\beta$ -CD-Urea and Thiourea polymers at $25^\circ\text{C}$ by SLS	86
4.2.1	Binding constants for binary inclusion complex	114
4.2.2	Stern-Volmer quenching constant for ternary inclusion complex	117
5.2.1	Aqueous solubility of corresponding complex at $25^\circ\text{C}$ and concentration of $\text{C}_{60}$ per mg of complex	149
6.1	Hypochromism constants for pristine and modified MWCNTs calculated from fluorescence intensities	182

## Abbreviations

AFM	Atomic Force Microscopy
AR	Analytical Reagent
BCS	Biopharmaceutical Classification System
C <sub>60</sub>	[60]Fullerene
C <sub>70</sub>	[70]Fullerene
CBZ	Carbamazepine
CC	Cyanuric Chloride
CDCl <sub>3</sub>	Deuterated Chloroform
CDs	Cyclodextrins
CGTase	Cyclodextrin Glycosyltransferase
CM	Carboxymethyl
CNTs	Carbon Nanotubes
D <sub>2</sub> O	Deuterium Oxide
DCC	<i>N,N'</i> -Dicyclohexylcarbodiimide
DEG	Diethylene Glycol
DMA	Dimethylacetamide
DMAO	Dimethyl(aminomethyl)phosphine oxide
DMF	<i>N,N'</i> -Dimethylformamide
DMSO	Dimethylsulfoxide
DMSO-d <sub>6</sub>	Deuterium Dimethylsulfoxide
DNA	Deoxy Ribonucleic Acid
DPPH	2,2'-Diphenyl-1-Picryl Hydrazyl
DS	Degree of substitution
EDC	1-Ethyl-3-(3-Dimethylamino Propyl) Carbodiimide Hydrochloride
EDS	Energy Dispersive Spectroscopy
EPH	Epichlorohydrine
FE-SEM	Field Emission Scanning Electron Microscopy
FTIR	Fourier Transform Infrared
GC	Gas Chromatography
HIV	Human Immunodeficiency Virus
HPLC	High Performance Liquid Chromatography

HP- $\beta$ -CD	Hydroxypropyl $\beta$ -Cyclodextrin
$K_b$	Binding Constant
$K_{SV}$	Stern-Volmer Constant
$Me_4Si$	Tetramethyl Silane
MeCN	Acetonitrile
MRI	Magnetic Resonance Imaging
$M_w$	Molecular weight
MWCNTs	Multi Wall Carbon Nanotubes
MWCO	Molecular Weight Cut Off
NMR	Nuclear Magnetic Resonance
PEG	Polyethylene Glycol
ppm	Parts Per Million
RT	Room Temperature
SEB- $\beta$ -CD	Sulfobutylether- $\beta$ -Cyclodextrin
SEM	Scanning Electron Microscopy
SLS	Static Light Scattering
SWCNTs	Single Wall Carbon Nanotubes
TBDMS	<i>ter</i> -Butyldimethylsilyl Chloride
TEM	Transmission Electron Microscopy
TGA	Thermogravimetric Analysis
THF	Tetrahydrofuran
TLC	Thin Layer Chromatography
TMS	Tetramethyl Silane
TsCl	Tosyl Chloride
UV-Vis	Ultraviolet Visible
XRD	X-ray Diffraction

***Chapter 1***  
***Introduction***

## Chapter 1

### Introduction

#### 1.1 Brief History of Cyclodextrins

Cyclodextrins were first described by a French scientist A. Villiers in 1891, where he explained the isolation of crystalline substance obtained from bacterial digestion of starch which appeared resistant towards acid hydrolysis and did not show reducing properties like ordinary sugar<sup>1</sup>. Subsequently, Australian microbiologist F. Schardinger laid the foundation of the cyclodextrin chemistry during 1903-1911. First he gave the name “cellulosine” for “crystalline dextrin” and later changed the name and identified two compounds as  $\alpha$ -cyclodextrin and  $\beta$ -cyclodextrin<sup>2,3</sup>. In the following years cyclodextrins were named as ‘Schardinger dextrins’ in his honor. In the 1935, K. Freudenberg and Jacobi identified  $\gamma$ -cyclodextrin and suggested that larger cyclodextrins could also exist<sup>4</sup>. K. Freudenberg and co-workers showed that cyclodextrins were cyclic oligosaccharides formed by glucose units and later F. Cramer and co-workers described their ability to form inclusion complexes<sup>5,6</sup>. By the early 1950s the basic physicochemical characteristics of cyclodextrins had been discovered, including their ability to solubilize and stabilize drugs. The first cyclodextrin-related patent was issued in 1953 to K. Freudenberg, F. Cramer and H. Plieninger<sup>7</sup>. After that American scientist D. French described the cyclodextrins and their inclusion complexes in a much better way<sup>8-10</sup>.

However, pure cyclodextrins that were suitable for pharmaceutical applications did not become available until about 25 years later and at the same time the first cyclodextrin-containing pharmaceutical product was marketed in Japan. Later cyclodextrin-containing products appeared on the European market and in 1997 also in the US. New cyclodextrin-based technologies are constantly being developed and, thus, 140 years after their discovery cyclodextrins are still regarded as novel with unexplored potential. Later D. French and co-workers have reported that more than eight glucose containing cyclodextrin also exist<sup>11</sup>. However, until the mid 1980s the large-ring cyclodextrins were ignored because of difficulties in their purification and preparation of reasonable yield and it was conceivable that they were identical with side chain containing cyclodextrins<sup>12,13</sup>. P. R. Sundararajan and V. S. R. Rao

demonstrated by conformational energy map calculations that cyclodextrins with less than six members cannot be formed for sterical reasons<sup>14</sup>. F. V. Lichtenthaler and S. Immel proposed the term cyclodextrins as a generic nomenclature for all cyclooligosaccharides composed of glucose units depending upon the numbers of glucose unit presence in a ring<sup>15</sup>.

The field of cyclodextrins has made tremendous advances since the discovery of the inclusion complexation properties. 44,877 papers and 9,213 patents on cyclodextrins were published during 1961-2010 (www.cyclolab.hu) in various areas, ranging from organic chemistry to pharmaceutical and analytical applications. The field is not only very large but also highly diversified and is expanding rapidly. Figure 1.1 shows the cyclodextrins papers and patents in last 5 decades.

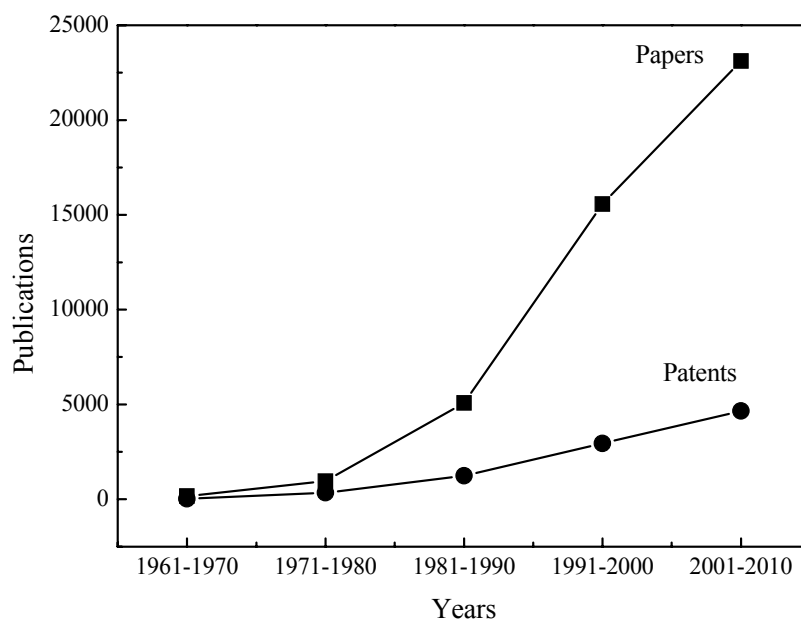


**Figure 1.1** Cyclodextrins papers and patents in Last 5 decades.

## 1.2 Structural Features of Cyclodextrins

Cyclodextrins (CDs) are water-soluble cyclic, non-reducing oligosaccharides consisting of D-glucopyranose units linked through  $\alpha$ -1,4-glycosidic linkages. The major and most common three cyclodextrins,  $\alpha$ -cyclodextrin,  $\beta$ -cyclodextrin and  $\gamma$ -cyclodextrin consist of six, seven and eight D-glucopyranose units, respectively. Pristine cyclodextrins are crystalline, non-hygroscopic, homogeneous substances,

which are torus (bucket) shaped macrocycles. In cyclodextrins, the glucose units adopt a  ${}^4C_1$  chair confirmation and orient themselves so that the molecule forms a toroidal truncated cone shaped structure. The cavity is lined by the hydrogen atoms and the glycosidic oxygen bridges. The non-bonding electron pairs of the glycosidic oxygen bridges are directed towards the inside of the cavity to produce a high electron density and lend it some Lewis base character<sup>16</sup>. Figure 1.2 shows the schematic structures of native  $\alpha$ -CD,  $\beta$ -CD and  $\gamma$ -CD.

The C-2 hydroxyl group of one glycopyranose unit can form a hydrogen bond with the C-3 hydroxyl group of the neighbouring glucopyranose unit<sup>17</sup>. In the  $\beta$ -CD molecule a complete secondary belt is formed by these hydrogen bonds, thus making it a rigid structure. The hydrogen ring is incomplete in the  $\alpha$ -CD molecule because one of the glycopyranose units is in a distorted position<sup>18,19</sup>; therefore, instead of the six possible hydrogen bonds, only four can be formed.

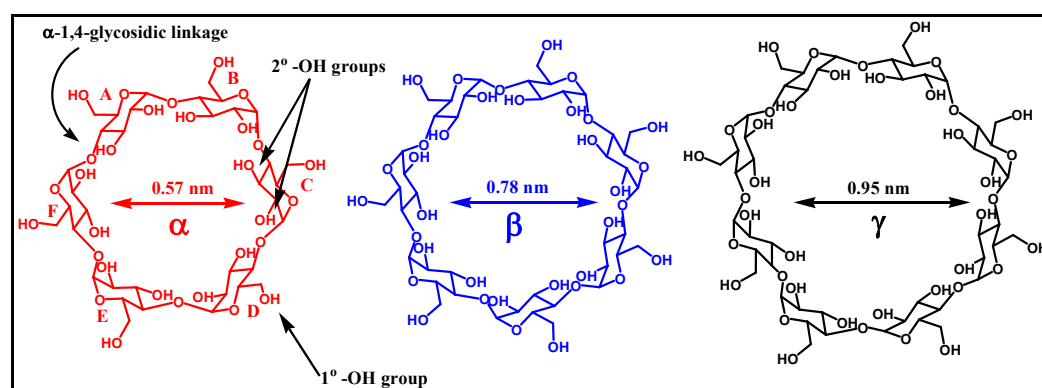


**Figure 1.2** Schematic structures of native  $\alpha$ -,  $\beta$ - and  $\gamma$ -cyclodextrins.

The  $\gamma$ -CD molecule has a more flexible structure and so is the most soluble of the three native CDs. The equilibrium constants for hydrogen-deuterium exchange in the secondary hydroxyl groups of  $\alpha$ -CD,  $\beta$ -CD and  $\gamma$ -CD also indicate that the strongest hydrogen bond system is formed in the  $\beta$ -CD molecule<sup>20</sup>. Table 1.1 summarizes the important physical properties of the three major and most common cyclodextrins<sup>21</sup>.

**Table 1.1** Physical properties of the three major cyclodextrins

<b>Cyclodextrin Type</b>	<b><math>\alpha</math>-CD</b>	<b><math>\beta</math>-CD</b>	<b><math>\gamma</math>-CD</b>
Number of glucose units	6	7	8
Mw (Da)	972	1135	1297
Solubility in water (g/100 mL, 25°C)	14.5	1.85	23.2
$[\alpha]_D$ at 25°C (°C)	150 ± 0.5	162.5 ± 0.5	177.4 ± 0.5
Cavity diameter (pm)	470 - 530	600 - 650	750 - 830
Height of torus (pm)	790 ± 10	790 ± 10	790 ± 10
Diameter of outer periphery (pm)	1460 ± 40	1540 ± 40	1750 ± 40
Approximate volume of cavity (10 <sup>6</sup> pm <sup>3</sup> )	174	262	427
Approximate cavity volume in 1 mol of CD (mL)	104	1257	256
Crystal form (from water)	hexagonal plates	monoclinic parallelogram	quadratic prisms
Surface tension (mN/m)	71	71	71
Melting range (°C)	255-260	255-265	240-245
Crystal water (wt. %)	10.2	13.2-14.5	8.13-17.7
Water molecules in cavity	6	11	17
Diffusion constant at 40°C	3.443	3.224	3.000
pK (by potentiometry) at 25°C	12.332	12.202	12.081
Partial Molar volumes in solution (mL mol <sup>-1</sup> )	611.4	703.8	801.2
Adiabatic compressibility in aqueous solution (10 <sup>4</sup> mLmol <sup>-1</sup> bar <sup>-1</sup> )	7.2	0.4	-5.0

Cyclodextrins are not hygroscopic, but form stable hydrates. Deuterium magnetic resonance spectra of powder and single crystal sample of  $\alpha$ -CD,  $\beta$ -CD and  $\gamma$ -CD crystallized from deuterated water showed 6.6 molecules of water per molecule of  $\alpha$ -CD, 11 molecules of water per molecule of  $\beta$ -CD and 17 molecules of water per molecule of  $\gamma$ -CD. A quasielastic neutron scattering study on  $\alpha$ -CD.6H<sub>2</sub>O,  $\beta$ -CD.11H<sub>2</sub>O and  $\gamma$ -CD.17H<sub>2</sub>O showed that 2, 6 and 8.8 water molecules are included in

the  $\alpha$ -CD,  $\beta$ -CD and  $\gamma$ -CD cavity, respectively with considerable positional disorder and rest of the water molecules are hydrogen bonded outside with hydroxyl groups of CDs; moreover, the hydroxyl group of  $\beta$ -CD shows extensive orientation disorder. According to neutron diffraction studies, in crystalline  $\gamma$ -CD molecule 8.8 water molecules are located in the hydrophobic cavity.

### 1.3 Shape and Size of Cyclodextrins

Cyclodextrins have truncated cone or bucket shape structure as shown in Figure 1.3. The native  $\beta$ -cyclodextrins have 14 secondary hydroxyl groups on the wider rim and 7 primary hydroxyl groups on the narrow rim. Cyclodextrins have inner non-polar hydrophobic cavity and polar hydrophilic exterior. The diameter of the cavity is smaller on the primary face and wider on secondary face. This is because the free rotation of the primary hydroxyl groups reduces the effective diameter of the cavity. Because of their torus-like geometry, relatively hydrophobic surface of the internal cavity and the hydrophilic character of external hydroxyl groups, these molecules easily form inclusion complexes with a wide variety of guest molecules. This complex-forming capacity is the reason for their widespread application in various fields of chemistry.

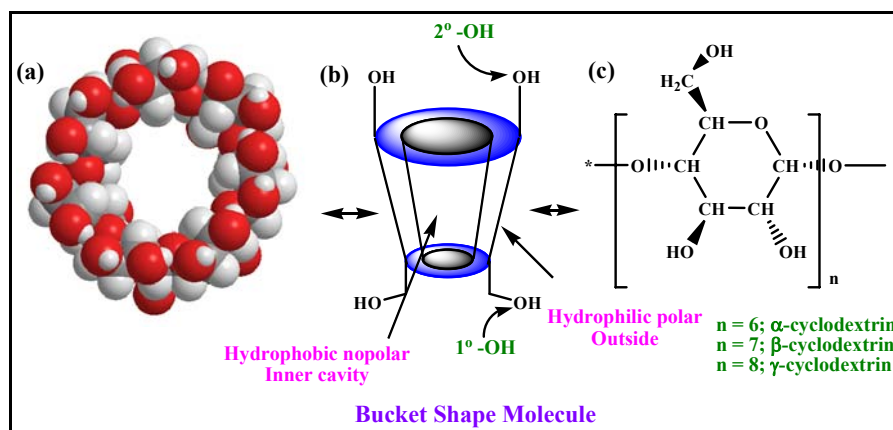


**Figure 1.3** (a) 3D Molecular structure of  $\beta$ -CD, (b) Torus (Bucket) shape of CD and (c) Common structure of CDs.

According to the molecular graphics computations  $\beta$ -CD has perfect symmetry, while  $\alpha$ -CD and  $\gamma$ -CD rings are slightly distorted. As the numbers of glucose units increases the cavity dimensions of the cyclodextrins increases as shown

in Figure 1.4. The inner diameter of the cavity in unmodified cyclodextrins varies from 5 to 10 Å and depth is same in all cyclodextrins about 8 Å. Depending upon the cavity size of the cyclodextrins and guest molecules, cyclodextrin can form an inclusion complex with different shape and size of molecules. As the CD cavity diameter increases, the apolar cavity can accommodate an increasing number of water molecules, and in aqueous medium these complexed water molecules will be energetically lost during the course of formation of an inclusion complex<sup>22</sup>.

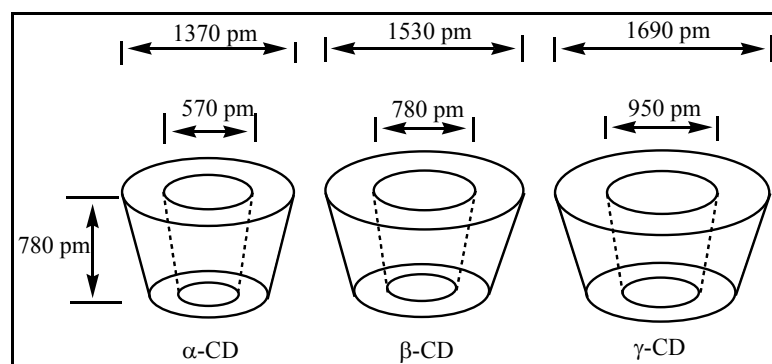


**Figure 1.4** Molecular dimensions of  $\alpha$ -,  $\beta$ - and  $\gamma$ -cyclodextrins.

#### 1.4 Solubility of Cyclodextrins

Solubility is the major parameter for the applications of cyclodextrins. The solubility of  $\beta$ -CD is only 1.85 g per 100 mL at ambient temperature<sup>23</sup>, while the solubility of  $\alpha$ -CD and  $\gamma$ -CD are higher at 14.5 and 23.2 g per 100 mL, respectively. The solubility of CDs depends strongly on the temperature<sup>24</sup>. At 50°C the solubility of the all three CDs are about three times that at 20°C. The water-solubility of the cyclodextrins and their derivatives varies in a rather surprising manner. The solubility of methylated CD decreases with an increase of temperature, while the pristine cyclodextrins are more soluble in water at higher temperature. The solubility of  $\beta$ -CD increases when upto two thirds of the all hydroxyl groups are methylated and then decreases when all hydroxyl groups are methylated. J. Szejtli<sup>25</sup> explained the low water-solubility displayed by  $\beta$ -CD by the fact that it has a rather rigid molecular structure consisting of a seven fold axis of symmetry, making it more prone to crystallization than  $\alpha$ -CD or  $\gamma$ -CD. The intermolecular interaction of  $\beta$ -CD molecules in the solid state requires a high energy to break the molecular association, due to the

greatest overall molecular dipole, thereby imparting a lower solubility than the  $\alpha$ - or  $\gamma$ -CD. Also, the interruption of  $\beta$ -CD crystalline nature can reduce the intermolecular interaction and in turn increase its aqueous solubility.

The temperature dependence of the solubility of the three cyclodextrins in water is described by equations (1.1-1.3), the parameters of the functions being determined by a least-squares method from the data of Jozwiakowski and Connors<sup>26</sup>.

$$c = (112.71 \pm 0.45) e^{-(3530 \pm 31)[(1/T) - (1/298.1)]} \quad (\text{for } \alpha\text{-CD}) \quad (1.1)$$

$$c = (18.3236 \pm 0.099) e^{-(14137 \pm 31)[(1/T) - (1/298.1)]} \quad (\text{for } \beta\text{-CD}) \quad (1.2)$$

$$c = (219.4 \pm 9.8) e^{-(3187 \pm 320)[(1/T) - (1/298.1)]} \quad (\text{for } \gamma\text{-CD}) \quad (1.3)$$

Where,  $c$  is the concentration of the CD in milligram per milliliter.  $T$  is the temperature in kelvin. The temperature dependence of water-solubility of three most common cyclodextrins are shown in Table 1.2.

**Table 1.2** Solubility of cyclodextrins in water as a function of temperature

Temperature (°C)	Solubility (mg/g water)		
	$\alpha$ -CD	$\beta$ -CD	$\gamma$ -CD
20	90	16.4	185
25	127	18.5	256
30	165	22.8	320
35	204	28.3	390
40	242	34.9	460
45	285	44.0	585
50	347	52.7	651

Relative to the solubilities of acyclic saccharides, the low solubilities of CDs are a consequence of the relatively unfavorable enthalpies of solutions, partially offset by the more favorable enthalpies of solution. The thermodynamic properties of  $\alpha$ -CD and  $\gamma$ -CD are very similar, whereas the much lower solubility of  $\beta$ -CD is a consequence of a less favorable (more positive)  $\Delta H^\circ$  and a less favorable (more

negative)  $\Delta S^\circ$ . Table 1.3 shows the thermodynamic parameters for CDs causing a compensation of the favorable enthalpy by the unfavorable entropy of solution<sup>27</sup>.

**Table 1.3** Thermodynamics parameters of three major cyclodextrins

CDs	$\Delta H^\circ$ kJmol <sup>-1</sup>	$\Delta S^\circ$ JK <sup>-1</sup> mol <sup>-1</sup>
$\alpha$ -CD	32.1	57.8
$\beta$ -CD	34.8	49.0
$\gamma$ -CD	32.4	61.5

In presence of organic solvents the solubility of CDs changes owing to the formation of inclusion complex. The solubility of  $\beta$ -CD as a mobile-phase additive was studied in methanol, ethanol, propanol, acetonitrile, THF and DMSO<sup>28</sup>. The solubility decreased monotonically with increasing methanol concentration, but increased to double its value in water with increasing acetonitrile concentration up to 30%<sup>29</sup>. Figure 1.5 shows the solubility of  $\beta$ -cyclodextrin in presence of cosolvents with water. In presence of relatively non-polar solvents the solubility of  $\beta$ -CD increases rapidly with increasing the concentration of cosolvent in water up to 50% after that the solubility decrease quickly, whereas in case of polar solvent the solubility remains constant up to 40% after that it increases rapidly.

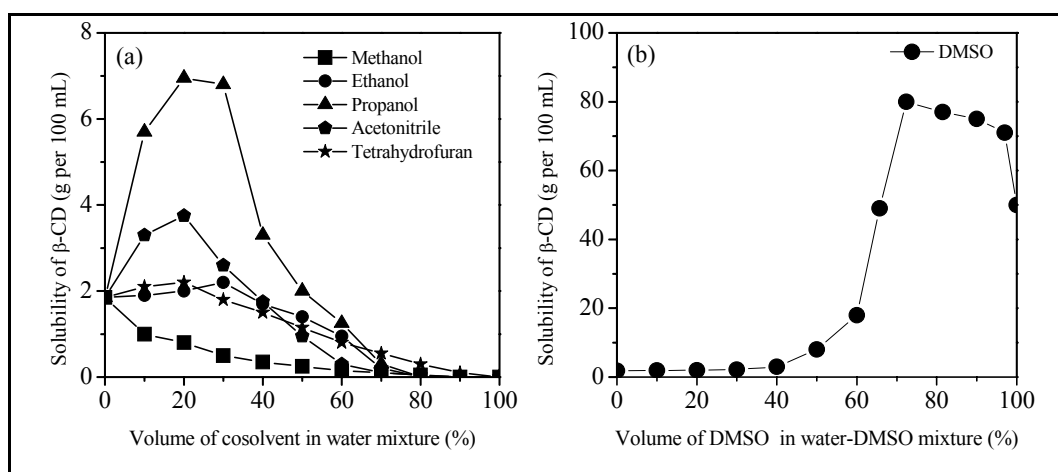


**Figure 1.5** (a) Solubility of  $\beta$ -CD as a function of different cosolvent in water mixture and (b) Solubility of  $\beta$ -CD as a function of DMSO in water-DMSO mixture.

## 1.5 Viscosity and Stability of Cyclodextrins

The viscosity of an aqueous cyclodextrin solution does not differ significantly from that of water. Measured at 25.1°C, the viscosity of pure water is  $8.93 \times 10^{-4}$  Pa s, whereas the viscosity of a  $9.5 \times 10^{-4}$  M  $\alpha$ -CD solution is  $8.99 \times 10^{-4}$  Pa s, and that of  $9.98 \times 10^{-3}$  M  $\beta$ -CD solution is  $9.4 \times 10^{-4}$  Pa s<sup>30</sup>. Both the concentration and temperature dependences of the viscosities of  $\alpha$ -CD and  $\gamma$ -CD solutions, and their apparent molar volumes, are similar to those of linear saccharides, such as maltose and maltotriose. This indicates that  $\alpha$ -CD and  $\gamma$ -CD are structural-forming solutes. The concentration dependences of the activity coefficients of CDs differ significantly from those of maltose and maltotriose due to dimerization<sup>31</sup>.

The cyclodextrins are thermally stable (up to at least 200°C). They are very stable in alkaline solutions (pH < 14) and moderately stable in acidic solutions (pH > 3). Cyclodextrins can be hydrolyzed in strong acidic condition. The rate of hydrolysis depends on the concentration of acid and the temperature<sup>32</sup>. Cyclodextrins are stable in presence of (enzymes) glucoamylases or  $\gamma$ -amylase and  $\beta$ -amylase and can be hydrolyzed by some  $\alpha$ -amylase<sup>33</sup>.

## 1.6 Host-Guest Inclusion Complex of Cyclodextrins

The most important, unique and exceptional property of cyclodextrins is that they can form inclusion complexes in solution as well as in crystalline solid form with wide varieties of molecules depending upon the size of the host and guest molecules<sup>34-37</sup>. This phenomenon is commonly known as host-guest inclusion complexation as shown Figure 1.6.

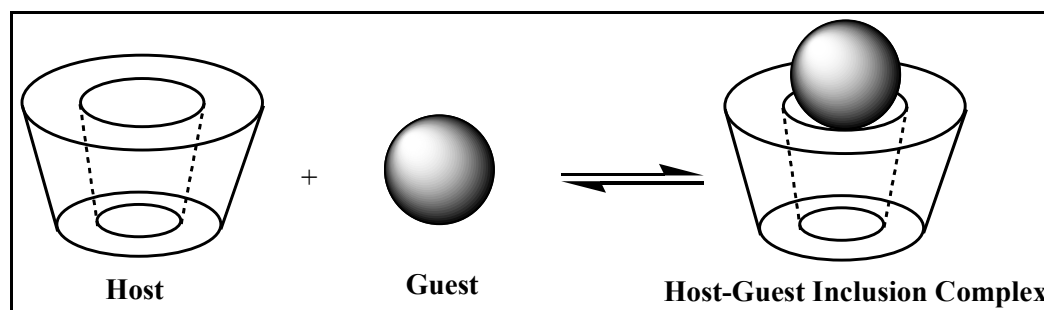


**Figure 1.6** Host-Guest Inclusion Complexation.

The word ‘inclusion complex’ was introduced by Schlenk in 1950<sup>38</sup>. Inclusion complexes are entities comprising two or more molecules; the ‘**host**’ includes a ‘**guest**’ molecule, totally or in part, by only physical forces, that is, without covalent bonding. CDs are typical host molecules and may include a great variety of molecules having the size of one or two benzene rings, or even larger compounds, which have a side chain of comparable size, to form crystalline inclusion complexes. Complexation occurs when there is a steric compatibility between the CD cavity and the guest molecule and the affinity of the guest molecule for the CD cavity is higher than for the other components present (*i.e.* solvent). It has been established that, besides steric compatibility, hydrophobic interactions<sup>39</sup>, van der Waals interactive forces<sup>40</sup> and hydrogen bonding<sup>41</sup> independently or in combination play a considerable role in the determination of the strength of inclusion complexes. Several techniques have been used for the formation of cyclodextrin inclusion complex these include: mixed solvent system, co-precipitation, slurry complexation, paste-complexation (kneading method), damp mixing and heating, extrusion and dry mixing. The stoichiometry of inclusion compounds is usually 1:1; however, complexes can be made of two or more guests (especially with the large  $\gamma$ -CD cavity) or with several CD molecules by the inclusion of different parts of a large guest molecule. Many physicochemical methods have been used for the study of the formation of inclusion complexes. Thus calorimetry<sup>42</sup>, spectrophotometry<sup>43</sup> and various liquid chromatographic methods, such as reverse-phase thin-layer and high-performance liquid chromatography<sup>44</sup>, has been successfully used for the assessment of the various aspects of host-guest interaction. It has also been deduced that the remarkable flexibility of the cyclodextrin ring can be responsible for the adaptation of molecules to a wide range of shapes.

The formation of a 1:1 inclusion complex of host and guest is an equilibrium process between the dissociated and associated species in solution (Eq. 1.4), which is characterized by the stability constant,  $K$  (Eq. 1.5). This is the simplest and more frequent case, however, 2:1, 1:2 or 2:2 stoichiometries can also exist for CD host-guest complexes.



$$K = \frac{[\text{Inclusion Complex}]}{[\text{Host}][\text{Guest}]} \quad (1.5)$$

The nature of interaction has been studied during the host-guest complexation as well as the structure of the CD complexes<sup>45</sup>. Molecular modeling, simulation, X-ray crystallography, NMR spectroscopy, optical spectroscopy (UV-Vis, fluorescence, circular dichroism) and thermal characterization methods have been used to determine the molecular structure of inclusion complex.

The ‘driving force’ of complexation is not yet fully understood. The following factors have been considered for the formation of an inclusion complex.

- (i) Substitution of the energetically unflavored-apolar interactions between the included water molecules and the CD cavity on one hand, and between water molecules and the guest on the other by the more favoured apolar-apolar interaction between the guest and the cavity, and polar-polar interaction between bulk water and the released cavity-water molecules.
- (ii) CD-ring strain release on complexation.
- (iii) van der Waals interaction.
- (iv) In the case of some guest, hydrogen bonding between host and guest.

### 1.7 Synthesis of Cyclodextrins

The synthesis of cyclodextrins involves treatment of ordinary starch with easily available enzymes. In nature, the enzymatic digestion of starch by cyclodextrins glycosyltransferase (CGTase) produces a mixture of cyclodextrin comprised of six, seven and eight glucose units ( $\alpha$ -,  $\beta$ -, and  $\gamma$ -cyclodextrin, respectively). Commercially, cyclodextrins are produced from starch, but more specific enzymes are used to selectively produce consistently pure  $\alpha$ -,  $\beta$ - and  $\gamma$ -cyclodextrin<sup>46,47</sup>. The typical enzymatic synthesis of cyclodextrins is shown in Figure 1.7. Cyclodextrins are obtained in a large scale by enzymatic degradation of starch, by making a use of a glycosyltransferase from *Bacillus macerans*<sup>48</sup>. Commercially

cyclodextrins are prepared by two major processes (i) solvent and (ii) non solvent process. These processes involve following main-steps:

- 1) Cultivation of the microorganism which produces the cyclodextrin glycosyltransferase (CGTase) enzyme.
- 2) Separation of the enzyme from the fermentation tank, followed by concentration and purification.
- 3) Enzymatic conversion of prehydrolysed starch to a mixture of cyclic and acyclic dextrins.
- 4) Separation of cyclodextrins from the conversion mixture with purification and crystallization.

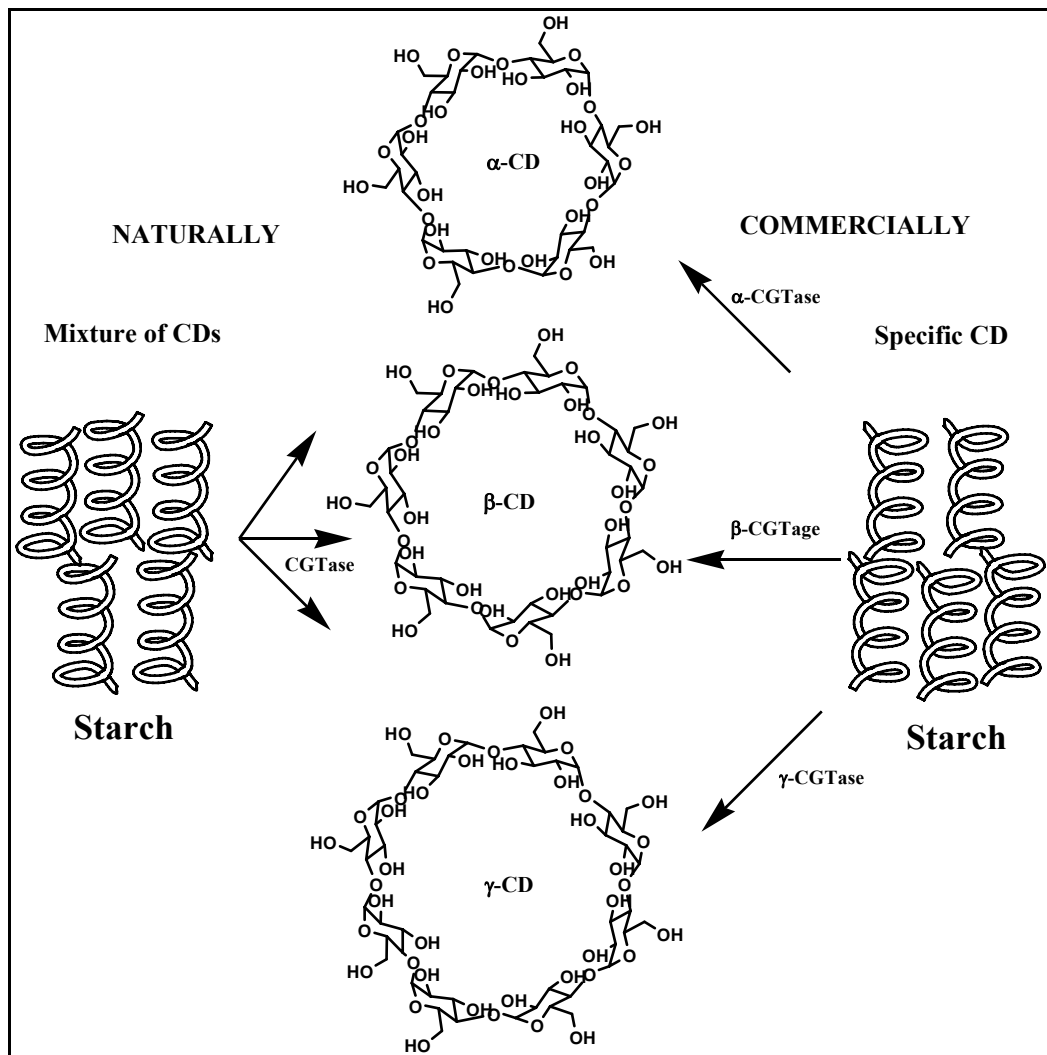


**Figure 1.7** Synthesis of cyclodextrins from starch by enzymatic digestion.

## 1.8 Chemical Modification of Cyclodextrins

In CDs every glucopyranose unit has three free OH groups, two of which (on C-2 and C-3) are secondary and one (C-6) primary<sup>49</sup>. As each of these free hydroxyl groups can be modified, by substituting the hydrogen atom or the hydroxyl group by a wide variety of substituents, the majority of simple synthetic reactions results in a number of positional isomers. Hydroxyl groups present at the 2-, 3-, and 6-positions compete for the reagent and make selective modification extremely difficult<sup>50</sup>.

Cyclodextrins are modified for a variety of reason. For example, if a highly water soluble cyclodextrin is desired, then a random conversion of hydroxyl groups to sulfate groups can be done<sup>51,52</sup>. However, if a cyclodextrin with a high solubility in organic solvents is desired then hydroxyl groups are converted to silyl ethers in a random fashion<sup>53</sup>. However, in both these cases, the final product is not homogeneous and cannot be accurately characterized by elemental analysis.

Selective and efficient modification especially mono or disubstitutions is complicated by the presence of similar functionalities<sup>54</sup>. Among the three hydroxyl groups in a glucopyranose unit, the primary hydroxyl groups on the C-6 has the highest reactivity, especially when bulky substitution reagents are used, and the secondary hydroxyl groups on C-3 has least reactivity. This has been attributed to the hydrogen bonding between the protons of the hydroxyl group on C-3 and the oxygen atom of the hydroxyl group on the C-2<sup>55</sup>. The hydroxyl groups on the C-3 can only react when all the primary and secondary hydroxyl groups are protected. The functional groups used in the chemical modification of cyclodextrins are alkyl-, amine-, hydroxylalkyl-, carboxyalkyl-, azide- etc<sup>56</sup>. The most of the synthesized cyclodextrin derivatives are complex mixture with different degree of substitution and positional isomers. Most commonly NMR, FTIR and Mass spectrometric analysis has been reported to be cheap, simple and rapid characterization techniques for the determination of substitution<sup>57</sup>.

## 1.9 Methods for Modification of Cyclodextrins

There are various chemical factors that are involved in the chemical modification of cyclodextrins<sup>58-60</sup>. The primary factors are the nucleophilicity of the hydroxyl groups and the ability of cyclodextrins to form complexes with the reagents

used. All modifications of cyclodextrins take place at the hydroxyl groups and since the hydroxyl groups are nucleophilic in nature, which initiate the reaction and directs the regioselectivity and the extent of modification (mono, di, tri, etc.) of all subsequent reactions and then an electrophile attack on these positions. As the cyclodextrin moiety has three types of hydroxyl groups, those at the 6-position are the most basic (and often most nucleophilic), those at the 2-position are the most acidic, and those at the 3-position are the most inaccessible<sup>61,62</sup>. General synthetic strategies for the selective modification of cyclodextrin are shown in Figure 1.8.

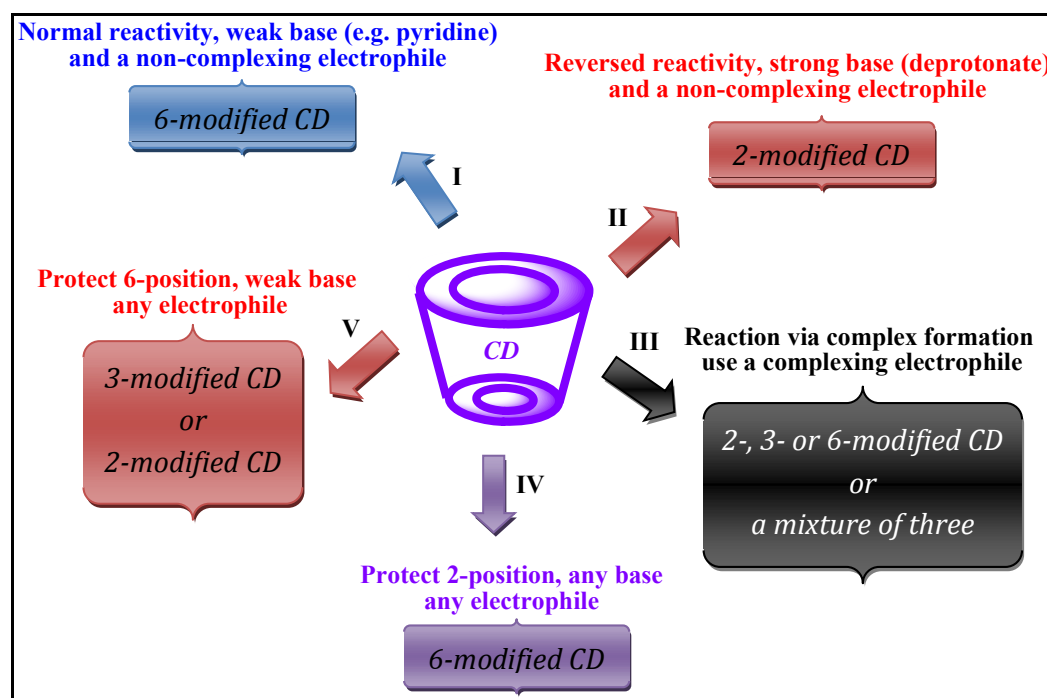


**Figure 1.8** Overview of the methods for modification of cyclodextrins.

Under the normal conditions an electrophilic reagent attacks at the 6-positions. However, more reactive reagent like trimethylsilyl chloride attacks the 6-positions less selectively<sup>63</sup> (I in Figure 1.8). Less reactive reagents like *ter*-butyldimethylsilyl chloride shown to react more selectively 6-position hydroxyl groups<sup>64</sup>. The most acidic 2-position hydroxyl groups have been found to be first deprotonated<sup>65</sup> that subsequently forms the oxyanion, which is more nucleophilic than the non-deprotonated 6-position hydroxyl groups (II in Figure 1.8). Proton transfer between the 2- and 6-positions hydroxyl groups lead to mixture of 2- as well as 6-position modified cyclodextrin derivatives.

The complex formation property of the cyclodextrin has been found to affect the modification of the hydroxyl groups (III in Figure 1.8) thus if the electrophilic reagents forms a complex with the cyclodextrin then the predominant product formed is dictated by the orientation of the reagent within the complex. On the other hand, if the complex is weak, then the product formation is directed by the reactive nucleophilicities of the hydroxyl groups. Solvents also play an important role in the orientation of the electrophilic agent in the cyclodextrin cavity. Tosyl chloride reacts with  $\alpha$ -cyclodextrin in pyridine to give 6-tosylated product, where as it gives the 2-tosylated product in an aqueous base<sup>66</sup>. The cavity size of the cyclodextrin also affects the strength and orientation of the complex and so affects the product of the reaction. Tosyl chloride reacts with  $\alpha$ -cyclodextrin to give the 2-positional substituted product; whereas  $\beta$ -cyclodextrin, gives the 6-positional substituted product<sup>67</sup>.

The method of protection and deprotection of the hydroxyl group is to overcome the complications arising due to the binding of reagent into the cavity of cyclodextrin. Thus, if 2-position of cyclodextrin is first protected, then the incoming electrophile selectively reacts with the 6-position hydroxyl group (IV in Figure 1.8). Takeo *et al* carried out permethylation of the primary side of the cyclodextrin by first protecting the secondary side by esterification<sup>64</sup>. The primary side is then reacted with alkyl halides. Similarly, protection of the primary side leads to the electrophile reacting with the hydroxyl group at the 2-position (V in Figure 1.8)<sup>68</sup>. Among the protecting groups *ter*-butyldimethylsilyl chloride (TBDMS) has been found to be easy to attach and easy to remove<sup>69</sup>. Fujita *et al* first reported the 3-position substituted  $\beta$ -cyclodextrin by the reaction of naphthalenesulfonyl chloride with  $\beta$ -cyclodextrin<sup>70,71</sup>. After that Tian *et al* demonstrated in the reaction of the electrophile *N*-methyl-4-(chloromethyl)-2-nitroaniline with 6-protected  $\beta$ -cyclodextrin which directed the electrophile to the 3-position instead of the expected 2-position<sup>72</sup>. In these reactions the complex formation has occurred with the primary hydroxyl group protected CD derivative due to the presence of a weak base after the orientation of reactive group towards the less nucleophilic hydroxyl group at the 3-position than the 2-position. Figure 1.9 shows the possible positional isomers of mono, di and tri-modified  $\alpha$ -CD and  $\beta$ -CD.

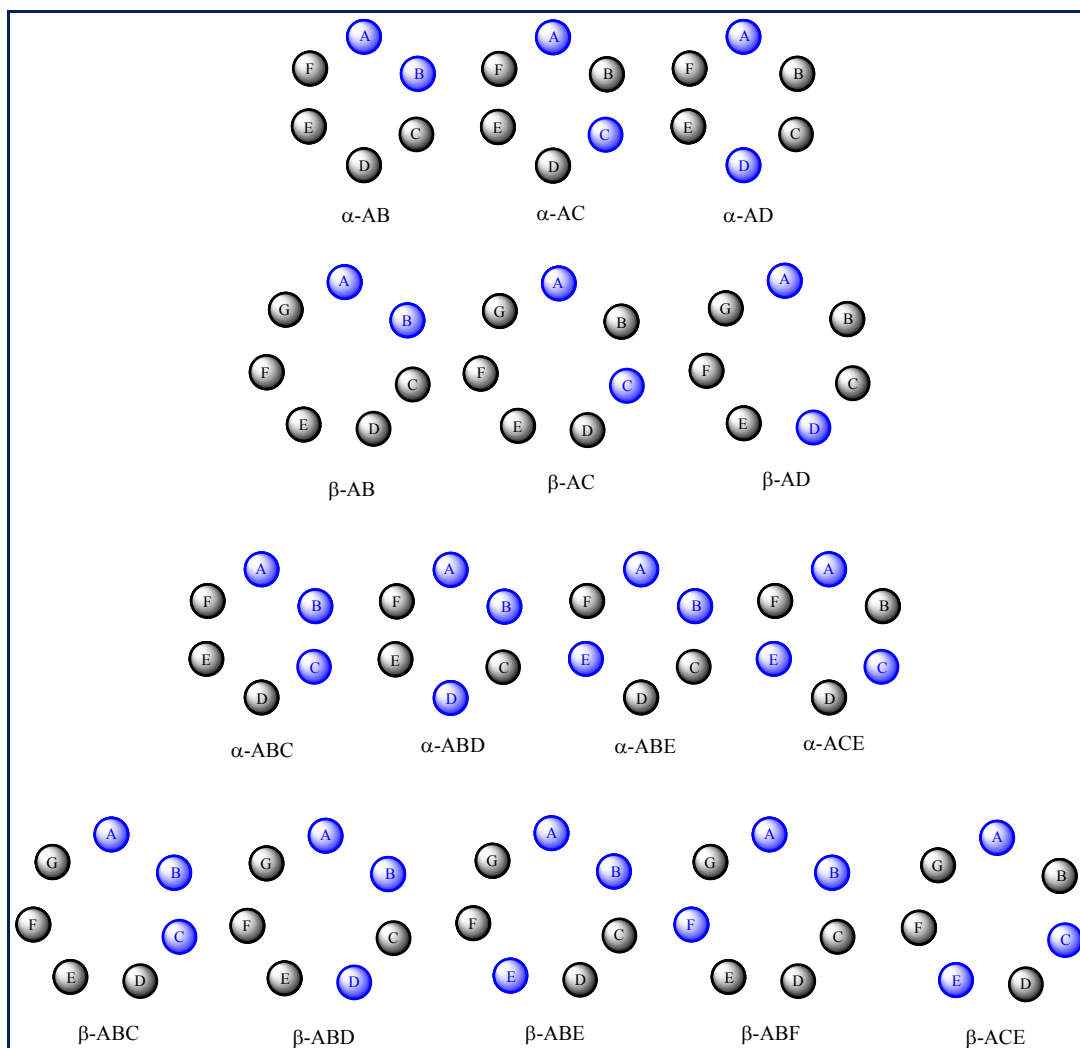


**Figure 1.9** Possible positional isomers of mono, di and tri-modified  $\alpha$ -CD and  $\beta$ -CD.

### 1.10 Mono-, di- and tri-substituted Cyclodextrins

Many of the cyclodextrin derivatives reported in literature are the complex mixture of compounds that contains number of positional isomers. The number of possible positions for a substituent is given by the number of possible positions at a glucose unit (2, 3 and 6) multiplied by the number of different glucose units A, B, C...in the cyclodextrins. These are shown in Figure 1.9. Thus mono-, di-, tri- and permodifications refers to modification at one, two, three or all hydroxyl groups at one site that is either the 2-, 3- or 6-positions of cyclodextrins<sup>58</sup>.

The possible positional isomers of di and tri substituted  $\alpha$ -cyclodextrin and  $\beta$ -cyclodextrin are shown in Figure 1.9. Disubstitution of  $\alpha$ -CD and  $\beta$ -CD at one site

(either 2- or 3- or -6) can give 3 positional isomers. However trisubstitution at one site (either 2- or 3- or -6) can give 4 positional isomers for  $\alpha$ -CD and 5 positional isomers in the case of  $\beta$ -CD.

The most popular common method for the monomodification at 6-position of cyclodextrin is by nucleophilic attack of a reagent containing appropriate group on mono-6-tosyl cyclodextrin. The monotosylated cyclodextrin derivatives are synthesized by reacting 1 equivalent of benzene or p-toluene-sulfonyl chloride with cyclodextrin in pyridine or DMF containing a base<sup>73-75</sup>. The monosubstituted 6-tosylcyclodextrins are important precursors for a variety of modified cyclodextrins. A nucleophilic displacement of the tosyl group by suitable nucleophiles such as iodide, azide, thioacetate, hydroxylamine, alkyl, or poly-(alkylamines) gives monoiodo-, azido-, thio-, (hydroxylamino)-, or (alkylamino)-cyclodextrins<sup>76-80</sup>.

Disubstituted cyclodextrins are obtained most easily by bridging the two primary hydroxyl groups of cyclodextrin molecule with difunctional reagent. In this method, disubstituted sulfonates of cyclodextrins are synthesized by reaction of arenedisulfonyl chlorides with cyclodextrin to give AB, AC and AD isomers<sup>81-83</sup>. Though disulfonyl chlorides give a mixture of regioisomers, they show distinct regiospecificity based on their geometrical structures. Trans-stilbene and biphenyl based capping reagents have been used to give AD isomers, benzophenone-based reagents to give AC isomers and 1,3-benzenedisulfonyl chlorides gives the AB isomers<sup>84-86</sup>. The other bulky sulfonyl chloride also used for the selective modification of cyclodextrins resulted in very low yield after HPLC purifications<sup>87-88</sup>. Figure 1.10 gives a schematic representation of the mono-, di-, and tri-substituted cyclodextrin using different strategies.

The synthesis and isolation of the trisubstituted cyclodextrin is very difficult because of the large number of possible positional isomers. Tosylation of cyclodextrin leads to 6<sup>A</sup>,6<sup>C</sup>,6<sup>E</sup>-tri-O-tosyl- $\beta$ -cyclodextrin with very low yield (2.6%)<sup>89,90</sup>. In contrast the tritylation of cyclodextrin in presence of enzyme gives 6<sup>A</sup>,6<sup>C</sup>,6<sup>E</sup>-trityl derivative in a reasonable yield of 43%<sup>91-92</sup>.

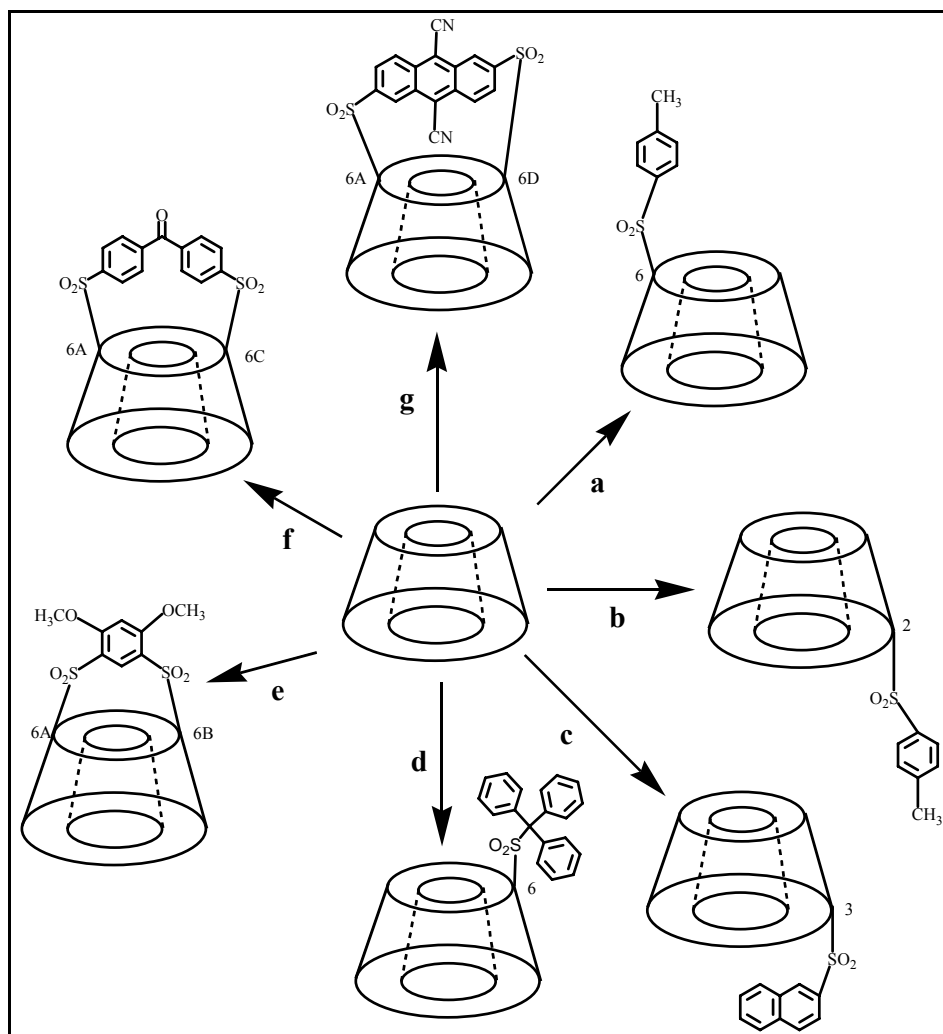


**Figure 1.10** Specific introductions of mono-, di- and tri- substituents to cyclodextrins.

*a) Ts/Pyridine, b) 3-nitrophenyltosylate/DMF/H<sub>2</sub>O (pH 10), c) NsCl/MeCN/H<sub>2</sub>O (pH 12), d) TritCl/Pyridine, e) 4,6-dimethoxy-benzene-1,3-sulfonyl chloride/Pyridine, f) Benzophenone-disulfonyl chloride and g) Bis(9,10-dicyano-anthracene-2,6-sulfonyl chloride)/Pyridine.*

### 1.11 Cyclodextrin Polymers

In recent years attention has been expanding from supramolecular chemistry of cyclodextrins to supramolecular chemistry of cyclodextrin based polymers owing to more sophisticated structures and advanced function have been achieved by the formation of supramolecular cyclodextrin polymers<sup>93</sup>. Compounds consisting of a number of covalent linked cyclodextrin rings are called cyclodextrin polymers. The

cyclodextrin fixed into polymeric structures behave differently from their monomeric derivatives<sup>94-97</sup>.

Cyclodextrin polymers can be classified into the following types. These are shown schematically in Figure 1.11.

- (a) Linear polymers
- (b) Cross-linked polymers
- (c) CDs immobilized by covalent bond to macromolecular support
- (d) CDs immobilized by physical bonding in/to macromolecular support
- (e) Necklace Type CD polymers (Polyrotaxanes)

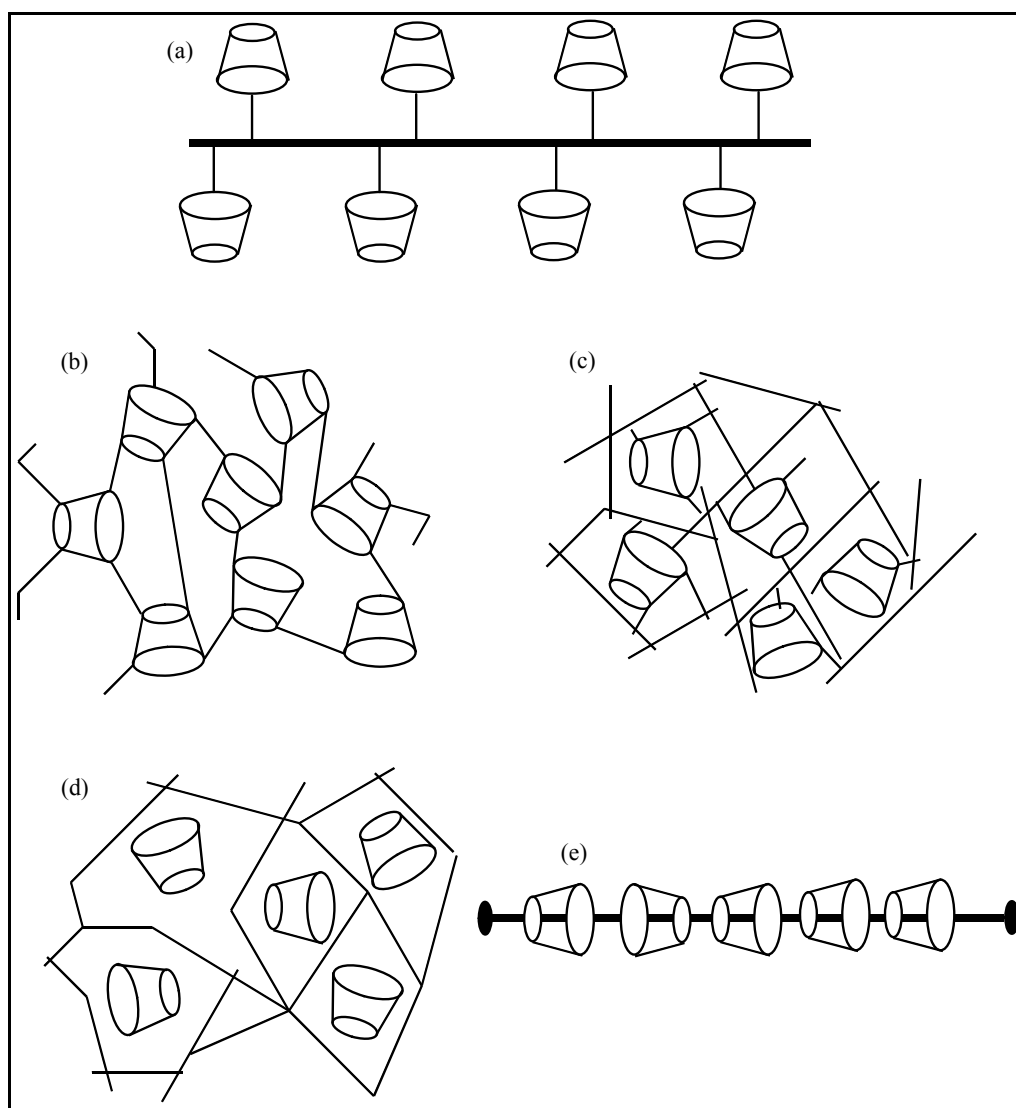


**Figure 1.11** Structural classifications of cyclodextrin polymers.

### (a) Linear polymers

Linear polymers containing CD residues on the side chain were synthesized by two methods such as addition polymerization and condensation polymerization. In the addition polymerization, the first step was the preparation of allyl group containing monomer, for example, acryloyl and methacryloyl cyclodextrins were obtained by reacting acryloyl nitrophenol with cyclodextrin<sup>98,99</sup>. The monomers were also copolymerized with other water-soluble monomers, such as acrylamide, acrylic acid and vinyl pyrrolidone. Linear or cross-linked structures were obtained based on the functionality of the comonomer. A typical synthesis of such polymers is shown in Figure 1.12.

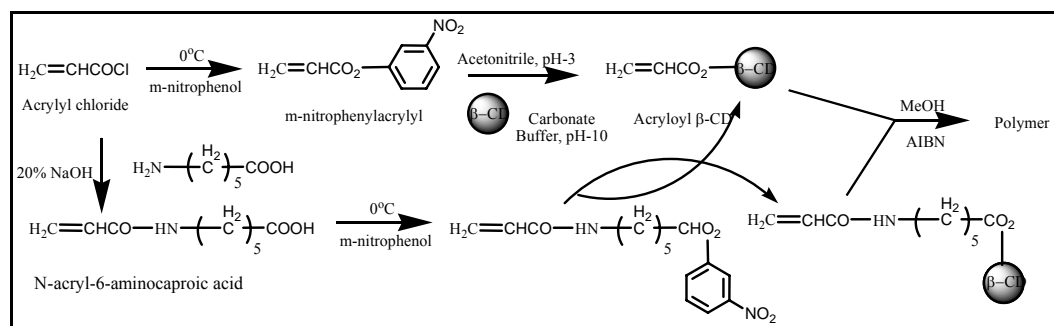


**Figure 1.12** Synthetic scheme of linear pendent-cyclodextrin polymer.

In a patent assigned to addition polymerizable monomers were by modifying monotosyl  $\beta$ -cyclodextrin into monomethylol cyclodextrin and vinylamine  $\beta$ -cyclodextrin which could be polymerized to give linear cyclodextrin based polymers. Similarly, Yoshinaga *et al* and Crini *et al* synthesized the functional  $\beta$ -cyclodextrin to get  $\beta$ -cyclodextrin based polymers<sup>100-101</sup>.

In the condensation polymerization, cyclodextrin was coupled with the presynthesized polymers by using the two different functionalities and coupling agent. Cyclodextrin was attached with polyallylamine<sup>102</sup> and caboxy methylated chitosan<sup>103</sup> using DMAO and EDC as coupling agents. A typical synthesis of such polymers is shown in Figure 1.13.

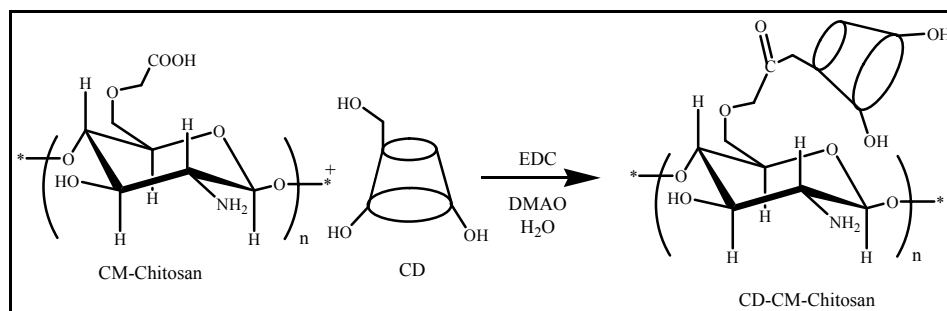


**Figure 1.13** Synthetic scheme of CD-CM-Chitosan polymer.

Covalent bonded cyclodextrin as pendent-chain polymers by condensation polymerization using tosylated  $\beta$ -CD and polyallylamine as monomers has been also reported<sup>104-106</sup>. In another variation of synthesizing polymers containing cyclodextrin as pendent group,  $\beta$ -cyclodextrin was grafted on to poly(methyl vinyl ether)-co-maleic anhydride where the monoalkoxide of  $\beta$ -cyclodextrin was prepared and then attached to the maleic anhydride site of the copolymer thus giving a polymers with pendent  $\beta$ -CD<sup>107</sup>. This is schematically shown in Figure 1.14.

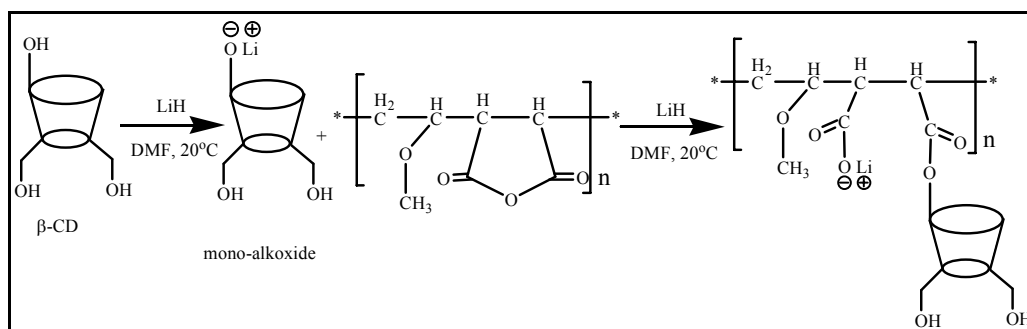


**Figure 1.14** Synthesis of novel linear water-soluble polymer.

A class of linear polymers that contains  $\beta$ -CD as part of the backbone was synthesized by Davis *et al*<sup>108-109</sup>. The key step in preparing this type of backbone containing polymer was the synthesis of difunctionalized  $\beta$ -CD-containing monomers. The synthesized difunctional monomers connect with therapeutic agents in a linear structure. Figure 1.15 illustrates the strategy of preparing either cationic or anionic polymers starting from difunctional  $\beta$ -CD-monomers.

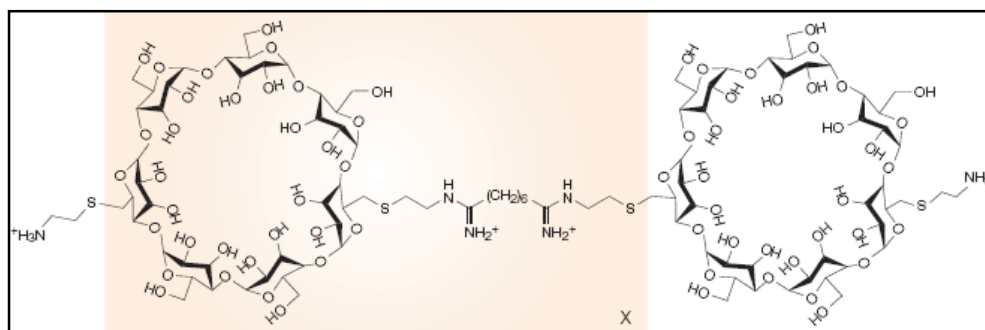


**Figure 1.15** Synthesis of linear cationic cyclodextrin main-chain polymer.

Linear cyclodextrin containing polymers have also been obtained by non-covalent interaction where the cyclodextrin units are not linked by any covalent bond. 6-deoxy-(6-*t*-butyl)- $\beta$ -cyclodextrin based polymers were synthesized where the *t*-butyl group of one is included into the cavity of the other monosubstituted cyclodextrins<sup>110</sup>. Similarly, 2-hydroxypropyl  $\beta$ -cyclodextrin has been prepared where the 2-hydroxypropyl  $\beta$ -cyclodextrin is included into the cyclodextrin nanocavity of the next molecule and helically extended polymeric structure is formed by repetition of the intermolecular inclusion<sup>111</sup>.

Masahiko *et al*<sup>112</sup> synthesized the supramolecular polymeric structure by preparing cinnamide functionality among on  $\alpha$ -CD at 6-position or 3-position. The cinnamide group was included into the nanocavity of cyclodextrin. This is depicted in Figure 1.16.

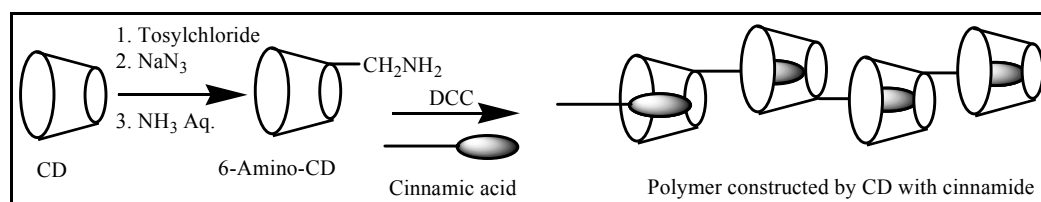


**Figure 1.16** Synthesis of supramolecular polymers constructed by cyclodextrins with cinnamide.

Iwata *et al*<sup>113</sup> attach the  $\beta$ -cyclodextrin on copolymers of glycidyl methacrylate and ethylene glycol methacrylate or via linking with the *N, N'*-carbonyldiimidazole.

## (b) Cross-linked polymers

Cross-linked polymers have been synthesized by reaction of cyclodextrins and cross-linking agents containing bi- or polyfunctional groups. Effective crosslinking agents that have been reported are: epichlorohydrin<sup>114-116</sup>, diisocyanates<sup>117</sup>, polycarboxylic acids<sup>118</sup>, anhydrides<sup>119</sup>, diepoxides<sup>120</sup> etc. These crosslinking nucleophilic substitution reactions with crosslinking agent usually occur in the alkaline medium. The water-solubility and molecular weight of the obtained polymers generally depends on the concentration of the crosslinking agent, pH of the reaction mixture and temperature of the reaction. Renard *et al*<sup>121</sup> have investigated the relation between preparation conditions and water-solubility of the cyclodextrin polymers. Usually, lower molar ratio of crosslinking agent gives water-soluble polymers whereas higher molar ratio of crosslinking agent gives water-insoluble polymers. Figure 1.17 shows the typical synthesis of cyclodextrin and epichlorohydrin cross-linked polymers.

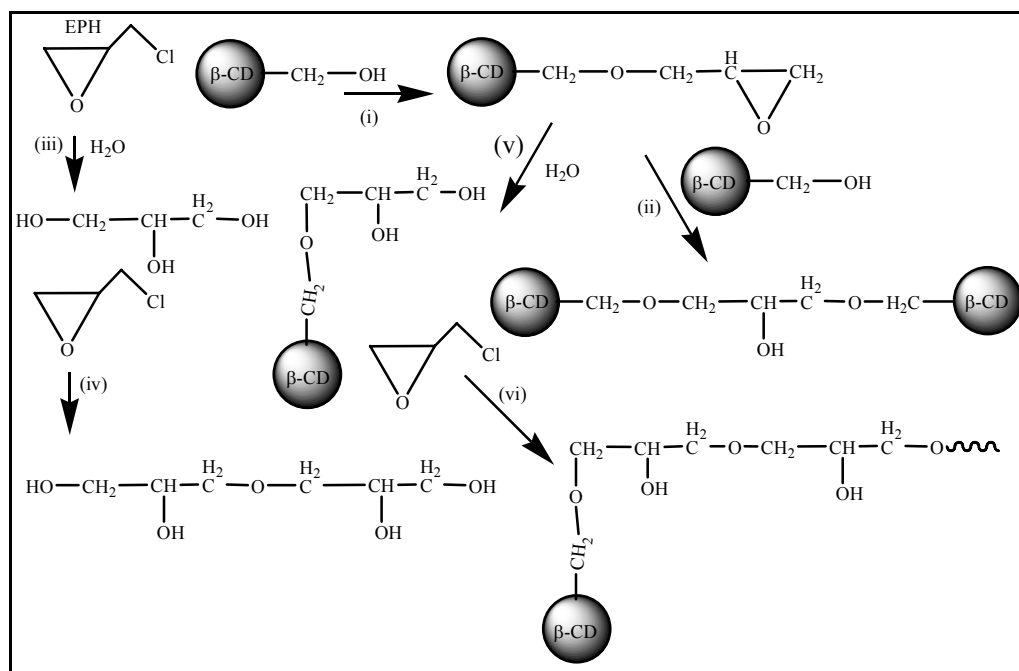


**Figure 1.17** Synthesis of  $\beta$ -cyclodextrin-epichlorohydrin polymer.

Thatiparti *et al*<sup>122</sup> synthesized cyclodextrin and diisocyanate crosslinked hydrogels by simple reaction of  $\beta$ -cyclodextrin with hexamethylene diisocyanate in dry DMF. This hydrogel was used for antibiotic delivery. Similarly, Bhaskar *et al*<sup>123</sup>

synthesized water-insoluble polyurethane using  $\beta$ -cyclodextrin and hexamethylene diisocyanate which was used as a column material for the extraction of aromatic amines from water. Figure 1.18 depicted the synthesis of cross-linked cyclodextrin and hexamethylene diisocyanate polymers.

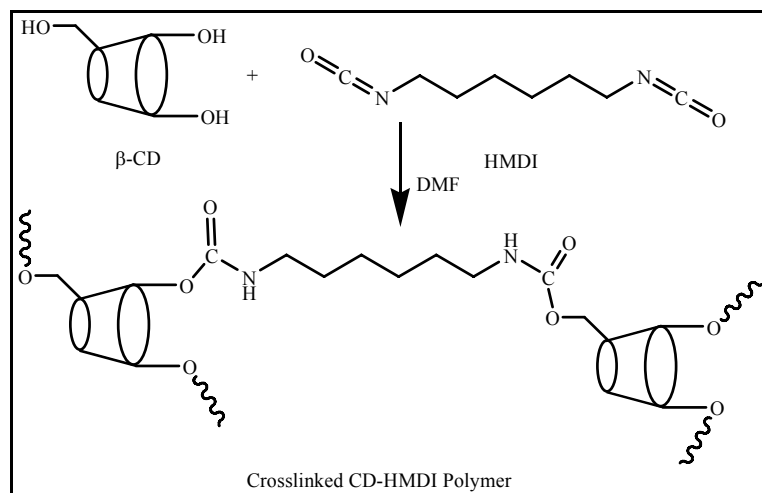


**Figure 1.18** Synthesis of  $\beta$ -cyclodextrin-hexamethylene diisocyanate polymer.

**(c) CDs immobilized by covalent bond to macromolecular support**

These types of polymers can be achieved by immobilization of cyclodextrins on polymer support by coupling agent. For example,  $\beta$ -cyclodextrin can be fixed on copolymers of glycidyl methacrylate and ethylene glycol methacrylate via linking with *N,N'*-carbonyldiimidazole<sup>124</sup> resulting in a polymer with 30% cyclodextrin content. Similarly, cyclodextrin has been immobilized on chlorinated silica gel<sup>125</sup>, polystyrene<sup>126</sup>, polyurethane<sup>127</sup>, polysiloxane<sup>128</sup> etc.

**(d) CDs immobilized by physical bonding in/to macromolecular support**

Polymeric products with immobilized cyclodextrins bound physically to the macromolecular support belong to this group as shown in Figure 1.19. In this type 'empty' cyclodextrins are incorporated into a polymer by simply blending with a solution of the macromolecular support and subsequent evaporation of the solvent<sup>129</sup>.

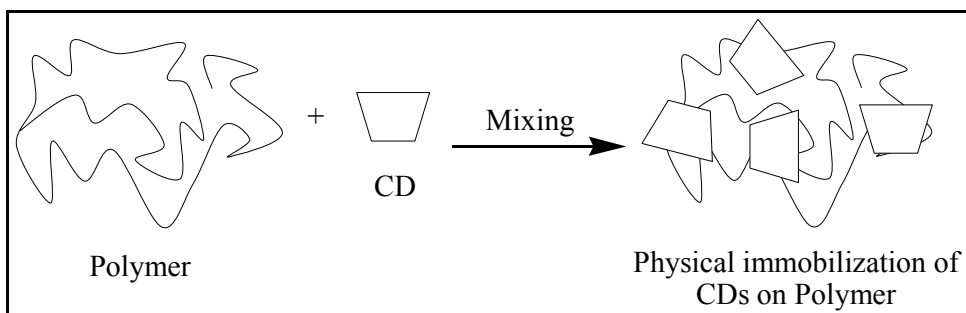


**Figure 1.19** Physical immobilization of CDs on polymer by physical mixing.

### (e) Necklace Type CD polymers (Polyrotaxanes)

The necklace type cyclodextrin polymers are mainly polyrotaxanes where cyclodextrin rings are strung on a polymer chain. Polyrotaxanes containing cyclodextrin can be synthesized by first threading many cyclodextrins on a polymer chain and then blocking the ends of the polymer chain with bulky groups<sup>130</sup>. Different types of polyrotaxanes are obtained, when a polymer with reactive groups in the main-chain is threaded by cyclodextrins<sup>131-133</sup>. These polyrotaxanes cyclodextrins polymers have been shown to remarkable structures<sup>134-136</sup>. Figure 1.20 shows the synthesis of polyrotaxane.

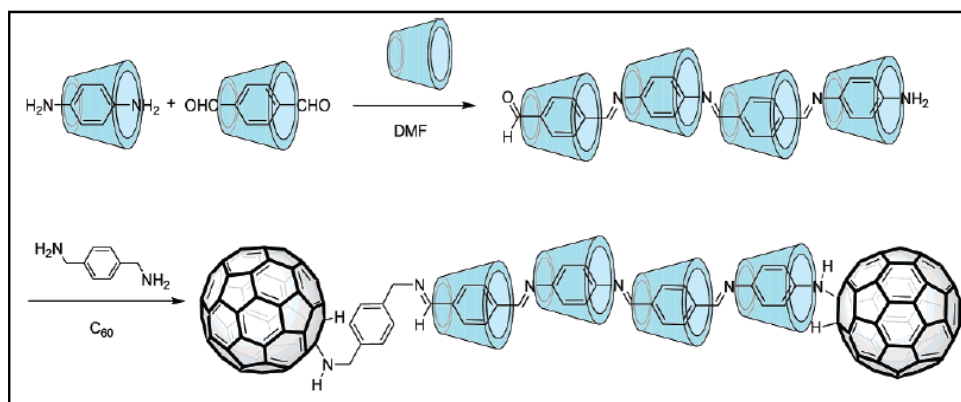


**Figure 1.20** Synthesis of Necklace Type CD polymers (Polyrotaxane).

## 1.12 Applications of Cyclodextrins and Cyclodextrin Polymers

Cyclodextrins are able to form host-guest complexes with wide range of molecules given the unique nature imparted by their structure. As a result, these molecules have found tremendous applications in a wide range of fields.

The major and potential application of cyclodextrin has been in drug delivery. Cyclodextrins act as drug delivery vehicle because of their ability to alter the physical, chemical and biological properties of the guest molecules through formation of inclusion complexes<sup>137</sup>. Various types of cyclodextrin derivatives and cyclodextrin polymers have been utilized for the effective drug delivery system<sup>138</sup>. Among the hydrophilic derivatives of cyclodextrin the hydroxylpropyl-CD<sup>139</sup> and methylated-CD<sup>140</sup> have been widely used for the solubilization of hydrophobic drugs in aqueous medium. Apart from the increasing the water-solubility of the natural cyclodextrin increasing the degree of substitution (methylation) decreases the hydrophilic nature of the parent cyclodextrin. This hydrophobic cyclodextrins have the ability to decrease the water-solubility of the guest molecules, thus having potential to be used as sustained-release drug carrier of water-soluble drugs and peptides<sup>141</sup>. The anionic cyclodextrins can modify the release rate of a drug depending on the pH of the medium and thus bind to the surface membrane of cells, for selective delivery of the drug across biological barriers<sup>142</sup>. The biocompatibility and multi-functional characteristics of cyclodextrins have been used to deliver the drugs in various routes of administration like oral, rectal, nasal, ocular, transdermal and dermal systems<sup>143</sup>. However, the low aqueous solubility and nephrotoxicity of specially  $\beta$ -cyclodextrin limits its use especially in parenteral route of drug delivery<sup>144</sup>.

Recently in the novel drug carrier systems, the cyclodextrin based polymers have been shown effective advances in drug delivery application owing to their improved water-solubility, biocompatibility and higher inclusion ability as compared to the parent cyclodextrins<sup>145,146</sup>. A number of reports are available in literature where cyclodextrin based polymers have been used for steroid<sup>147</sup>, anti-inflammatory<sup>148</sup>, insulin<sup>149</sup>, and anti-cancer drug formulations<sup>150</sup>. Cyclodextrin polymers have a wide range of potential applications, including the controlled release of a soluble substance across membrane<sup>151</sup>. Several groups have reported the synthesis of cyclodextrin based polymers using different techniques and their use for the drug delivery application<sup>152-</sup>  
156

The most common used approach to study inclusion complexation of guest molecules is the phase solubility (Figure 1.21) method described by Higuchi and Connors<sup>157</sup>, which examines the effect of a solubilizer, i.e. CD on the guest being

solubilized, i.e. drug. The phase solubility diagrams are categorized into A and B types; A type curves indicate the soluble inclusion complexes while B type suggest the formation of soluble inclusion complexes with poor solubility. A B<sub>S</sub> type response denotes complexes of limited solubility and a B<sub>I</sub> curve indicates insoluble complexes. A-type curves are subdivided into A<sub>L</sub> (linear increase of drug solubility as a function of CD concentration), A<sub>P</sub> (positive deviating isotherms), and A<sub>N</sub> (negative deviating isotherms) subtypes. β- CD often gives rise to B-type curves due to the poor water-solubility whereas the chemically modified CDs like HP-β-CD, SEB-β-CD and β-CD polymers usually produce soluble complexes and thus give A-type curves. S<sub>0</sub>, S<sub>t</sub> and S<sub>c</sub> indicate the intrinsic solubility, total molar solubility and decrease solubility of the guest, respectively.

In case of a 1:1 inclusion complex, depending on phase solubility diagram the equilibrium binding or association constant *K*, was determined by using following equation.

$$K = \frac{\text{Slope}}{S_0 (1 - \text{slope})} \quad (1.6)$$

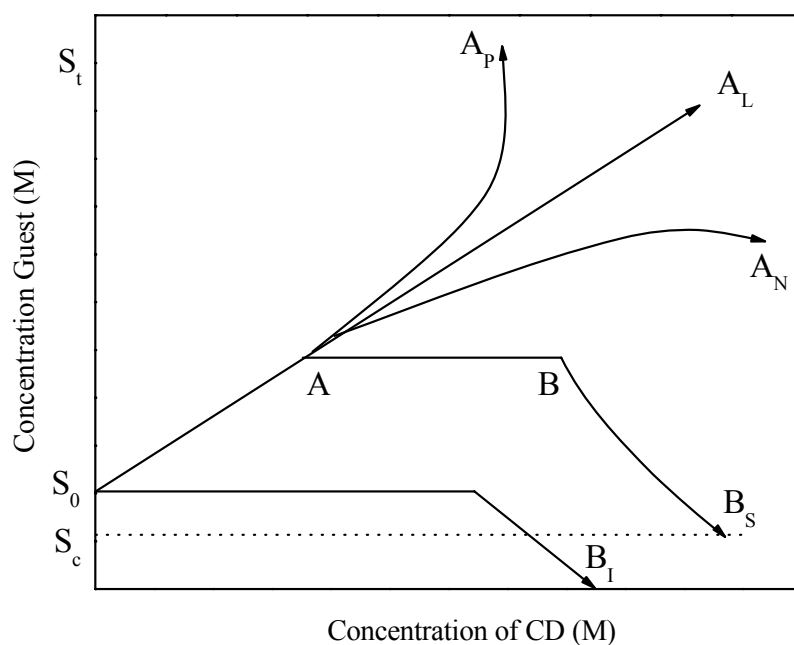


**Figure 1.21** Theoretical phase-solubility diagram.

The practical analytical applications of cyclodextrins and cyclodextrin based polymers shows the advantages of stationary phases in GC when they are used for the separation of structurally related compounds and positional and material isomers<sup>158,159</sup>. The inclusion complex formation, as a new principal of molecular interaction used in GC, has shown the advantages resulting from the high selectivity. The main achievement was the introduction of CDs and their derivatives as chiral stationary phase in capillary GC<sup>160</sup>. However, there is limitation of use to volatile compounds and substances that can be vaporized without decomposition. The great choice and variety of CDs derivatives allows separation of almost any kind of chiral compounds from apolar to highly polar compounds<sup>161-163</sup>. The field of applications ranges from stereochemical analysis of natural compounds including essential oils, flavors and fragrances, pheromones, drugs, agrochemicals, etc<sup>164,165</sup>.

Apart from these applications cyclodextrin and cyclodextrin based polymers have applications in modern textiles<sup>166</sup>, agrochemicals<sup>167</sup>, food<sup>168</sup>, cell biology<sup>169</sup>, environmental remedation<sup>170</sup>, catalysis<sup>171</sup>, pesticides<sup>172</sup>, cosmetics and toiletries<sup>173</sup> etc. Figure 1.22 shows the trends of cyclodextrins science and technology in last 5 decades in different field of chemistry.

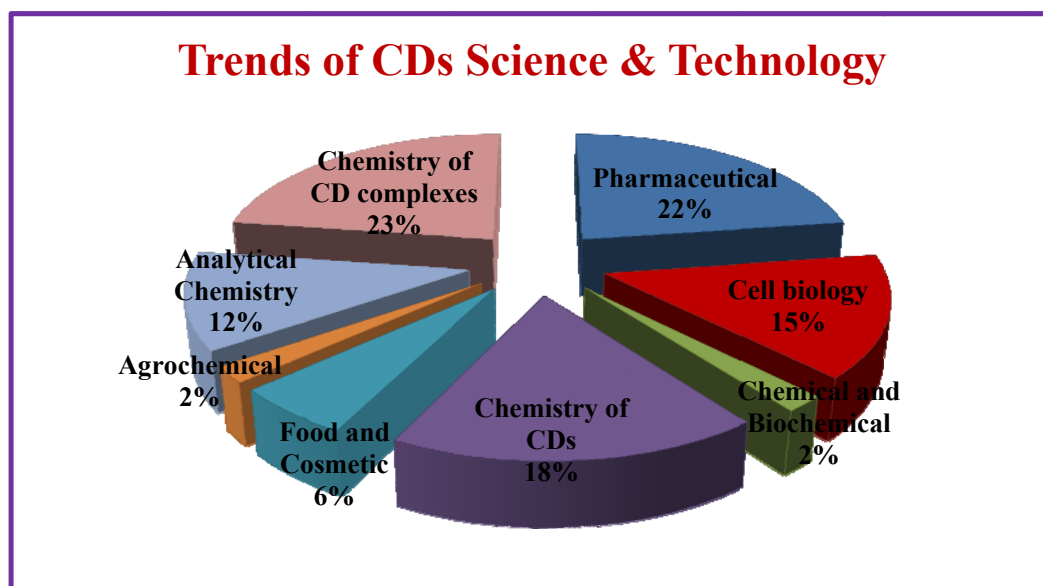


**Figure 1.22** Trends of cyclodextrins science and technology.

### 1.13 Aim of the Thesis

Although three most common cyclodextrins ( $\alpha$ -CD,  $\beta$ -CD and  $\gamma$ -CD consisting six, seven and eight D-glucopyranose units, respectively) is available commercially. Among these three cyclodextrins,  $\beta$ -cyclodextrin is cheapest and most widely used in material and pharmaceutical science as its cavity size is compatible with wide variety of molecules. The presence of similar functionality and comparatively low aqueous solubility of the  $\beta$ -CD as compared to other cyclodextrins limits its applications and also the cytotoxicity of  $\beta$ -CD alters the permeability properties of the cell membranes. Thus, aim of the thesis is to enhance the reactivity and aqueous solubility of parent  $\beta$ -cyclodextrin by selective functionalization of primary hydroxyl groups of  $\beta$ -cyclodextrin for the polymerization reaction and simultaneously use these enhanced reactivity and solubility of  $\beta$ -CD to enhance the aqueous solubility of two carbon allotropes (fullerenes and carbon nanotubes), fluorescence properties of pyrene and aqueous solubility of hydrophobic antiepileptic drug carbamazepine.

Carbon allotrope such as fullerenes and carbon nanotubes, which has a  $\pi$ -electron system, shows interesting magnetic, superconductivity, electrical and biochemical properties. It is not surprising that carbon allotropes and their derivatives have attracted a lot of attention in recent years and have been successfully applied to materials science and biological technology. However, the biomedical applications of carbon allotropes and their derivatives are limited, owing to their low solubility in water and other frequently used solvents. In recent research several approaches have been explored for the preparation of water-soluble fullerenes and carbon nanotubes. Cyclodextrins has been frequently used for the solubilization of carbon allotropes as it has unique molecular recognition and self-assembling behavior in aqueous solution. In literature, investigation on molecular recognition between cyclodextrins and carbon allotropes has been centered only on non-covalent supramolecular inclusion complexes and well documented.

However, a competitive guest molecule in a biological media can displace encapsulated guest molecule from the cyclodextrin cavity. Therefore, our secondary aim of the thesis is to covalently functionalize two carbon allotropes (fullerenes and carbon allotropes) by selectively modified  $\beta$ -cyclodextrin derivatives for the aqueous solubilization.

**Based on the above intensions aim of the thesis divided as below.**

First aim of the thesis is to improve water-solubility of cheapest  $\beta$ -cyclodextrin and toxicity as compared parent  $\beta$ -CD,  $\alpha$ -CD and  $\gamma$ -CD. To achieve this aim, the objective is to prepare  $\beta$ -cyclodextrin based highly water-soluble derivatives (monomers) and prepare linear  $\beta$ -cyclodextrin polymers consisting  $\beta$ -cyclodextrin as a part of the main-chain of polymers.

Utilize the selectively modified CDs derivatives to prepare linear main-chain  $\beta$ -CD based polymers by using short linker between two CDs.

Utilize these modified  $\beta$ -CD based derivatives and linear main-chain polymers to improve water-solubility of hydrophobic poorly water-soluble drug carbamazepine, enhance fluorescence properties of pyrene and aqueous solubilization of completely water-insoluble carbon allotropes Fullerenes and carbon nanotubes.

## References

1. A. Villiers, *Rend. Acad. Sci.*, **1891**, 112, 536-538.
2. F. Schardinger, *Wien. klin. Wochschr.*, **1904**, 17, 207.
3. F. Schardinger, *Parasitenkd. Abt. II* 29, **1911**, 188-197.
4. K. Freudenberg and R. Jacobi, *Ann. Chem.*, **1935**, 518, 102-108.
5. K. Freudenberg and M. Meyer-Delius, *Ber. Chem.*, **1938**, 71, 1596-1600.
6. F. Cramer, *Chem. Ber.*, **1951**, 84, 851.
7. K. Freudenberg, F. Cramer and H. Plieninger, *Germany, Patent No. 895,769*, 5 November **1953**.
8. D. French, *Adv. Carbohydr. Chem.*, **1957**, 12, 189-260.
9. D. French, A. O. Pulley, J. A. Effenberger, M. A. Rougvie and M. Abdullah, *Arch. Biochem. Biophys.*, **1965**, 111, 153-160.
10. A. O. Pulley and D. French, *Biochem. Biophys. Res. Commun.*, **1961**, 5, 11.
11. D. French and R. E. Rundle, *J. Am. Chem. Soc.*, **1942**, 64, 1651-1653.
12. H. Ueda, *J. Incl. Phenom. Macrocycl. Chem.*, **2002**, 44, 53-56.
13. K. Koizumi, T. Utamura, M. Sota, and Y. Yagi, *Carbohydr. Res.*, **1986**, 153, 55.
14. P. R. Sundarajan and V. S. R. Rao, *Carbohydr. Res.*, **1970**, 13, 351.
15. F. V. Lichtenthaler and S. Immel, *Tetrahedron: Asymmetry*, **1994**, 5, 2045.
16. J. Szejtli, *Cyclodextrin and their inclusion complexes*, Akademiai Kiado, Budapest, **1982**.
17. B. Gillet, D. J. Nicole and J. J. Delpuech, *Tetrahedron Lett.*, **1982**, 23, 65.
18. D. A. Rees, *J. Chem. Soc. (B)*, **1970**, 877.
19. B. P. Schonberger, A. C. A. Jansen and L. H. M. Janssen, in 'Proceedings of the 4<sup>th</sup> International Symposium on Cyclodextrins, Munich, 1988', eds. O. Huber and J. Szejtli, Kluwer, Dordrecht, **1988**, p. 61.
20. B. Casu, G. G. Gallo, M. Reggiani and A. Vigevani, *J. Chem. Soc. Spec. publ.*, **1968**, 23, 217
21. J. L. Atwood, J. E. D. Davies, D. D. Macnicol and F. Vogtle, *Comprehensive Supramolecular Chemistry*, Volume 3 (Cyclodextrin); 1<sup>st</sup> edn; J. Szejtli and T. Osa, Eds.; Elsevier Science Ltd: New York, **1996**.
22. H. S. Choi, *J. Korean Chem. Soc.*, **1992**, 36, 324. (*Chem. Abstr.* **1992**, 116, 236011)

23. D. French, M. L. Lewine, J. H. Pazur and E. Norberg, *J. Am. Chem. Soc.*, **1949**, 71, 353.
24. K. Harata, C. T. Rao and J. Pitha, *J. Carbohydr. Res.*, **1993**, 83, 247.
25. J. Szejtli, *J. Incl. Phenom. Mol. Recogn. Chem.*, **1992**, 14, 25.
26. M. J. Jozwiakowski and K. A. Connors, *J. Carbohydr. Res.*, **1985**, 143, 51.
27. W. Linert, P. Margl and F. Renz, *Chem. Phys.*, **1992**, 162, 327.
28. A. K. Chatijigaski, C. Donze, A. W. Coleman and P. Cardot, *Anal. Chem.*, **1992**, 64, 1632
29. M. Taghvaei and G. H. Stewart, *Anal. Chem.*, **1991**, 63, 1902.
30. K. Flohr, R. N. Paton and E. T. Kaiser, *J. Am. Soc.*, **1975**, 97, 1209
31. K. Miyajima, M. Sawada and M. Nakagaki, *Bull. Chem. Soc. Jpn.*, **1993**, 56, 3556.
32. K. Myrback and T. Jarnestrom, *Ark. Kemi*, **1949**, 1, 129.
33. I. Jodal, L. Kandra, J. Harangi, P. Nanasi and J. Szejtli, *Starch*, **1984**, 36, 140.
34. L. Yu and C. You, *J. Phys. Org. Chem.*, **2001**, 14(1), 11.
35. I. Kim, S. Park and H. Kim, *J. Chromatogr.*, **2000**, A 877(1&2), 217.
36. J. Bergamini, M. Belabbas, M. Jouini, S. Aeiyaach, J. Lacroix, K. Chane-Ching and P. Lacaze, *J. Electroanal. Chem.*, **2000**, 482(2), 156.
37. W. Herrmann, S. Wehrle and G. Wenz, *Chem. Commun.*, **1997**, 18, 1709.
38. F. Cramer, 'Einschlussverbindungen' Springer Berlin, **1954**
39. B. V. Muller and E. Albers, *J. Pharm. Sci.*, **1991**, 80, 599-604.
40. M. Suzuki, M. Kajtir, J. Szejtli, M. Vikman, E. Fenyvesi and L. Szente, *Carbohydr. Res.*, **1991**, 214, 25-33.
41. J. H. Park, M. D. Jang and M. J. Sain, *J. Chromatogr.*, **1992**, 595, 45-52.
42. G. Castronuovo, V. Elia, D. Fessas, A. Giordano and F. Velleca, *Carbohydr. Res.*, **1995**, 272, 31-40.
43. Y. L. Loukas, E. A. Vyza and A. V. Valiraki, *Analyst*, **1995**, 120, 333-338.
44. T. Cserhiti and E. Forgacs, *Anal. Biochem.*, **1997**, 246, 206-209.
45. K. A. Connors, *Chem. Rev.*, **1997**, 97, 1325-1358.
46. S. Kitahata, S. Okada and T. Fukuji, *Agric. Biol. Chem.*, **1978**, 42, 2369
47. M. Yamamoto and K. Horikoshi, *Starch*, **1981**, 33, 24.
48. H. Bender, *Carbohydr. Res.*, **1983**, 124, 225.
49. D. W. Armstrong, *J. Liq. Chromatogr.*, **1980**, 3, 895-899.
50. A. Ueno and R. Breslow, *Tetrahedron Lett.*, **1982**, 23, 3451.

51. P. B. Weisz, M. M. Joullie, C. M. Hunter, K. M. Kumor, Z. Zhang, E. Levine, E. Macarak, D. Weiner, and E. S. Barnathan, *Biochem. Pharm.*, **1997**, 54, 149.
52. J. Folk, P. B. Weisz, M. M. Joullie, W. W. Li and W. R. Ewing, *Science*, **1989**, 243, 1490.
53. D. W. Armstrong, *U.S. Pat.* 4539399, **1985** (*Chem. Abstr.* **1985**, 103, 226754).
54. B. Joshua, J. C. Richard and L. Jean-Marie, *Helvetica Chemica Acta.*, **1978**, 61, 2190.
55. F. M. Menger and M. A. Dulany, *Tetrahedron Lett.*, **1985**, 26, 267.
56. C. O Mellet, J. M. Bento, J. M. G. Fernandez, H. L. K. Chmurski, J. Defaye, M. L. O'Sullivan, and H. N. Carlo, *Chem. Eur. J.*, **1998**, 4, 2523.
57. J. Jindrich, J. Pitha, B. Lindberg, P. Suffer and K. Harata, *Carbohydr. Res.*, **1995**, 266, 75.
58. A. R. Khan, P. Forg, K. J. Stine and V. T. D'Souza, *Chem. Rev.*, **1998**, 1977-1996.
59. P. Fugedi and P. Nanasi, *Carbohydr. Res.*, **1988**, 175, 173.
60. K. Fujita, T. Ishizu, K. Oshiro, and K. Obe, *Bull. Chem. Soc. Jpn.*, **1989**, 62, 2960.
61. A. Hybl, R. E. Rundle, and D. E. William, *J. Am. Chem. Soc.*, **1965**, 87, 2779.
62. W. Saenger, M. Noltemeyer, P. C. Manor, B. Himgerty, B. Klar, *Bioorg. Chem.*, **1976**, 5, 187.
63. F. Cramer, G. Mackensen, and K. Kense, *Chem. Ber.*, **1969**, 102, 494.
64. K. Takeo, K. Uemura and H. Mitoh, *J. Carbohydr. Chem.*, **1988**, 7, 293.
65. D. Rong and V. T. D'Souza, *Tetrahedron Lett.*, **1990**, 31, 4275.
66. K. Fujita, S. Nagamura and T. Imoto, *Tetrahedron Lett.*, **1984**, 25, 5673.
67. K. Takahashi, K. Hattori and F. Toda, *Tetrahedron Lett.*, **1984**, 25, 3331.
68. J. H. Coates, C. J. Easton, S. F. Lincoln, S. J. Van Eyk, B. L. May, M. L. William, S. E. Brown, A. Lepore M. L. Liao, Y. Luo, V. Macolino, D. S. Schiesser, C. B. Whalland and I. S. C. McKenzie, *PCT Int. Apl.*, WO 9113100, **1991** (*Chem. Abstr.* **1992**, 117, 29142).
69. K. Takeo, H. Mitoh and K. Uemura, *Carbohydr. Res.*, **1989**, 187, 203.
70. K. Fujita, S. Nagamura, T. Imoto, T. Tahara and T. Koga, *J. Am. Chem. Soc.*, **1985**, 107, 3233.
71. K. Fujita, T. Tahara, T. Imoto and T. Koga *J. Am. Chem. Soc.*, **1986**, 108, 2030.
72. S. Tian, P. Forgo and V. T. D'Souza, *Tetrahedron Lett.*, **1996**, 37, 8309.

73. R. C. Petter, J. S. Salek, C. T. Sikorsky, G. Kumaravel and F. T. Lin, *J. Am. Chem. Soc.*, **1990**, 112, 3860.
74. X. M. Gao, L. H. Tong, Y. Inoue, and A. Tai, *Synth. Commun.*, **1995**, 25, 703.
75. K. A. Martin and A. W. Czarnik, *Tetrahedron Lett.*, **1994**, 35, 6781.
76. A. Ueno, F. Moriwaki, T. Osa, F. Hamada and K. Murai, *Tetrahedron*, **1987**, 43, 1571.
77. K. Tsujihara, H. Kurita and M. Kawazu, *Bull. Chem. Soc. Jpn.*, **1977**, 50, 1567.
78. D. W. Griffiths and M. L. Bender, *Adv. Catal.*, **1973**, 54, 625.
79. B. Siegel, *J. Inorg. Nucl. Chem.*, **1979**, 41, 609.
80. L. E. Fikes, D. T. Winn, R. W. Sweger, M. P. Johnson and A. W. Crarnik, *J. Am. Chem. Soc.*, **1992**, 114, 1493.
81. I. Tabushi, K. Shimkawa and K. Fujita, *Tetrahedron Lett.*, **1977**, 18, 1527.
82. I. Tabushi, Y. Kuroda, K. Yokota and L. C. Yuan, *J. Am. Chem. Soc.*, **1981**, 103, 711.
83. I. Tabushi, K. Shimokawa, N. Shimizu, H. Shirakata, and K. Fujita, *J. Am. Chem. Soc.*, **1976**, 98, 7855.
84. I. Tabushi, K. Yamamura and T. Nabeshima, *J. Am. Chem. Soc.*, **1984**, 106, 5267-5270.
85. G. Yi, J. S. Bradshaw, B. E. Rossiter, S. L. Rees, P. Petesson, K. E. Markides and M. L. Lee, *J. Org. Chem.*, **1993**, 58, 2561.
86. R. Breslow, J. W. Canary, M. Varney, S. T. Waddell, D. Yang, *J. Am. Chem. Soc.*, **1990**, 112, 5212.
87. A. M. Aquino, C. J. Abelt, K. L. Berger, C. M. Darragh, S. E. Kelley and M. V. Cossette, *J. Am. Chem. Soc.*, **1990**, 112, 5819.
88. M. F. Acquavella, M. F. Evans, S. W. Farrah, L. J. Nevoret and C. J. Abelt, *J. Org. Chem.*, **1994**, 59, 2894.
89. K. Fujita, T. Tahara and T. Koga, *Chem. Lett.*, **1989**, 821.
90. K. Fujita, T. Tahara, H. Yamamura, T. Imoto, T. Koga, T. Fujioka, K. Mihashi, K. *J. Org. Chem.*, **1990**, 55, 877.
91. J. Boger, D. G. Brenner and J. R. Knowles, *J. Am. Chem. Soc.*, **1979**, 101, 7630.
92. S. Cottaz and H. Driguez, *Chem. Commun.*, **1989**, 16, 1088.
93. W. H. Binder and R. Zirbs, *Adv. Polym. Sci.*, **2007**, 207, 1-78.
94. A. Harada, Y. Takashima and H. Yamaguchi, *Chem. Soc. Rev.*, **2009**, 38, 875-882.

95. G. Mocanu, D. Vizitiu and A. Carpov, *J. Bioact. Comp. Polym.*, **2001**, 16, 315-342.
96. S. Loethen, J. M. Kim and D. H. Thompson, *Polym. Rev.*, **2007**, 47, 383-418.
97. A. Harada, A. Hashidzume and Y. Takashima, *Adv. Polym. Sci.*, **2006**, 201, 1-43.
98. A. Harada, M. Furue and S. Nozakura, *Macromolecules*, **1976**, 9, 701.
99. M. Furue, A. Harada and S. Nozakura, *Polym. Lett. Ed.*, **1975**, 13, 357.
100. M. Yoshinaga, *Jpn. Kokai, Tokkyo Koho*, 04025503, **1992**, (*Chem. Abstr.* 116, 8168)
101. G. Crini, G. Torri, M. Guerrini, B. Martel Y. Leckhiri and M. Morcellet, *Eur. Polym. J.*, **1997**, 33, 1143.
102. A. Ruebner, G. L. Statto and M. R. James, *Macromol. Chem. Phys.*, **2000**, 201, 1185-1188.
103. A. Binello, B. Robaldo, A. Barge and R. Cavalli, G. Cravotto, *J. Appl. Polym. Sci.*, **2008**, 107, 2549-2557.
104. T. Seo, T. Kajihara and T. Iijima, *Macromol. Chem.*, **1987**, 188, 2071.
105. A. Ruebner, G. L. Statton and M. R. James, *Macromol. Chem. Phys.*, **2000**, 201, 1185.
106. P. Caliceti, S. Salmaso, A. Semenzato, T. Carofiglio, R. Fornasier, M. Fermeglia, M. Ferrone, and S. Pricl, *Biconjugate Chem.*, **2003**, 14, 899-908.
107. E. Renard, G. Gisele and C. Amiel, *Polym. Int.*, **2004**, 54, 594-599
108. S. J. Hwang, N. C. Bellocq and M. E. Davis, *Biconjugate Chem.*, **2001**, 12, 280-290.
109. S. R. Popielarski, S. Mishra, and M. E. Davis, *Biconjugate Chem.*, **2003**, 14, 672-678.
110. K. Hirotsu, T. Higuchi, K. Fujita, T. Ueda, A. Shinoda, T. Tomoto and I. Tabushi. *J. Org. Chem.*, **1982**, 47, 1143.
111. K. Harata, C. T. Rao and J. Pitha, *J. Carbohydr. Res.*, **1993**, 247, 83.
112. M. Masahiko, K. Yoshinori and H. Akira, *J. Incl. Phenom. Macrocycl. Chem.*, **2004**, 50, 57.
113. K. Itawa and S. Moriguchi, *Jpn. Kokai, Tokkyo Koho*, **1990** (02228558) (*Chem. Abstr.* 114, 177692).
114. G. Crini, S. Bertini, G. Torri, A. Naggi, D. Sforzini, C. Vecchi, L. Janus, Y. Lekchiri, and M. Morcellet, *J. Appl. Polym. Sci.*, **1998**, 68(12), 1973-1978.

115. G. Crini, C. Cosentino, S. Bertini, A. Naggi, G. Torri, C. Vecchi, L. Janus, and M. Morcellet, *Carbohydr. Res.*, **1998**, 308(1-2), 37-45
116. M. Kitaoka, and K. Hayashi, *J. Incl. Phenom. Macrocycl. Chem.*, **2002**, 44(1), 429-431.
117. F. Zha, S. Li, and Y. Chang, *Carbohydr. Polym.*, **2008**, 72(3), 456-461
118. L. Ducoroy, B. Martel, B. Bacquet, and M. Morcellet, *J. Incl. Phenom. Macrocycl. Chem.*, **2007**, 57(1), 271-277.
119. S. Berto, M. C. Bruzzoniti, R. Cavalli, D. Perrachon, E. Prenesti, T. Sarzanini, F. Trotta, and W. Tumiatti, *J. Incl. Phenom. Macrocycl. Chem.*, **2007**, 57(1), 631-636.
120. M. Kitaoka and K. Hayashi, *J. Incl. Phenom. Macrocycl. Chem.*, **2002**, 44, 429-431.
121. E. Renard, A. Deratani, G. Volet and B. Sebillier, *Eur. Polym. J.*, **1997**, 33, 49.
122. T. R. Thatiparti and H.A. von Recum, *Macromol. Biosci.*, **2010**, 10, 82-90.
123. M. Bhaskar, P. Aruna, R. Jeevan, G. Jeevan, G. Radhakrishnan, *Ana. Chemica Acta.*, **2004**, 509, 39.
124. M. Horie and M. Chiwa, *Jpn. Kokai, Tokkyo, Koho*, 63 314201, **1988** (*Chem. Abstr.* 110, 175437)
125. S. Shiraishi, M. Komiyama and H. Hirai, *Bull. Chem. Soc. Jpn.*, **1986**, 59(2), 507.
126. I. Tabushi, N. Shimizu, and K. Yamamura, *Jpn. Kokai, Tokkoyo, Koho*, 79 60761, **1979**, (*Chem. Abstr.* 91, 162667)
127. M. Yoshinaga, *Jpn. Kokai, Tokkoyo, Koho*, 05 032704, **1993**, (*Chem. Abstr.* 119, 10738)
128. V. Schurig, D. Schmalzing and M. Schleimer, *Angew. Chem.*, **1991**, 103, 994.
129. S. A. Buckler, R. R. Martel and R. J. Moshy, *US. Pat.*, 3472835, **1969**.
130. A. Harada, J. Li and M. Kamachi, *Macromolecules*, **1994**, 27, 4538.
131. A. Harada, J. Li and M. Kamachi, *Nature*, **1992**, 356, 325.
132. A. Harada, J. Li and M. Kamachi, *Nature*, **1993**, 364, 516.
133. A. Harada, *Supramol. Sci.*, **1996**, 3, 19.
134. I. Tomatsu, A. Hashidzume and A. Harada, *J. Am. Chem. Soc.*, **2006**, 128, 2226.
135. H. Murakani, A. Kawabuchi, R. Matsumoto, T. Ido, and N. Nakashima, *J. Am. Chem. Soc.*, **2005**, 127, 15891.
136. K. Ohga, Y. Takashima, H. Takahashi, Y. Kawaguch, H. Yamaguchi and A. Harada, *Macromolecules*, **2005**, 38, 5897.
137. T. Loftsson, D. Duchene, *Int. J. Pharm.*, **2007**, 329, 1-11.

138. X. Li and X. J. Loh, *Adv. Drug Del. Rev.*, **2008**, 60, 1000-1017.
139. S. M. Sammeta, S. R. Vaka and S. N. Murthy, *J. Control Release*, **2010**, 142(3), 361-7
140. M. R. Caira, W. T. Mhlongo and J. Li, *J. Optoelect. Adv. Mater.*, **2008**, 10(9), 2255-2260.
141. A. Rasheed, A. C. K. Kumar and V. N. S. S. Sravanthi, *Sci. Pharma.*, **2008**, 76, 567-598.
142. V. A. Jabor, V. L. Lanchote and P. S. Bonato, *Electrophoresis*, **2002**, 23(17), 3041-7.
143. A. L. Laza-Knoerr, R. Gref and P. Couvreur, *J. Drug. Target*, **2010**, 18(9), 645-56.
144. K. Shiotani, T. Irie, K. Uekama and Y. Ishimaru, *E. J. Pharm. Sci.*, **1995**, 3(3), 139-151.
145. J. Zhou and H. Ritter, *Polym. Chem.*, **2010**, 1, 1552-1559.
146. E. Setihadi, L. Tao, J. Lu, Z. Jia, C. Boyer and T. P. Davis, *Biomacromolecules*, **2009**, 10(9), 2699-2707.
147. W. Cai, T. Sun, P. Liu, C. Chipot and X. Shao, *J. Phys. Chem. B*, **2009**, 113(22), 7836-7843.
148. J. Hwang, K. Rodgers, J. C. Oliver and T. Schlupe, *Int. J. Nanomedicine*, **2008**, 3(3), 359-372.
149. N. Zhang, W. Jiang, C. Ren, J. Li, J. Xin, and K. Li, *Int. J. Pharma.*, **2010**, 393(1-2), 212-8.
150. Y. Cirpanli, E. Bilensoy, D. A. Lale and S. Calis, *Eur. J. Pharm. Biopharma.*, **2009**, 73(1), 82-9.
151. R. Challa, A. Ahuja, J. Ali, R. K. Khar, *AAPS Pharm. Sci. Tech.*, **2005**, 6, 329.
152. F. van de Manakker, T. Vermonden, C. F. van Nostrum and W. E. Hennik, *Biomacromolecules*, **2009**, 10(12), 3157-3175.
153. T. T. Nielsen, V. Wintgens, K. L. Larsen and C. Amiel, *J. Incl. Phenom. Macrocycl. Chem.*, **2009**, 65, 341-348.
154. Y. Iwasaki and K. Akiyoshi, *Biomacromolecules*, **2006**, 7(5), 1433-1438.
155. H. Choi, T. Ooya, K. M. Huh, and N. Yui, *Biomacromolecules*, **2005**, 6(3), 1200-1204.
156. S. Daoud-Mahammed, P. Couvreur, K. Bouchemal, M. Cheron, G. Lebas, C. Amiel and R. Gref, *Biomacromolecules*, **2009**, 10(3), 547-554

157. T. Higuchi and K. A. Connors, *Adv. Anal. Instrum.*, **1965**, 4, 117-212.
158. D. W. Armstrong, W. Li, C. D. Chang and J. Pitha, *Anal. Chem.*, **1990**, 62(9), 914-923.
159. A. Wilfried, K. D. Icheln, T. Runge, I. Pforr, A. Krebs, *J. High Resolution Chromatography*, **1990**, 13(10), 702-707.
160. G. Shen, J. Cui and Y. Ling, *J. Sep. Sci.*, **2009**, 32(1), 79-87.
161. W. C. E. Schofield and J. P. S. Badyal, *ACS Appl. Mater. Interfaces*, **2011**, 3(6), 2051-2056.
162. Z. Zhang, M. Wu, R. Wu, J. Dong, J. Ou, and H. Zou, *Anal. Chem.*, **2011**, 83(9), 3616-3622.
163. G. G. Mironov, V. Okhonin, S. I. Gorelsky, and M. V. Berezovski, *Anal. Chem.*, **2011**, 83(6), 2364-2370.
164. C. Bicchì, V. Manzin, A. D'Amato and P. Rubiolo, *Flavour and Fragrance Journal*, **1995**, 10(3), 127-137.
165. J. Szejtli, B. Zsádon, and T. Cserhati, *Ordered Medium in Chemical Separations, Chapter 11*, **1987**, 200-217.
166. H. J. Buschmann, D. Knittel and E. Schollmeyer, *J. Incl. Phenom. Macrocycl. Chem.*, **2001**, 40(3), 169-172.
167. L. D. Wilson, M. H. Mohamed, R. Guo, D. Y. Pratt, J. H. Kwon and S. T. Mahmud, *J. Agrochemedecine*, **2010**, 15(2), 105-16.
168. A. Binello, B. Robaldo, A. Barge, R. Cavalli and G. Cravotto, *J. Appl. Polym. Sci.*, **2008**, 107(4), 2549-2557.
169. R. Zidovetzki and I. Levitan, *Biochim. Biophys Acta.*, **2007**, 1768(6), 1311-1324.
170. B. Sancey, G. Trunfio, J. Charles, P.-M. Badot and G. Crini, *J. Incl. Phenom. Macrocycl. Chem.*, **2011**, 70, 315-320.
171. A. Harada, M. Osaki, Y. Takashima and H. Yamaguchi, *Acc. Chem. Res.*, **2008**, 41(9), 1143-1152.
172. H. Liu, X. Cai, Y. Wang and J. Chen, *Water Res.*, **2011**, 45(11), 3499-511.
173. J. Szejtli, *Starch*, **1982**, 34(11), 379-385.

*Chapter 2*  
*Synthesis of Difunctionalized  $\beta$ -Cyclodextrin Monomers*

## Chapter 2

### Synthesis of Difunctionalized $\beta$ -Cyclodextrin Monomers

#### 2.1 Introduction

The cyclodextrin molecule has six, seven and eight primary hydroxyl groups for  $\alpha$ -,  $\beta$ - and  $\gamma$ -cyclodextrin on narrow rim. Apart from this there are twelve, fourteen and sixteen secondary hydroxyl groups for  $\alpha$ -,  $\beta$ - and  $\gamma$ -cyclodextrin, respectively on wider rim<sup>1</sup>. Thus, theoretically it is possible for these primary and secondary hydroxyl groups to react under suitable condition. The primary hydroxyl groups are more reactive than the secondary hydroxyl groups. However, under a given reaction condition all the primary hydroxyl groups are equally reactive. Thus, all the six primary hydroxyl groups in case of  $\alpha$ -CD, seven primary hydroxyl groups of  $\beta$ -CD and eight primary hydroxyl groups of  $\gamma$ -CD are equally reactive. Therefore, to synthesize a mono functionalized cyclodextrin is extremely difficult and tricky. Consequently to make selective difunctionalized cyclodextrin is a challenging task and purification is tedious process<sup>2,3</sup>.

To use cyclodextrin molecule as a monomer for the polymer formation, its functionality should be two i.e. it should be difunctionalized. Therefore, pristine cyclodextrin molecules cannot be used as it is for the polymerization reaction. Thus, here we tried tosylation reaction of cyclodextrin with bulky biphenyl 4,4'-disulfonyl chloride as the disulfonating agent for the synthesis of selective difunctional  $\beta$ -cyclodextrin<sup>4</sup>. The structural dimension of this molecule is shown in Figure 2.1. The distance between the two terminal chlorine atoms in this molecule is 12.3 Å and therefore it can form a bridge where the two hydroxyl groups are separated by comparable distance. The disubstituted biphenyl 4,4'-disulfonylbridged- $\beta$ -cyclodextrin can be formed after the structural distortion and the orientation of the reactive chlorine groups towards the AD and AE hydroxyl groups at the 6-position of the  $\beta$ -cyclodextrin. This is schematically shown in Figure 2.1. Though biphenyl forms inclusion complex with  $\beta$ -cyclodextrin, the sulfonyl chloride groups attached to the biphenyl molecule prevents it from doing so. Thus, the biphenyl always will form a bridge between the hydroxyl groups of the same cyclodextrin molecule.

One of the key steps of the present synthesis is the reaction of  $\beta$ -cyclodextrin with bulky biphenyl 4,4'-disulfonyl chloride to form a bisulfonate ester on the smaller primary rim of  $\beta$ -cyclodextrin. This bisulfonate ester was further reacted with potassium iodide to give 6<sup>A</sup>,6<sup>D</sup>-diiodo 6<sup>A</sup>,6<sup>D</sup>-dideoxy  $\beta$ -cyclodextrin. The obtained 6<sup>A</sup>,6<sup>D</sup>-diiodo 6<sup>A</sup>,6<sup>D</sup>-dideoxy  $\beta$ -cyclodextrin further react with sodium azide to give 6<sup>A</sup>,6<sup>D</sup>-diazido 6<sup>A</sup>,6<sup>D</sup>-dideoxy  $\beta$ -cyclodextrin followed by reduction to form 6<sup>A</sup>,6<sup>D</sup>-diamino 6<sup>A</sup>,6<sup>D</sup>-dideoxy  $\beta$ -cyclodextrin. The schematic of the reaction is shown in Scheme 2.1.

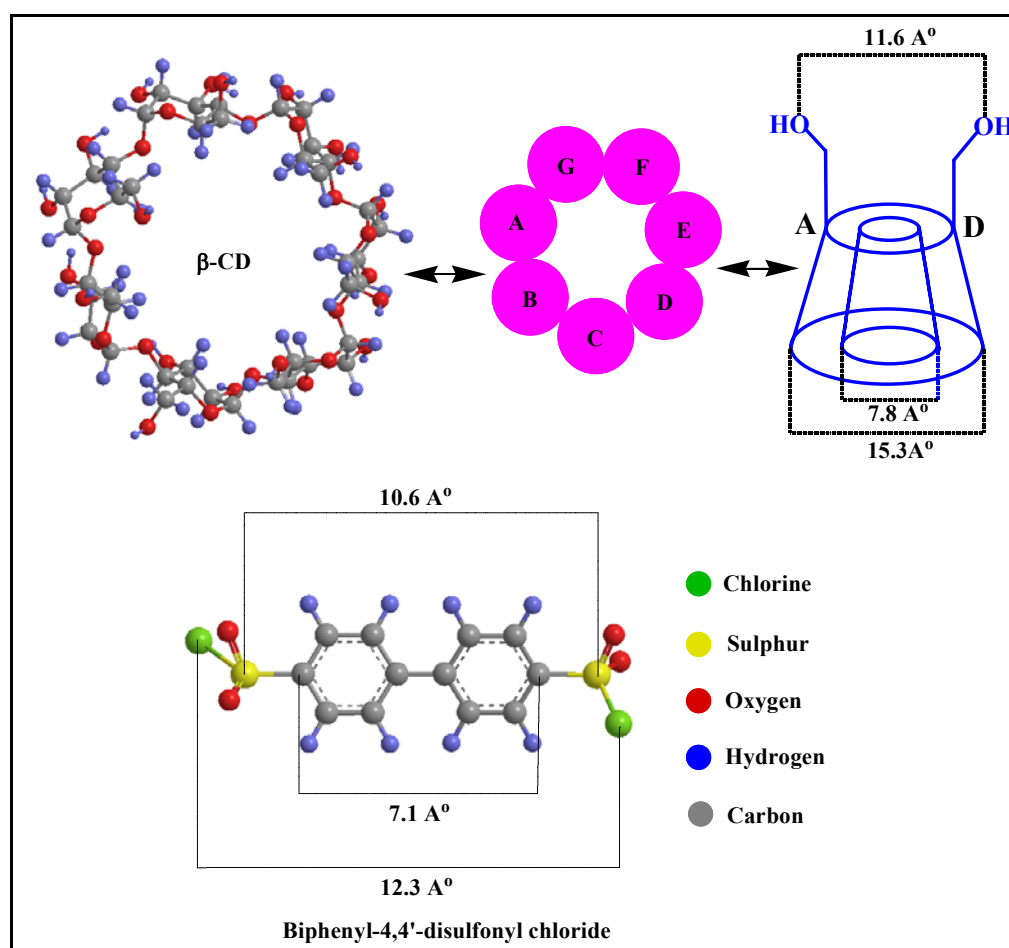


**Figure 2.1** Structural dimension of the  $\beta$ -cyclodextrin and biphenyl-4,4'-disulfonyl chloride.

## 2.2 Experimental

### 2.2.1 Materials

$\beta$ -Cyclodextrin was obtained from Signet Chemical Corporation, Mumbai as a gift sample and dried overnight under a vacuum oven at 60°C, then used without further purification. Biphenyl-4,4'-disulfonyl chloride (recrystallized from chloroform), potassium iodide, sodium azide and triphenylphosphine were purchased from Sigma-Aldrich. *N,N'*-dimethylformamide (DMF), pyridine, and tetrachloroethylene were purchased from Merck (Germany) and dried over molecular sieves for 1 day then distilled under reduced pressure before use. All other chemicals were procured locally and used without further purifications. Double distilled water was used during the all experiments.

### 2.2.2 Measurements

The FTIR spectra of the compounds were recorded on a Shimadzu 8400S Fourier Transform Infrared Spectrometer by KBr pellet method at  $10^{-4}$  resolution and 30 scans at room temperature. AR grade KBr was used for the preparation of the pellet. The UV-Visible absorbance spectra were recorded on a Shimadzu UV-Vis-2450, spectrophotometer.  $^1\text{H}$  and  $^{13}\text{C}$  NMR spectra were recorded on a Bruker spectrometer operating at 400 MHz at room temperature where tetra-methylsilane (TMS) was used as internal standard. The chemical shifts are given in  $\delta$  ppm from TMS signal. TLC was carried out on silica gel plates (Merck 60-F254). CDs derivatives were detected with UV light and with anisaldehyde reagent. The CDs amino derivatives were detected by ninhydrin test. For the structural drawing and molecular modeling studies, the software Chem Office 2004 (Chem 3D Ultra 8.0version) was used.

### 2.2.3 Synthesis of 6<sup>A</sup>,6<sup>D</sup>-biphenyl bridged $\beta$ -Cyclodextrin (2)

A 500 mL three neck round bottom flask equipped with a magnetic stir bar, a Schlenk adapter and a rubber septum was charged with 11.35 g (0.01 mole) of dry  $\beta$ -cyclodextrin (1) and 150 mL of anhydrous pyridine. The resulting solution was stirred at 50°C under nitrogen atmosphere, while 3.51 g (0.01 mole) of biphenyl-4,4'-disulfonyl chloride dissolved in 100 mL pyridine was cautiously added drop wise in 1

h. After that the reaction mixture was allowed to stir at 50°C for an additional 3 h in the same conditions. The solvent was removed under vacuum on a rotary evaporator at 40°C and the residue obtained was subjected to reversed-phase column chromatography using a gradient elution of 0-40% acetonitrile in water. After, removing the bulk of the acetonitrile on a rotary evaporator, the resulting aqueous suspension was lyophilized to dryness. This afforded 6.15 g (40%) of 6<sup>A</sup>,6<sup>D</sup>-biphenyl bridged β-cyclodextrin as a colorless solid.

#### 2.2.4 Synthesis of 6<sup>A</sup>,6<sup>D</sup>-diiodo 6<sup>A</sup>,6<sup>D</sup>-dideoxy β-Cyclodextrin (3)

A 100 mL three neck round bottom flask equipped with a magnetic stirbar, a Schlenk adapter and a rubber septum was charged with 5.42 g (3.52 mmole) of 6<sup>A</sup>,6<sup>D</sup>-biphenyl bridged β-cyclodextrin (2), 17.53 g (0.106 mole) of dry, powdered potassium iodide and 15 mL of anhydrous *N,N'*-dimethylformamide (DMF). The resulting suspension was stirred at 80°C under nitrogen atmosphere for 2 h. After cooling to room temperature, the solids were separated by centrifugation and the supernatant was decanted. The solid precipitate was washed with a second portion of anhydrous DMF and the supernatants were combined and concentrated in vacuum. The residue was then dissolved in 14 mL of water and cooled in an ice bath before 0.75 mL (7.3 mmole) of tetrachloroethylene was added with rapid stirring. The precipitated inclusion complex was filtered and washed with a small portion of acetone after it was dried under vacuum. This gave 4.69 g (90% yield) of 6<sup>A</sup>,6<sup>D</sup>-diiodo 6<sup>A</sup>,6<sup>D</sup>-dideoxy β-cyclodextrin as a slightly yellow solid.

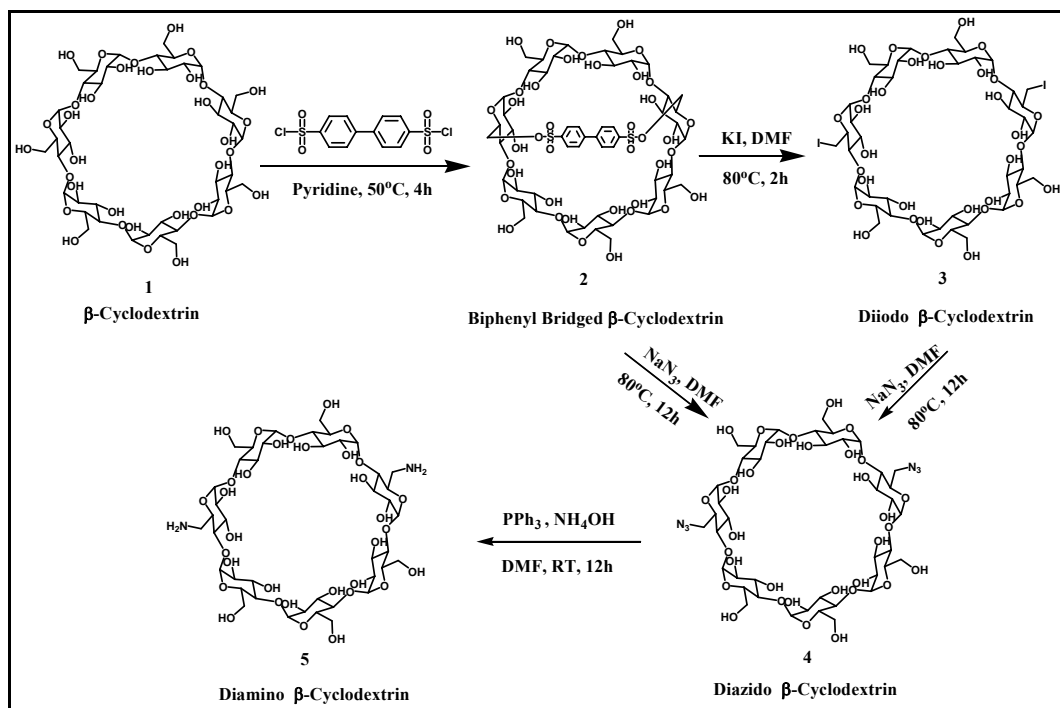
#### 2.2.5 Synthesis of 6<sup>A</sup>,6<sup>D</sup>-diazido 6<sup>A</sup>,6<sup>D</sup>-dideoxy β-Cyclodextrin (4)

A 100 mL three neck round bottom flask equipped with a magnetic stir bar coated with Teflon, a Schlenk adapter and a septum was charged with 3.90 g (2.88 mmole) of β-cyclodextrin diiodide (3), 1.12 g (0.019 mole) of sodium azide and 10 mL of anhydrous *N,N'*-dimethylformamide (DMF). The resulting suspension was stirred at 80°C under nitrogen atmosphere for 12 h. The solvent was removed on a rotary evaporator under reduced pressure and obtained residue was dissolved in 150 mL of water. This diluted solution was subjected to ultrafiltration by using polymer membrane filtration (MWCO 650 Da) to remove the excess salt. After removing salt

the resulting aqueous suspension was freeze-dried to get 3.54 g (90%) white solid which was used for the next stage.

### **2.2.6 Synthesis of 6<sup>A</sup>,6<sup>D</sup>-diamino 6<sup>A</sup>,6<sup>D</sup>-dideoxy β-Cyclodextrin (5)**

A 100 mL three neck round bottom flask equipped with a magnetic stirbar and a septum was charged with 1.232 g (1.04 mmole) of β-cyclodextrin bisazide (4) in 50 mL of anhydrous *N,N'*-dimethylformamide (DMF). To this stirring solution 0.898 g (3.42 mmole) triphenylphosphine was added. The resulting suspension was stirred for 1 h at ambient temperature after this 10 mL of ammonium hydroxide was added. The addition of ammonium hydroxide was accompanied by a rapid gas evolution and the solution became homogeneous. After 12 h, solvent was removed under vacuum rotavapor and obtained residue was mixed with water and washed twice with benzene to remove the phosphonium oxides. The solution was adjusted to pH-7 by addition of 0.1N HCl solution and diluted with 100 mL of water. This diluted solution was subjected to ultrafiltration by using polymer membrane (MWCO 650 Da). The resulted aqueous solution was freeze dried to get dry 1.10 g (90%) white product of diamino β-cyclodextrin.



**Scheme 2.1** Synthetic scheme for the synthesis of selectively difunctionalized  $\beta$ -cyclodextrins.

## 2.3 Characterization of Difunctionalized $\beta$ -Cyclodextrin Monomers

The regioselectively modified 6<sup>A</sup>,6<sup>D</sup>-diamino 6<sup>A</sup>,6<sup>D</sup>-dideoxy  $\beta$ -cyclodextrin was synthesized by the route shown in Scheme 2.1 following the primary reports of I. Tabushi *et al*<sup>5</sup>. The capping reaction illustrated was carried out by treating the  $\beta$ -cyclodextrin with biphenyl 4,4'-disulfonyl chloride, which has enough long geometry that it can direct the reaction on A to D position hydroxyl groups of  $\beta$ -cyclodextrin on the primary rim. The reaction of biphenyl bridged- $\beta$ -cyclodextrin with dry powder potassium iodide in dry DMF gave the diiodo  $\beta$ -CD derivative, which further reacts with sodium azide to afford diazido  $\beta$ -CD derivative. The reaction of diazido  $\beta$ -CD with triphenylphosphine in DMF followed by hydrolysis of iminophosphorane intermediate with ammonium hydroxide gave the 6<sup>A</sup>,6<sup>D</sup>-diamino 6<sup>A</sup>,6<sup>D</sup>-dideoxy  $\beta$ -cyclodextrin.

### 2.3.1 6<sup>A</sup>,6<sup>D</sup>-biphenyl bridged $\beta$ -Cyclodextrin (2)

The FTIR spectrum of 6<sup>A</sup>,6<sup>D</sup>-biphenyl bridged  $\beta$ -cyclodextrin is shown in Figure 2.2. The spectrum exhibited the major stretching absorbance bands of parent  $\beta$ -cyclodextrin at 3368 cm<sup>-1</sup>, 2920 cm<sup>-1</sup>, 1660 cm<sup>-1</sup>, 1155 cm<sup>-1</sup>, 1029 cm<sup>-1</sup> and strong stretching absorbance bands at 1176 cm<sup>-1</sup>, 2900 cm<sup>-1</sup> and 820 cm<sup>-1</sup> which could be assigned to -SO<sub>2</sub> stretching, -CH<sub>2</sub> stretching and para-substituted benzene stretching absorption bands of 4,4'-biphenyl disulfonyl chloride. This result confirmed the formation of biphenyl-bridge between two primary hydroxyl groups of  $\beta$ -cyclodextrin. The band at 3368 cm<sup>-1</sup> is broad due to the -OH groups was extended hydrogen bonded with other -OH groups and it indicates that the crystalline nature of  $\beta$ -cyclodextrin was retained after biphenyl capping.

Figure 2.3 shows the UV-Vis absorption spectra of biphenyl-4,4'-disulfonyl chloride in chloroform,  $\beta$ -cyclodextrin in water and biphenyl bridged  $\beta$ -cyclodextrin in water. The UV-Vis absorbance spectra also support the formation of biphenyl bridged between two primary hydroxyl groups of  $\beta$ -cyclodextrin. The UV-Vis absorbance spectrum of biphenyl-4,4'-disulfonyl chloride shows absorbance maxima at around 326 nm in chloroform which is completely insoluble in water, whereas the  $\beta$ -cyclodextrin in water does not show any absorbance in this region. However, the

UV-Vis absorbance spectrum of biphenyl bridged  $\beta$ -cyclodextrin in water showed the typical absorbance of biphenyl-4,4'-disulfonyl chloride at around 263 nm which was observed to blue shifted by few nanometer due to the formation of bridge between two primary hydroxyl groups of  $\beta$ -cyclodextrin and biphenyl moiety was attracted towards the non-polar cavity of  $\beta$ -cyclodextrin due to nonpolar-nonpolar interaction.

The  $^1\text{H}$ -NMR spectra of unsubstituted  $\beta$ -cyclodextrin and biphenyl bridged  $\beta$ -cyclodextrin in  $\text{DMSO-d}_6$  are shown in Figure 2.4 and Figure 2.5. The spectrum of biphenyl bridged  $\beta$ -cyclodextrin showed a distinct separation of proton signals that are obtained from the protons attached to the aromatic nucleus of the biphenyl ring of biphenyl 4,4'-disulfonyl chloride and  $\beta$ -cyclodextrin of glucose units. Thus, clusters of proton signals can be observed between 2 to 5.5 ppm of  $\beta$ -cyclodextrin's glucose units' protons {4.95 ppm (br S, 7H-1 anomeric proton), 3.3-4.7 ppm (54 H, H-3, H-5, H-6, H-2, and H-4)} and proton signals of 7.5-8.9 ppm (8H, ArH) which could be assigned to the aromatic protons of biphenyl ring. The intensity of the aromatic protons was observed to be very less compared to the glucose unit's protons of  $\beta$ -cyclodextrins. This suggests that biphenyl moiety was attracted towards the non-polar cavity of  $\beta$ -cyclodextrin. Similar observation has been observed when  $^1\text{H}$  NMR of  $\beta$ -cyclodextrin and biphenyl bridged  $\beta$ -cyclodextrin has been also carried out in  $\text{D}_2\text{O}$  as shown in Figure 2.6 and Figure 2.7. There is no much change in the results when the solvent was changed. The comparison of protons signal of unsubstituted  $\beta$ -CD and substituted  $\beta$ -CD in two different solvents are shown in Table 2.1 and Table 2.2.

The  $^{13}\text{C}$  NMR spectra of unsubstituted  $\beta$ -cyclodextrin (in  $\text{D}_2\text{O}$  and  $\text{DMSO-d}_6$ ) are shown in Figure 2.8 and Figure 2.9. The  $^{13}\text{C}$  NMR spectrum of biphenyl bridged  $\beta$ -cyclodextrin (in  $\text{DMSO-d}_6$ ) is shown in Figure 2.10. The  $^{13}\text{C}$  NMR spectra of  $\beta$ -CD in two different solvents shows the similar carbon chemical shifts for glucose units carbons at  $\delta$ ppm 101.10 (C-1), 71.85 (C-2), 73.21 (C-3), 81.18 (C-4), 72.16 (C-5) and 60.30 (C-6). The spectrum of biphenyl bridged  $\beta$ -cyclodextrin (in  $\text{DMSO-d}_6$ , Figure 2.9) showed the typical biphenyl aromatic carbons chemical shifts of biphenyl moiety at  $\delta$ ppm 126.17, 126.80, 127.23, 128.23, 139.78, 142.23, 146.10 and 147.31 due to changes in the symmetry of the  $\beta$ -CD molecule after the bridge formation with the primary hydroxyl groups, where as the only biphenyl aromatic system showed carbon

chemical shift at  $\delta$ ppm: 143.0 (C-1,1'), 127.3 (C-2,2'), 128.6 (C-3,3') and 143.4 (C-4,4'). The  $^{13}\text{C}$ -NMR spectrum also showed carbon chemical shifts of  $\beta$ -cyclodextrin at  $\delta$ ppm 102.08 (C-1), 71.66 (C-2), 73.21 (C-3), 81.55 (C-4), 72.89 (C-5) and 59.76 (C-6), and also one more carbon chemical shift was observed due to primary hydroxyl group substitution C-6 at 59.76  $\delta$ ppm (adjacent to  $-\text{OH}$  group) of the  $\beta$ -CD goes up field shows the C-6' at 41.67  $\delta$ ppm (adjacent to biphenyl ring). The comparison of chemical shifts of unsubstituted  $\beta$ -CD and substituted  $\beta$ -CD are shown in Table 2.3. These NMR data shows that the biphenyl-4,4'-disulfonyl chloride subsequently attached with the primary hydroxyl and making bridged on the primary side of  $\beta$ -CD molecule as shown in Scheme 1.

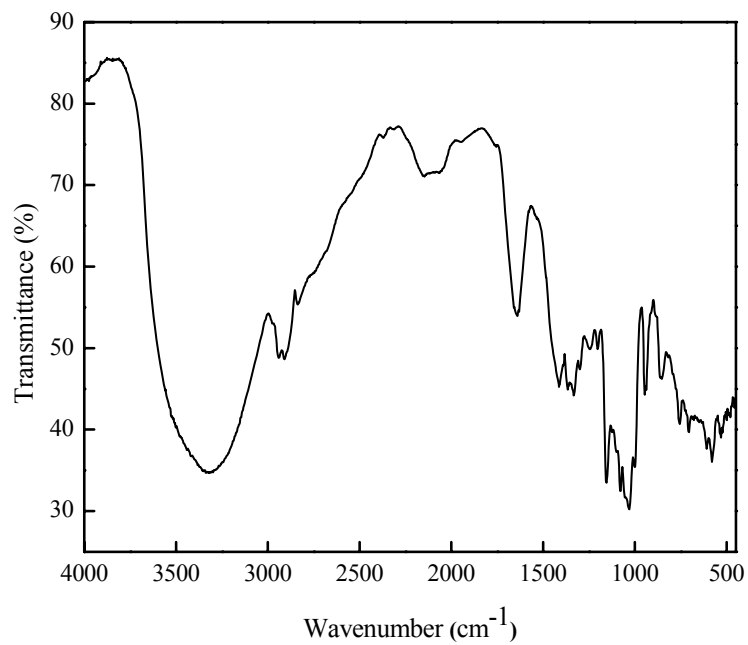


**Figure 2.2** FTIR spectrum of 6<sup>A</sup>,6<sup>D</sup>-biphenyl bridged  $\beta$ -cyclodextrin.

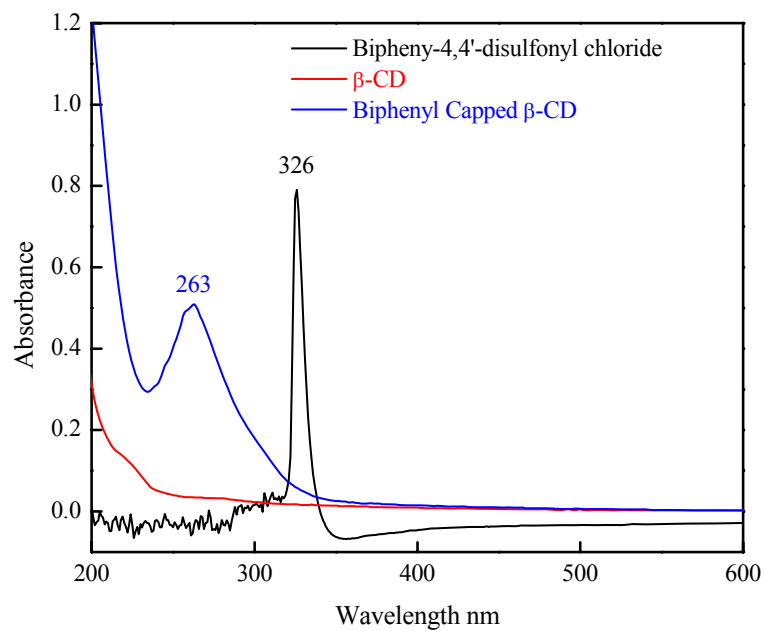


**Figure 2.3** UV-Vis spectra of biphenyl-4,4'-disulfonyl chloride in chloroform,  $\beta$ -cyclodextrin in water and biphenyl bridged  $\beta$ -cyclodextrin in water.

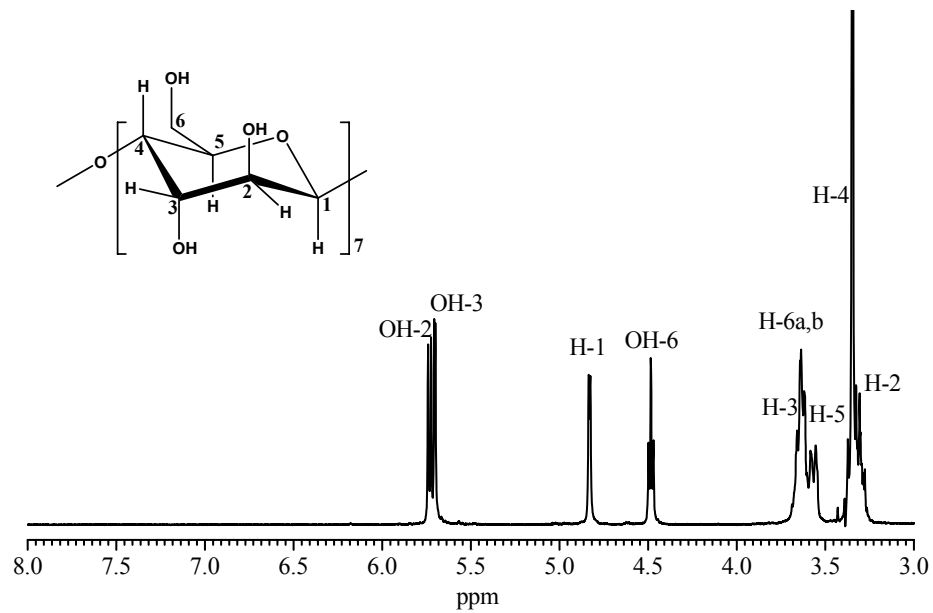


**Figure 2.4**  $^1\text{H}$  NMR spectrum of  $\beta$ -cyclodextrin in  $\text{DMSO-d}_6$ .

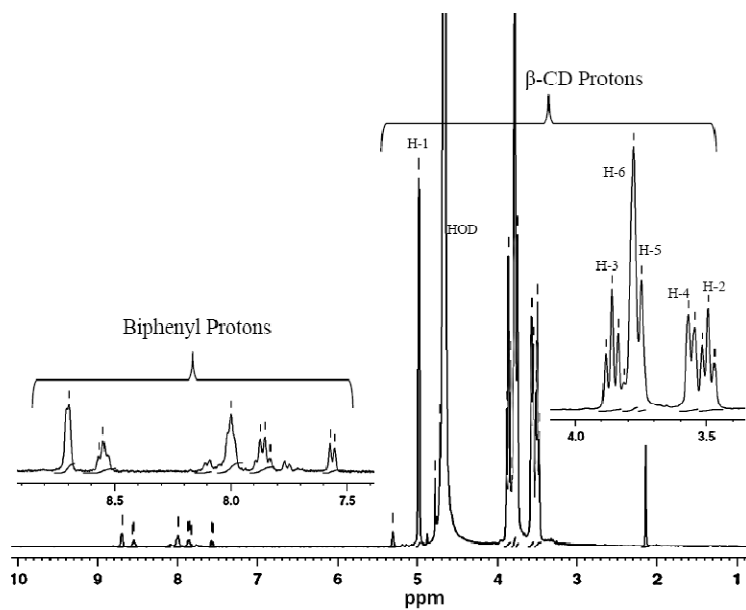


**Figure 2.5**  $^1\text{H}$  NMR spectrum of biphenyl bridged  $\beta$ -cyclodextrin in  $\text{DMSO-d}_6$ .

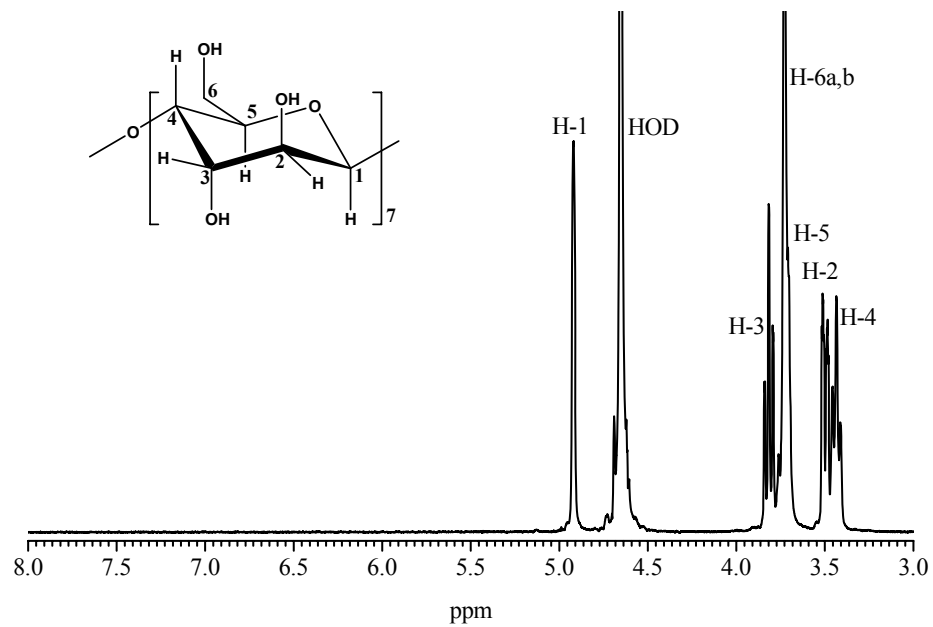


**Figure 2.6**  $^1\text{H}$  NMR spectrum of  $\beta$ -cyclodextrin in  $\text{D}_2\text{O}$ .

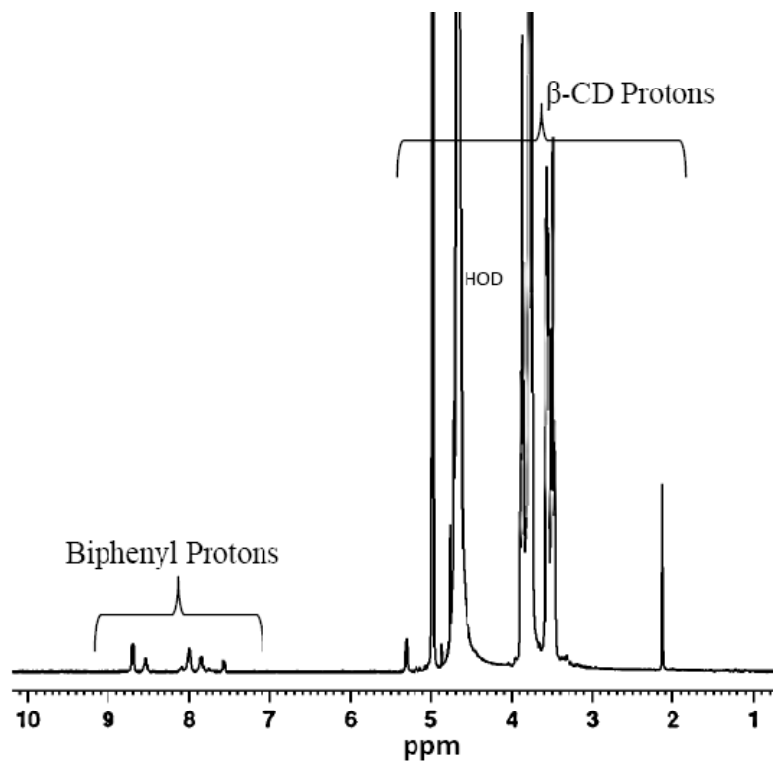


**Figure 2.7**  $^1\text{H}$  NMR spectrum of biphenyl bridged  $\beta$ -cyclodextrin in  $\text{D}_2\text{O}$ .

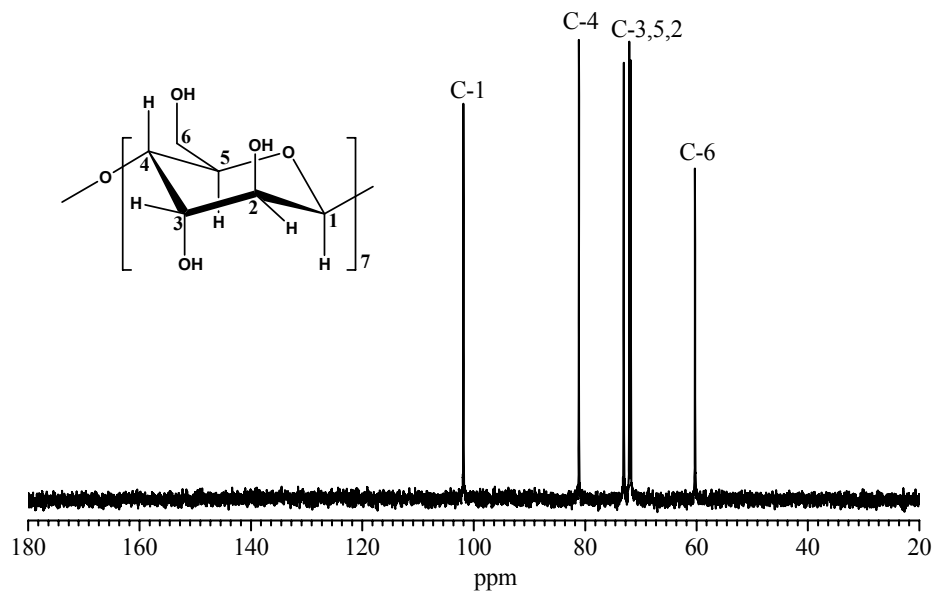


**Figure 2.8**  $^{13}\text{C}$  NMR spectrum of  $\beta$ -cyclodextrin in  $\text{D}_2\text{O}$ .

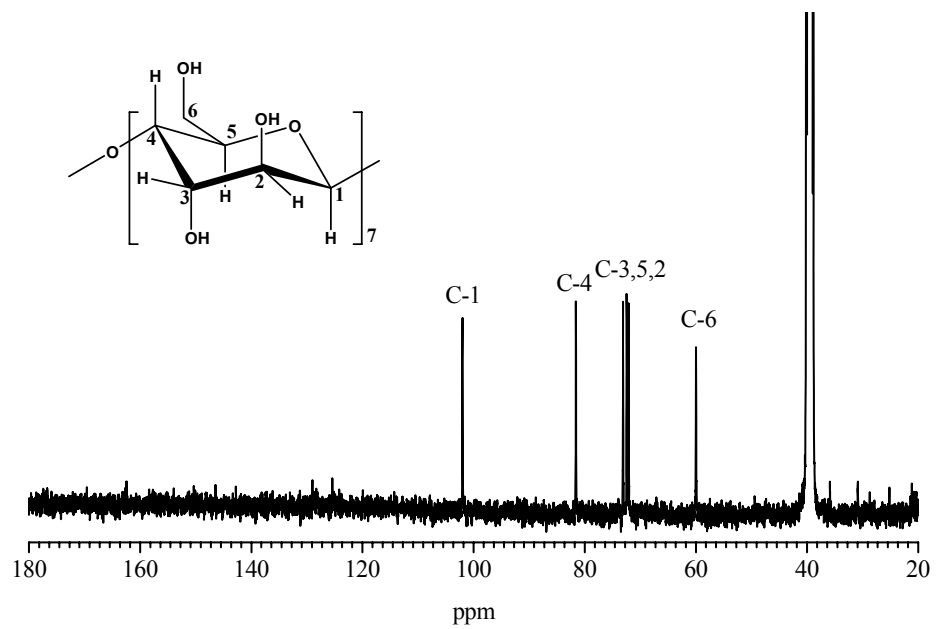


**Figure 2.9**  $^{13}\text{C}$  NMR spectrum of  $\beta$ -cyclodextrin in  $\text{DMSO-d}_6$ .

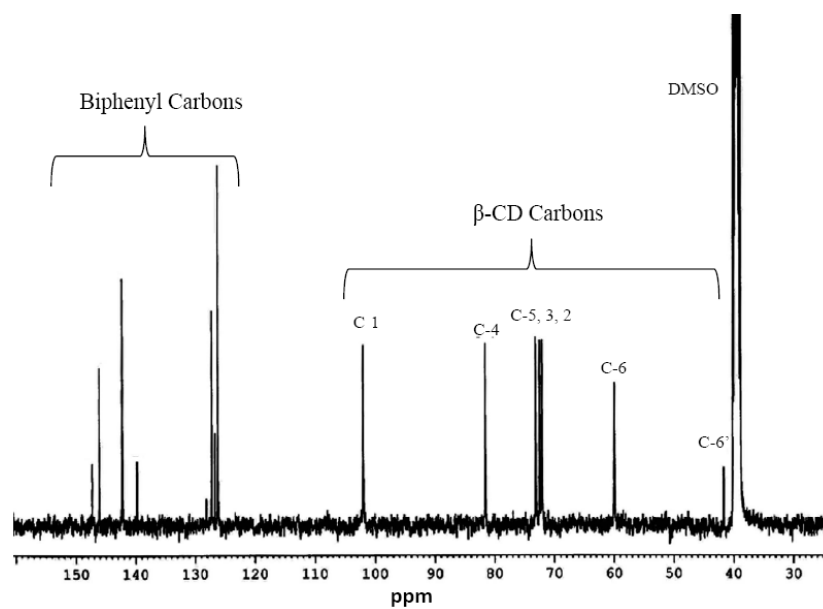


**Figure 2.10**  $^{13}\text{C}$  NMR spectrum of biphenyl bridged  $\beta$ -cyclodextrin in  $\text{DMSO-d}_6$ .

### 2.3.2 6<sup>A</sup>,6<sup>D</sup>-diiodo 6<sup>A</sup>,6<sup>D</sup>-dideoxy β-Cyclodextrin (3)

The FTIR spectrum of 6<sup>A</sup>,6<sup>D</sup>-diiodo 6<sup>A</sup>,6<sup>D</sup>-dideoxy β-cyclodextrin is shown in Figure 2.11. The spectrum depicted the absorbance band at 3400 cm<sup>-1</sup> and 1156 cm<sup>-1</sup> peak was observed due to –OH stretching and –CH<sub>2</sub>-I stretching (rocking and wagging band), which confirms that biphenyl ring easily removed from the biphenyl bridged β-cyclodextrin by the nucleophilic addition of the potassium iodide.

The <sup>1</sup>H NMR spectrum of the 6<sup>A</sup>,6<sup>D</sup>-diiodo 6<sup>A</sup>,6<sup>D</sup>-dideoxy β-cyclodextrin is shown in Figure 2.12. The spectrum shows only the typical glucose unit's proton signals of β-cyclodextrin at δppm: 4.92 (d, 7H, H-1), 3.49 (m, 7H, H-2), 3.82 (m, 7H, H-3), 3.40 (m, 7H, H-4) 3.69 (m, 7H, H-5), 3.72 (d, 12H, H-6) and peaks at 2.70-2.86 (dd, 2H, H-6') along with removal of aromatic biphenyl protons in aromatic region. These results confirmed that the biphenyl ring was completely removed from the biphenyl bridged β-cyclodextrin due to the nucleophilic substitution. The comparison of protons signal of unsubstituted β-CD and diiodo β-CD are shown in Table 2.1.

The <sup>13</sup>C NMR spectrum of 6<sup>A</sup>,6<sup>D</sup>-diiodo 6<sup>A</sup>,6<sup>D</sup>-dideoxy β-cyclodextrin is shown in Figure 2.13 also support the same observation showed all the typical carbon chemical shifts of cyclodextrin glucose units at δppm: 101.85 (C-1), 72.42 (C-2), 73.04 (C-3), 82.29 (C-4), 72.26 (C-5), 6.27 (C-6) along with one new carbon chemical shift C-6' at 10 ppm (adjacent to –I) due to the substitution of two primary hydroxyl groups of the β-CD. The comparison of carbon chemical shifts of unsubstituted β-CD and diiodo β-CD are shown in Table 2.3.

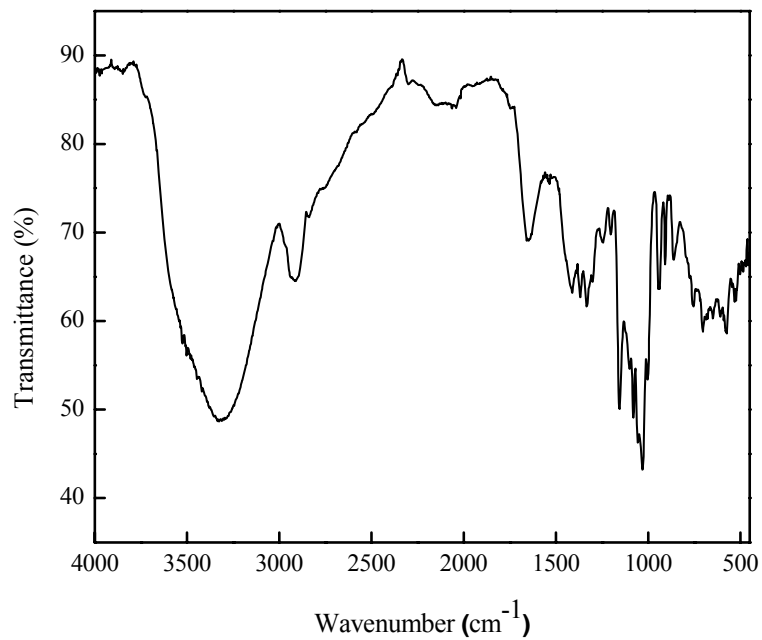


**Figure 2.11** FTIR spectrum of  $6^A,6^D$ -diiido  $6^A,6^D$ -dideoxy  $\beta$ -cyclodextrin.

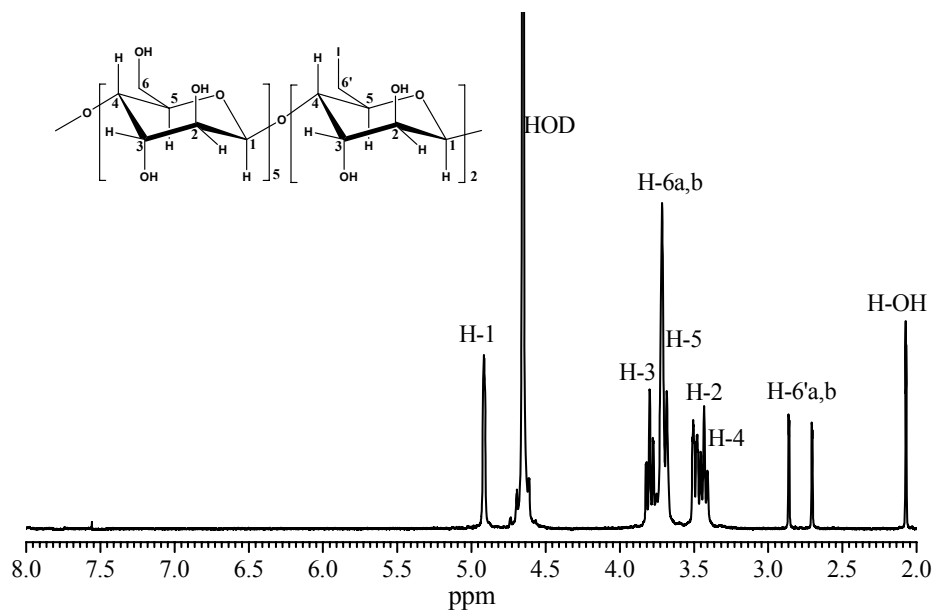


**Figure 2.12**  $^1\text{H}$  NMR spectrum of  $6^A,6^D$ -diiido  $6^A,6^D$ -dideoxy  $\beta$ -cyclodextrin in  $\text{D}_2\text{O}$ .

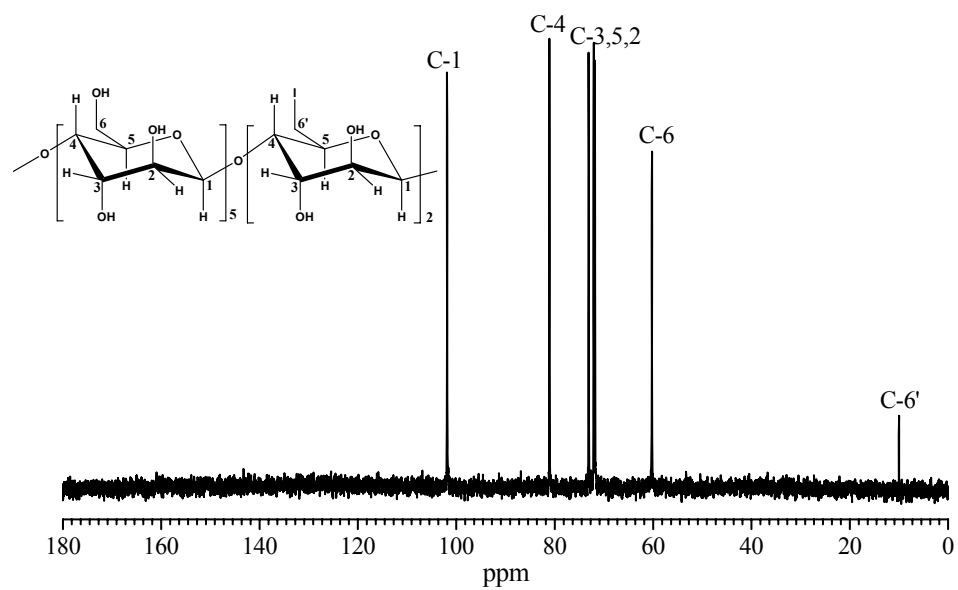


**Figure 2.13**  $^{13}\text{C}$  NMR spectrum of  $6^A,6^D$ -diiodo  $6^A,6^D$ -dideoxy  $\beta$ -cyclodextrin in  $\text{D}_2\text{O}$ .

### 2.3.3 6<sup>A</sup>,6<sup>D</sup>-diazido 6<sup>A</sup>,6<sup>D</sup>-dideoxy β-Cyclodextrin (4)

The FTIR spectrum of the 6<sup>A</sup>,6<sup>D</sup>-diazido 6<sup>A</sup>,6<sup>D</sup>-dideoxy β-cyclodextrin is shown in Figure 2.14. The spectrum exhibited the absorbance band at 3400 cm<sup>-1</sup> and 2037 cm<sup>-1</sup> were observed due to presence –OH stretching and -N<sub>3</sub> asymmetrical stretching, which confirms that replacement of two iodo groups from the 6<sup>A</sup>,6<sup>D</sup>-diiodo 6<sup>A</sup>,6<sup>D</sup>-dideoxy β-cyclodextrin by the nucleophilic addition of the sodium azide.

The <sup>1</sup>H-NMR (Figure 2.15) and <sup>13</sup>C-NMR (Figure 2.16) also confirmed the removal of iodo groups from 6<sup>A</sup>,6<sup>D</sup>-diiodo 6<sup>A</sup>,6<sup>D</sup>-dideoxy β-cyclodextrin showed only protons and carbon chemical shifts of β-cyclodextrin's glucose units along with substituted protons and carbon shifts at two C-6' position of β-cyclodextrin. The comparison of protons signal and carbon chemical shifts of unsubstituted β-CD and diazido β-CD are shown in Table 2.1 and Table 2.3.

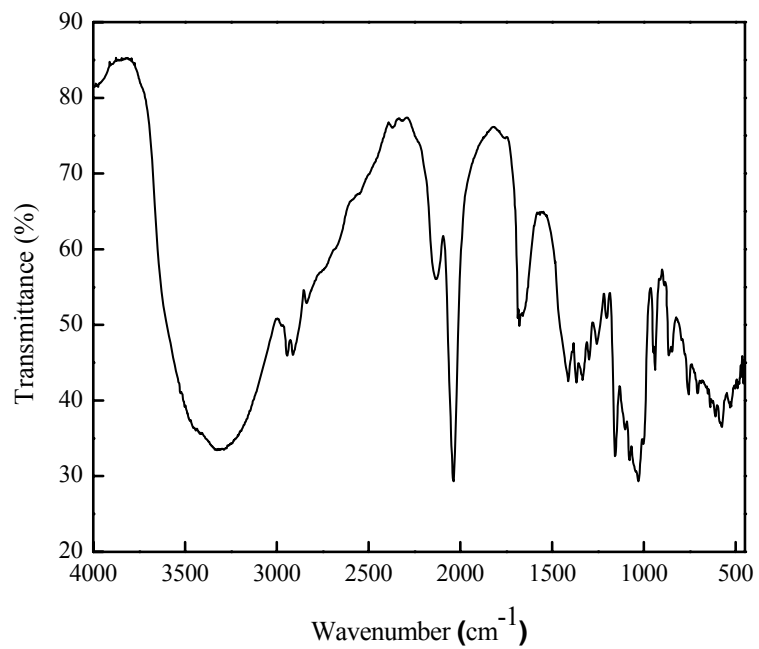


**Figure 2.14** FTIR spectrum of  $6^A,6^D$ -diazido  $6^A,6^D$ -dideoxy  $\beta$ -cyclodextrin.

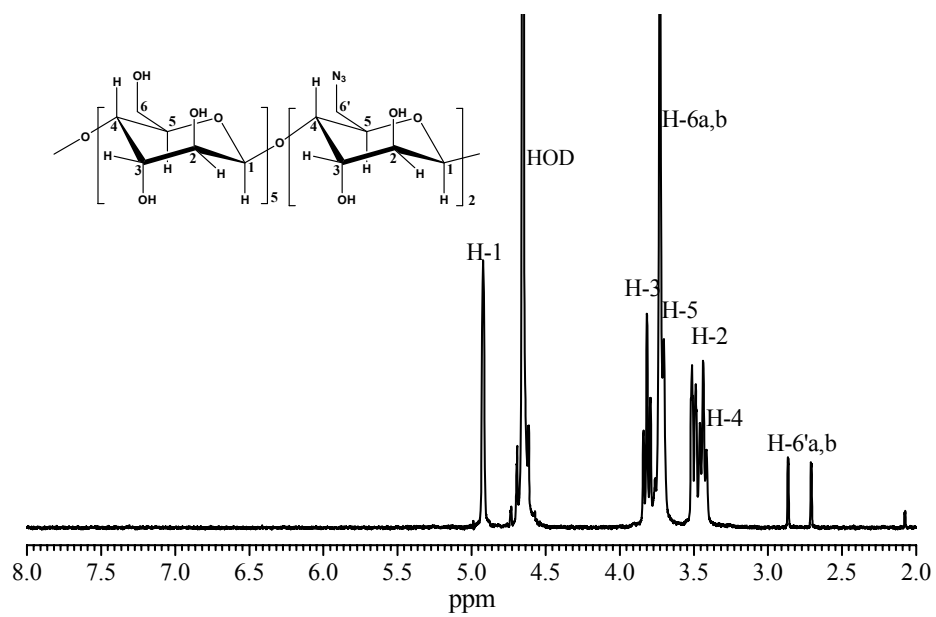


**Figure 2.15**  $^1\text{H}$  NMR spectrum of  $6^A,6^D$ -diazido  $6^A,6^D$ -dideoxy  $\beta$ -cyclodextrin  $\text{D}_2\text{O}$ .

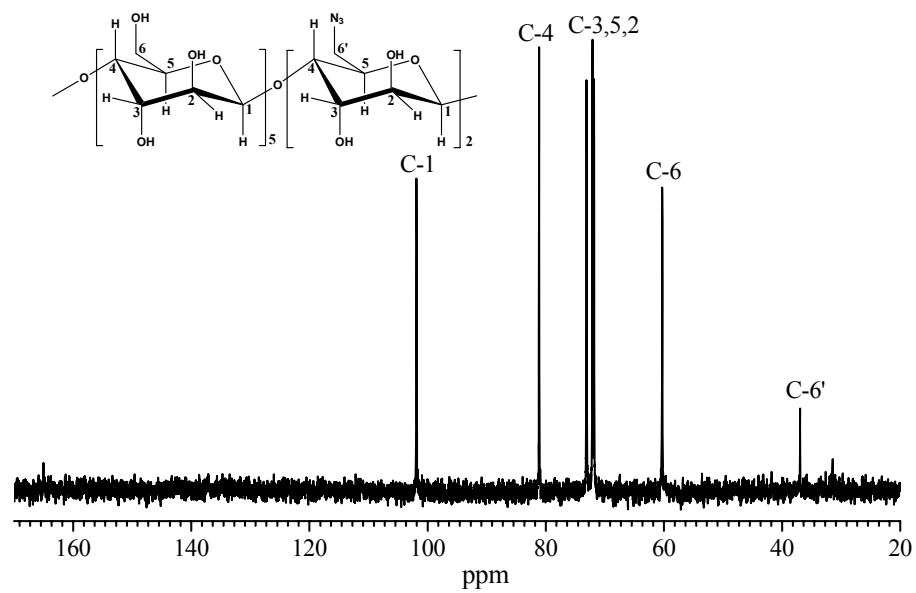


**Figure 2.16** <sup>13</sup>C NMR spectrum of 6<sup>A</sup>,6<sup>D</sup>-diazido 6<sup>A</sup>,6<sup>D</sup>-dideoxy β-cyclodextrin in D<sub>2</sub>O.

### 2.3.4 6<sup>A</sup>,6<sup>D</sup>-diamino 6<sup>A</sup>,6<sup>D</sup>-dideoxy β-Cyclodextrin (5)

The FTIR spectrum of the 6<sup>A</sup>,6<sup>D</sup>-diamino 6<sup>A</sup>,6<sup>D</sup>-dideoxy β-cyclodextrin is shown in Figure 2.17. The spectrum depicted the absorbance at 3400 cm<sup>-1</sup> and 3200 cm<sup>-1</sup> were observed due to -OH stretching hydrogen bonded and stretching of -NH<sub>2</sub>, 2900 cm<sup>-1</sup> (-CH stretching), 1620 cm<sup>-1</sup>, 1490 cm<sup>-1</sup> (ammonium combination bands). Moreover, the disappearances of azide stretching band at 2037 cm<sup>-1</sup> suggest that complete reduction of azide functional groups into amine functional groups.

Figure 2.18 and Figure 2.19 shows the <sup>1</sup>H-NMR spectra of 6<sup>A</sup>,6<sup>D</sup>-diamino 6<sup>A</sup>,6<sup>D</sup>-dideoxy β-cyclodextrin in D<sub>2</sub>O and DMSO-d<sub>6</sub>, respectively. The <sup>1</sup>H NMR spectra of 6<sup>A</sup>,6<sup>D</sup>-diamino 6<sup>A</sup>,6<sup>D</sup>-dideoxy β-cyclodextrin in D<sub>2</sub>O in Figure 2.18 shows the protons signals at δppm: 4.93 (d, 7H, H-1), 3.50 (m, 7H, H-2), 3.83 (m, 7H, H-3), 3.42 (m, 7H, H-4) 3.69 (m, 7H, H-5), 3.70 (d, 12H, H-6) and peaks at 2.70-2.85 (dd, 2H, H-6') due to substitution of two primary hydroxyl groups with two amino functional groups. The <sup>1</sup>H NMR spectra in Figure 2.19 showed the δppm: 4.82 (m, 7H, H-1), 4.27 (m, 7H, H-2), 3.65 (m, 7H, H-3), 3.35 (m, 7H, H-4) 3.55 (m, 7H, H-5), 3.62 (d, 12H, H-6) and peaks at 2.73-2.89 (dd, 2H, H-6') the observed upfield shifts in proton signals and existence of one new peak is due to substitution of two -OH groups with -NH<sub>2</sub> groups. The anisotropic effects of the σ electrons of a C-C bond are small compared to the circulating π electrons and the axis of the C-C bond is the axis of the deshielding cone. Due to anisotropic cone in a rigid cyclodextrin an equatorial proton (α-D-glucose unit) at H-1 gives a signal around δppm 4.93 (downfield). The chemical shifts of protons, i.e., O-H protons in alcohols and N-H protons in amines depend on the concentration. In concentrated solutions of these protons are deshielded by hydrogen bonding when these absorb at lower field (δ 3.5 amine, N-H, δ 4.5 for an alcohol O-H). For <sup>1</sup>H-NMR 6<sup>A</sup>,6<sup>D</sup>-diamino 6<sup>A</sup>,6<sup>D</sup>-dideoxy β-cyclodextrin is diluted with a non-hydrogen bonding solvent (DMSO), hydrogen bonding becomes less important and consequently these resonances are observed at higher field at δppm 2.0. The comparison of protons signal of unsubstituted β-CD and substituted β-CD in two different solvents are shown in Table 2.1 and Table 2.2.

The <sup>13</sup>C NMR spectrum of 6<sup>A</sup>,6<sup>D</sup>-diamino 6<sup>A</sup>,6<sup>D</sup>-dideoxy β-cyclodextrin is shown in Figure 2.20. The spectrum showed aliphatic carbon chemical shifts of β-

cyclodextrin's glucose unit's at  $\delta$ ppm: 101.85 (C-1), 72.42 (C-2), 73.04 (C-3), 82.29 (C-4), 72.26 (C-5), 6.27 (C-6) and one new peak at 30.27 (C-6') due to substitution of two hydroxyl groups on the primary side. It is observed that due to the primary hydroxyl group substitution the signal of the substituted C-6 carbon of the  $\beta$ -cyclodextrin shift upfield from 60.27 ppm to 30.27 ppm (C-6'). These NMR spectra confirmed that the  $-\text{NH}_2$  groups has been attached at the primary hydroxyl side of  $\beta$ -cyclodextrin molecule.

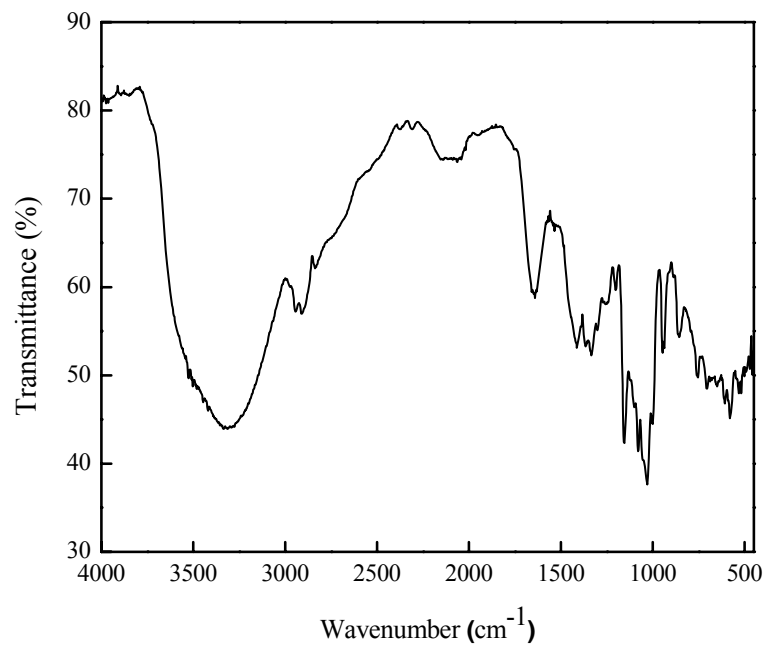


**Figure 2.17** FTIR spectrum of  $6^A,6^D$ -diamino  $6^A,6^D$ -dideoxy  $\beta$ -cyclodextrin.

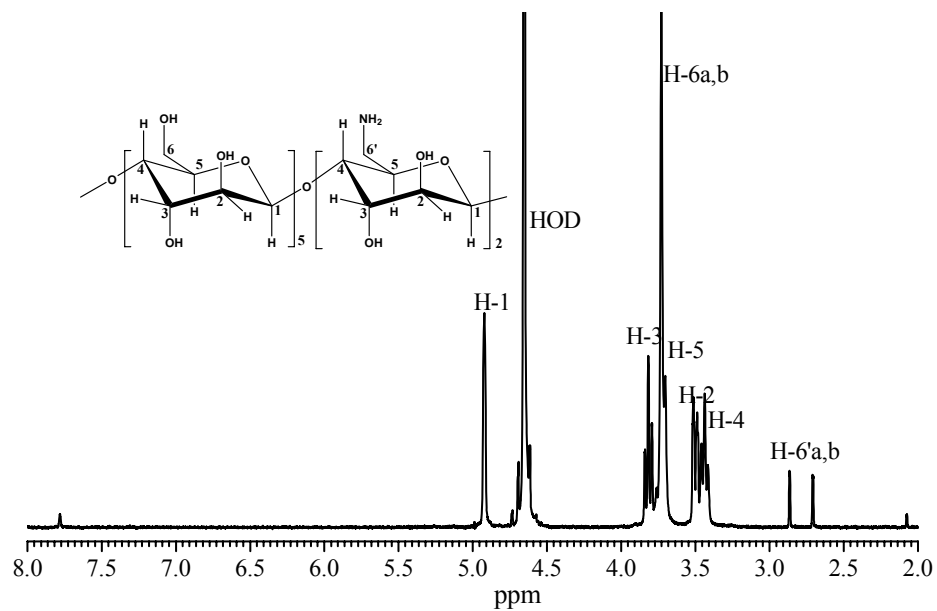


**Figure 2.18**  $^1\text{H}$  NMR spectrum of  $6^A,6^D$ -diamino  $6^A,6^D$ -dideoxy  $\beta$ -cyclodextrin in  $\text{D}_2\text{O}$ .

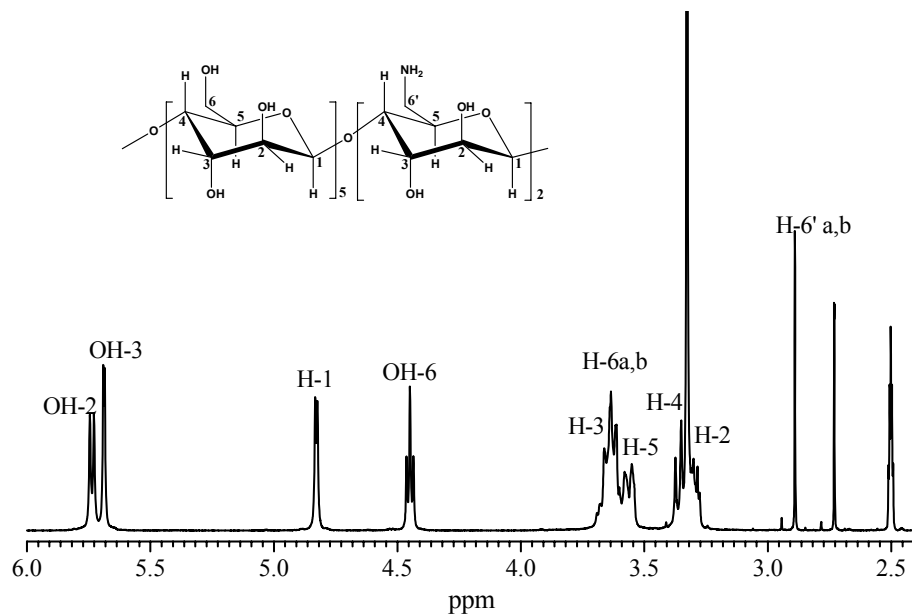


**Figure 2.19**  $^1\text{H}$  NMR spectrum of  $6^A,6^D$ -diamino  $6^A,6^D$ -dideoxy  $\beta$ -cyclodextrin in  $\text{DMSO-d}_6$ .

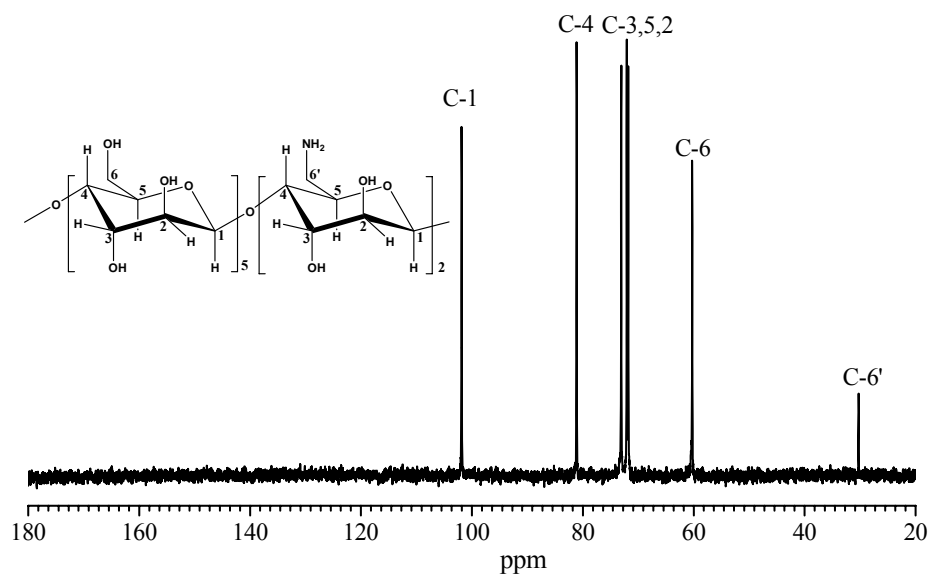


**Figure 2.20**  $^{13}\text{C}$  NMR spectrum of  $6^A,6^D$ -diamino  $6^A,6^D$ -dideoxy  $\beta$ -cyclodextrin in  $\text{D}_2\text{O}$ .

**Table 2.1**  $^1\text{H}$  NMR chemical shifts,  $\delta(\text{ppm})$ , of C-H protons in unsubstituted  $\beta$ -CD and substituted  $\beta$ -CD in  $\text{D}_2\text{O}$ .

CDs	H-1	H-2	H-3	H-4	H-5	H-6a,b	H-6'a,b	H-Ar
$\beta$ -CD	4.92	3.51	3.83	3.42	3.70	3.72	-	-
Bicapped $\beta$ -D	4.93	3.52	3.84	3.42	3.70	3.71	5.20	7.50-8.90
Diiodo $\beta$ -CD	4.92	3.49	4.82	3.40	3.69	3.72	2.70-2.86	-
Diazido $\beta$ -CD	4.92	3.50	3.82	3.41	3.71	3.72	2.70-2.85	-
Diamino $\beta$ -CD	4.93	3.50	3.83	3.42	3.69	3.70	2.70-2.85	-

**Table 2.2**  $^1\text{H}$  NMR chemical Shifts,  $\delta(\text{ppm})$ , of C-H protons in unsubstituted  $\beta$ -CD and substituted  $\beta$ -CD in  $\text{DMSO-d}_6$ .

CDs	H-1	H-2	H-3	H-4	H-5	H-6a,b	H-6'a,b	H-Ar
$\beta$ -CD	4.83	3.26	3.66	3.35	3.55	3.63	-	-
Bicapped $\beta$ -CD	4.99	3.38	3.98	3.59	3.69	3.70	5.2	7.50-8.90
Diamino $\beta$ -CD	4.82	3.27	3.65	3.35	3.55	3.62	2.73-2.89	-

**Table 2.3**  $^{13}\text{C}$  NMR chemical Shifts,  $\delta(\text{ppm})$ , of unsubstituted  $\beta$ -CDs and substituted  $\beta$ -CD.

CDs	C-1	C-2	C-3	C-4	C-5	C-6	C-6'	C-Ar
$\beta$ -CD in $\text{D}_2\text{O}$	101.10	71.85	73.21	81.18	72.16	60.30	-	-
$\beta$ -CD in $\text{DMSO-d}_6$	102.08	71.66	73.21	81.55	72.89	59.76	-	-
Bicapped $\beta$ -CD in $\text{DSMO-d}_6$	102.10	71.67	73.22	81.57	72.89	60.01	41.67	126-147
Diiodo $\beta$ -CD in $\text{D}_2\text{O}$	101.84	72.12	73.40	81.15	72.35	60.21	10.08	-
Diazido $\beta$ -CD in $\text{D}_2\text{O}$	101.79	71.88	73.35	81.27	72.76	60.40	36.90	-
Diamino $\beta$ -CD in $\text{D}_2\text{O}$	101.82	71.60	73.21	81.28	72.58	60.18	30.16	-

## 2.4 Conclusions

In summary, the short and effective synthesis of the selectively difunctionalized derivatives of  $\beta$ -cyclodextrin such as biphenyl bridge A,D capped  $\beta$ -CD, diiodo  $\beta$ -CD, diazido  $\beta$ -CD and diamino  $\beta$ -CD were described by simple oxidoreductive substitution reactions without protection of hydroxyl groups. In this synthesis procedure we introduced selectively more reactive arene sulfonyl ester functional groups on the primary hydroxyl side of  $\beta$ -cyclodextrin. These modified di-substituted  $\beta$ -cyclodextrin derivatives shows higher water solubility and moderate reactivity over the parent  $\beta$ -cyclodextrin. This selectively functionalized  $\beta$ -cyclodextrins are useful monomers for the synthesis of cyclodextrin polymers in which  $\beta$ -cyclodextrins are incorporated into the main-chain of the polymers.

## References

1. J. Szejtli, *Chem. Rev.*, **1998**, 98, 1743-1753.
2. K. Fujita, A. Matsunaga and T. Imoto, *J. Am. Chem. Soc.*, **1984**, 106, 5740-5741.
3. S. M. Zarcero A. L. Crego I. del Hierro, I. Sierra and M. L. Marina, *Electrophoresis*, **2008**, 29(22), 4575-4582.
4. I. Tabushi and K. Yamamur and T. Nabeshima, *J. Am. Chem. Soc.*, **1984**, 106, 5267-5270.
5. I. Tabushi and Y. Kuroda, *J. Am. Chem. Soc.*, **1984**, 106, 4580-4584.

*Chapter 3*  
*Synthesis of Cyclodextrin based Polymers*

## Chapter 3

### Synthesis of Cyclodextrin based Polymers

#### 3.1 Introduction

In recent years, many interesting cyclodextrin-containing polymeric systems have been described in literature. These systems have to be optimized and extensively evaluated in different field of chemistry concerning their safety and efficacy, making future novel applications of these materials in the biomedical and pharmaceutical field feasible. The excellent enhanced properties of cyclodextrin polymers have inspired the developments of novel synthesis of cyclodextrin polymers and biomaterials<sup>1,2</sup>. Cyclodextrin based polymers are well known host materials for the formation of inclusion complexes (ICs) with specific drug molecules via non-covalent interaction with their hydrophobic cavities. This characteristic makes them invaluable in the field of pharmaceutical and drug delivery. The most common pharmaceutical application of CDs and their chemical derivatives are to enhance the aqueous solubility of the complex species, photo stability and bioavailability of the complex drugs and eventually to reduce side effects<sup>3-8</sup>. The weaker aqueous solubility of the cheapest  $\beta$ -cyclodextrin can limit its practical application towards drug delivery systems<sup>9</sup>. One of the effective approaches to improve the aqueous solubility of  $\beta$ -cyclodextrin is to prepare  $\beta$ -cyclodextrin based polymers consisting  $\beta$ -cyclodextrin as a part of the main-chain<sup>10,11</sup>. The reported methods of synthesis of  $\beta$ -cyclodextrin polymers only deal with crosslinking of  $\beta$ -cyclodextrin with different reactants or attachment of  $\beta$ -cyclodextrin on the synthesized polymers<sup>12-17</sup>. Linear cyclodextrins based polymers have several advantages, such as higher water-solubility, inclusion ability and moderate cavity size<sup>18,19</sup>. Controlling the degree of substitution and reactivity is an important phenomenon in balancing the water-solubility of the  $\beta$ -cyclodextrin based polymers. For this purpose, it is necessary to design the synthesis methods which have controlled the reactivity with no more crosslinking<sup>20</sup>. However, there still exists a need in the art for linear cyclodextrin polymers in which the cyclodextrin moiety is part of the main chain and not a pendant moiety off the main chain and a method for their preparation<sup>21</sup>.

Cyclodextrin polymers are of interest of many researchers owing to their unique complex forming property and higher hydrophilicity. Solubilization of hydrophobic drug with biocompatibility and controlled release across a membrane and increased stability constant are some of the major applications of water-soluble cyclodextrin based polymers<sup>22</sup>. The first cyclodextrin polymers reported were prepared by cross-linking with epichlorohydrine<sup>23</sup>. A crosslinked structure is produced when cyclodextrins are reacted with bi- or polyfunctional reagents. The most widely used crosslinking agents are diepoxides and diisocyanate. The major problem in polycondensation of cyclodextrin with cross-linking agent is no control over the degree of cross-linking and resulted product has less water-solubility<sup>24</sup>.

Thus, the aim of this chapter was to design the synthesis of highly water-soluble  $\beta$ -cyclodextrin polymers consisting  $\beta$ -cyclodextrin in the main chain of the polymers. For this purpose, reagent cyanuric chloride (CC) has been chosen as a short linking to connect  $\beta$ -cyclodextrin and PEG in the main-chain of the polymers. The chemistry of cyanuric chloride is that it contains three chlorine atoms and the uniqueness is that all these three chlorine atoms react at three different temperature regions. First chlorine atom react at 0-5°C, second chlorine atom react at 25-30°C and third chlorine atom react at more than 60°C. Using this controlled temperature dependent reactivity of cyanuric chloride, linear  $\beta$ -cyclodextrin and PEG based polymers was synthesized. Furthermore, the selectively functionalized  $\beta$ -cyclodextrin described in second chapter also used as monomer for the preparation of linear water-soluble polymers using short linker urea or thiourea to connect  $\beta$ -cyclodextrin in the main-chain of the polymers. In this chapter, we adopted two methods for the preparation of water-soluble  $\beta$ -cyclodextrin based polymers (i) using the temperature controlled reactivity of the linker cyanuric chloride and (ii) using the difunctional  $\beta$ -cyclodextrins connected with a short linker.

## **3.2 Experimental**

### **3.2.1 Materials**

$\beta$ -Cyclodextrin was obtained from Signet Chemical Corporation, Mumbai as a gift sample and dried overnight under a vacuum oven at 60°C, then used without further purification. Cyanuric chloride, PEG with different molecular weight, urea, thiourea and sodium carbonate were purchased from Merck India. Diiodo  $\beta$ -cyclodextrin synthesized in Chapter 2 was used as monomer. Double distilled water was used throughout the experiments.

### **3.2.2 Measurements**

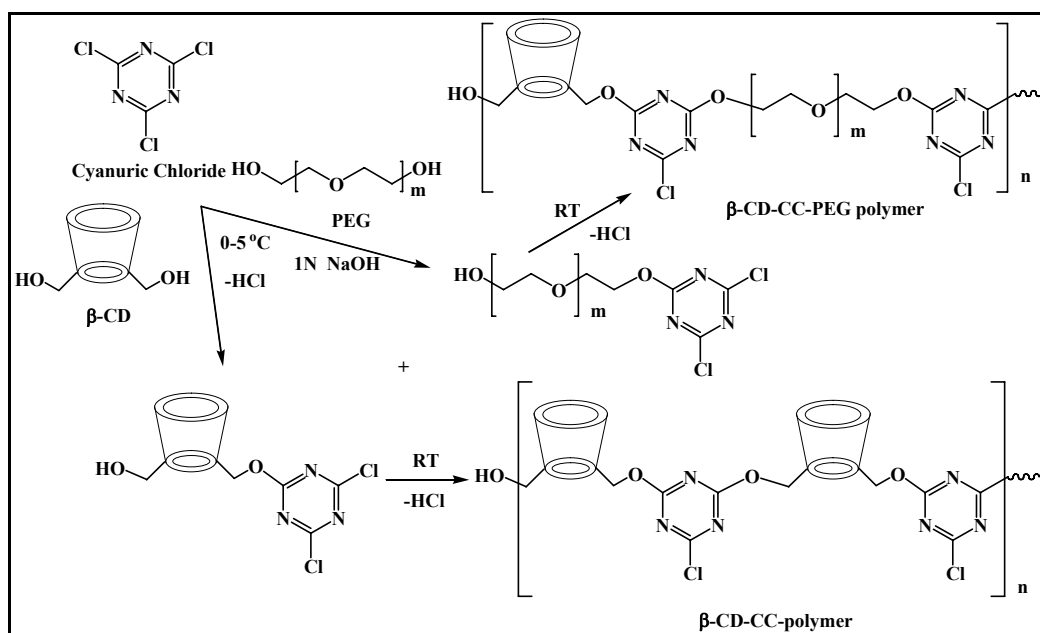
Fourier transform infrared spectra (FTIR) were recorded on a Shimadzu (8400s) spectrophotometer at 30 scans by KBr pellet method at  $10^{-4}$  resolution. Thermogravimetric analysis (TGA) was made on a Shimadzu, TGA-50 system with a heating rate of 10°C/min in the temperature range of 25-700°C. X-ray powder diffraction patterns were taken on a computer-controlled RIGAKUDMAX-2200. NMR spectra were recorded on a Bruker Avance spectrometer operating at 400 MHz at room temperature. Samples were prepared in D<sub>2</sub>O containing TMS as an internal standard. The weight average molecular weight of the polymers was determined by Static Laser Light Scattering technique with Ga-As semiconductor laser (mini Dawn Tri-Star, Wyatt Technology) instrument at laser wavelength 690 nm.

### **3.2.3 Synthesis of $\beta$ -Cyclodextrin and Cyanuric chloride as Linker based Polymers**

$\beta$ -CD based homopolymer and  $\beta$ -cyclodextrin-polyethylene glycols based copolymers were synthesized by one-step condensation polymerization using short linker cyanuric chloride. The reactions were shown in Scheme 3.1. Typically, a measured quantity of  $\beta$ -CD (1 mole) and cyanuric chloride (1 mole) were taken in different flasks and dissolved separately in the required amount of distilled water and pH (>12) was maintained using 1N NaOH solution. 10 mL of this  $\beta$ -CD solution of predetermined pH (>12) was taken in a round bottom flask and kept in ice bath with continuous stirring, the temperature being maintained between 0-5°C. To this, 10 mL of the

cyanuric chloride solution was added drop wise with the help of pressure equalizing funnel. During the addition, temperature was maintained between 0-5°C. After the addition the reaction was continued with stirring, temperature was maintained between 0-5°C for 4-5h. Stirring was continued for 12h while the contents were allowed to attain ambient temperature (30°C). The polymerization was stopped by addition of 0.1N HCl solution. The polymers were purified in aqueous solution by membrane filtration using a polymer membrane with a molecular mass cut-off of 1000 Da. Residual unpolymerized and substituted  $\beta$ -CD monomers were removed in order to investigate the properties of the high molecular weight polymer fractions only. The solution obtained was directly freeze-dried to get an off-white fluffy product.

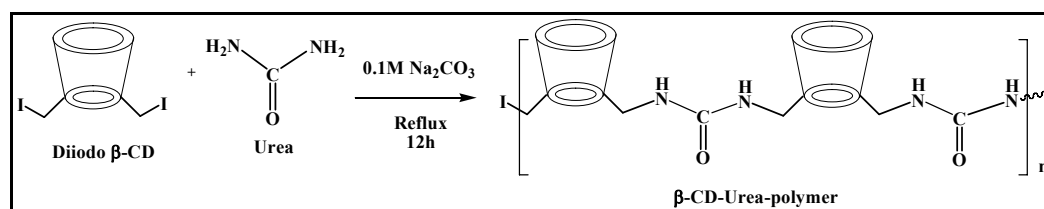
Similarly  $\beta$ -Cyclodextrin and polyethylene glycols based copolymers were also synthesized utilizing temperature dependent reactivity of short linker cyanuric chloride by taking 0.5: 1: 0.5 mole ratio of  $\beta$ -CD: cyanuric chloride: polyethylene glycols.



**Scheme 3.1** Synthesis of  $\beta$ -cyclodextrin-cyanuric chloride and PEG based polymers.

### 3.2.4 Synthesis of $\beta$ -Cyclodextrin and Urea or Thiourea as Linker based Polymers

$\beta$ -Cyclodextrin based polymers were synthesized by the condensation polymerization of difunctional  $\beta$ -CD monomer with difunctional short linker (urea or thiourea) to give linear main-chain  $\beta$ -CD polymers as shown in Scheme 3.2. Diiodo  $\beta$ -CD (1.355 g, 1 mmole) was dissolved in 0.1 M sodium carbonate stirred and degassed with nitrogen atmosphere after obtained clear solution, short linker urea (0.06 g, 1 mmole) or thiourea (0.076 g, 1 mmole) was added. The solution was stirred under reflux for 12 hrs. The progress of the polymerization was monitored by viscosity measurements during the course of reaction. The viscosity of the solution increased with reaction time. After cooling to room temperature and acidifying with 0.1N HCl, the solution was subjected to ultrafiltration using polymer membrane MWCO of 1K to remove unreacted monomers. The resulted concentrated solution was lyophilized to obtained solid white polymers. The polymers were dried under vacuum overnight at room temperature.



**Scheme 3.2** Reaction scheme for the synthesis of  $\beta$ -cyclodextrin polymer with short linker Urea.

### 3.2.5 Determination of Aqueous Solubility of Polymers

The aqueous solubility of the synthesized  $\beta$ -CD polymers were measured using a simple technique. 0.1 g of  $\beta$ -cyclodextrin polymer was added to 0.5 mL of water to ensure the solution reaching saturation. The solution was mechanically shaken for 4 h and then incubated overnight at room temperature. The solution was then filtered through a microfilter-syringe. The filtrate was dried in an oven for sufficient period until a constant weight was reached. The solubility was estimated in terms of the

weight of sample in the saturated solution and solution volume. This was repeated to get constant values within an error of  $\pm 0.05$  g.

### 3.3 Results and Discussion

The  $\beta$ -cyclodextrin-cyanuric chloride polymer and  $\beta$ -cyclodextrin-cyanuric chloride-polyethylene glycols based copolymers were successfully synthesized under controlled temperature condition by using cyanuric chloride (2,4,6-trichloro-1,3,5-triazine) as the short linking agent between  $\beta$ -cyclodextrin monomers in alkaline medium. Cyanuric chloride can act as an excellent central linker because of all three chlorine atoms react at different temperatures region. This allows a possible synthetic methodology for forming linear highly water-soluble polymers. The first step in the synthesis of the  $\beta$ -cyclodextrin polymers was the preparation of dichlorotriazine sodium salt from the dispersion of cyanuric chloride in alkaline water. The second step is the condensation reaction of two chlorine groups of dichlorotriazine sodium salt with  $\beta$ -cyclodextrin and PEG under alkaline conditions, controlled pH (<10) and controlled temperature (<30°C). The preparation of the dichlorotriazine sodium salt reduces the degree of substitution (DS) of the reactive groups from DS = 1.0 to 0.4 due to the precomplexation effect. This implies that there are only 2–3 reactive triazine groups per cyclodextrin molecule whose reactivity has been shown to be between 2.3–2.7. If the degree of substitution is higher, it would lead to the formation of crosslinked and hence insoluble polymers by reaction with itself. However, all the synthesized polymers showed higher solubility than the pristine  $\beta$ -cyclodextrin even though the linker cyanuric chloride is insoluble in water. This implies that the polymers obtained were linear with very low degree of branching.

Similarly,  $\beta$ -cyclodextrin-urea or thiourea based polymers were synthesized by condensation reaction in aqueous alkaline medium. The urea and thiourea has been effectively used as linking agent between diiodo functionalized  $\beta$ -cyclodextrin.

#### 3.3.1 Aqueous Solubility of $\beta$ -CD Polymers

As expected, after polymerization there is a significant enhancement of the aqueous solubility of  $\beta$ -CD. The solubility values for  $\beta$ -CD polymers at 25°C are shown in Table 3.1. The water-solubility of the synthesized  $\beta$ -CD polymers is almost seven times higher than that of the pristine  $\beta$ -CD. The low water-solubility of pristine  $\beta$ -CD is attributed to the intramolecular hydrogen bonding between the secondary hydroxyl groups, which are unfavorable to the interaction between  $\beta$ -CD and

surrounding water molecules. The  $\beta$ -CD molecule is rigid as compared to the  $\alpha$ -CD and  $\gamma$ -CD. The reason for this difference in water-solubility is the presence of one glucopyranose unit in distorted form in the  $\alpha$ -CD and the non-polar flexible structure of the  $\gamma$ -CD. The introduction of cyanuric chloride or thiourea as linker via condensation reaction disrupts this intramolecular hydrogen bonding, thus increasing the aqueous solubility even though the triazine linker is insoluble in water. In case of polyethylene glycols based copolymers, PEG provides the unique chemical functionality as water-solubility with the biocompatibility, increases the aqueous solubility and the flexibility of the polymers. Since all of the  $\beta$ -CD polymers are highly water-soluble it implies that there was no cross linking occurring during the polycondensation reaction. The solubility data reported here are average of two reading and have an accuracy of  $\pm 0.1$ . However, a general observation is that the  $\beta$ -CD-CC polymer has a lower water-solubility as compared to the other  $\beta$ -CD polymers. The increase in the distance between the two cyclodextrins with PEG linkers increased the water-solubility of the  $\beta$ -CD polymers.

**Table 3.1** Aqueous solubility of  $\beta$ -CD polymers at 25°C

<b>Samples</b>	<b>Aqueous solubility mg/mL</b>	<b>Solubility Relative to <math>\beta</math>-CD</b>
$\beta$ -CD	18.5	1.00
$\beta$ -CD-CC-Polymer	124	6.70
$\beta$ -CD:CC:DEG-Polymer	132	7.14
$\beta$ -CD:CC:TEG-Polymer	134	7.24
$\beta$ -CD:CC:PEG 400- Polymer	137	7.40
$\beta$ -CD-Urea-Polymer	126	6.81
$\beta$ -CD-Thiourea-Polymer	128	6.91

### 3.3.2 Characterization of $\beta$ -Cyclodextrin and Cyanuric chloride as Linker based Polymers

#### 3.3.2.1 Fourier Transform Infrared Spectroscopy (FTIR)

The FTIR spectra of the  $\beta$ -CD,  $\beta$ -CD-CC polymer and  $\beta$ -CD-CC-DEG copolymer are shown in Figure 3.1. The FTIR spectrum (Figure 3.1 a) of pristine  $\beta$ -CD showed the typical characteristic absorption bands at  $3331\text{ cm}^{-1}$  (-OH stretching hydrogen bonded),  $2930\text{ cm}^{-1}$  (C-H stretching),  $1641\text{ cm}^{-1}$  (OH bending),  $1365\text{ cm}^{-1}$  (OH deformation),  $1168\text{ cm}^{-1}$  (C-O-C stretching and OH bending),  $1080\text{ cm}^{-1}$  and  $1032\text{ cm}^{-1}$  for (C-O-C stretching). The FTIR spectra of the  $\beta$ -CD-CC polymer and  $\beta$ -CD-CC-DEG polymer (Figure 3.1 b and c) showed all the typical characteristic absorption bands of  $\beta$ -CD and also absorption bands arising due to the linker cyanuric chloride at  $1724\text{ cm}^{-1}$  assigned to the -C=N stretching vibration of the cyanuric chloride which is absent in the spectrum of the pristine  $\beta$ -CD. This suggests that triazine is now part of the polymer chain.

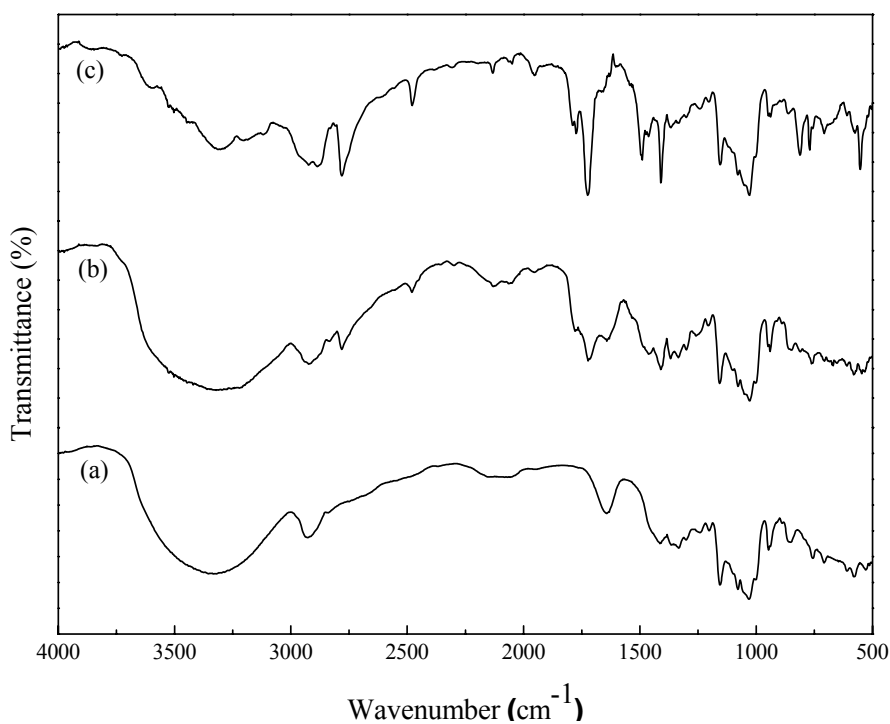


**Figure 3.1** FTIR spectra of (a)  $\beta$ -CD, (b)  $\beta$ -CD-CC polymer and (c)  $\beta$ -CD-CC-DEG polymer.

### 3.3.2.2 Nuclear Magnetic Resonance Spectroscopy (NMR)

The  $^1\text{H}$  NMR spectra of the  $\beta$ -CD,  $\beta$ -CD-CC polymer and  $\beta$ -CD-CC-DEG polymer are shown in Figure 3.2. The  $^1\text{H}$  NMR spectral resonance signals of  $\beta$ -CD and  $\beta$ -CD polymer look similar due to similar structure. The pristine  $\beta$ -CD (Figure 3.2 a) showed the proton signals at  $\delta$ ppm: 4.92 (s, 7H, C<sup>1</sup>H), 3.81 (t, 7H, C<sup>3</sup>H), 3.72 (m, 14H, C<sup>6</sup>H, C<sup>5</sup>H), 3.51 (d, 7H, C<sup>2</sup>H) and 3.43 (m, 7H, C<sup>4</sup>H). The  $^1\text{H}$  NMR spectra of  $\beta$ -CD-CC polymer and  $\beta$ -CD-CC-DEG polymer (Figure 3.2 b and c) showed all the typical proton signals of parent  $\beta$ -CD, except some upfield shift of proton signals and a shoulder signal at 3.30  $\delta$ ppm. This shoulder peak was observed in the spectra of polymers may be due to the presence of linker between  $\beta$ -CDs which afford the changes in the chemical environment of  $\beta$ -CD after polymerization. In case of DEG based polymer, one extra proton signal arising at 3.60  $\delta$ ppm was observed due to the  $-\text{CH}_2-\text{CH}_2-$  linkage of the DEG, which is absent in the spectra of  $\beta$ -CD and  $\beta$ -CD-CC polymer.

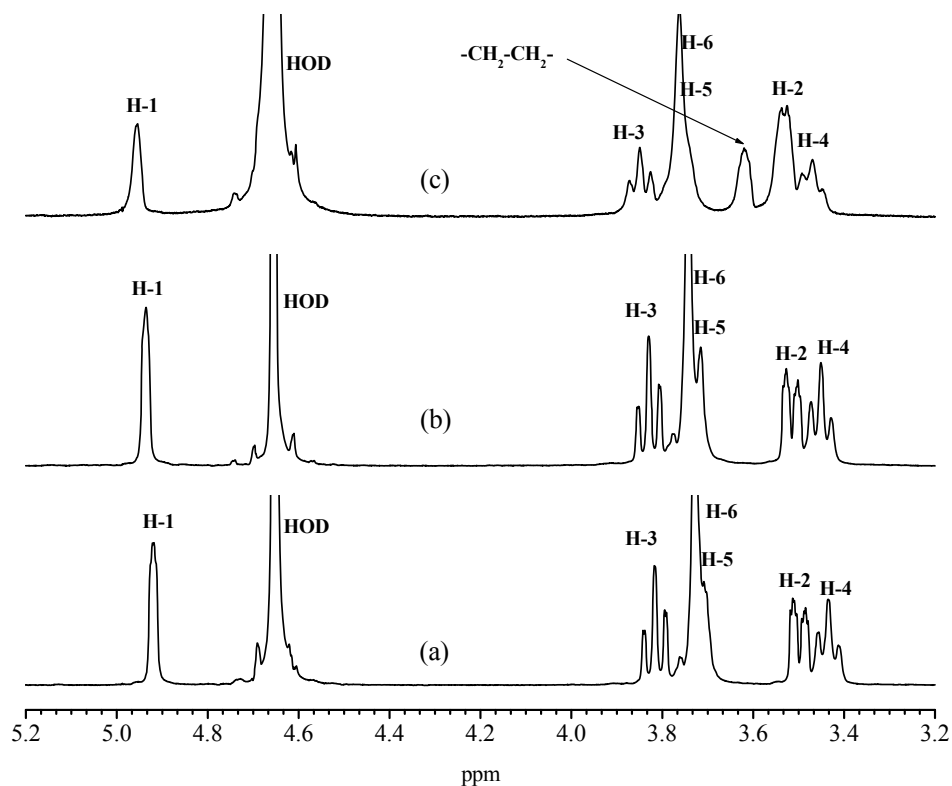


**Figure 3.2**  $^1\text{H}$  NMR spectra of (a)  $\beta$ -CD, (b)  $\beta$ -CD-CC polymer and (c)  $\beta$ -CD-CC-DEG polymer in  $\text{D}_2\text{O}$ .

The  $^{13}\text{C}$  NMR spectra of the  $\beta$ -CD,  $\beta$ -CD-CC polymer and  $\beta$ -CD-CC-DEG polymer are shown in Figure 3.3. The  $^{13}\text{C}$  NMR spectrum of pristine  $\beta$ -CD (Figure 3.3 a) showed the typical glucose unit's carbon chemical shifts at  $\delta\text{ppm}$ : 101.2 (C-1), 81.1 (C-4), 73.1 (C-3), 72.0 (C-5), 71.8 (C-2) and 60.3 (C-6). The  $^{13}\text{C}$  NMR spectra of  $\beta$ -CD-CC polymer and  $\beta$ -CD-CC-DEG polymer (Figure 3.3 b and c) showed all these typical carbon chemical shifts of pristine  $\beta$ -CD and also some extra carbon chemical shifts at 154  $\delta\text{ppm}$  (C=N), 71.6  $\delta\text{ppm}$  (C-Cl) and 60.1  $\delta\text{ppm}$  (C-CH<sub>2</sub>-) arising from linker cyanuric chloride and DEG. This result confirmed the incorporation of linker in to the main-chain of the polymers.

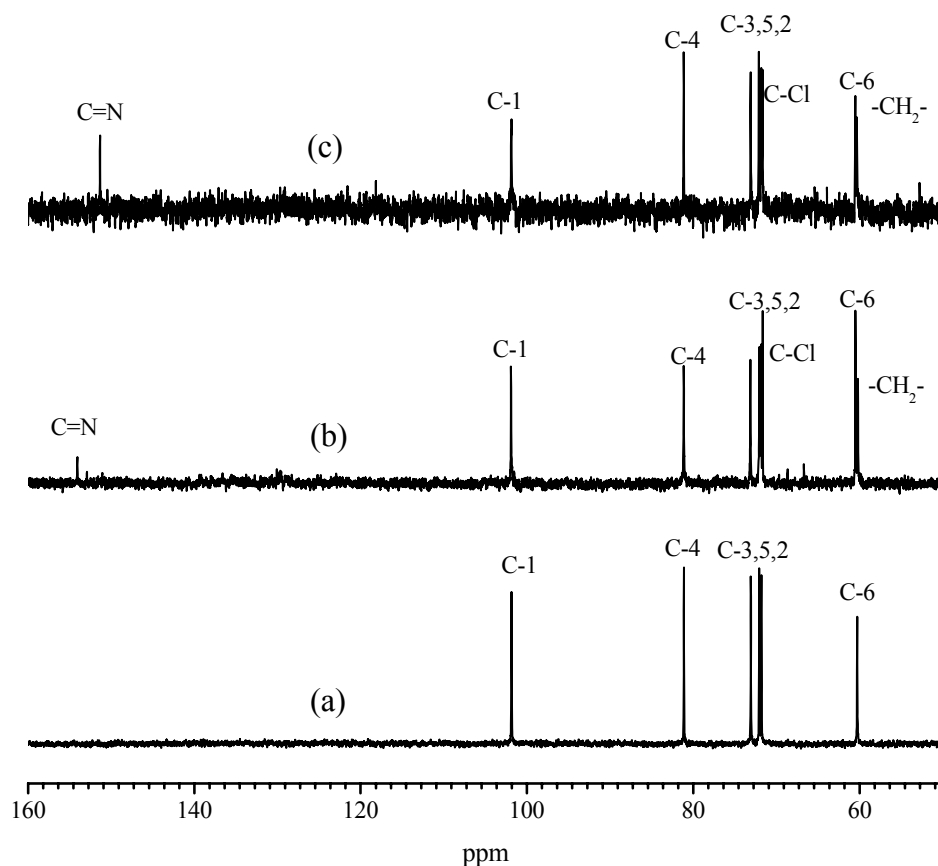


**Figure 3.3**  $^{13}\text{C}$  NMR spectra of (a)  $\beta$ -CD, (b)  $\beta$ -CD-CC polymer and (c)  $\beta$ -CD-CC-DEG polymer in  $\text{D}_2\text{O}$ .

### 3.3.2.3 Thermogravimetric Analysis (TGA)

Thermogravimetric analysis gives the thermal stability of the polymers and also gives an idea about the presence of different structural units through their degradation pattern. The thermal analysis of the  $\beta$ -CD,  $\beta$ -CD-CC polymer and  $\beta$ -CD-CC-DEG polymer are shown in Figure 3.4. The degradation pattern showed weight loss at three different temperature regions. The first weight loss at 106°C was due to the loss of moisture, the second weight loss at 300°C as dehydration of  $\beta$ -CD, and third weight loss at 367°C as a decomposition of glucose in  $\beta$ -CD. However, in case of the  $\beta$ -CD-CC polymer and  $\beta$ -CD-CC-DEG polymer, the thermogram was different; the first weight loss at around the same temperature due to the loss of moisture but second weight loss was at a lower temperature due to the formation of polymers of the  $\beta$ -CD unit with the resulting loss of the crystalline nature of the  $\beta$ -cyclodextrin molecule. Subsequent loss occurs due to the decomposition of the glucose and triazine linker after  $\beta$ -CD polymers are quite stable above 500°C.

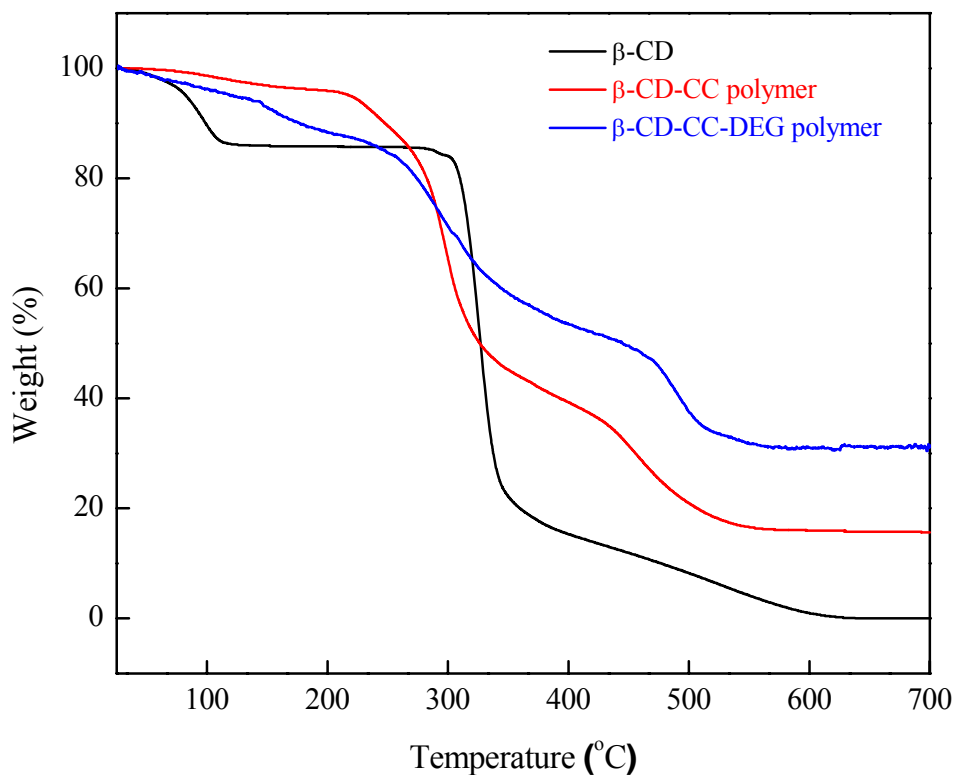


**Figure 3.4** TGA curves of  $\beta$ -CD,  $\beta$ -CD-CC polymer and  $\beta$ -CD-CC-DEG polymer.

### 3.3.2.4 X-ray Diffraction (XRD)

The X-ray diffraction pattern of the  $\beta$ -CD,  $\beta$ -CD-CC polymer and  $\beta$ -CD-CC-DEG polymer are shown in Figure 3.5. The X-ray diffraction pattern of the synthesized  $\beta$ -CD-CC polymer and  $\beta$ -CD-CC-DEG polymer (Figure 3.5 b and c) showed that the polymers do not have typical  $2\theta$  values of the pristine  $\beta$ -CD. It can be seen that the synthesized polymers have a different structure than that of the pristine  $\beta$ -CD ( $2\theta = 9, 12.5, 19.6, 23.0, 27.0, \text{ and } 34.88$ ) with the total suppression of the crystalline nature of the pristine  $\beta$ -CD. XRD data showed that the  $\beta$ -CD was modified due to the condensation reaction with cyanuric chloride and converted to amorphous polymers.

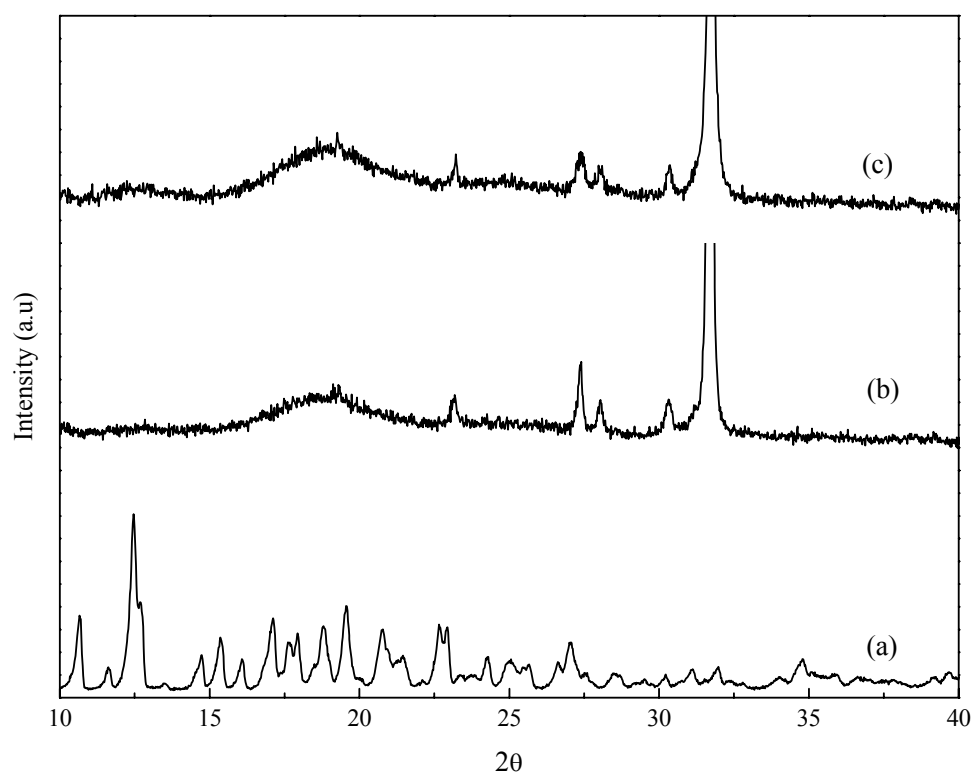


**Figure 3.5** XRD patterns of (a)  $\beta$ -CD, (b)  $\beta$ -CD-CC polymer and (c)  $\beta$ -CD-CC-DEG polymer.

### 3.3.2.5 Molecular Weight (Mw)

The solid polymers obtained after purification by ultrafiltration and freeze drying, the average molecular mass was determined by static laser light scattering technique (SLS) using Debye plot. The scattering intensity of the dilute solution was used to measure the molecular weight of the polymer. The molecular weight was determined by using Rayleigh ratio described as given below, where K is an optical constant, C is the polymer concentration, M is the weight average molecular weight, and  $A_2$  is the 2nd virial coefficient (representative of the magnitude of polymer particle-solvent interactions).

*Rayleigh ratio*

$$\frac{KC}{R\theta} = \frac{1}{M} + 2A_2C \quad (3.1)$$

The Rayleigh expression given above is represented graphically in the form of a Debye plot showing the concentration  $KC/R\theta$  as shown in Figure 3.6. The average molecular weights of the polymers were obtained and shown in Table 3.2

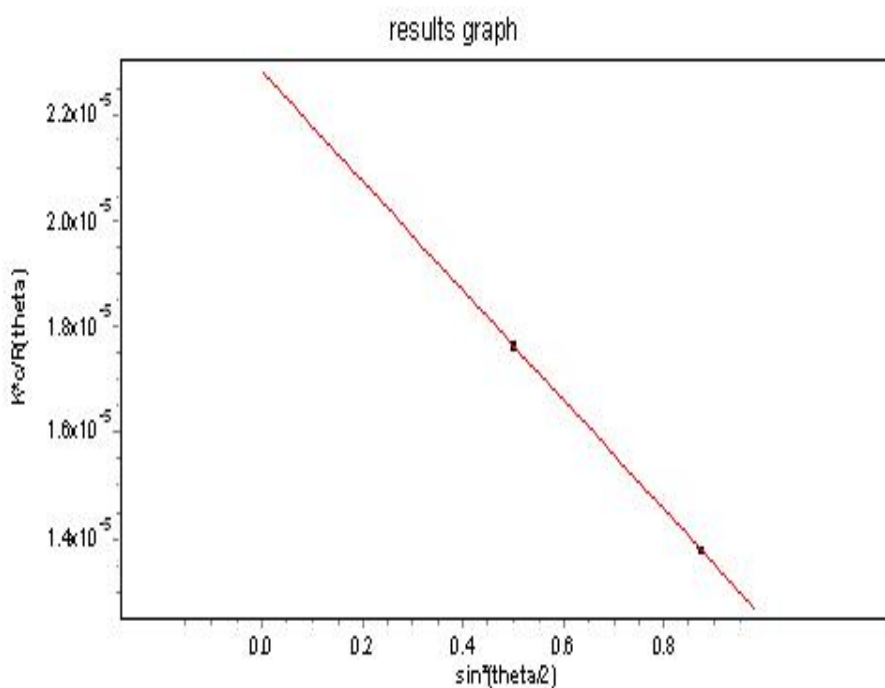


**Figure 3.6** Debye plot of  $\beta$ -CD-CC polymer.

**Table 3.2** Molecular Weight of  $\beta$ -CD-CC-PEG polymers at 25°C by SLS

<b>Samples</b>	<b>Molecular Weight (SLS)</b>
$\beta$ -CD	1,135
$\beta$ -CD-CC-Polymer	26,578
$\beta$ -CD:CC:DEG-Polymer	27,234
$\beta$ -CD:CC:TEG-Polymer	27,648
$\beta$ -CD:CC:PEG 400-Polymer	28,786

### 3.3.3 Characterization of $\beta$ -cyclodextrin and urea or thiourea as linker based polymers

#### 3.3.3.1 Fourier Transform Infrared Spectroscopy (FTIR)

The FTIR spectra of diiodo  $\beta$ -CD, Urea and  $\beta$ -CD-Urea polymer are presented in Figure 3.7. The FTIR spectral data of polymer (Figure 3.7 c) clearly showed an evidence of polycondensation between diiodo  $\beta$ -CD and Urea with the appearance of a new absorption band ascribed to the secondary amide ( $-\text{NH}-\text{C}=\text{O}$ ) stretching vibration at  $1632\text{ cm}^{-1}$  arising near to the primary amide ( $-\text{NH}_2-\text{C}=\text{O}$ ) stretching vibration at  $1668\text{ cm}^{-1}$  and also disappearance of  $1159\text{ cm}^{-1}$  band characteristic absorption band of  $-\text{CH}_2-\text{I}$  was observed due to the condensation of diiodo  $\beta$ -CD and Urea.

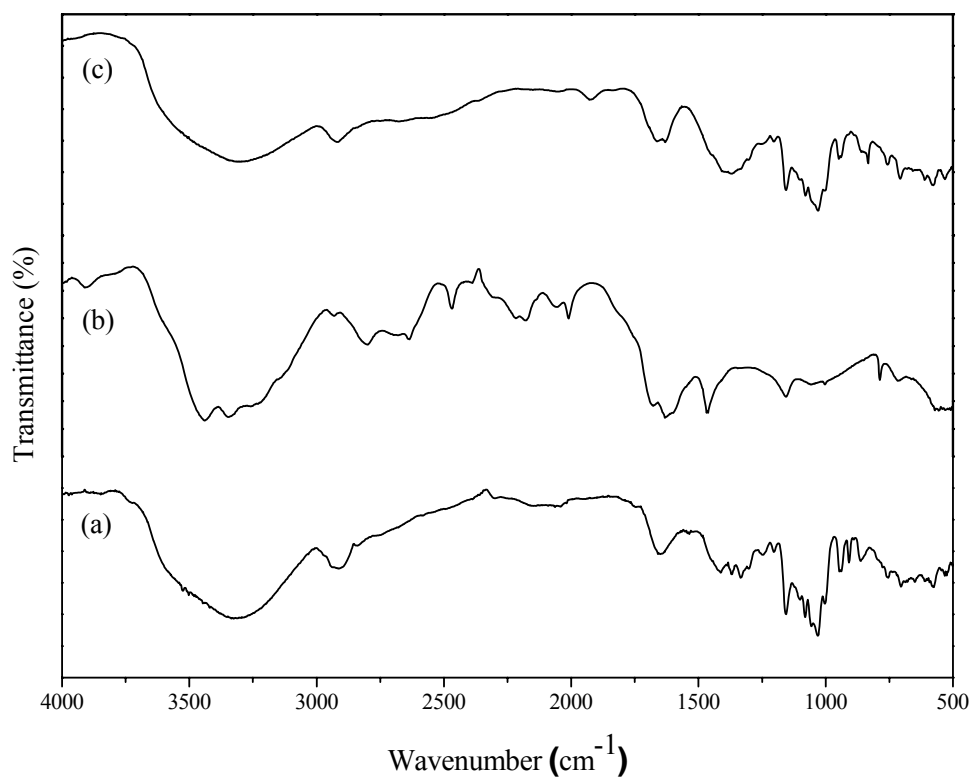


**Figure 3.7** FTIR spectra of (a) diiodo  $\beta$ -CD, (b) Urea and (c)  $\beta$ -CD-Urea polymer.

### 3.3.3.2 Nuclear Magnetic Resonance Spectroscopy (NMR)

Further corroboration of condensation reaction between selectively difunctionalized  $\beta$ -CD and short linker urea comes from the NMR analysis. The  $^1\text{H}$  and  $^{13}\text{C}$  NMR spectra of diiodo  $\beta$ -CD and  $\beta$ -CD-Urea polymer are shown in Figure 3.8 and Figure 3.9, respectively. The  $^1\text{H}$  NMR spectra of diiodo  $\beta$ -CD and  $\beta$ -CD-Urea polymer look similar due to the same structural features except one new proton signal was observed at 5.94  $\delta$ ppm for the  $\beta$ -CD-Urea polymer correspond to the proton of urea linker. Similarly  $^{13}\text{C}$  NMR spectra of the diiodo  $\beta$ -CD and  $\beta$ -CD-Urea polymer shows all the carbon chemical shifts of the modified  $\beta$ -CD along with one extra carbon chemical shift at 162.6  $\delta$ ppm carbonyl ( $-\text{C}=\text{O}$ ) carbon due to the incorporation of urea linker in to the main-chain of the polymer with  $\beta$ -CD and it was also observed that the C-6' (10  $\delta$ ppm) of diiodo  $\beta$ -CD (adjacent to  $-\text{I}$ ) shifted to downfield (30  $\delta$ ppm) due to more electro-negativity of nitrogen (adjacent to  $-\text{NH}$ ).

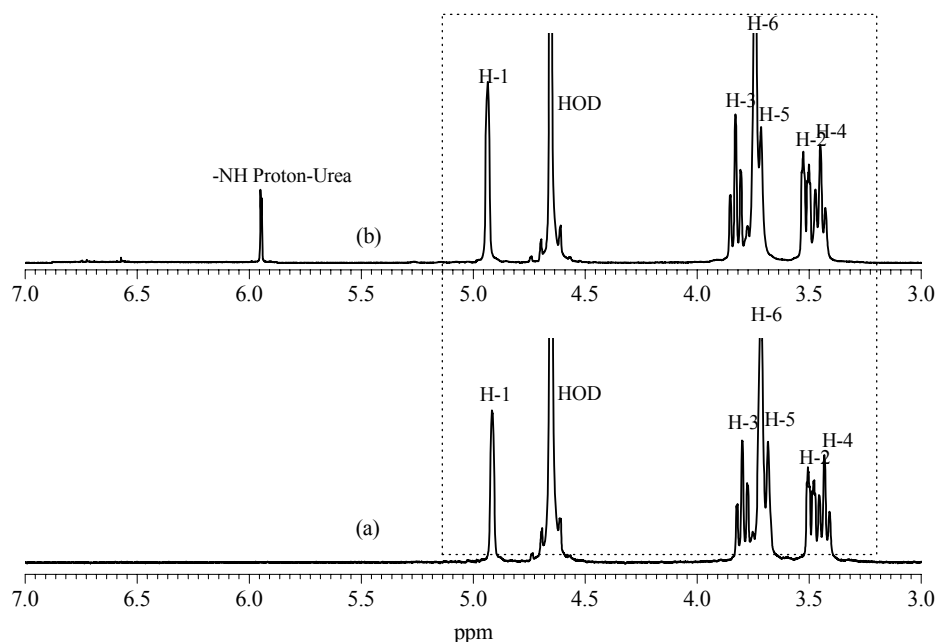


**Figure 3.8**  $^1\text{H}$  NMR spectra of (a) diiodo  $\beta$ -CD and (b)  $\beta$ -CD-Urea polymer in  $\text{D}_2\text{O}$ .

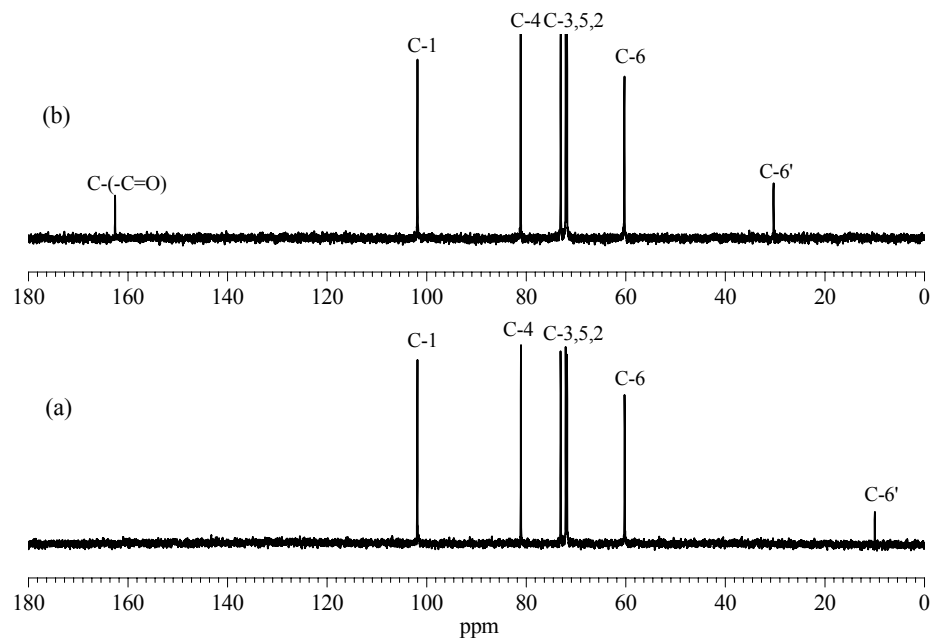


**Figure 3.9**  $^{13}\text{C}$  NMR spectra of (a) diiodo  $\beta$ -CD and (b)  $\beta$ -CD-Urea polymer in  $\text{D}_2\text{O}$ .

### 3.3.3.3 Thermogravimetric Analysis (TGA)

The thermal analysis of  $\beta$ -CD and  $\beta$ -CD polymer are shown in Figure 3.10. The degradation pattern showed weight loss at three different temperature regions. The first weight loss at  $106^\circ\text{C}$  was observed due to the loss of moisture and structural water molecules, the second mass loss at  $285^\circ\text{C}$  as dehydration of  $\beta$ -CD, and third mass loss at  $335^\circ\text{C}$  as a decomposition of glucose in  $\beta$ -CD. However, in case of  $\beta$ -CD polymer the thermogram was different; the first weight loss at around the same temperature due to the loss of moisture and structural water molecules but second weight loss was at a lower temperature due to the formation of polymer of the  $\beta$ -CD unit with the resulting loss of the crystalline nature of the cyclodextrin molecule. Subsequent weight loss occurs due to the decomposition of the glucose and urea linker after that  $\beta$ -CD polymer is quite stable above  $500^\circ\text{C}$ .

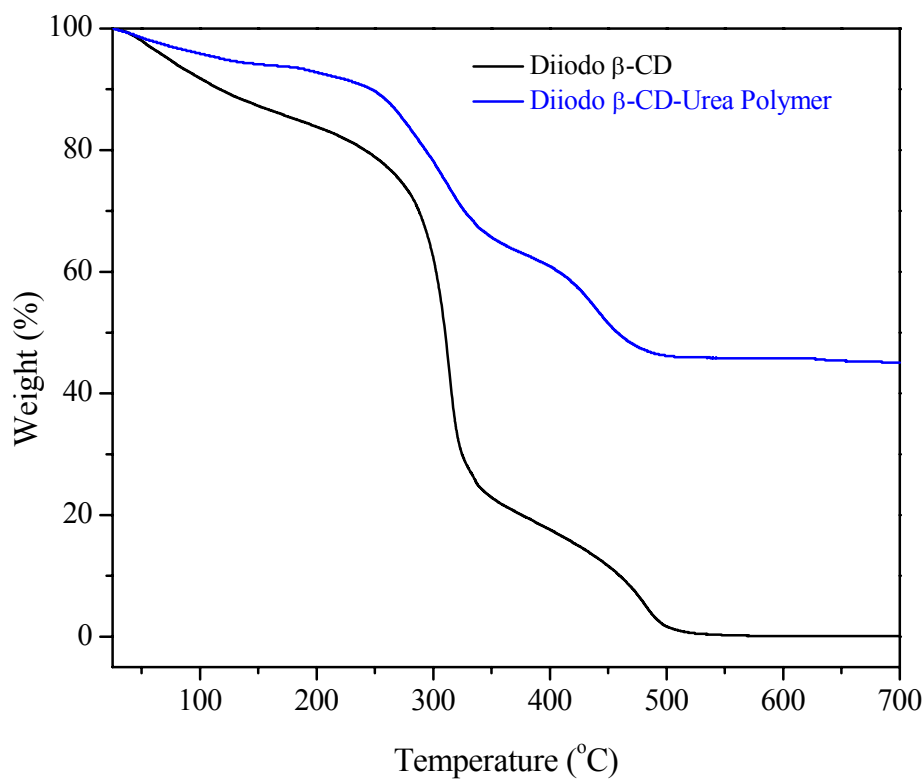


**Figure 3.10** TGA curves of diiodo  $\beta$ -CD and  $\beta$ -CD-Urea polymer.

### 3.3.3.4 X-ray Diffraction (XRD)

The X-ray diffraction patterns of diiodo  $\beta$ -CD and  $\beta$ -CD-Urea polymer are shown in Figure 3.11. The synthesized  $\beta$ -cyclodextrin-polymer (Figure 3.11 b) does not have typical  $2\theta$  values of the diiodo  $\beta$ -CD. It can be seen that the synthesized polymer have a different structure than that of the diiodo  $\beta$ -CD ( $2\theta = 9, 12.5, 19.6, 23.0, 27.0, \text{ and } 34.88$ ) (Figure 3.11 a) with the total suppression of the crystalline nature of the  $\beta$ -CD. The XRD pattern of the  $\beta$ -CD-Urea polymer showed that broadening of peak is due to the condensation reaction and converted to an amorphous polymer.

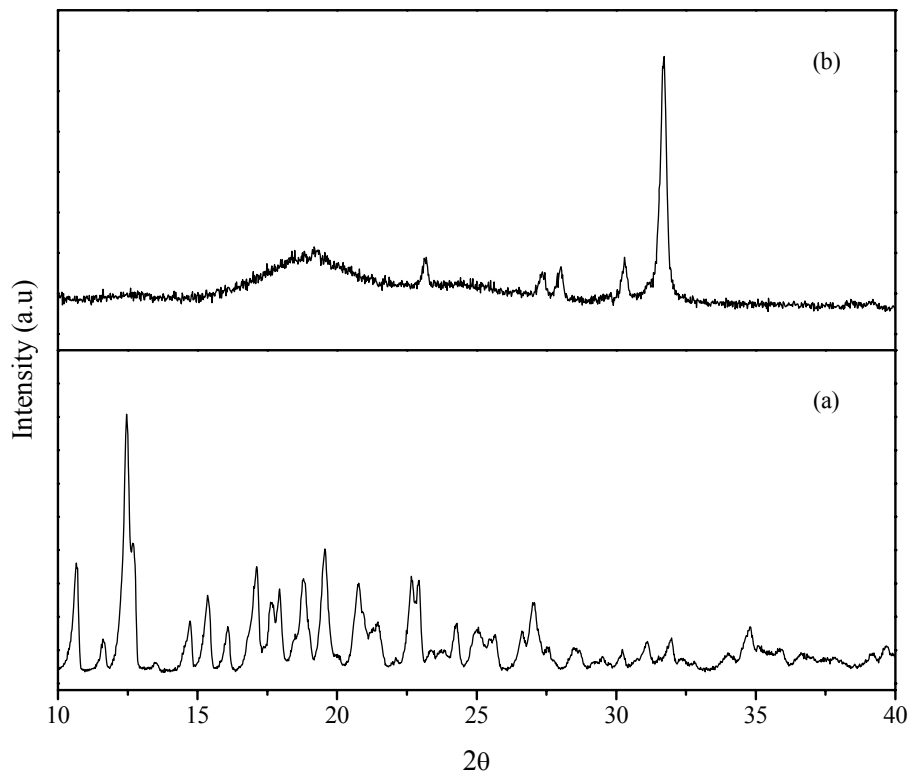


**Figure 3.11** XRD curves of (a) diiodo  $\beta$ -CD and (b)  $\beta$ -CD-Urea polymer.

### 3.3.3.5 Molecular Weight (Mw)

The solid polymers obtained after purification by ultrafiltration and freeze drying, the average molecular mass was determined by static laser light scattering technique (SLS) using Debye plot as method shown above. The average molecular weights of the polymers were obtained and shown in Table 3.3.

**Table 3.3** Molecular Weight of  $\beta$ -CD-Urea and Thiourea polymers at 25°C by SLS

<b>Samples</b>	<b>Molecular Weight (SLS)</b>
$\beta$ -CD-Urea-Polymer	31,163
$\beta$ -CD-Thiourea-Polymer	31,426

### 3.4 Conclusions

In this work linear highly water-soluble main-chain  $\beta$ -CD-CC and  $\beta$ -CD-CC-PEG based polymers, with hydroxyl functional groups have been synthesized by using short linker cyanuric chloride (CC) between two  $\beta$ -CDs by condensation polymerization procedure. Cyanuric chloride used as a short linker between two  $\beta$ -CDs, owing to its temperature dependent reactivity of all the three chlorine atoms, which controlled the cross-linking and formation of insoluble polymers. Similarly, using condensation polymerization procedure linear polymers of  $\beta$ -CD and urea or thiourea were also synthesized by connecting the diiodo functionalized  $\beta$ -CD with urea or thiourea as a linker. These synthesized  $\beta$ -CD polymers are highly water-soluble and biocompatible materials, characterized successfully by FTIR, NMR, XRD and TG analysis.

## References

1. S. Srinivasachari and T. M. Reineke, *Biomaterials*, **2009**, 30, 928-938.
2. S. J. Hwang, N. C. Bellocq, M. E. Davis, *Bioconjugate Chem.* **2001**, 12, 280-290.
3. T. Loftsson and M. E. Brewster, *J. Pharm. Sci.*, **1996**, 85, 1017-1025.
4. P. Caliceti, S. Salmaso, A. Semenzato, T. Carofiglio R. Fornasier, M. Fermeglia, M. Ferrone, S. Sabrina Pricl, *Bioconjugate Chem.* **2003**, 14, 899-908.
5. A. Rasheed, A. C. K. Kumar and V. V. N. S. S. Sravanthi, *Sci. Pharm.*, **2008**, 76, 576-598.
6. F. Csempez, A. Süle, I. Puskás, *Colloids and Surfaces A: Physicochem. Eng. Aspects*, **2010**, 354, 308-313.
7. K. Uekama, F. Hirayama, and T. Irie, *Chem. Rev.*, **1998**, 98, 2045-2076.
8. M. Valero and C. A. Dreiss, *Langmuir*, **2010**, 26, 10561-10571.
9. M. Wulff, M. Aldén, and J. Tegenfeldt, *Bioconjugate Chem.*, **2002**, 13, 240-248.
10. M. E. Davis and M. E. Brewster, *Nature Rev.*, **2004**, 3, 1023-1035.
11. F. Yhaya, J. Lim, Y. Kim, M. Liang, A. M. Gregory, and M. H. Stenzel, *Macromolecules*, **2011**, 44, 8433-8445.
12. G. Crini, S. Bertini, G. Torri, A. Naggi, D. Sforzini, C. Vecchi, L. Janus, Y. Lekchiri, and M. Morcellet, *J. Appl. Polym. Sci.*, **1998**, 68, 1973-1978.
13. G. Crini, C. Cosentino, S. Bertini, A. Naggi, G. Torri, C. Vecchi, L. Janus, and M. Morcellet, *Carbohydr. Res.*, **1998**, 308, 37-45
14. M. Kitaoka, and K. Hayashi, *J. Incl. Pheno. Macrocycl. Chem.*, **2002**, 44, 429-431.
15. F. Zha, S. Li, and Y. Chang, *Carbohydr. Polym.*, **2008**, 72, 456-461
16. L. Ducoroy, B. Martel, B. Bacquet, and M. Morcellet, *J. Incl. Pheno. Macrocycl. Chem.*, **2007**, 57, 271-277.
17. S. Berto, M. C. Bruzzoniti, R. Cavalli, D. Perrachon, E. Prenesti, T. Sarzanini, F. Trotta, and W. Tumiatti, *J. Incl. Pheno. Macrocycl. Chem.*, **2007**, 57, 631-636.
18. C.N. Murthy, S.J. Choi and K.E. Geckeler, *J. Nanosci. Nanotech.*, **2002**, 2, 129-132.
19. I. Shown, S. Banerjee, A.V. Ramchandran, K. E. Geckeler, C. N. Murthy, *Macromol. Symp.*, **2010**, 287, 51-59.
20. I. Shown and C. N. Murthy, *Supramol. Chem.*, **2008**, 20(6), 573-578.

21. O. Jazkewitsch, A. Mondrzyk, R. Staffel, and H. Ritter, *Macromolecules*, **2011**, 44(6), 1365-1371
22. F. van de Manakker, T. Vermonden, C. F. van Nostrum and W. E. Hennink, *Biomacromolecules*, **2009**, 10(12), 3157-3175.
23. A. Harada, M. Furue, S. Nozakura, *Macromolecules*, **1976**, 9(5), 701-704.
24. D. Zhao, L. Zhao, C. Zhu, Z. Tian, X. Shen, *Carbohydr. Polym.*, **2009**, 78(1), 125-130.

***Chapter 4***  
***Applications of Cyclodextrin based Polymers***

## Chapter 4

### Applications of Cyclodextrin based Polymers

#### 4.1 Aqueous Solubilization of Carbamazepine by Cyclodextrin based Polymers

##### 4.1.1 Introduction

In pharmaceuticals, about 90% of medicines, the active ingredients are in the form of solid materials. The number of newly developed drugs having a poor solubility and thus exhibiting bioavailability problems after oral administration is steadily increasing. Estimates by the pharmaceutical companies are that about 40% of the drugs in the pipeline are poorly soluble, and as high as 60% of compounds come directly from the synthesis route<sup>1</sup>. The solubility of drug plays an important role in disposition, since the maximum rate of drug transport across a biological membrane is the result of permeability and solubility. According to the biopharmaceutical classification system (BCS), aqueous solubility and permeability are the most important parameters affecting drug bioavailability. Carbamazepine (CBZ) is one among the poorly water-soluble drug. Carbamazepine chemically 5H-dibenzo[b,f]azepine-5-carboxamide was discovered by chemist Walter Schindler at J. R. Geigy AG (now part of Novartis) in Basel, Switzerland, in 1953 is an antiepileptic drug widely used in the treatment of epilepsy and bipolar disorder<sup>2</sup>. Carbamazepine (CBZ) is used for anticonvulsant and anti-neuralgic effects. The popularity of this drug is related to several beneficial properties, including proven efficacy in controlling different types of seizures<sup>3,4</sup>. CBZ is poorly soluble in water with erratic oral absorption and bioavailability less than 70%<sup>5,6</sup>. CBZ comes under Biopharmaceutical Classification System (BCS) Class II drugs which exhibits very low aqueous solubility and high permeability characteristics<sup>7</sup>. The controlled delivery system for CBZ would also be beneficial for patients with epileptic seizures, because CBZ will be released in a controlled manner<sup>8-12</sup>. The aqueous solubility of CBZ at 25°C is 0.1 mg/mL nearly practically insoluble in water<sup>13</sup>. Thus, the absorption dissolution rate of CBZ is very poor.

CBZ is known to form an inclusion complex with cyclodextrins, which increase the aqueous solubility, dissolution and bioavailability in aqueous media<sup>14,15</sup>.

Cyclodextrins can both enhance and hamper drug delivery through artificial membranes<sup>16</sup>. The composition of the drug formulation and the physicochemical and physiological composition of the membrane will determine what kind of effect is obtained<sup>17</sup>. Cyclodextrin will enhance drug delivery through a diffusion-controlled barrier but will hamper drug delivery through a lipophilic membrane controlled barrier. Cyclodextrins enhance drug delivery through porous membranes depending on the relative pore size compared with the effective diameter of the drug/cyclodextrin complex<sup>18</sup>. Through cyclodextrin complexation, it is possible to enhance aqueous solubility and drug bioavailability for oral administration<sup>19</sup>. The parent cyclodextrins, in particular  $\beta$ -cyclodextrin have limited aqueous solubility and its complex formation with lipophilic drug like CBZ often results in precipitation of solid drug/cyclodextrin complex. In general, the complexation efficiency of parent  $\beta$ -cyclodextrin is low and thus a relatively large amount of  $\beta$ -cyclodextrin is needed to complex small amount of drug CBZ<sup>20</sup>. Due to toxicological consideration, formulation and production cost, it is important to use as little  $\beta$ -cyclodextrin as possible in pharmaceutical formulations<sup>21</sup>. Thus, the increased water-solubility of parent  $\beta$ -cyclodextrin after polymerization was effectively used to stop the precipitation of complex and reduced the production cost. Cyclodextrin based polymers have been well known matrixes for potential carriers for a range of drugs in pharmaceutical formulations as well as DNA delivery applications. The kinetics of the release performance of these CD polymeric carriers has been also been investigated in several reports<sup>22-26</sup>.

Thus, the cyclodextrin based polymers synthesized in previous Chapter 3 were used as a carrier for the poorly water-soluble antiepileptic drug carbamazepine, with the intention that these synthesized cyclodextrin based polymers can change the solubility of CBZ and alter the stability of the drug CBZ/cyclodextrin polymers inclusion complex with better release performance.

## **4.1.2 Experimental**

### **4.1.2.1 Materials**

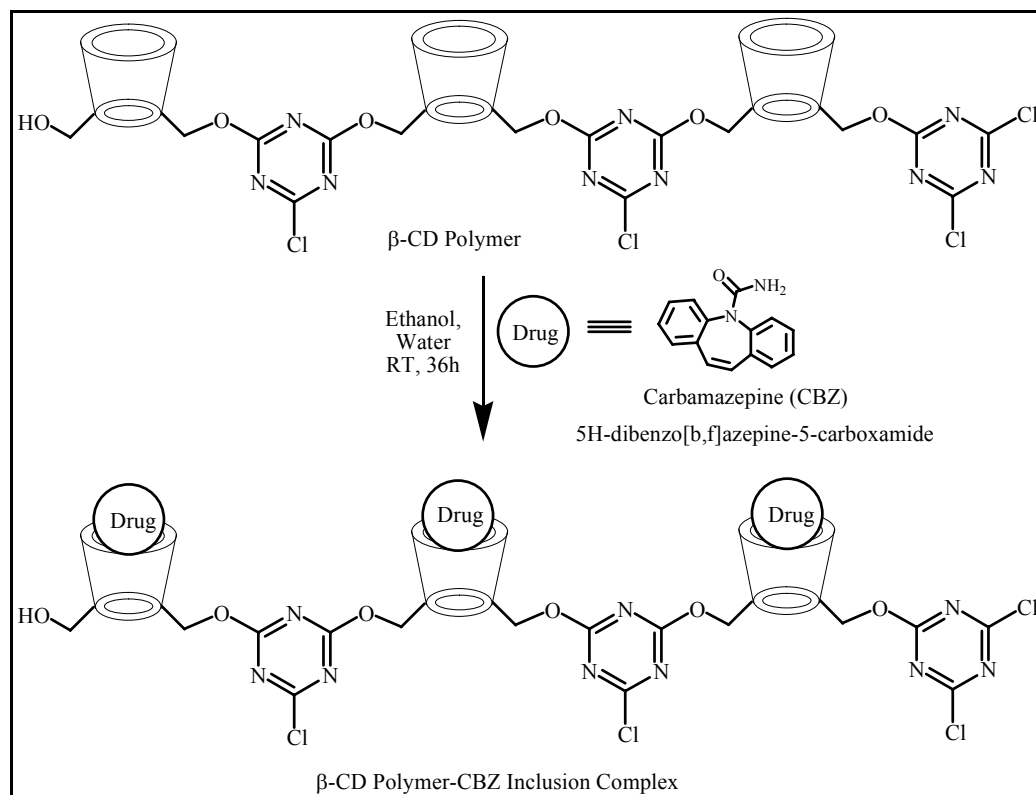
$\beta$ -Cyclodextrin based polymers were synthesized in Chapter 3 was used for solubilization of drug carbamazepine (CBZ). Carbamazepine (Mw = 236 g/mole) was purchased from Sigma-Aldrich.

### **4.1.2.2 Measurements**

The FTIR spectra were recorded on a Shimadzu (8400S) infrared spectrophotometer at 30 scans by using a KBr pellet method at  $10^{-4}$  resolution. UV-Visible spectra were recorded on a Shimadzu UV-2450 spectrophotometer.  $^1\text{H-NMR}$  spectra were recorded on a Bruker Avance spectrometer operating at 400 MHz at room temperature. Samples were prepared in  $\text{D}_2\text{O}$  (except Carbamazepine in  $\text{CDCl}_3$ ) containing TMS as an internal standard. Thermogravimetric analysis (TGA) was recorded on a Shimadzu, TGA-50 system with a heating rate of  $10^\circ\text{C}/\text{min}$  under air atmosphere in the temperature range of  $30\text{-}800^\circ\text{C}$ .

### **4.1.2.3 Synthesis of $\beta$ -CD-P-CBZ Inclusion Complex**

The synthesis of the  $\beta$ -CD-P-CBZ inclusion complex (Scheme 4.1.1) was achieved in a mixed aqueous solvent system containing ethanol and water (typically 50:50, v:v), where both  $\beta$ -CD-P and CBZ formed a homogeneous reaction medium. The inclusion of the CBZ into the  $\beta$ -CD-P was monitored over a period of 4 hrs by UV-Vis spectroscopy. The  $\beta$ -CD-P-CBZ inclusion complex was isolated by removing the ethanol by rota vapor and subsequent addition of distilled water. The complex was purified in aqueous solution by membrane filtration using a polymer membrane with a molecular mass cut-off of 650 Da and finally freeze-drying of the aqueous suspension yield the white solid powder of  $\beta$ -CD-P-CBZ inclusion complex. The formation of CBZ and  $\beta$ -CD-P inclusion complex is shown in Scheme 4.1.1.



**Scheme 4.1.1** Scheme shows the formation of inclusion complex of drug CBZ with  $\beta$ -CD-CC-P in mixed solvents system.

#### 4.1.2.4 Phase Solubility

The phase solubility studies give an idea of the ease with which CBZ forms an inclusion complex. The phase solubility of the CBZ with pristine  $\beta$ -CD and synthesized  $\beta$ -CD polymers was measured using a simple one pot technique. The phase solubility studies were carried out in phosphate buffer solution according to the method described by Higuchi and Connors. Accurately weighed sample of CBZ in quantities exceeding its aqueous solubility (100 mg) was added into vials containing 10 mL of 7.2 pH phosphate buffer solution (PBS) of various concentration of  $\beta$ -CD or  $\beta$ -CD polymer (10 mg, 20 mg, 30 mg, 40 mg, 50 mg). All solutions were prepared in a glass vials which shaken at constant temperature (25°C) until equilibrium was achieved (48 h). This amount of time was considered sufficient to reach equilibrium and then filtered through a 0.45  $\mu$ m membrane filter to obtain a clear solution and insoluble residue was omitted. The CBZ concentration was determined by measuring

the UV absorbance of the saturated solutions at 285 nm wavelength and compared with the calibration curve. The apparent binding constant of the CBZ/ $\beta$ -CD polymer inclusion complex was calculated from the slope and intercept of the straight line of the phase solubility diagram, using the well known Higuchi-Connors equation.

*Higuchi-Connors equation*

$$K_{1:1} = \frac{\text{Slope}}{\text{Intercept} (1 - \text{Slope})} \quad (4.1.1)$$

#### **4.1.2.5 Dissolution Studies**

The release performance of the CBZ drug with the synthesized polymers was measured by dissolution studies. The dissolution of  $\beta$ -CD-P-CBZ inclusion complex was determined by adopting the procedure described by M. J. Arias *et al*<sup>27</sup> and P. Mura *et al*<sup>28</sup>. Samples were analyzed spectrophotometrically at 285 nm for CBZ. The freeze dried inclusion complex of drug with polymers (100 mg) was added to 75 mL of water in a 150 mL beaker and stirred at 100 rpm with a glass three-blade propeller centrally immersed in a beaker 20 mm from the bottom. At appropriate time intervals, suitable aliquots were withdrawn with a filter-syringe (pore size 0.45  $\mu$ m) and absorbance was measured. CBZ concentration in the phosphate buffer solution was obtained by UV-Vis spectrophotometer measurements after calibration at definite intervals of time. Fresh dissolution medium was added to maintain a constant volume after each sampling.

### 4.1.3 Results and Discussion

#### 4.1.3.1 Molecular Modeling

Energy-minimized space-filling molecular models of the three-dimensional conformation of the cyclic  $\beta$ -cyclodextrin-host, drug carbamazepine-guest and  $\beta$ -cyclodextrin-carbamazepine-inclusion complex are shown in Figure 4.1.1. The host and guest molecules are independently built up, and their geometry is optimized. The overall structure of these possible models of inclusion complexes is again subjected to energy minimization. The final energy-minimized molecular model indicates that carbamazepine molecule is included in the  $\beta$ -cyclodextrin host cavity. The dimension of molecules was studied in details and final molecular models suggested that only 1:1 inclusion complex is possible in case of carbamazepine and  $\beta$ -cyclodextrin. Similarly in case of  $\beta$ -CD polymer only one molecule of carbamazepine is included in the cavity of each  $\beta$ -CD units of the polymer main-chain.

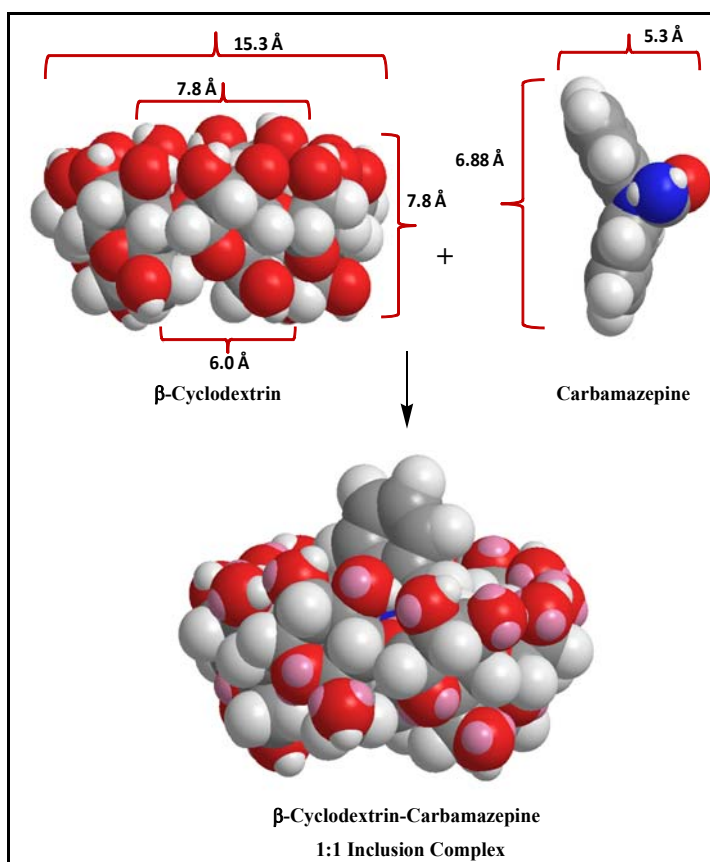


**Figure 4.1.1** Energy-minimized space-filling molecular model of inclusion complex.

#### 4.1.3.2 Fourier Transform Infrared Spectroscopy (FTIR)

It has been demonstrated that FTIR spectroscopy is a very powerful tool to prove the presence of both host and guest components in inclusion compounds. The FTIR spectra of the  $\beta$ -CD-CC-P,  $\beta$ -CD-Urea-P, CBZ and CBZ encapsulated  $\beta$ -CD-CC-P and  $\beta$ -CD-Urea are shown in Figure 4.1.2 a, b, c, d, e in the region of 2500-500  $\text{cm}^{-1}$ . The FTIR spectrum of CBZ (Fig. 4.1.2 c) exhibited the absorption band at 1678  $\text{cm}^{-1}$  arising due to the C=O stretching of primary amide along with typical aromatic stretching bands. In the FTIR spectrum of CBZ encapsulated  $\beta$ -CD-CC-P (Fig. 4.1.2 d), sharp absorption bands were noticed at 1726  $\text{cm}^{-1}$  and 1680  $\text{cm}^{-1}$  assigned to the C=N stretching vibration of the  $\beta$ -CD polymers arising from cyanuric chloride and amide of CBZ, respectively. In the FTIR spectrum of CBZ encapsulated  $\beta$ -CD-Urea (Fig. 4.1.2 e), a distinct band notice for the CBZ at 1678  $\text{cm}^{-1}$ , this typical absorption band was shifted to a higher frequency at 1684  $\text{cm}^{-1}$  due to the formation of the inclusion complex. It was also observed that spectra of CBZ encapsulated  $\beta$ -CD polymers, displayed that the peaks of CBZ almost disappear whereas the characteristic peaks of  $\beta$ -CD polymers remains strong. Thus, the positions and relative intensities of few bands were affected due to host-guest interaction, which confirmed the formation of an inclusion complex between CBZ and  $\beta$ -CD polymers. If it were not so, then the spectra of CBZ encapsulated would resemble that of a physical mixture of CBZ with  $\beta$ -CD polymers with no shift in the characteristic bands.

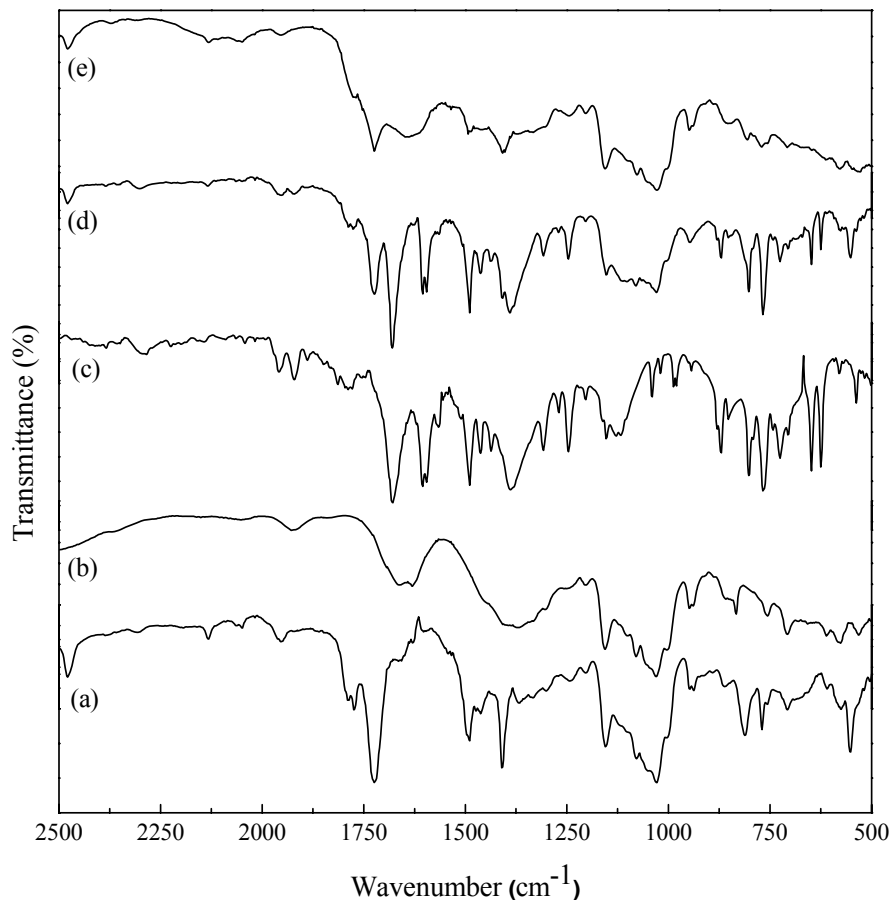


**Figure 4.1.2** FTIR spectra of (a)  $\beta$ -CD-CC-P, (b)  $\beta$ -CD-Urea-P, (c) CBZ, (d) CBZ encapsulated  $\beta$ -CD-CC-P and (e) CBZ encapsulated  $\beta$ -CD-Urea.

#### 4.1.3.3 UV-Visible Spectroscopy (UV-Vis)

The UV-Vis spectroscopy is also an effective tool to characterize the host-guest interaction between drug CBZ and  $\beta$ -CD polymers. The UV-Vis absorbance spectra of CBZ in ethanol,  $\beta$ -CD polymer in water and CBZ encapsulated  $\beta$ -CD polymer in water was shown in Figure 4.1.3. The CBZ drug shows two absorbance maximum at around 243 nm and 286 nm in ethanol and it was water-insoluble, whereas the  $\beta$ -CD polymer shows no absorbance in this region. However, the spectrum of the CBZ- $\beta$ -CD-P inclusion complex in water showed the typical absorbance peak corresponding to the CBZ drug with considerable blue shift in the absorbance maximum implying that the drug CBZ has been encapsulated into the non-polar cavity of  $\beta$ -CD-P. This shift can be attributed to change in dielectric properties and deformation of host-guest

molecules in solution. The observed shift in the spectrum might be the included drug molecule is in a more favorable environment as compared to the molecule in pure solution<sup>29</sup>. The  $\beta$ -CD-P offers non-polar inner cavity and polar outside environment for the drug CBZ and thus has been “solubilized” in water.

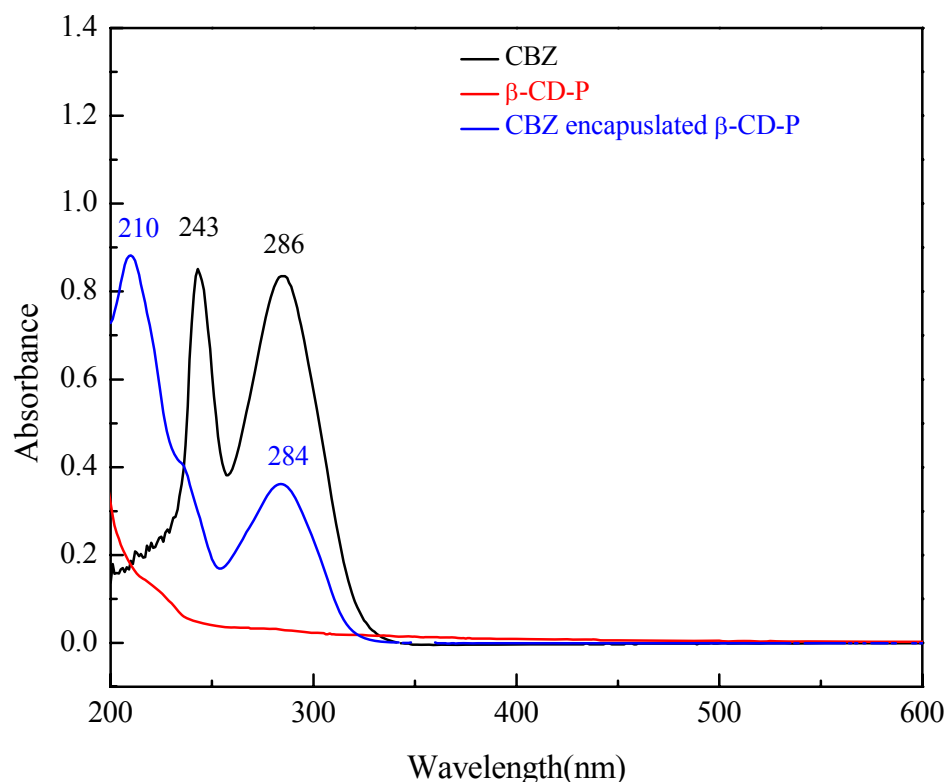


**Figure 4.1.3** UV-Vis spectra of CBZ in ethanol,  $\beta$ -CD polymer in water and CBZ encapsulated  $\beta$ -CD polymer in water.

#### 4.1.3.4 Nuclear Magnetic Resonance Spectroscopy (NMR)

The  $^1\text{H}$  NMR spectra of the  $\beta$ -CD-CC-P,  $\beta$ -CD-Urea-P, CBZ and CBZ encapsulated  $\beta$ -CD-CC-P and  $\beta$ -CD-Urea are shown in Figure 4.1.4 a, b, c, d, e in the region of 8-3  $\delta$ ppm in  $\text{D}_2\text{O}$  as a solvent except CBZ in  $\text{CDCl}_3$ . It was evident from the spectra shown in Fig, 4.1.4 c, d and e, that the peaks observed in the range of 7.0 -7.5 ppm of CBZ, assigned to the aromatic protons and also noticed in the inclusion complex as well in the addition to the characteristic peaks  $\beta$ -CD polymer. In addition, the aromatic protons of the CBZ are shifted considerably upfield after the formation of inclusion complex. The upfield shift observed due to the guest protons inside the

cavity of the host has been considered as an evidence for the formation of an inclusion complex.

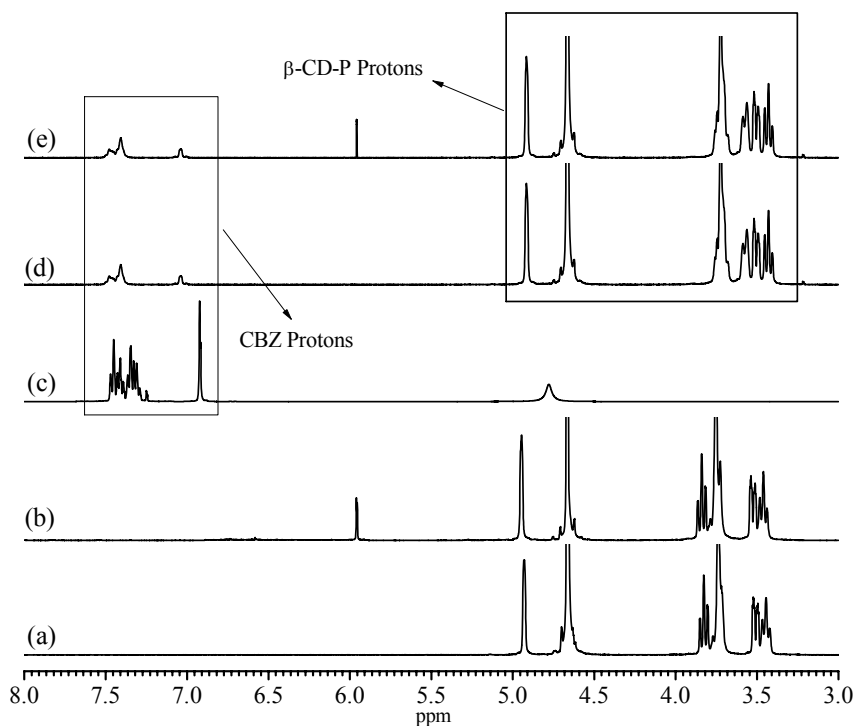


**Figure 4.1.4**  $^1\text{H}$  NMR spectra of (a)  $\beta$ -CD-CC-P, (b)  $\beta$ -CD-Urea-P, (c) CBZ, (d) CBZ encapsulated  $\beta$ -CD-CC-P and (e) CBZ encapsulated  $\beta$ -CD-Urea.

#### 4.1.3.5 Thermogravimetric Analysis (TGA)

In order to study the thermal stability and stoichiometry of the inclusion complex thermogravimetric analysis are recorded in an air atmosphere. TGA curves of (a)  $\beta$ -CD, (b) CBZ and (c) CBZ encapsulated  $\beta$ -CD. Inset TGA curves of (a)  $\beta$ -CD-CC-P, (b) CBZ and (c) CBZ encapsulated  $\beta$ -CD-CC-P are shown in Figure 4.1.5. From the TG curves, it was found that  $\beta$ -CD and CBZ encapsulated  $\beta$ -CD showed at the beginning a small weight loss due to the loss of water molecules, this weight loss was found to be small in case of CBZ encapsulated  $\beta$ -CD as compared to pristine  $\beta$ -CD, owing to loss of water molecules from the  $\beta$ -CD cavity (escape from  $\beta$ -CD cavity) during the formation of inclusion complex. The second weight loss was observed at  $300^\circ\text{C}$  in case of pristine  $\beta$ -CD due to the decomposition of glucose units,

this weight loss was observed at lower temperature for CBZ encapsulated  $\beta$ -CD due to the formation of inclusion complex which breaks the rigid hydrogen bonding in  $\beta$ -CD cavity. In most cases,  $\beta$ -CD can form inclusion complexes with guest molecules in a molar ratio of 1:1, 2:1 or 1:2. The theoretical, calculated mass content CD in the complex of these three ratios could be 82.78, 70.62 and 90.58% respectively. The TGA data of the CBZ encapsulated  $\beta$ -CD showed that the total weight loss at 360°C is 82.05%. The value indicates that the ratio between  $\beta$ -CD and CBZ complex is of 1:1 type. The similar observation has been drawn in case of CBZ encapsulated  $\beta$ -CD polymer as shown in Figure 4.1.5 (Inset).

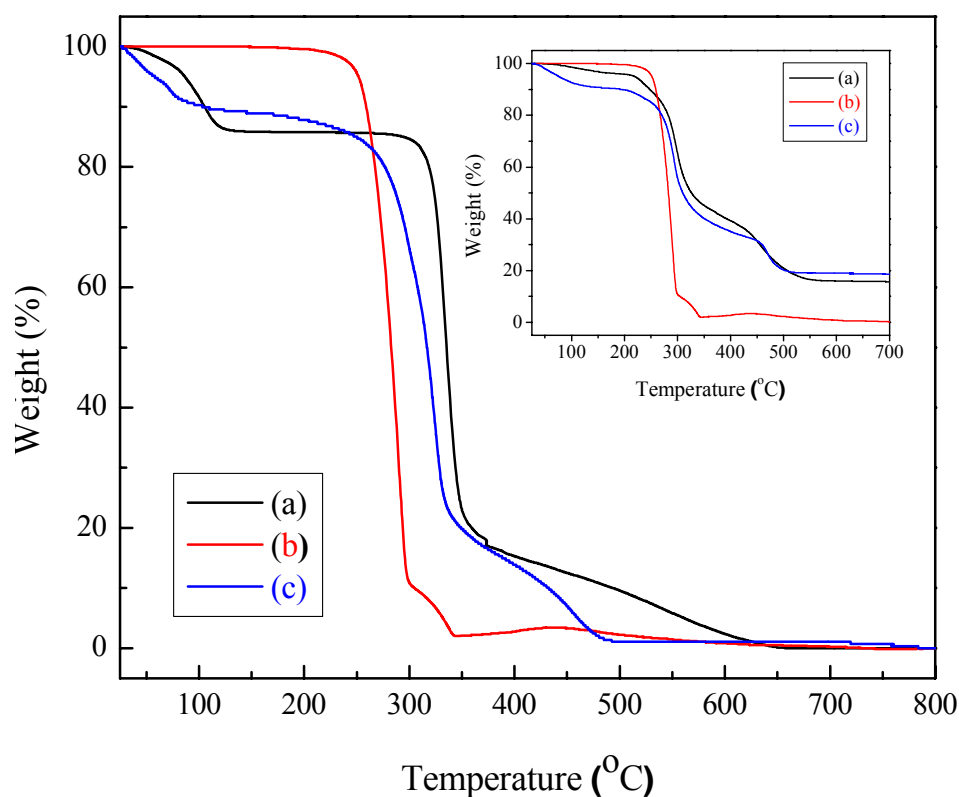


**Figure 4.1.5** TGA curves of (a)  $\beta$ -CD, (b) CBZ and (c) CBZ encapsulated  $\beta$ -CD. Inset TGA curves of (a)  $\beta$ -CD-CC-P, (b) CBZ and (c) CBZ encapsulated  $\beta$ -CD-CC-P.

#### 4.1.3.6 Phase Solubility Diagrams of the $\beta$ -CD-P/CBZ inclusion complex

The phase solubility diagrams for the formation of inclusion complex between CBZ and  $\beta$ -CD or  $\beta$ -CD polymers presented in Figure 4.1.6. These plots illustrated that the aqueous solubility of the drug CBZ increases linearly as a function of  $\beta$ -CD or  $\beta$ -CD polymers over the entire concentration range studied and can be classified as  $A_L$ -type diagram according to Higuchi and Connors. According to Higuchi and Connors theory, this may be attributed to the formation of 1:1 stoichiometry water-soluble inclusion complexes. The order of the stability according to the obtained stability constants, was  $\beta$ -CD ( $1066 \text{ M}^{-1}$ ) <  $\beta$ -CD homopolymer ( $1136 \text{ M}^{-1}$ ) <  $\beta$ -CD-DEG copolymer ( $1174 \text{ M}^{-1}$ ). From the phase solubility plot the slope of the diagram is less than one proved the inclusion complexes 1:1 stoichiometry. The values of the stability constant  $K_{1:1}$  was within the range of 1000 to  $1500 \text{ M}^{-1}$  considered the ideal complex. Specific guest-cyclodextrin interactions (van der Waals and hydrophobic forces) appear to play an important role in determining stability constants, i.e., guest molecular structure determines the magnitude of stability constant. The apparent solubility enhancement was evaluated by the UV-Vis comparing with standard curve. According to the comparison study the synthesized  $\beta$ -CD polymers showed better solubilization power of drug CBZ as compared to the native  $\beta$ -CD. The solubility of CBZ was linearly increased from 0.05 mM to about 0.7 mM with the increasing of polymers concentration, which could be attributed to better inclusion complex formation ability of cyclodextrin based polymers through non-polar-non-polar interaction of hydrophobic drug CBZ and non-polar cyclodextrin cavity.

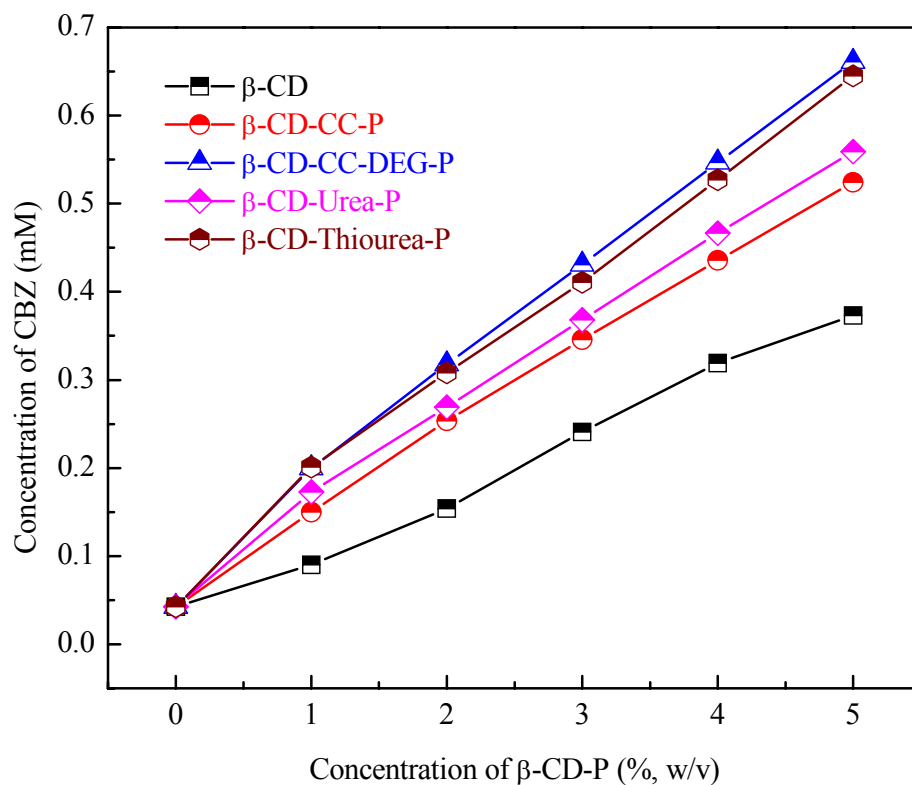


**Figure 4.1.6** Phase solubility diagrams of CBZ in  $\beta$ -CD and  $\beta$ -CD polymers.

#### 4.1.3.7 Dissolution Studies

The dissolution profiles of the freeze dried inclusion complexes of the CBZ with the synthesized  $\beta$ -CDs polymers are compared with the CBZ/ $\beta$ -CD were shown in Figure 4.1.7. CBZ/ $\beta$ -CD polymers samples showed the better dissolution rate and higher cumulative release of the drug dissolution as compared to the pristine  $\beta$ -CD. This was due to the high hydrophilic nature of the synthesized polymers, lowering the interfacial tension in between the highly water insoluble drug CBZ and water. The high amorphous nature of the synthesized polymers and their water-solubility showed a positive impact on the cumulative release of the drug CBZ, thus leading to higher dissolution rate.

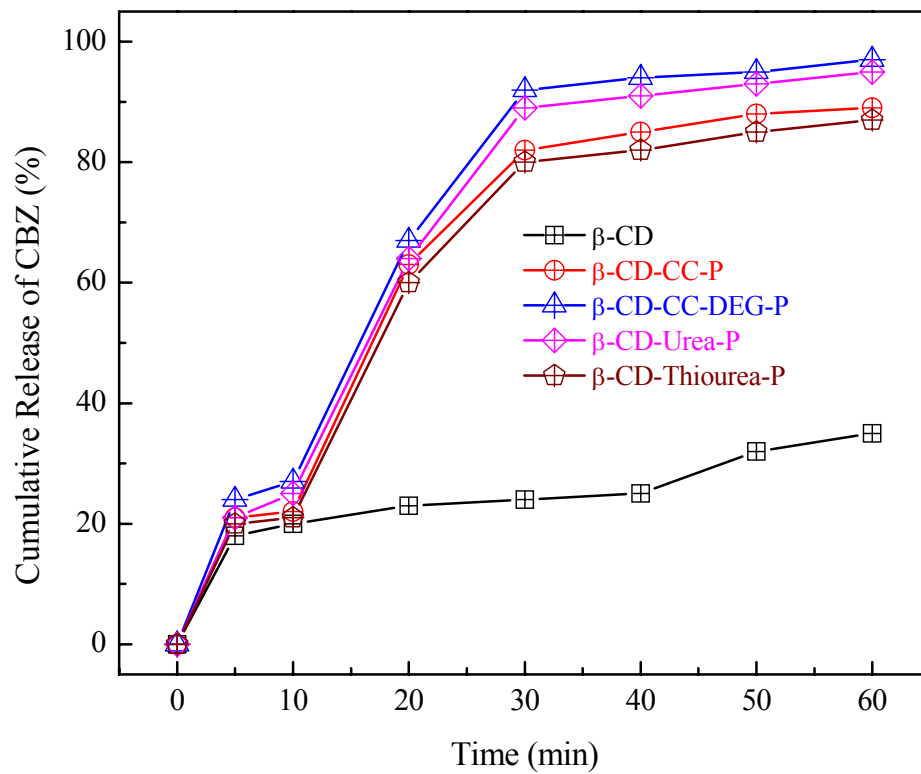


**Figure 4.1.7** Dissolution curves of CBZ with  $\beta$ -CD and  $\beta$ -CD polymers.

#### **4.1.4 Conclusions**

In conclusion, we have successfully prepared a novel inclusion complex of poorly water-soluble antiepileptic drug carbamazepine (CBZ) with  $\beta$ -CD and  $\beta$ -CD based polymers, so as to improve water-solubility and biocompatibility in aqueous medium. The results show that the inclusion complex is of 1:1 type. Interestingly it was found that the  $\beta$ -CD based polymers considerably enhance the water-solubility of CBZ as compared to the pristine  $\beta$ -CD. It is also worthwhile to mention here that the solubility was enhanced seven times higher than the intrinsic water-solubility of drug CBZ in presence of  $\beta$ -CD based polymers.

## 4.2 Fluorescence Sensitizing of Pyrene by Cyclodextrin based Polymers

### 4.2.1 Introduction

Molecular luminescence spectrometry, especially molecular fluorescence spectrometry, has become a routine technique in many analytical applications<sup>30,31</sup>. In many cases, molecular luminescence spectrometry can yield a lower detection limit and greater selectivity than molecular absorption spectrometry. However, although most fluorophore show strong fluorescence in non-polar solvents, the solubility and intensity of luminescence is rather weak in polar solvents<sup>32,33</sup>. Cyclodextrins, which form inclusion complexes with fluorophore molecules in aqueous solution, can result in significant enhancement of the fluorescence. The unique torus structural conformation of the CDs protects the fluorescing singlet state or the phosphorescing triplet state of the fluorophore from external quenchers<sup>34-38</sup>. The effective microenvironment of the cyclodextrin non-polar cavity is likely to be similar to that of such non-polar oxygenated solvents as dioxane, *t*-amyl alcohol, or 1-octanol<sup>39,40</sup>. The CDs solution can improve the lower detection limit for hydrophobic fluorophore in aqueous solution by increasing their solubility or for hydrophilic fluorophore by increasing solubility of the water-insoluble fluorescent compounds into which the fluorophore are incorporated<sup>41</sup>.

Fluorescence is widely used in microscopic imaging, dating in archaeology, medical research, forensic science, biotechnology and diagnosis<sup>42-44</sup>. The enhanced fluorescence has attracted great attention in recent years, in terms of the quantum yield and photostability of the fluorophore<sup>45,46</sup>. It is available from the number of reports that cyclodextrin enhance the fluorescence property of the fluorophores due to formation of an inclusion complex. Pyrene is a water-insoluble polycyclic aromatic hydrocarbon (PAH) consisting of four fused benzene rings, resulting in a flat (planar) aromatic molecule. Pyrene is smallest peri-fused colorless solid and useful fluorescence probe for studying the microenvironment within the cyclodextrin cavity. The fluorescence intensity of pyrene is very less in polar medium. The fluorescence property of pyrene is very sensitive to solvent polarity and microenvironmental changes<sup>47,48</sup>.

In literature, most of the studies on the cyclodextrin host-guest inclusion complexation were focused on binary system, although recently attention has been drawn towards ternary complexes in which third components such as alcohols, alkylamines and surfactant also participate in the inclusion processes<sup>49-55</sup>. The results obtained from ternary inclusion complex revealed interesting intramolecular and intermolecular interaction, which can be useful for the sensitizing applications<sup>56</sup>. However, complexation involving more than three different components has not been well explored till now owing to their higher levels of complexity.

In this work, we describe the systematic study of the absorbance and fluorescence enhancement of pyrene in the presence of  $\beta$ -CD and  $\beta$ -CD polymer. The study was conducted over a wide range of concentration and binding constants were calculated for pyrene inclusion complex with  $\beta$ -CD and  $\beta$ -CD polymer using Benesi-Hildebrand equation<sup>57</sup>. Moreover, the quenching phenomenon of the pyrene inclusion with  $\beta$ -CD and  $\beta$ -CD polymer in presence of third component adamantol also carried out for the dynamic equilibrium of pyrene-cyclodextrin inclusion complex and quenching constants were determined using Stern-Volmer coordinates<sup>58</sup>.

## 4.2.2 Experimental

### 4.2.2.1 Materials

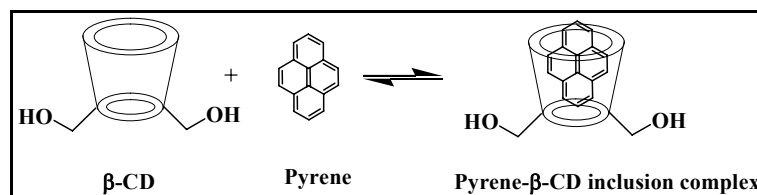
$\beta$ -Cyclodextrin-CC polymer synthesized in Chapter 3 using the temperature reactivity of cyanuric chloride under controlled condition was used as reactant. Pyrene and adamantol were purchased from Merck (Germany) and recrystallized from ethanol. Double distilled water was used throughout the experiments.

### 4.2.2.2 Measurements

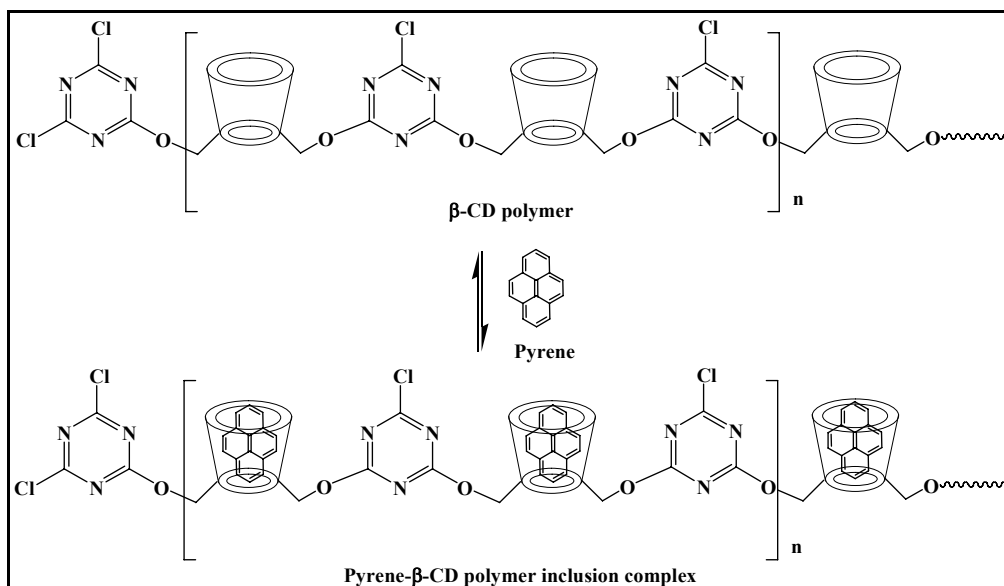
All the fluorescence spectra were taken on a RF-5301PC spectrophotometer at room temperature. A 450-W Xenon CW lamp was used as the excitation source. Slit width was set 1.5 nm for excitation and emission respectively. The scan rate was  $1 \text{ nm s}^{-1}$ . The UV-Vis spectra were recorded on a Shimadzu UV-Vis-2450 spectrophotometer.

### 4.2.2.3 Procedure of binary pyrene- $\beta$ -CD or $\beta$ -CD polymer inclusion complex

The pyrene  $1 \times 10^{-5} \text{ M}$  solution was prepared in absolute dry ethanol and 1% w/v  $\beta$ -CD and  $\beta$ -CD polymer solutions were separately prepared in double distilled water 7.0 pH was maintained. From the pyrene solution  $1 \text{ cm}^3$  was added to the different volumes ( $1\text{-}5 \text{ cm}^3$ ) of  $\beta$ -CD or  $\beta$ -CD polymer solution and then total volume of the mixture was made up to  $6 \text{ cm}^3$  with double distilled water. The mixtures were stirred for 8 h and then allowed to equilibrate overnight. The Schemes for the formation of pyrene- $\beta$ -CD and pyrene- $\beta$ -CD binary inclusion complex are shown in Scheme 4.2.1 and Scheme 4.2.2.



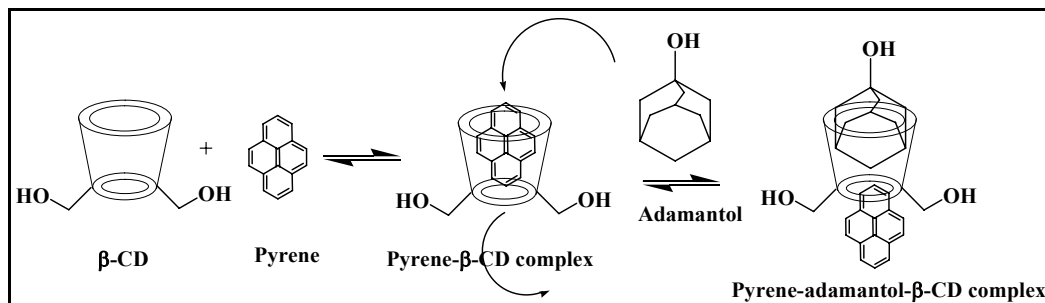
**Scheme 4.2.1** Scheme for the formation of binary pyrene- $\beta$ -CD inclusion complex in mixed solvent system.



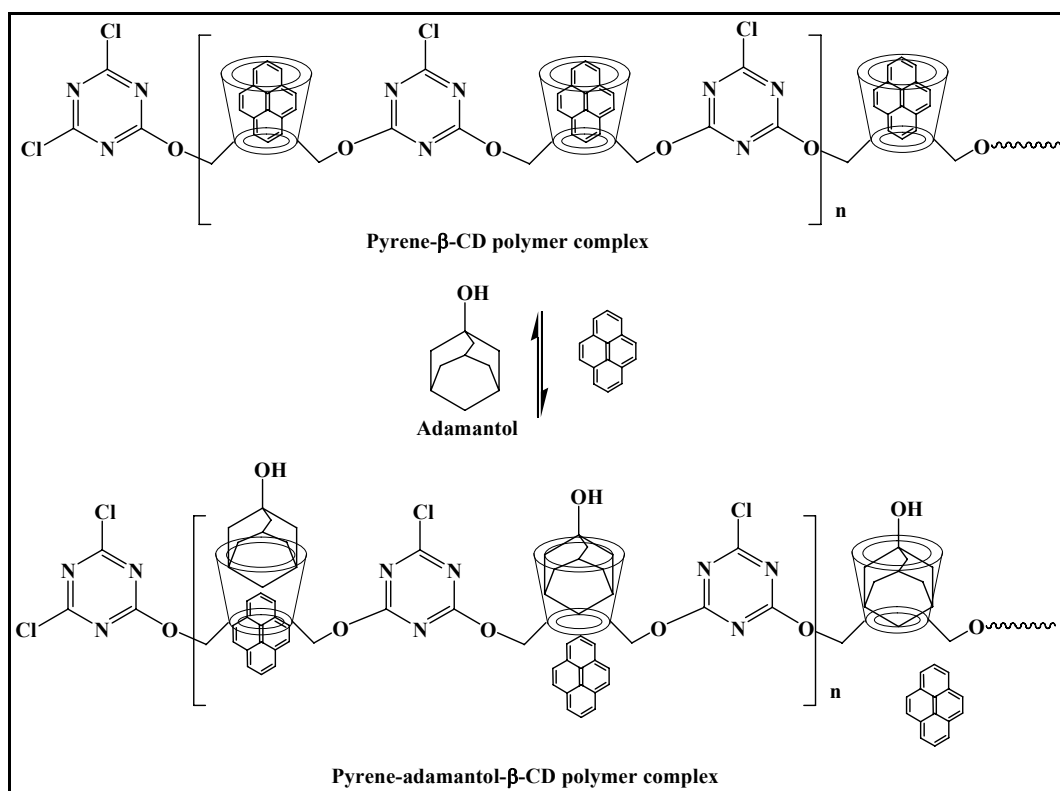
**Scheme 4.2.2** Scheme for the formation of binary pyrene-β-CD-P inclusion complex in mixed solvent system.

#### 4.2.2.4 Procedure of ternary pyrene-adamantol-β-CD or pyrene-adamantol-β-CD polymer inclusion complex

For the fluorescence quenching of Pyrene-β-CD or β-CD polymer inclusion complexes the concentration of pyrene and β-CD or β-CD polymer was kept constant. 1 cm<sup>3</sup> each was added to the different volumes (1-6 cm<sup>3</sup>) of the adamantol solution then adjusted to be total volume of the mixture was made up to 8 cm<sup>3</sup> with double distilled water. The mixtures were stirred for 8 h and then allowed to equilibrate overnight. The Schemes for the formation of pyrene-adamantol-β-CD and pyrene-adamantol-β-CD ternary inclusion complex were shown in Scheme 4.2.3 and Scheme 4.2.4.



**Scheme 4.2.3** Scheme for the formation of ternary pyrene-adamantol- $\beta$ -CD inclusion complex in mixed solvent system.



**Scheme 4.2.4** Scheme for the formation of ternary pyrene-adamantol- $\beta$ -CD-P inclusion complex in mixed solvent system.

## 4.2.3 Results and Discussion

### 4.2.3.1 Molecular Modeling

Energy-minimized space-filling molecular models of the three-dimensional conformation of the cyclic  $\beta$ -cyclodextrin-host, planar pyrene-guest and  $\beta$ -cyclodextrin-pyrene-inclusion complex are shown in Figure 4.2.1. The host and guest molecules are independently built up, and their geometry is optimized. The overall structure of these possible models of inclusion complexes is again subjected to energy minimization. The final energy-minimized molecular model indicates that pyrene molecule is included in the  $\beta$ -cyclodextrin host cavity. The dimension of molecules was studied in details and final molecular models suggested that only 1:1 inclusion complex is possible in case of pyrene and  $\beta$ -cyclodextrin. Similarly in case of  $\beta$ -CD polymer only one molecule of pyrene is included in the cavity of each  $\beta$ -CD units of the polymer main-chain.

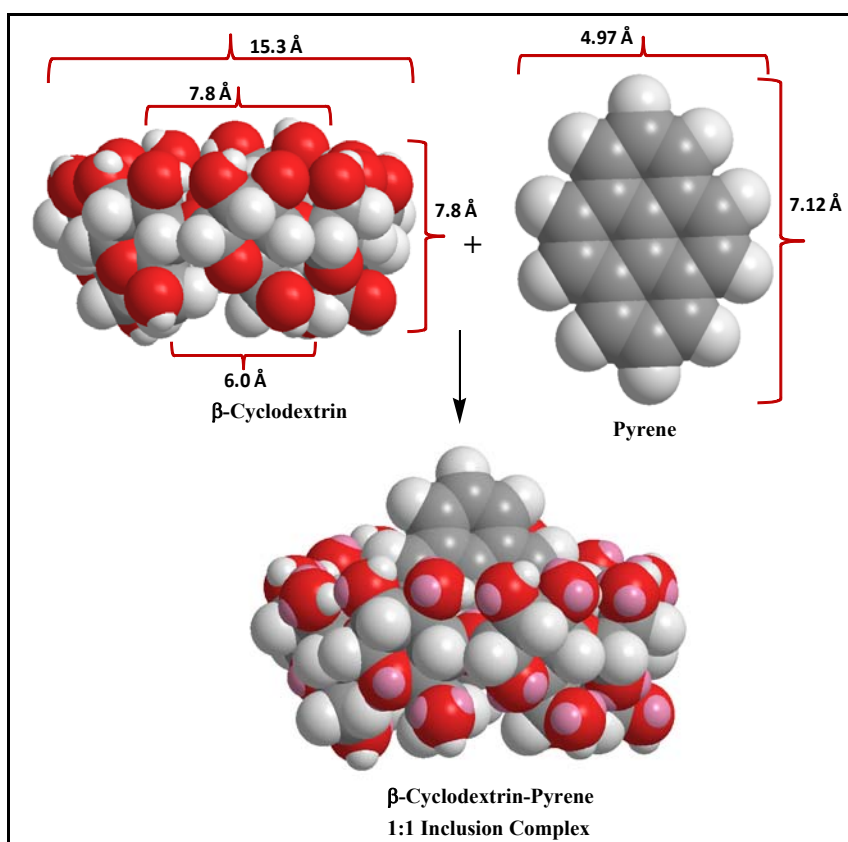


**Figure 4.2.1** Energy-minimized space-filling molecular model of inclusion complex.

#### 4.2.3.2 UV-Visible Spectroscopy (UV-Vis)

Formation of inclusion complex between pyrene and  $\beta$ -CD or  $\beta$ -CD polymer was confirmed by UV-Vis absorbance spectra. Figure 4.2.2 shows absorbance spectra of pyrene ( $1.66 \times 10^{-6}$ M) in aqueous solutions containing various concentrations of  $\beta$ -CD or  $\beta$ -CD polymer. The absorbance maxima of pyrene in the absence of  $\beta$ -CD or  $\beta$ -CD polymer are located at 335, 319, 305, 273 and 262 nm. On addition of  $\beta$ -CD or  $\beta$ -CD polymer the absorbance bands of pyrene were slightly shift to red shift (ca. 4 nm) with increase in oscillator strength. The absorbance intensity of pyrene increases with increasing concentration of  $\beta$ -CD or  $\beta$ -CD polymer. This phenomenon was observed due to the fact that encapsulation of pyrene and electronic properties of pyrene are favorable in presence of non-polar hydrophobic cavity of  $\beta$ -CD.

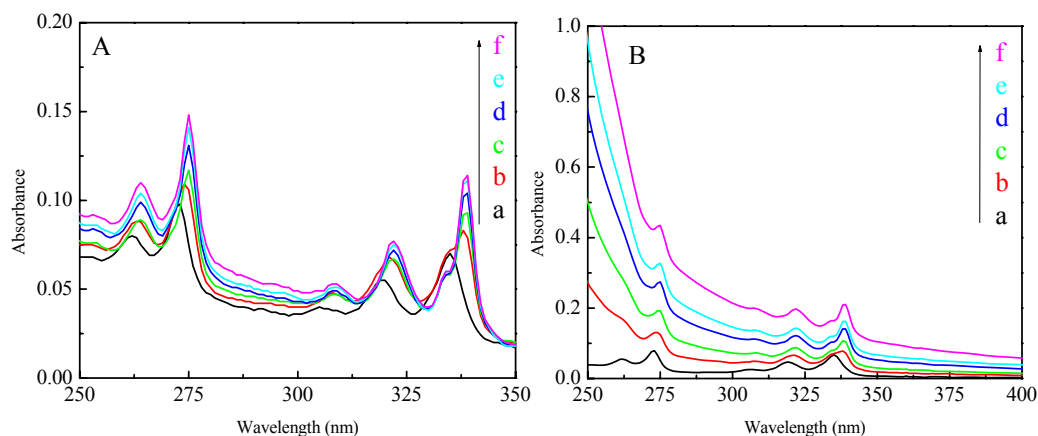


**Figure 4.2.2** UV-Vis spectra of pyrene ( $1.66 \times 10^{-6}$ M) in aqueous solution of (A)  $\beta$ -CD and (B)  $\beta$ -CD-polymer at different concentrations: (a) 0.00 %, (b) 0.166 %, (c) 0.333 %, (d) 0.500 %, (e) 0.666 %, (f) 0.833 %.

#### 4.2.3.3 Fluorescence Emission Spectra

The photoluminescence emission spectra (excited at 340 nm) of the pyrene in aqueous solution containing various concentration of  $\beta$ -CD or  $\beta$ -CD polymer are shown in Figure 4.2.3. The fluorescence emission intensity was enhanced upon the addition of  $\beta$ -CD or  $\beta$ -CD polymer to a solution of pyrene ( $1.66 \times 10^{-6}$ M) in the range of 370 to 410 nm fluorescence band is attributed to the formation of pyrene monomer

in non-polar cavity. Also there was no broadening of peak was observed after 410 nm which ascribed there was no pyrene dimer formation in the cavity. The molecular sizes of pyrene and  $\beta$ -CD cavity (internal diameter = 7.8 Å) is capable of including only one pyrene molecule within the inner cavity. This phenomenon was observed due to the formation of inclusion complex which afford the rotation of the pyrene molecule is hindered, and the relaxation of the solvent molecules is considerably decreased. Both of these effects can result in a decrease in the vibrational deactivation. The non-polar cavity of  $\beta$ -CD protects the quenching of the pyrene emission by water molecule. The CDs cavity behaves similarly to the organic solvent which gives non-polar surrounding for the included molecule. This altered microenvironment can provide favorable polarity for enhanced quantum efficiencies and hence the intensities of fluorescence increase.

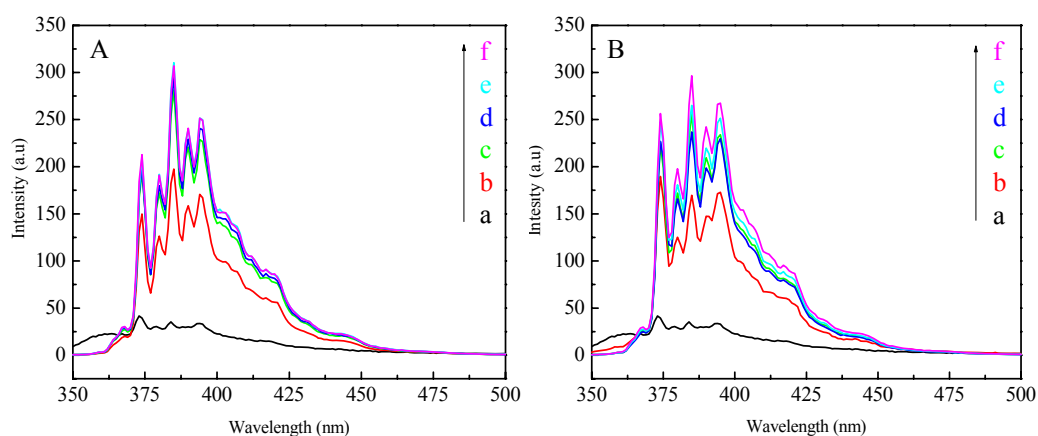


**Figure 4.2.3** Fluorescence spectra (excited at 340 nm) of pyrene ( $1.66 \times 10^{-6}$ M) in aqueous solution of (A)  $\beta$ -CD and (B)  $\beta$ -CD-polymer at different concentrations: (a) 0.00 %, (b) 0.166 %, (c) 0.333 %, (d) 0.500 %, (e) 0.666 %, (f) 0.833 %.

It was reported that while pyrene molecule is fluorescent in aprotic medium, the fluorescence yield drops rapidly due to hydrogen bond donating solvents<sup>59</sup>. Thus the enhancement of the fluorescence of the pyrene on the addition of  $\beta$ -CD or  $\beta$ -CD polymer is a reflection of the passage molecule into the non-polar host cavity. On comparing the effect of  $\beta$ -CD and  $\beta$ -CD polymer, for the same concentration the fluorescence enhancement is higher for  $\beta$ -CD polymer due to the higher order of inclusion ability. These are shown in Scheme 4.2.1 and Scheme 4.2.2. Higher

enhancement in  $\beta$ -CD polymer in aqueous solution indicates that encapsulation is more favored in this case owing to each  $\beta$ -CD unit in of the  $\beta$ -CD polymer include pyrene molecule. Using the Benesi-Hildebrand equation binding constants were also calculated from the fluorescence data on the basis of 1:1 association between pyrene and  $\beta$ -CD as shown below.

*Benesi-Hildebrand Equation*

$$\frac{[Py]}{I} = \frac{1}{K_b \epsilon} \frac{1}{[CD]} + \frac{1}{\epsilon} \quad (4.2.1)$$

Where, [Py] = Concentration of Pyrene, I = Fluorescence Intensity of Pyrene,  $K_b$  = Binding Constant and  $\epsilon$  = Extinction Coefficient.

The plot of [Py]/I Vs 1/[ $\beta$ -CD] and 1/[ $\beta$ -CD polymer] gave a straight line with a slope and intercept are shown in Figure 4.2.4. A good linear fit to the experiment data obtained for all the inclusion complexes, indicating that a 1:1 inclusion complex is formed. The spectral maximum is observed at around 374 nm wavelength was used for the calculation. The extinction coefficient at 374 nm for the free pyrene,  $\beta$ -CD encapsulated-pyrene and  $\beta$ -CD polymer encapsulated-pyrene are  $1.579 \times 10^7 \text{ cm}^{-1}\text{M}^{-1}$ ,  $8.514 \times 10^7 \text{ cm}^{-1}\text{M}^{-1}$  and  $10.297 \times 10^7 \text{ cm}^{-1}\text{M}^{-1}$ , respectively. The binding constant  $K_b$  calculated from the emission spectra for the  $\beta$ -CD polymer is  $2000 \text{ M}^{-1}$  which is higher than the value of the  $\beta$ -CD which is  $600 \text{ M}^{-1}$  (Table 4.2.1). Thus the qualitative comparison of the binding constants of the two complexes suggests that  $\beta$ -CD polymer provide a better fit for the pyrene guest molecule.

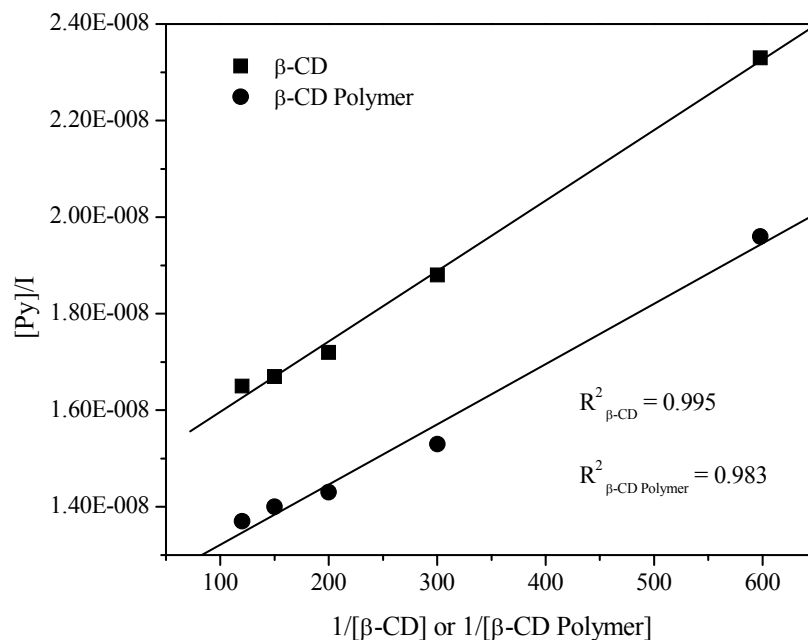


**Figure 4.2.4** Benesi-Hildebrand plot of  $[Py]/I$  Vs  $1/[\beta\text{-CD}]$  and  $[Py]/I$  Vs  $1/[\beta\text{-CD Polymer}]$ .

**Table 4.2.1** Binding constants for binary inclusion complex

Inclusion Complex	Binding Constant $K_b$
Pyrene- $\beta\text{-CD}$	$6.0 \times 10^2 \text{ M}^{-1}$
Pyrene- $\beta\text{-CD polymer}$	$2.0 \times 10^3 \text{ M}^{-1}$

We also studied the fluorescence quenching for the pyrene constituting pyrene-adamantol- $\beta\text{-CD}$  or  $\beta\text{-CD}$  polymer ternary complex with increasing concentration of adamantol. It was observed that CDs can increase the fluorescence intensity. However, adamantol can selectively quench the fluorescence emission intensity as shown in Figure 4.2.5 of pyrene inclusion complex with  $\beta\text{-CD}$  and  $\beta\text{-CD}$  polymer due to adamantol can also encapsulated into the same cavity of the host and competes for the accommodation in hydrophobic cavity. The fluorescence emission intensity of the pyrene- $\beta\text{-CD}$  or  $\beta\text{-CD}$  polymer inclusion complex decrease as the concentration of adamantol increase due to the formation of ternary inclusion

complex with  $\beta$ -CD or  $\beta$ -CD polymer in which adamantol can accommodate with pyrene or slowly kick out the pyrene molecule from the non-polar cavity of the guest molecule as shown in Figure 4.2.6 molecular model of ternary inclusion complex. This is completely dynamic process and it is not easily to determine that in aqueous solution weather pyrene was completely removed from the non-polar cyclodextrin cavity. In aqueous solution both the guest molecules are competes for the inclusion and thus the pyrene molecule was slowly exposed to the bulk aqueous solution and therefore the fluorescence intensity of pyrene was decreased in presence of adamantol.

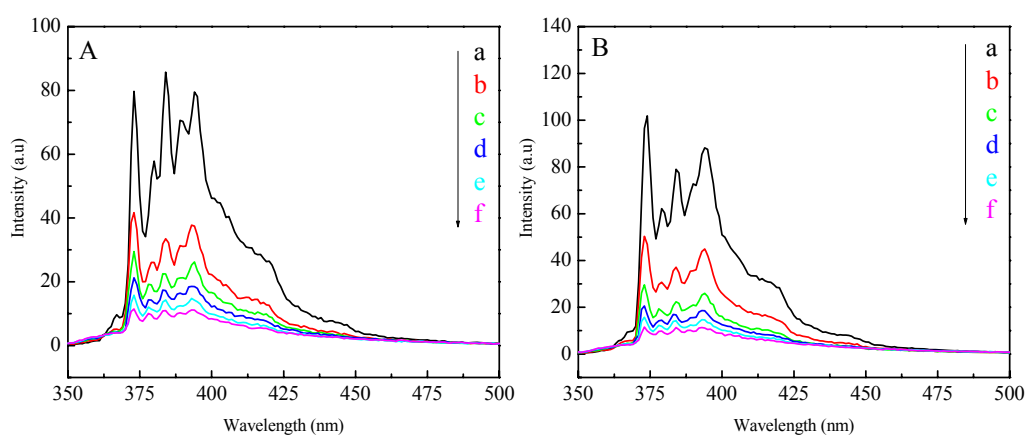


**Figure 4.2.5** Fluorescence spectra (excited at 340 nm) of pyrene ( $1.25 \times 10^{-6}$  M) in presence (0.166 %) of (A)  $\beta$ -CD and (B)  $\beta$ -CD-polymer at different concentration of adamantol: (a)  $1.25 \times 10^{-6}$  M, (b)  $2.50 \times 10^{-6}$  M, (c)  $3.75 \times 10^{-6}$  M (d)  $5.00 \times 10^{-6}$  M, (e)  $6.25 \times 10^{-6}$  M, (f)  $7.50 \times 10^{-6}$  M.

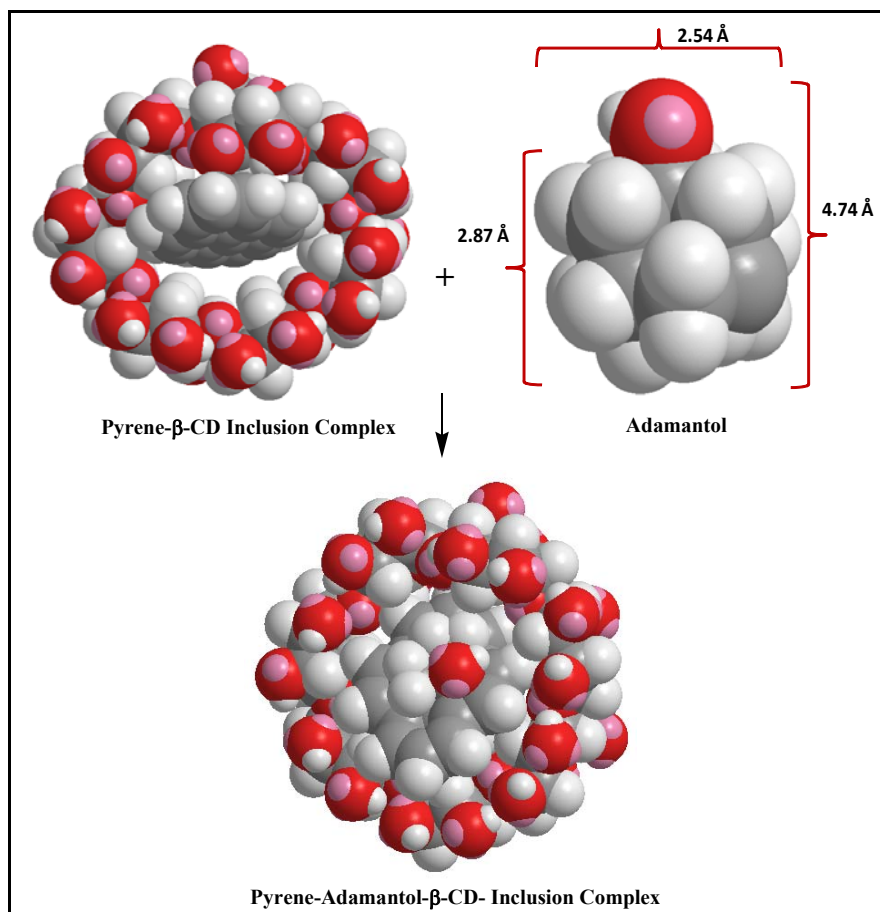


**Figure 4.2.6** Energy-minimized space-filling molecular model of ternary inclusion complex.

Using the Stern-Volmer equation and plot (Figure 4.2.7), the Stern-Volmer quenching constants  $K_{sv}$  (shown in Table 4.2.2) were also calculated from the fluorescence data as shown below.

*Stern-Volmer Equation*

$$\frac{I_0}{I} = 1 + K_{sv}[Q] \quad (4.2.2)$$

Where,  $I_0$  = Fluorescence Intensity in absence of Adamantol,  $I$  = Fluorescence Intensity of Pyrene in presence of Adamantol,  $K_{sv}$  = Stern-Volmer Quenching Constant and  $[Q]$  = Concentration of Quencher.

The extinction coefficient at 374 nm for the  $\beta$ -CD encapsulated-pyrene in absence and presence of adamantol are  $3.611 \times 10^7 \text{ cm}^{-1}\text{M}^{-1}$  and  $5.115 \times 10^6 \text{ cm}^{-1}\text{M}^{-1}$ . Similarly for the  $\beta$ -CD polymer encapsulated-pyrene in absence and presence of adamantol are  $5.430 \times 10^7 \text{ cm}^{-1}\text{M}^{-1}$  and  $5.286 \times 10^6 \text{ cm}^{-1}\text{M}^{-1}$ . It was observed that Stern-Volmer quenching constant for pyrene encapsulated  $\beta$ -CD polymer is more as compared to the pyrene encapsulated  $\beta$ -CD. Thus, the quenching phenomenon is fast in case of pyrene encapsulated  $\beta$ -CD polymer as after polymerization the cavity of  $\beta$ -CD become more flexible and competition for the inclusion formation with guest molecules happen to fast as compared the more rigid parent  $\beta$ -CD.

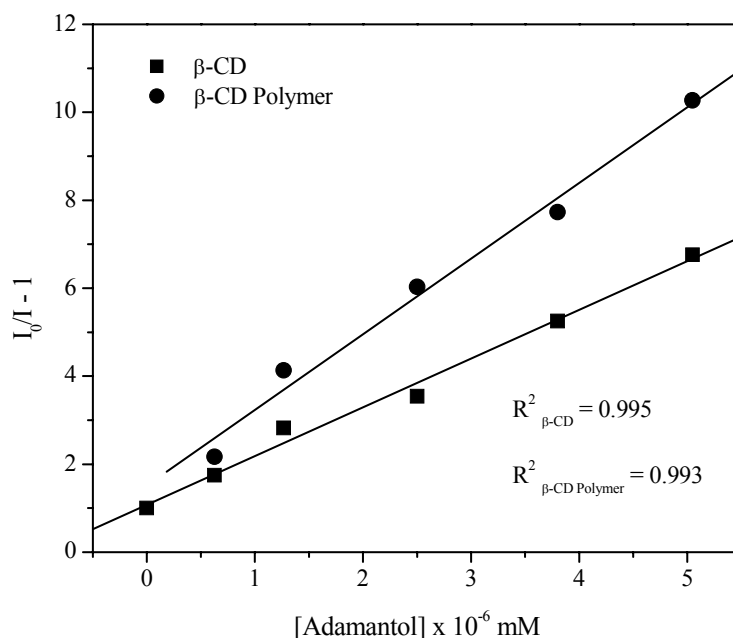


**Figure 4.2.7** Stern-Volmer plots of  $I_0/I$  Vs [Adamantol] for  $\beta$ -CD and  $\beta$ -CD polymer.

**Table 4.2.2** Stern-Volmer quenching constant for ternary inclusion complex

Inclusion Complex	Quenching Constant $K_{sv}$
Pyrene- $\beta$ -CD-Adamantol	$1.146 \times 10^8 \text{ M}^{-1}$
Pyrene- $\beta$ -CD polymer-Adamantol	$1.720 \times 10^8 \text{ M}^{-1}$

#### 4.2.4 Conclusions

The steady state absorbance and fluorescence spectra of pyrene inclusion complex with pristine  $\beta$ -CD and polymeric  $\beta$ -CD in mixed aqueous medium were studied effectively to increase the fluorescence intensity of pyrene in aqueous medium. The binding constant obtained from the Benesi-Hildebrand equation for the pyrene- $\beta$ -CD polymer inclusion complex was more than three times greater than the pyrene- $\beta$ -CD inclusion complex due to the more inclusion ability of  $\beta$ -CD polymer. The quenching study of the pyrene inclusion complex of  $\beta$ -CD and  $\beta$ -CD polymer in presence of third component adamantol gives the information of dynamic equilibrium of the inclusion complex. The quenching in fluorescence emission intensity of pyrene by adamantol occurs due to the collision between two molecules in hydrophobic cavity and competes for the accommodation in hydrophobic cavity.

## References

1. E. Merisko-Liversidge, *Nanocrystals*: In: Marty JJ. Ed. Particles. Orlando: Marcel Dekker, **2002**.
2. W. Schindler, F. Hafliger, *Helvetica Chimica Acta*, **1954**, 37(2), 472-483.
3. M. Sitges, L.M. Chiu, V. Nekrassov, *Neurochem. Int.*, **2006**, 49, 55-61.
4. K.A. Voudris, A. Attilakos, E. Katsarou, A. Drakatos, S. Dimou, S. Mastroianni, A. Skardoutsou, A. Prassouli, A. Garoufi, *Epilepsy Res.*, **2006**, 70, 211-217.
5. Eds P. O. Anderson, *Handbook of Clinical Drug Data*, 9<sup>th</sup> Ed., Appelton & Lange, **1999**.
6. W. Liu, L. Dang, S. Black and H. Wei, *J. Chem. Eng. Data*, **2008**, 53(9), 2204-2206.
7. H. van de Waterbeemd, *Eur. J. Pharm. Sci.*, **1998**, 7, 1-3.
8. H. El-Zein, L. Riad, A. A. El-Bary, *Int. J. Pharm.*, **1998**, 168, 209-220.
9. E. Chan, H.S. Lee, S. S. Hue, *Br. J. Clin. Pharmacol.*, **2001**, 51, 567-576.
10. J. H. Hu, K.P. Johnston, R. O. Williams, *Eur. J. Pharm. Sci.*, **2003**, 20, 295-303.
11. D. Douroumis, A. Fahr, *Eur. J. Pharm. Biopharm.*, **2006**, 63, 173-175.
12. H. Friedrich, B. Fussnegger, K. Kolter, R. Bodmeier, *Eur. J. Pharm. Biopharm.*, **2006**, 62, 171-177.
13. J. S. Smith, R. J. MacRae and M. J. Snowden, *Eur. J. Pharm. Biopharm.*, **2005**, 60, 73-80.
14. L. S. Koester, C. R. Xavier, P. Mayorga and V. L. Bassani, *Eur. J. Pharm. Biopharm.*, **2003**, 55(1), 85-91.
15. A. S. Jain, A. A. Date, R. R. S. Pissurlenkar, E. C. Coutinho and M. S. Nagarsenker, *AAPS PharmScitech.*, **2011**, 12(4), 1163-1175.
16. T. Loftsson, S. B. Vogensen, M. E. Brewster, F. Konraosdottir, *J. Pharm. Sci.*, **2007**, 96(10), 2532-2546.
17. M. Rajkumar and S. B. Bhise, *J. Young Pharm.*, **2010**, 2(1), 7-14.
18. T. Loftsson, S. D. Sigfusson, H. H. Sigurdsson and M. Masson, *S. T. P. Pharm Sci.*, **2003**, 13, 125-132.
19. L. S. Koester, J. B. Bertuol, K. R. Groch, C. R. Xavier, R. Moellerke, P. Mayorga, T. D. Costa and V. L. Bassani, *Eur. J. Pharm. Sci.*, **2004**, 22, 201-207.
20. E. Redenti, L. Szente and J. Szejtli, *J. Pharm. Sci.*, **2000**, 89(1), 1-8.

21. K. Toyoda, T. Shoda, C. Uneyama, K. Takada and M. Takahashi, *Food and Chemical Toxicology*, **1997**, 35, 331-336.
22. J. Zhou and H. Ritter, *Polym. Chem.*, **2010**, 1, 1552-1559.
23. J. Li, H. Xiao, J. Li and Y. Zhong, *Int. J. Pharm.*, **2004**, 278, 329-342.
24. V. Burckbuchler, V. Wintgens, C. Leborgne, S. Lecomte, N. Leygue, D. Scherman, A. Kichler and C. Amiel, *Bioconjugate Chem.*, **2008**, 19(12), 2311-2320.
25. J. Zhao, D. Q. Lin, Y. C. Wang, S. J. Yao, *Carbohydr. Polym.*, **2010**, 80(4), 1085-1090.
26. J. Li, H. Xiao, J. Li, Y. P. Zhong, *Int. J. Pharm. Sci.*, **2004**, 278, 329-342.
27. M. J. Arias, J. R. Moyano, J. M. Gines, *Int. J. Pharm.*, **1997**, 153, 181.
28. P. Mura, M. T. Faucci, S. Maestrelli, S. Furlanetto and S. Pinzauti, *J. Pharm. Biomed. Anal.*, **2002**, 29, 1015.
29. M. J. Frampton and H. L. Anderson, *Angew. Chem., Int. Ed.*, **2007**, 46, 1028-1064.
30. A. M. de la Pena, T. T. Ndou, V. C. Anigbogu and I. M. Warner, *Ana. Chem.*, **1991**, 63, 1018-1023.
31. X. Wang, H. Zeng, Y. Wie and Jin-Min Lin, *Sensors and Actuators B*, **2006**, 114, 565-572.
32. T. Kinoshita, F. Linuma, A. Tsuji, *Biochem. Biophys. Res. Commu.*, **1976**, 51, 666.
33. T. Kinoshita, F. Linuma, A. Tsuji, *Anal. Biochem.*, **1971**, 61, 632.
34. K. Kano, I. Takenoshita, T. Ogawa, *J. Phys. Chem.*, **1982**, 86, 1833.
35. K. Tanaka and A. Okamoto, *Bioorg. Med. Chem.*, **2008**, 16, 400-404.
36. C. D. Tran, J. H. Fendler, *J. Phys. Chem.*, **1984**, 88, 2167.
37. N. J. Turro, T. Okuba, G. Weed, *Photochem. Photobiol.*, **1982**, 35, 325.
38. N. J. Turro, G. S. Cox, X. Ki, *Photochem. Photobiol.*, **1983**, 36, 149.
39. H. Kondo, H. Nakatani, K. Hiromi, *J. Biochem.*, **1976**, 79, 393.
40. K. W. Street, *J. Liq. Chromatogr.*, **1987**, 10, 655.
41. F. Cramer, W. Saenger, H. C. Spatz, *J. Am. Chem. Soc.*, **1967**, 89, 14.
42. B. Bohunicky and S. A. Mousa, *Nanotech. Sci. Appl.*, **2011**, 4, 1-10.
43. F. A. Morsy, S. I. El-Sherbiny and M. Awadalla, *Foren. Sci. J.*, **2005**, 4, 1-13.
44. J. K. Feathers, *Meas. Sci. Technol.*, **2003**, 14, 1493-1509.

45. J. Lukomska, J. Malicka, I. Gryczynski, Z. Leonenko and J. R. Lokowicz, *Biopolymers*, **2005**, 77, 31-37.
46. O. Stainik, H. M. McEvoy, C. MacDonagh and B. D. MacCraith, *Sensors and Actuators B*, **2005**, 107, 148-153
47. M. G. Kuzmin, *Pure & Appl. Chem.*, **1993**, 65, 1653-1658.
48. Y. Fujiwara and Y. Amao, *Sensors and Actuators B*, **2003**, 89, 187-191.
49. K. Kano, I. Takenoshita, and T. Ogawa, *Chem. Lett.* **1980**, 1035.
50. A. Ueno, K. Takahashi, Y. Hino, and T. Osa, *J. C. S. Chem. Commun.* **1981**, 194.
51. S. Hashimoto and J. K. Thoms, *J. Am. Chem. Soc.*, **1985**, 107, 4655.
52. G. Patonay, K. Fowler, A. Shapira, G. Nelson, and I. M. Warner, *J. Incl. Phenom.*, **1987**, 5, 717.
53. G. Nelson, G. Patonay, and I. M. Warner, *Anal. Chem.* **1988**, 60, 274-279.
54. S. Hamai *J. Phys. Chem.* **1988**, 92, 6140.
55. J. M. Schuette, T. T. Ndou, A. Munoz de la Pena, S. Jr. Mukundau, and I. M. Warner, *J. Am. Chem. Soc.*, **1993**, **115**, 292.
56. T. Kida, T. Iwamoto, Y. Fujino, N. Tohnai, M. Miyata, and M. Akashi, *Org. Lett.*, **2011**, 13(17), 4570-4573.
57. J. Rima, S. Kyriacos and M. A. Rida, *Spectrochimica Acta Part A*, **2009**, 74, 10-15.
58. W. Hui, M. Minghua, X. Hongzhi, F. Yu, Z. Xiaohong and W. Shikang, *ARKIVOC*, **2003**, 173-181.
59. G. Patonay, A. Shapira, P. Diamond and I. M. Warner, *J. Phys. Chem.*, **1986**, 90(9), 1963-1966.

*Chapter 5*  
*Solubilization of Fullerenes*

## Chapter 5

### Solubilization of Fullerenes

#### 5.1 Solubilization of [60]Fullerene by Modified $\beta$ -Cyclodextrin

##### 5.1.1 Introduction

Buckminsterfullerene  $C_{60}$ , the third carbon allotrope has been the subject of many interesting applications during the last two and half decades because of its unique physical, chemical and biological properties<sup>1-5</sup>. The continuing interest in this molecule is evident from the number of papers that appear every year in the literature<sup>6-9</sup>. This is due to its biological activity including DNA-cleaving ability, radical scavenging, MRI enhancement and anti-HIV activity<sup>10-13</sup>. A number of such biological applications emerge from the fullerenes behaving as an efficient radical scavenger and known as ‘free radical sponge’. However, the potential biomedical applications of fullerenes are hindered due to its hydrophobicity and biomedical applications of fullerenes require genuine water-solubility with no agglomeration. The first report on aqueous solubilization of [60]fullerene with cyclodextrins was described by Andersson *et al*<sup>14</sup> where [60]fullerene was taken into alcoholic boiling aqueous solution with  $\gamma$ -CD. The authors concluded that due to the inner cavity size of 0.950 nm, only  $\gamma$ -CD can form inclusion complex with [60]fullerene and  $\alpha$ -CD and  $\beta$ -CD with inner cavity size of 0.57 nm and 0.78 nm respectively cannot form inclusion complex with [60]fullerene having a 1 nm diameter. Subsequently, Murthy *et al*<sup>15</sup> showed that not only  $\gamma$ -CD but also  $\beta$ -CD can form inclusion complex with [60]fullerene given the right reaction conditions arguing that  $\beta$ -CD can form 2:1 inclusion complex with fullerene. After that several methods have been developed and described for the preparation of water-soluble fullerenes by forming complexes with water-soluble calix[n]arenes,<sup>16,17</sup> polyvinyl alcohols,<sup>18</sup> and polyvinyl pyrrolidone<sup>19,20</sup>, however cyclodextrins being naturally occurring and water-soluble seem to be the ideal hosts and has been comprehensively investigated for aqueous solubilization of fullerenes for biomedical applications.

The unique ability of cyclodextrins is that they can encapsulate the [60]fullerene molecule (depending upon the size of the non-polar inner cavity) non-covalently into the non-polar cavity and make it water-soluble<sup>14,15</sup>. However, a

competitive guest molecule in the biological media can displace [60]fullerene from the CDs cavity, thus defeating the purpose of using CDs for encapsulating [60]fullerene. Therefore covalently linked fullerene with CDs would be a better solution to overcome this problem. The high chemical reactivity of the fullerene molecules allows the synthesis of an enormous number of fullerene derivatives for biocompatible materials and biological applications<sup>21</sup>. The reaction of [60]fullerene with azides under elevated temperature has been well studied in literature. The azides are known to add to C<sub>60</sub> via cycloaddition reaction by forming triazoline intermediate, which then decompose to yield the desired product by elimination of N<sub>2</sub>, or by the formation of a nitrene, that adds to C<sub>60</sub> double bond. It has been found to be an efficient process resulting in fullerene derivatives containing an expanded cage of fullerene as azafullerenes C<sub>60</sub>N<sup>22</sup>.

The synthesis of water-soluble  $\beta$ -CD-[60]fullerene adduct by adopting supramolecular covalent as well as non-covalent interactions of [60]fullerene with selectively diazide functionalized  $\beta$ -CD is described.

## 5.1.2 Experimental

### 5.1.2.1 Materials

[60] Fullerene purity (99.9%) was purchased from Sigma-Aldrich. Dimethylsulfoxide (DMSO) and toluene were purchased from Merck (India) and dried over calcium hydride for 24h and then distilled under reduced pressure before use. Diazido  $\beta$ -cyclodextrin synthesized in Chapter 2 was used. Double distilled water was used during the experimental work.

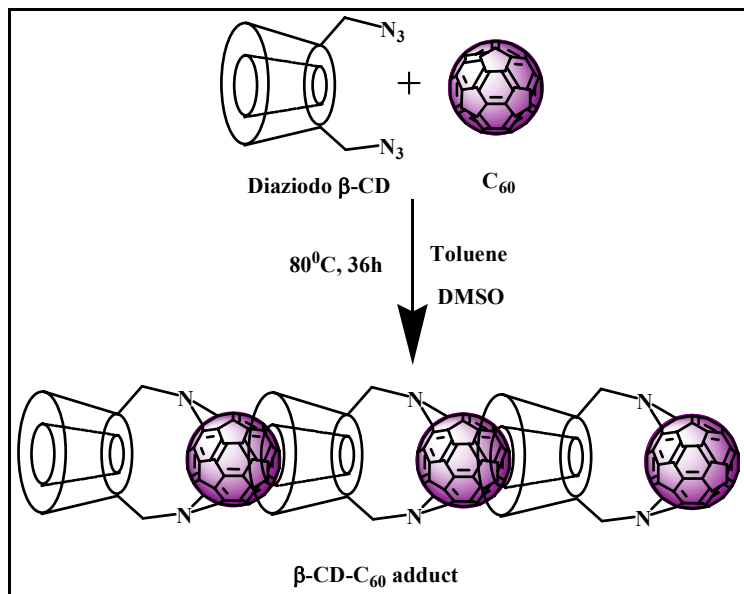
### 5.1.2.2 Measurements

The FTIR spectra of the compounds were recorded on a Shimadzu 8400S Fourier Transform Infrared Spectrometer by KBr pellet method at  $10^{-4}$  resolution and 30 scans at room temperature. AR grade KBr was used for the preparation of pellet. The UV-Vis spectra were recorded on a Shimadzu UV-Vis-2450 spectrophotometer.  $^1\text{H}$  and  $^{13}\text{C}$  NMR spectra were recorded on a Bruker spectrometer operating at 400 MHz at room temperature where TMS was used as internal standard. Thermogravimetry analysis (TGA) was recorded on a Shimadzu, TGA-50 system with a heating rate of  $10^\circ\text{C}/\text{min}$  under air atmosphere in the temperature range of  $30\text{-}800^\circ\text{C}$ . XRD patterns were measured on a Rikagu diffractometer with  $\text{CuK}\alpha$  radiation ( $\lambda = 0.15406\text{ nm}$ ) at 40 kV and 40 mA. To study the morphology and particle size of adduct, an energy-filtering transmission electron microscopy (TEM) [EF-TEM, EM 912 OMEGA (ZEISS, S-4700), 120 kV] was used. For TEM observation, the 1% adduct solution in double distilled water was drop casted on 400 mesh carbon-coated copper grids and annealed at  $100^\circ\text{C}$  for 12 hours before measurement. The measurements of scanning electron microscopy of powders on the carbon tape after gold-coating were performed on a JEOL JSM-6500F at an operation voltage of 20 kV. AFM measurements were carried out on a Nanoscope III (Digital Instruments) in air. The  $\text{D}_2\text{O}$  solution of adduct was deposited on a mica plate and the  $\text{D}_2\text{O}$  was evaporated under reduced pressure. Tapping mode analysis was carried out on the plate.

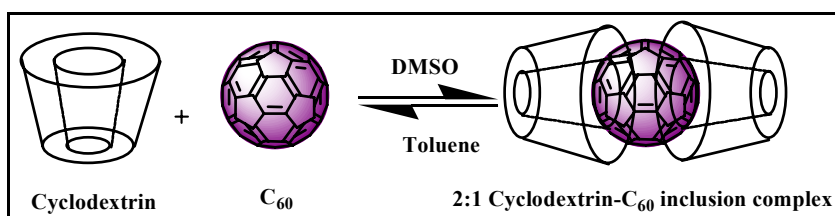
### 5.1.2.3 Synthesis of $\beta$ -Cyclodextrin-[60]Fullerene Adduct

The water-soluble  $\beta$ -cyclodextrin-[60]fullerene adduct as shown in Scheme 5.1.1 was synthesized using a mixed solvent system to bring water-soluble and toluene soluble reactants into one homogeneous phase. Thus, a 0.1 mmol solution of 6<sup>A</sup>,6<sup>D</sup>-diazido-6<sup>A</sup>,6<sup>D</sup>-dideoxy- $\beta$ -cyclodextrin in DMSO and a 0.1 mmol solution of [60]fullerene in toluene were mixed and stirred for 36h at 80°C under nitrogen atmosphere, during which the deep purple homogeneous solution turned to deep brown. The progress of the reaction was monitored by withdrawing aliquots of the reactant solution in intervals of 4h and measuring the UV-Vis absorbance. After the above mentioned time period, the product formed was isolated by removing the organic solvents under vacuum on a rotary evaporator. The brown colored solid was extremely water-soluble giving a light yellow aqueous solution. This aqueous solution was filtered through 0.45  $\mu\text{m}$  syringe-filter to remove undissolved residue and then the filtrate was subjected to ultrafiltration over a polymer membrane with a molar mass cut-off of 2 kg mol<sup>-1</sup> for the removal of excess of diazido  $\beta$ -cyclodextrin. The resultant concentrated aqueous solution was freeze-dried to get a deep brown colored adduct, which is soluble in water.

The 2:1 inclusion complex of  $\beta$ -cyclodextrin and [60]fullerene was prepared according to the literature<sup>15</sup> and adopting the same procedure as shown in Scheme 5.1.2 for the comparison studies.



**Scheme 5.1.1** Covalent and Non-covalent interaction of modified  $\beta$ -CD and [60]fullerene.



**Scheme 5.1.2** Non-covalent 2:1 inclusion complex of  $\beta$ -CD and [60]fullerene.

### 5.1.3 Results and Discussion

The solubility of the  $\beta$ -CD-[60]fullerene adduct in water was measured and found to be  $6.5 \text{ mg mL}^{-1}$ , which is greater than that of 2:1 inclusion complex of  $\beta$ -cyclodextrin<sup>9</sup>. Usually, apart from the solubility of fullerenes in aqueous solution, the stability of the aqueous solution of fullerenes is a major problem, owing to their tendency to agglomerate after storage for longer periods. Hence, the stabilization of aqueous solution of solubilized fullerenes with higher stability is a pivotal issue and, therefore, is a challenge to produce aqueous solution of fullerenes with higher stability to explore their potential in biomedical applications. The previously described methods for the aqueous solubilization only deal with the non-polar interaction of the [60]fullerene molecule with cyclodextrins<sup>14,15</sup>. However, a competitive guest molecule in the biological media can displace [60]fullerene from the cyclodextrin cavity. Tethering the [60]fullerene molecule to the improved water-soluble selectively functionalized cyclodextrin molecule is an effective option of overcoming this problem. It also takes into account the advantage of more [60]fullerene surface area, which is not in the case of 2:1 inclusion complex. The  $\beta$ -CD-[60]fullerene adduct was stable and fullerene was not extractable from this complex.

To see the visible evidence of covalent-noncovalent interactions and stability of the  $\beta$ -CD-[60]fullerene adduct in polar and non-polar solvents, the extraction experiment was conducted in vials. [60]Fullerene in toluene shows deep purple color (Figure 5.1.1 [A]) and it is completely insoluble in polar solvents. Diazido  $\beta$ -CD is completely soluble in polar DMSO (Figure 5.1.1 [B]). These two solutions when mixed together in inert atmosphere and after evaporation of organic solvents, resulted in a yellowish brown color water-soluble  $\beta$ -CD-[60]fullerene adduct (Figure 5.1.1 [C]). When toluene was added to the solid  $\beta$ -CD-[60]fullerene adduct (Figure 5.1.1 [D]), it was observed that  $\beta$ -CD-[60]fullerene adduct was stable enough and [60]fullerene does not go into the toluene layer and it settled at the bottom of the vial. When toluene was added to the aqueous solution of  $\beta$ -CD-[60]fullerene adduct (Figure 5.1.1 [E]), it was observed that aqueous solution of  $\beta$ -CD-[60]fullerene adduct was stable enough and [60]fullerene does not go into the toluene layer. Thus, the  $\beta$ -CD-[60]fullerene adduct was stable in both the polar and non-polar solutions,

whereas, this is completely inverted in the case of 2:1 inclusion complex of  $\beta$ -CD with [60]fullerene. When toluene was added to the solid  $\beta$ -CD-[60]fullerene 2:1 inclusion complex (Figure 5.1.2 [D]), it was observed that [60]fullerene can easily go into the toluene solution and also similar observation has been seen when toluene was added to the aqueous solution of  $\beta$ -CD-[60]fullerene 2:1 inclusion complex (Figure 5.1.2 [E]), since toluene can penetrate into the non-polar cavity of  $\beta$ -CD and act as competitive guest molecule it can displace [60]fullerene from the non-polar cavity of  $\beta$ -CD and itself occupy into the non-polar cavity of  $\beta$ -CD.

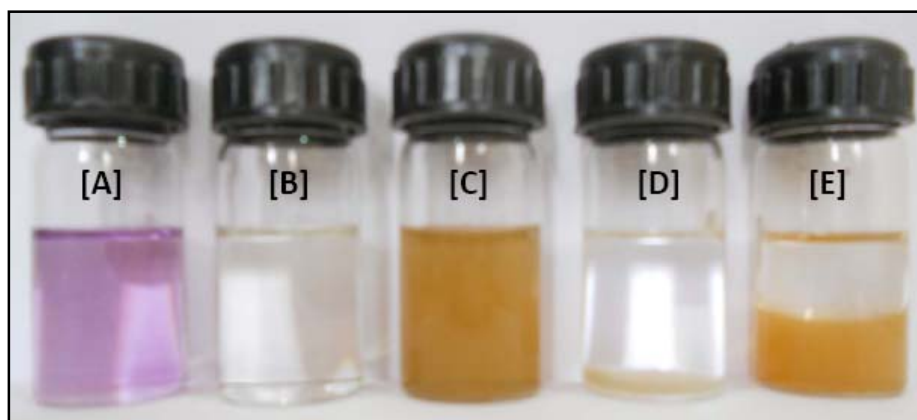


**Figure 5.1.1** Photograph of [A]  $C_{60}$  in toluene, [B] Diazido  $\beta$ -CD in DMSO, [C]  $\beta$ -CD- $C_{60}$  adduct in water, [D]  $\beta$ -CD- $C_{60}$  adduct in toluene and [E]  $\beta$ -CD- $C_{60}$  adduct in water + toluene.

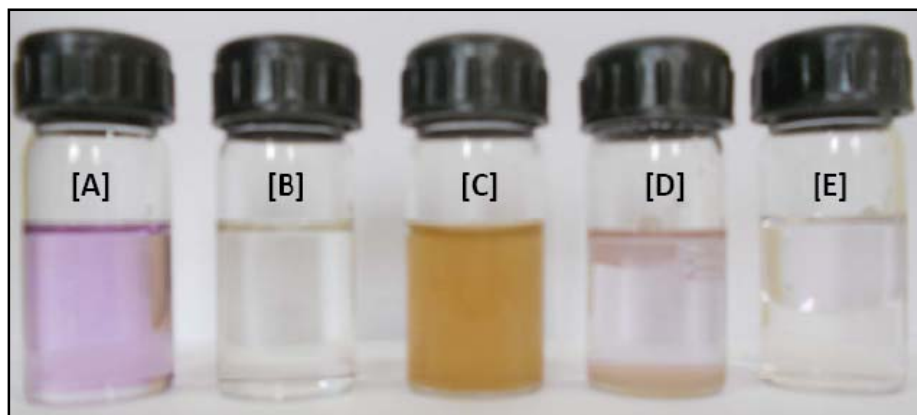


**Figure 5.1.2** Photograph of [A]  $C_{60}$  in toluene, [B]  $\beta$ -CD in DMSO, [C]  $\beta$ -CD- $C_{60}$  inclusion complex in water, [D]  $\beta$ -CD- $C_{60}$  inclusion complex in toluene and [E]  $\beta$ -CD- $C_{60}$  inclusion complex in water + toluene.

The more specific evidence for the covalent as well as non-covalent interactions between selectively diazido functionalized  $\beta$ -cyclodextrin and [60]fullerene comes from the conventional techniques like FTIR, UV-Vis,  $^1\text{H}$  NMR,  $^{13}\text{C}$  NMR and TGA of the  $\beta$ -CD-fullerene adduct.

### 5.1.3.1 Fourier Transform Infrared Spectroscopy (FTIR)

The FTIR spectra of diazido  $\beta$ -CD,  $\text{C}_{60}$  and  $\beta$ -CD-[60]fullerene adduct is depicted in Figure 5.1.3. The FTIR spectrum of the diazido functionalized  $\beta$ -CD (Figure 5.1.3 a) showed an absorbance stretching band at  $2037\text{ cm}^{-1}$  for asymmetrical azide ( $-\text{N}_3$ ) functionality along with all the absorbance bands of the parent  $\beta$ -cyclodextrin, whereas there was no signal in this region in the FTIR spectrum (Figure 5.1.3 c) of the  $\beta$ -CD-[60]fullerene adduct. The spectrum of pristine  $\text{C}_{60}$  (Figure 5.1.3 b) showed four characteristic absorption bands at  $1429\text{ cm}^{-1}$ ,  $1183\text{ cm}^{-1}$ ,  $578\text{ cm}^{-1}$  and  $527\text{ cm}^{-1}$ . The  $\beta$ -CD-[60]fullerene adduct showed the typical sharp peaks of [60]fullerene at  $527\text{ cm}^{-1}$  and  $583\text{ cm}^{-1}$ . The disappearance of absorbance band of azide ( $-\text{N}_3$ ) and presence of [60]fullerene absorbance bands confirmed the covalent attachment of fullerene with modified  $\beta$ -CD.

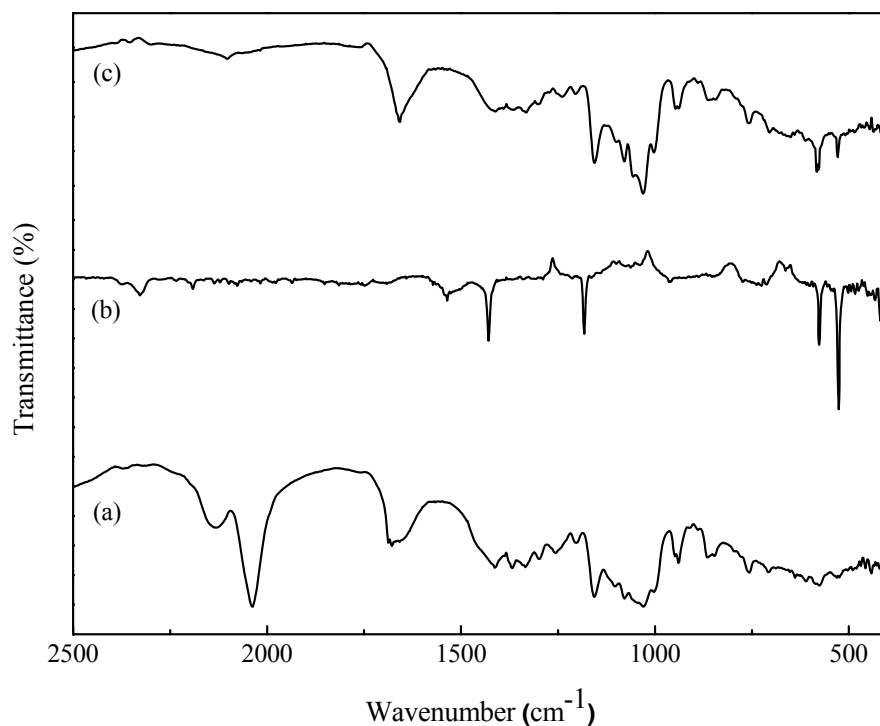


**Figure 5.1.3** FTIR spectra of (a) diazido  $\beta$ -CD, (b)  $\text{C}_{60}$ , (c)  $\beta$ -CD- $\text{C}_{60}$  adduct.

### 5.1.3.2 UV-Visible Spectroscopy (UV-Vis)

The UV-Vis absorbance spectra of  $C_{60}$  in toluene, diazido  $\beta$ -CD in water and  $\beta$ -CD-[60]fullerene adduct in water is shown in Figure 5.1.4. The UV-Vis absorbance spectrum of [60]fullerene showed absorbance maxima at around 334 nm in toluene and it is completely insoluble in water, whereas the diazido  $\beta$ -cyclodextrin does not show any absorbance in this region. However, the spectrum of  $\beta$ -CD-fullerene adduct in water showed the typical absorbance maxima at around 348 nm of [60]fullerene which is red shifted by few nanometers and there was peak broadening of the absorbance beyond 406 nm typical of the [60]fullerene absorbance in toluene.

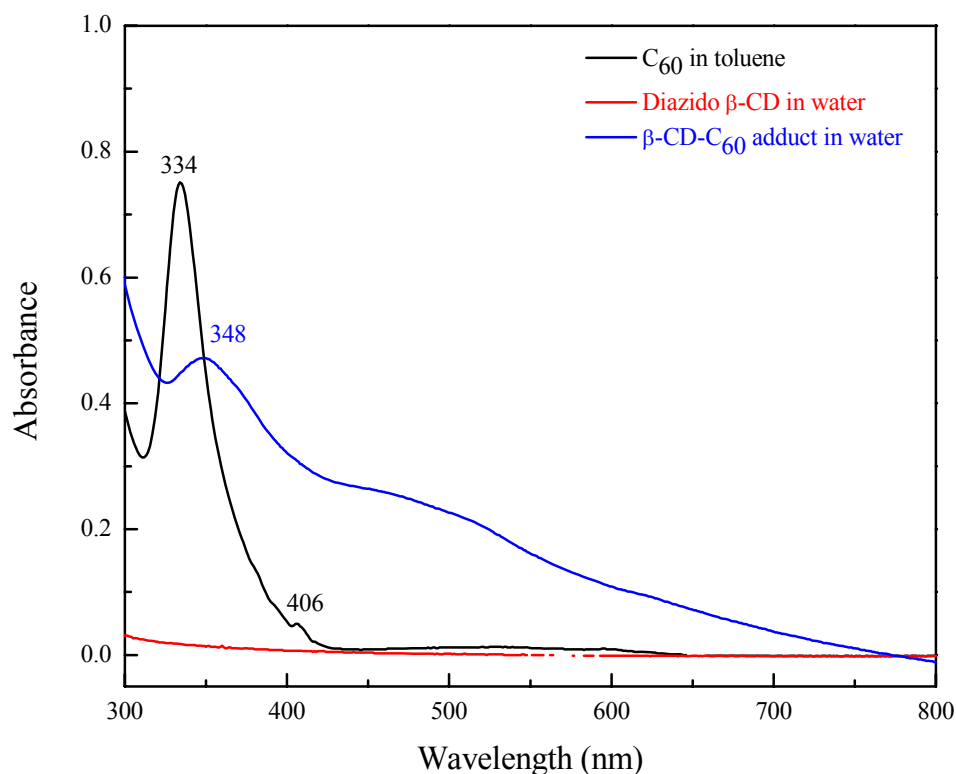


**Figure 5.1.4** UV-Vis spectra of  $C_{60}$  in toluene, diazido  $\beta$ -CD in water and  $\beta$ -CD- $C_{60}$  adduct in toluene.

The supramolecular interaction of [60]fullerene with the modified  $\beta$ -CD was confirmed by extracting [60]fullerene with a competitive guest molecule. Thus, when toluene was added (toluene acts as competitive guest molecule and also solvent for fullerene) to the aqueous solution of the modified  $\beta$ -CD-[60]fullerene adduct as well

as to a 2:1 inclusion complex of  $\beta$ -CD/[60]fullerene and shaken, the toluene layer was characterized by UV-Vis spectroscopy, it showed that 2:1 inclusion complex of  $\beta$ -CD/[60]fullerene shows an absorbance at 335 nm of [60]fullerene (Figure 5.1.5) whereas the toluene layer of the modified  $\beta$ -CD-[60]fullerene adduct did not show any absorbance. This indicates that the [60]fullerene was covalently attached to modified  $\beta$ -CD and also forms an inclusion complex with another molecule of modified  $\beta$ -CD. This behavior proved that in a competitive milieu the modified  $\beta$ -CD-[60]fullerene adduct is more stable than the 2:1 inclusion complex of  $\beta$ -CD/[60]fullerene.

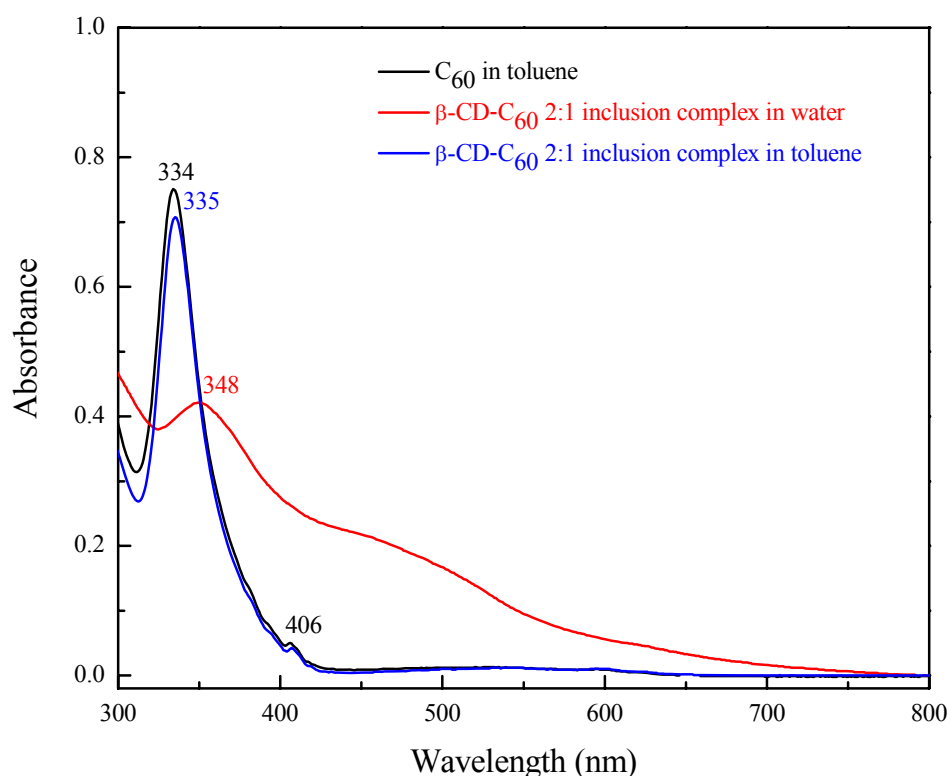


**Figure 5.1.5** UV-Vis spectra of C<sub>60</sub> in toluene,  $\beta$ -CD-C<sub>60</sub> 2:1 inclusion complex in water and  $\beta$ -CD-C<sub>60</sub> 2:1 inclusion complex in toluene.

### 5.1.3.3 Nuclear Magnetic Resonance Spectroscopy (NMR)

The type of interactions between [60]fullerene and modified  $\beta$ -cyclodextrin was further confirmed by <sup>1</sup>H and <sup>13</sup>C NMR. The <sup>1</sup>H NMR spectra of the diazide functionalized  $\beta$ -CD and  $\beta$ -CD-[60]fullerene adduct was taken in two different

solvents DMSO-d<sub>6</sub> and D<sub>2</sub>O shown in Figure 5.1.6 and Figure 5.1.7, respectively. The <sup>1</sup>H NMR spectra of diazido β-CD and adduct shows the similar proton signal due to the similar hydrogen structure, except upfield shifts was observed. The <sup>1</sup>H NMR spectra given in Figure 5.1.6 of the β-CD-[60]fullerene adduct showed all the proton signals of the glucose units of the cyclodextrin at δppm: 4.81 (d, 7H, H-1), 3.27 (m, 7H, H-2), 3.66 (m, 7H, H-3), 3.36 (m, 7H, H-4) 3.56 (m, 7H, H-5), 3.63 (d, 12H, H-6) and it was observed that the proton signals in adduct shows upfield shifts compared to the diazido β-CD, which confirms the formation of inclusion complex. The spectra was similar when it was taken in a different solvent i.e. D<sub>2</sub>O with no observable shifts in the positions of the peaks.

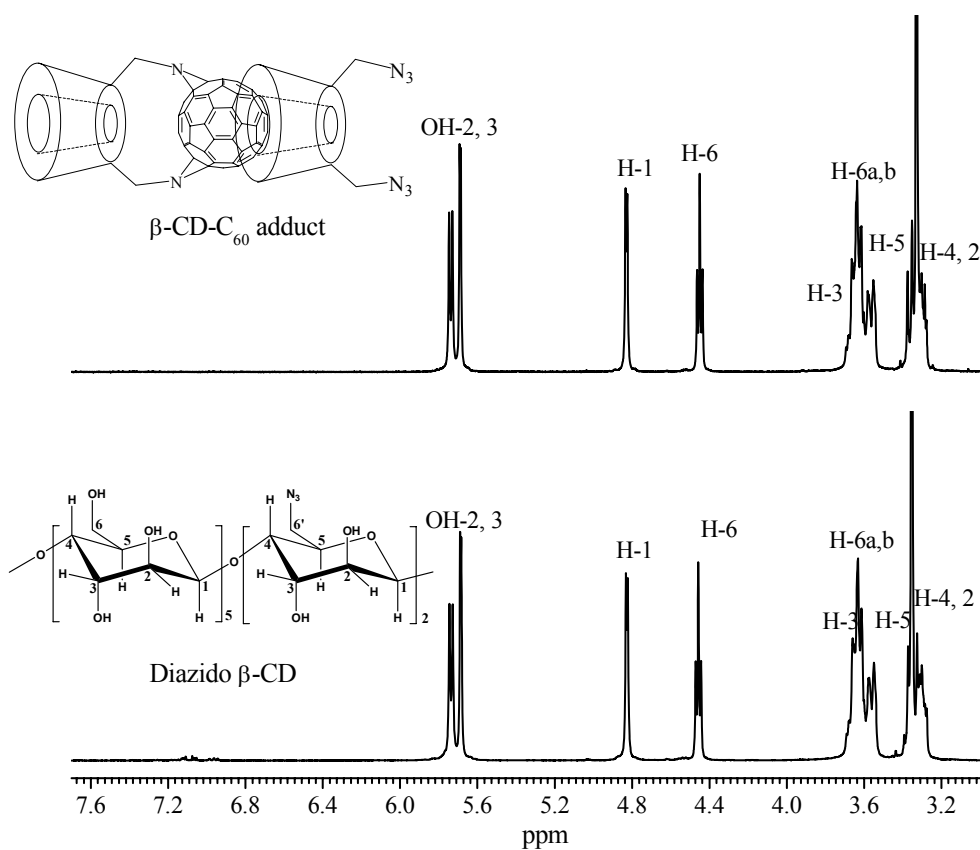


**Figure 5.1.6** <sup>1</sup>H NMR spectra of diazido β-CD and β-CD-C<sub>60</sub> adduct in DMSO-d<sub>6</sub>.

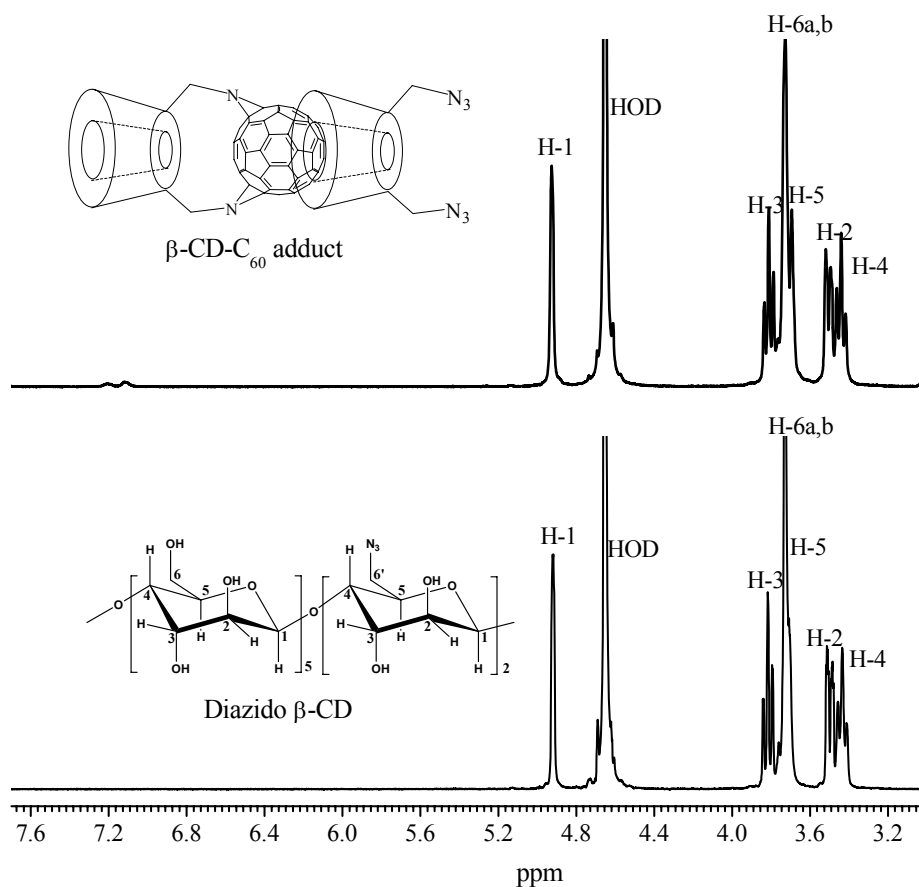


**Figure 5.1.7** <sup>1</sup>H-NMR spectra of diazido β-CD and β-CD-C<sub>60</sub> adduct in D<sub>2</sub>O.

The <sup>13</sup>C NMR spectra of β-CD-[60]fullerene adduct in two different solvents D<sub>2</sub>O and DMSO-d<sub>6</sub> is shown in Figure 5.1.8. The <sup>13</sup>C NMR spectra of the β-CD-[60]fullerene adduct in both the solvents showed all the expected six carbon chemical shift of glucose units at δppm: 101.85 (C-1), 72.42 (C-2), 73.04 (C-3), 82.29 (C-4), 72.26 (C-5), 6.27 (C-6) along with three new carbon chemical shifts. The one at 32 δppm is due to the primary substituted carbon (C-6') of β-CD and the other two at 70.7 δppm and at 165 δppm are due to the formation of [5,6] closed azafullerene structure with β-CD. It is interesting to note that the <sup>13</sup>C NMR is clean with new peaks confirming the formation of covalent bonds as determined by reaction between olefinic double bond and an azide. The spectra in both the solvents look similar due to the same structural carbon skeleton.

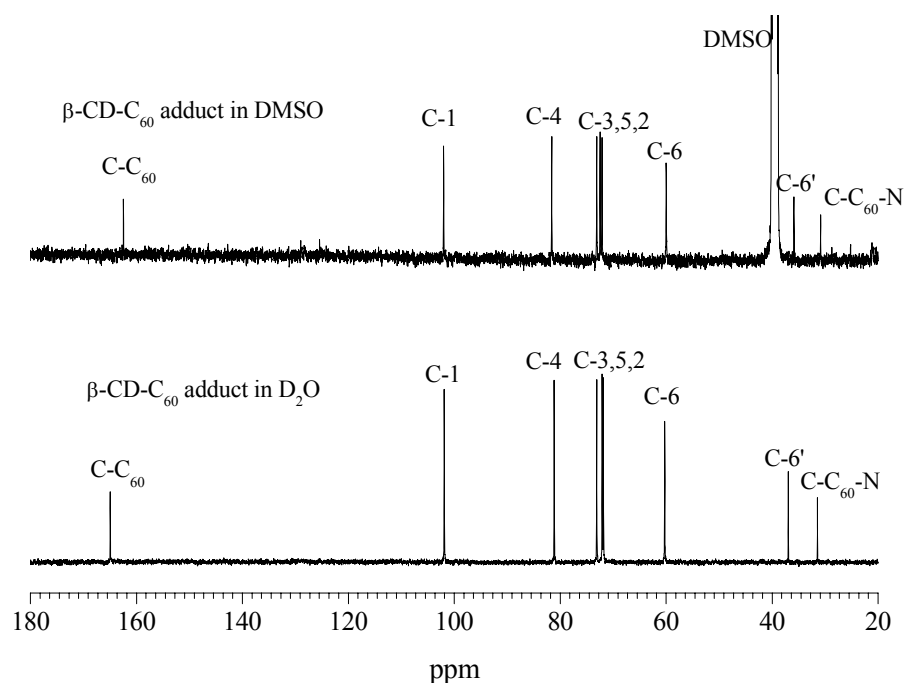


**Figure 5.1.8**  $^{13}\text{C}$ -NMR spectrum of  $\beta\text{-CD-C}_{60}$  adduct in  $\text{D}_2\text{O}$  and  $\text{DMSO-d}_6$ .

#### 5.1.3.4 Thermogravimetric Analysis (TGA)

In order to assess the thermal stability of the  $\beta$ -cyclodextrin derivative and  $\beta\text{-CD-[60]fullerene}$  adduct, a thermogravimetric study was conducted. The degradation pattern of parent cyclodextrin shows mass loss in three different temperature regions (Figure 5.1.9 a). The first mass loss at around  $105^\circ\text{C}$  is due to the loss of moisture, the second mass loss at  $300^\circ\text{C}$  as dehydration of  $\beta\text{-CD}$ , and third mass loss at  $367^\circ\text{C}$  as a decomposition of glucose units in  $\beta\text{-CD}$ . However, in case of the diazido  $\beta\text{-CD}$  (Figure 5.1.9 b) the thermogram is same, except that the second mass loss is at a lower temperature of  $250^\circ\text{C}$  due to the modification of cyclodextrin. The thermogram of pristine [60]fullerene (Figure 5.1.9 c) shows the mass loss after  $500^\circ\text{C}$ . The thermogram of  $\beta\text{-cyclodextrin-[60]fullerene}$  adduct (Figure 5.1.9 d) showed that the mass loss of the  $\beta\text{-cyclodextrin}$  at  $327^\circ\text{C}$  was 75%. This result indicates that one [60]fullerene molecule was sandwiched between two cyclodextrins supporting the structure of adduct as shown in Scheme 5.1.1.

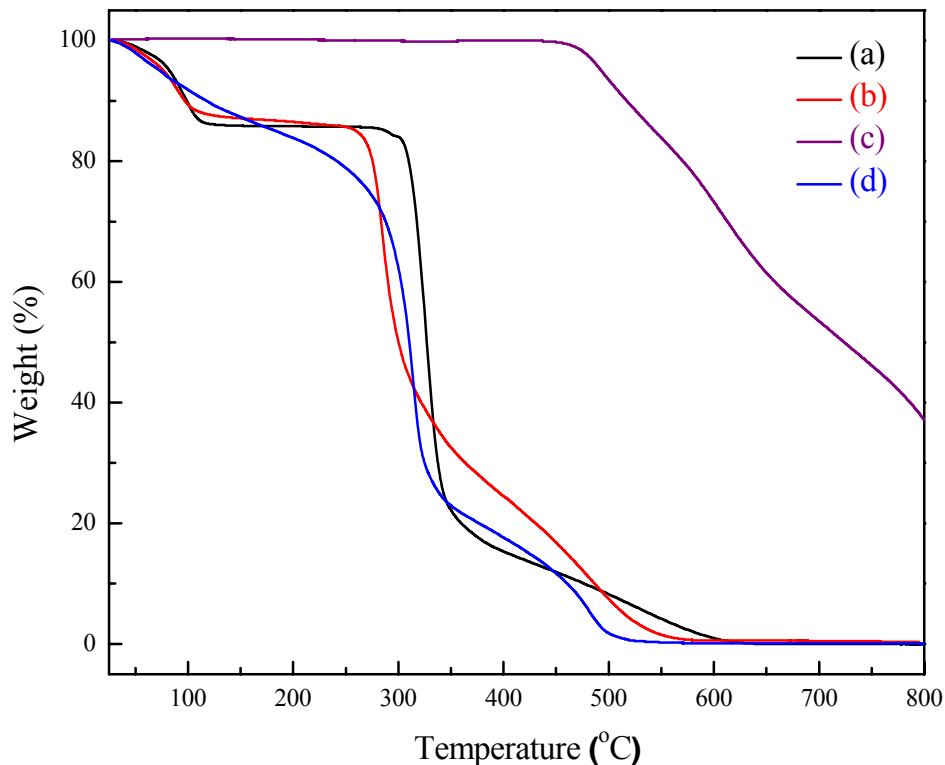


**Figure 5.1.9** TGA curves of (a)  $\beta$ -CD, (b) diazido  $\beta$ -CD, (c)  $C_{60}$  and (d)  $\beta$ -CD- $C_{60}$  adduct.

### 5.1.3.5 X-ray Diffraction (XRD)

XRD is widely used technique for the study of supramolecular aggregates to depict the aggregate structure. The X-ray diffraction pattern of  $C_{60}$ , diazido  $\beta$ -CD and  $\beta$ -CD- $C_{60}$  adduct is shown in Figure 5.1.10. The X-ray diffractogram pattern of the formed  $\beta$ -CD-[60]fullerene adduct (Figure 5.1.10 c) showed that the adduct has neither the typical  $2\theta$  values of functionalized  $\beta$ -CD (Figure 5.1.10 b) nor those of [60]fullerene (Figure 5.1.10 a). It can be seen that the  $\beta$ -CD- $C_{60}$  adduct has a different structure to the functionalized  $\beta$ -CD ( $2\theta = 10.7, 12.5, 19.5, 22.7, 27.0, 34.7^\circ$ ) and [60]fullerene ( $2\theta = 11.0, 17.5, 21.7^\circ$ ), with total suppression of the crystalline structure of  $\beta$ -CD. This type of phenomenon also observed for the  $\beta$ -CD/[60]fullerene inclusion complex.

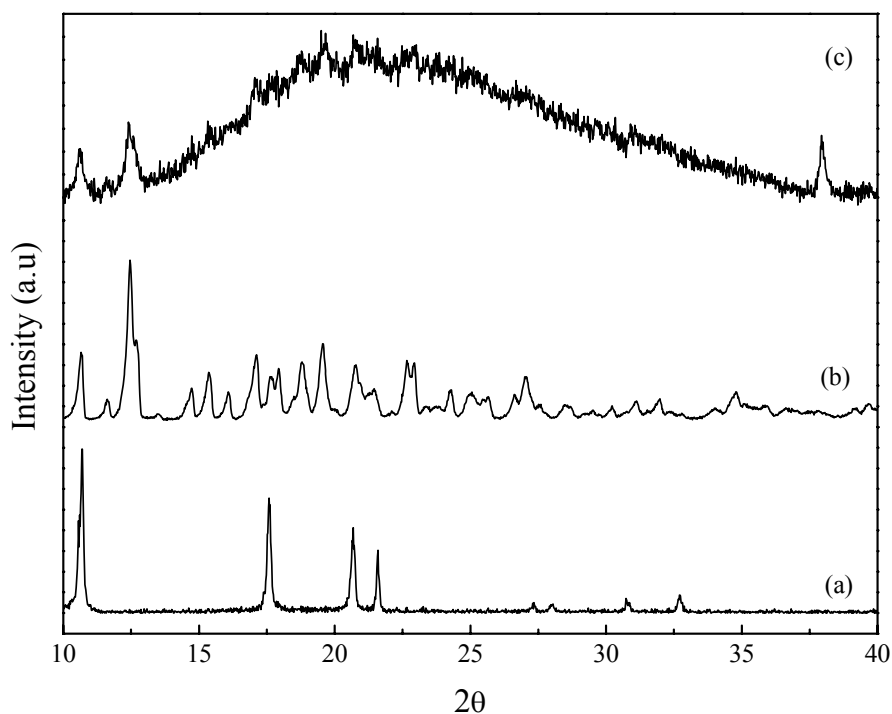


**Figure 5.1.10** X-ray diffractogram of (a)  $C_{60}$ , (b) diazido  $\beta$ -CD and (c)  $\beta$ -CD- $C_{60}$  adduct.

### 5.1.3.6 Transmission Electron Micrograph (TEM) and Field Emission Scanning Electron Microscopy (FE-SEM)

The most direct and visible evidence for the supramolecular self-assembly and formation of liner  $\beta$ -CD-[60]fullerene adduct is given by TEM and FE-SEM as shown in Figure 5.1.11. The TEM image (Figure 5.1.11 a) of  $\beta$ -CD-[60]fullerene adduct provides the confirmation for the presence of linear supramolecular nanostructure of 2000-2500 nm, which are joint together linearly through approximately 1000-1200 units of the  $\beta$ -CDs and [60]fullerene molecules. The same nanostructure of  $\beta$ -CD-[60]fullerene adduct also supports from the FE-SEM image (Figure 5.1.11 b). On the basis of TEM and FE-SEM results we suggest, here in a possible structural model of supramolecular self-assembly as shown in Figure 5.1.11 c. The model shows that  $\beta$ -CD- $C_{60}$  adduct is arranged in a channel through a head-to-tail arrangement and forms micrometer size supramolecular self-assembly. Similarly, 2:1 inclusion complex of  $\beta$ -CD and [60]fullerene form unique supramolecular self-assembly was confirmed by TEM as shown in Figure 5.1.12. The size of the self-assembly was found to be

approximately 1000 nm. These self-assemblies were observed due to the strong non-covalent integrations such as van der Waals forces, hydrogen-bonding, hydrophilic/hydrophobic interactions,  $\pi$ - $\pi$  stacking interaction, electrostatic interactions, donor and acceptor interactions, etc.

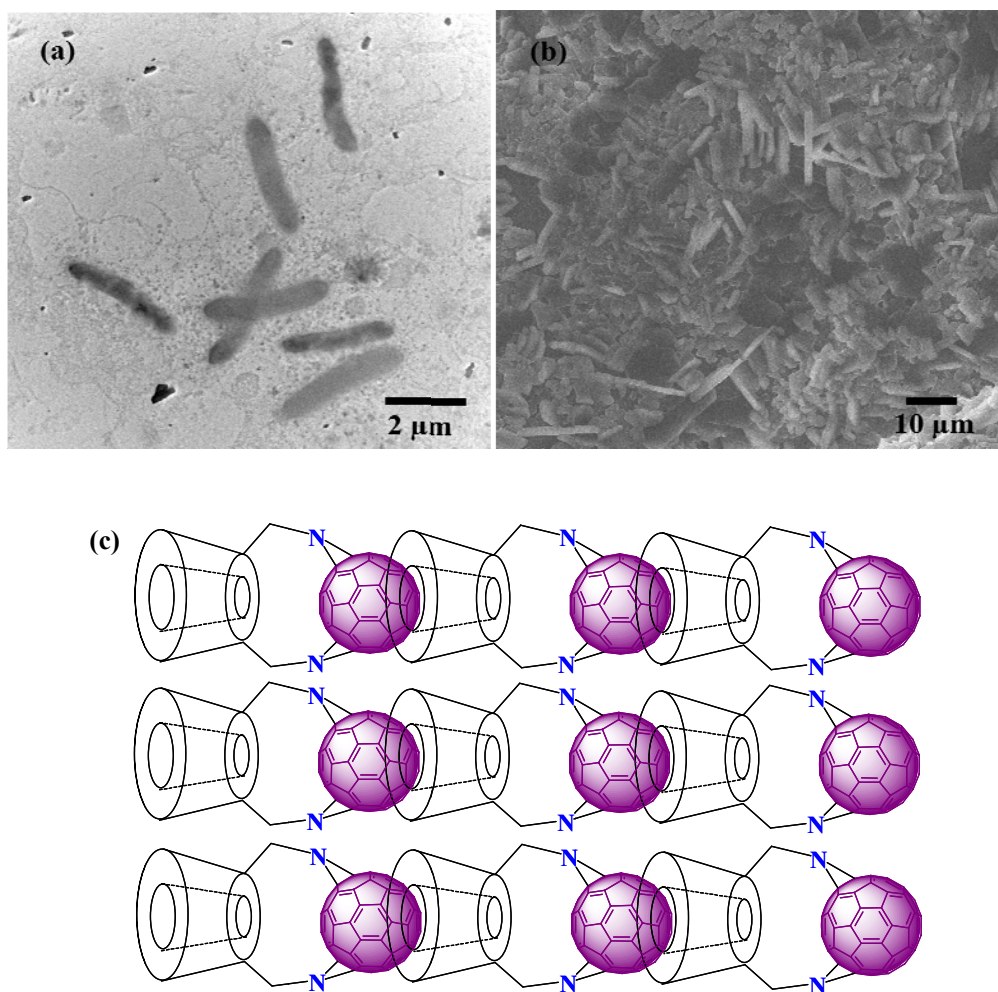


**Figure 5.1.11** (a) TEM image (b) FE-SEM image and (c) Schematic illustration of the proposed supramolecular self-assembly of  $\beta$ -CD-C<sub>60</sub> adduct.

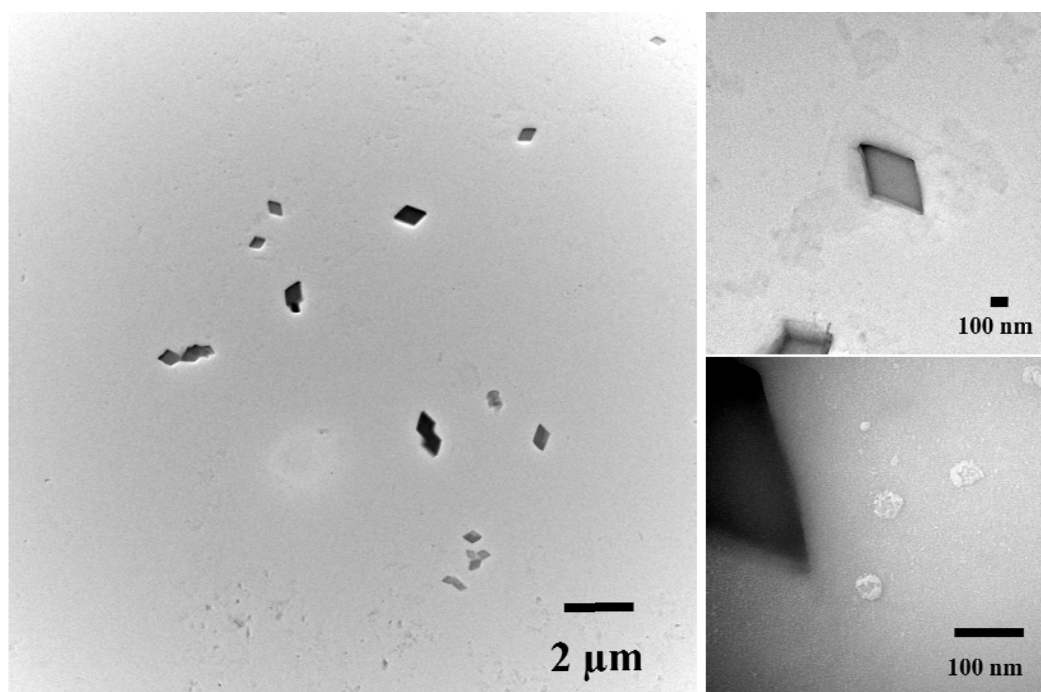


**Figure 5.1.12** TEM image of self-assembly of 2:1 inclusion complex of  $\beta$ -CD and [60]fullerene.

### 5.1.3.7 Atomic Force Microscopy (AFM)

The freeze-dried  $\beta$ -CD-[60]fullerene adduct was redispersed in distilled water then drops of solution spread over a sheet of mica and dried at room temperature. The picture of a  $1 \mu\text{m}^2$  surface of  $\beta$ -CD-[60]fullerene adduct is depicted in Figure 5.1.13. It can be clearly seen that the solid sample contains rather uniformly stacked nanostructure of 200 nm width, which appear to be built up from the conjugation and supramolecular self-assembly of functionalized  $\beta$ -CD and [60]fullerene in a linear manner, which was also supported from TEM and FE-SEM results.

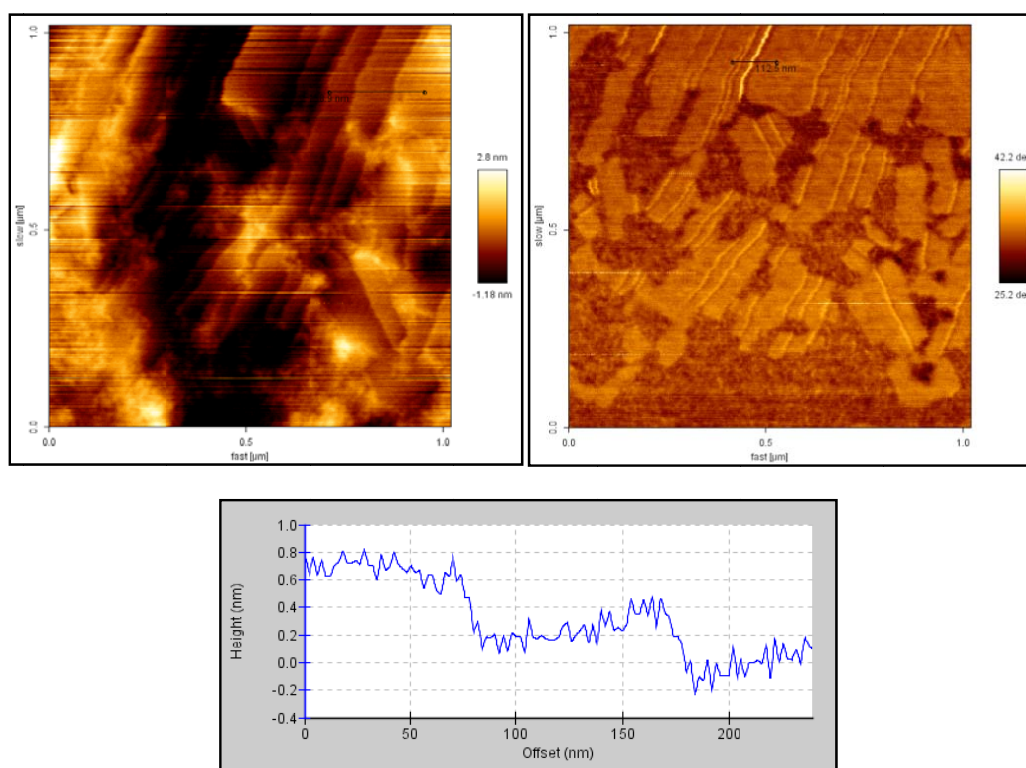


**Figure 5.1.13** AFM images of  $\beta$ -CD-[60]fullerene adduct.

#### 5.1.4 Conclusions

Diazido functionalized  $\beta$ -CD synthesized in Chapter 2 was used as reactant and it easily reacts with the double bond of the [60]fullerene via a [2+3] 1,3-dipolar nucleophilic cycloaddition reaction. Thus, the covalent linking of the highly water-insoluble [60]fullerene to a highly water-soluble cyclodextrin derivative gives the water-soluble adduct. The formation of covalent bond and non-covalent inclusion complex in aqueous media between [60]fullerene and diazido modified cyclodextrin has been confirmed from absorbance studies, and the stability of the complex (head-tail structure) has been confirmed from extraction experiment and spectroscopic studies. The supramolecular self-assembly of adduct has been further confirmed from the microscopic (TEM, FE-SEM and AFM) results, which suggest the linear rod like nanostructure of adduct. The tethering of the [60]fullerene molecule to the water-soluble  $\beta$ -cyclodextrins by both covalent linkage and non-covalent interaction has potential biomedical applications, where [60]fullerene properties can be used in aqueous medium.

## 5.2 Solubilization of [60]Fullerene and [70]Fullerene by Disaccharides

### 5.2.1 Introduction

Since the discovery of the novel biomedical applications of [60]fullerene attempts have been made to make it water-soluble<sup>23-31</sup>. Various techniques have been applied to make it water-soluble that include covalent functionalization,<sup>32-34</sup> emulsion formation<sup>35,36</sup> complexation with biomaterials<sup>37,38</sup> and non-covalent guest-host systems<sup>39-41</sup>. Among the guest-host systems, cyclodextrins are widely studied and successfully utilized including several patents<sup>42,43</sup>. One of the fundamental logic of guest-host system is that the fullerene molecule occupies the hydrophobic cavity of the cyclodextrins. Based on this premise it was argued that only  $\gamma$ -cyclodextrin (cavity size = 0.950 nm) could include the [60]fullerene (diameter = 0.7 nm) thus forming a 1:1 inclusion complex which was subsequently modified to show that even  $\beta$ -cyclodextrin (cavity size = 0.78 nm) could include a [60]fullerene molecule forming a 1:2 inclusion complex<sup>44,45</sup>. This was possible due to the formation of a self-assembled structure which included the [60]fullerene in the cavity formed by two cyclodextrin units<sup>46,47</sup>. If one were to look at the cyclodextrin structure closely, the glucose units are linked in by the  $\alpha$ -1,4-glycoside linkages<sup>48</sup>. How important is it for the [60]fullerene molecule to sit inside a cavity made by these bucket structures? If two  $\beta$ -cyclodextrins could include the [60]fullerene molecule then by the same logic it should be possible for a disaccharide to encircle a [60]fullerene molecule due to the same hydrophobic interactions. In fact some early studies have shown that fullerene/carbohydrates compositions were possible by mechanochemical method that led to fullerene aggregates in carbohydrate shell and that surface carbohydrate layer formed a van der Waals complex with fullerene<sup>49,50</sup>. Subsequent molecular modelling studies and theoretical calculations have shown that the enthalpy of formation of fullerene/sucrose complex was 3.5 kcal/mole<sup>51</sup>. If that is the case a few number of disaccharides could be used to isolate [60]fullerene in aqueous media or in other words solubilise [60]fullerene.

This chapter describes the preparation of crystalline highly water-soluble [60]fullerene/[70]fullerene by complexation with very inexpensive naturally and commercially available, nontoxic disaccharides (lactose, maltose and sucrose) in comparison with very expensive and difficult to synthesize and toxic host molecules.

Disaccharides can easily interact with [60]fullerene/[70]fullerene and convert this highly water-insoluble molecules into the highly water-soluble complex. Enthalpy and entropy calculation of interaction between [60]fullerene and disaccharides also support the formation of non-covalent complex<sup>51</sup>. The non-covalent interaction between [60]fullerene and disaccharides were characterized by using conventional characterization techniques like UV-Vis, FTIR, NMR, XRD, TGA analysis. The morphology and particles size of the complex was determined by Transmission Electron Micrograph (TEM) and Static Light Scattering (SLS).

## 5.2.2 Experimental

### 5.2.2.1 Materials

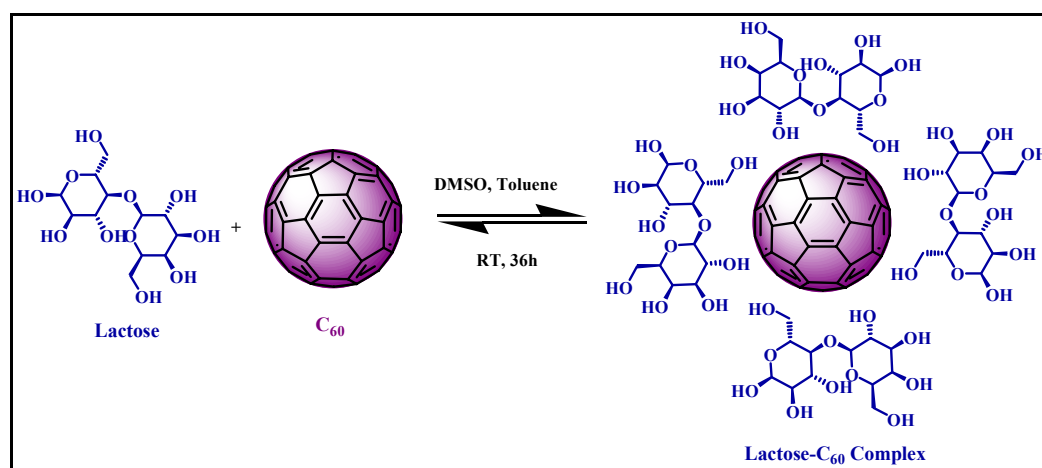
[60]Fullerene (purity 99.9%), [70]fullerene (purity 99%) and the most stable free radical 2,2'-diphenyl-1-picrylhydrazyl (DPPH) (stored in dry ice) were purchased from Sigma-Aldrich and used as received. Maltose monohydrate, lactose monohydrate, sucrose and spectrophotometric grade toluene, DMSO was purchased from Merck, Mumbai, India. Double distilled water was used during the experimental work.

### 5.2.2.2 Measurements

The UV-Visible spectra of the solutions were recorded on a Shimadzu-2450, spectrophotometer. The FTIR spectra of the freeze-dried compounds was recorded on a Shimadzu 8400S, Fourier Transform Infrared Spectrometer by using KBr pellet method at 30 scans and  $10^{-4}$  resolution at room temperature. XRD patterns were measured on a Rigaku diffractometer with  $\text{CuK}\alpha$  radiation ( $\lambda = 0.15406$  nm) at 40 kV and 40 mA.  $^1\text{H}$  and  $^{13}\text{C}$  NMR spectra were recorded on a JEOL JNM-LA300WB; 400 MHz instrument. All spectra were measured in  $\text{D}_2\text{O}$  as solvent and the chemical shifts were referenced to tetramethylsilane (TMS) at 0 ppm. Thermogravimetric analysis (TGA) was recorded on a Shimadzu, TGA-50 system with a heating rate of  $10^\circ\text{C}/\text{min}$  under air atmosphere in the temperature range of  $30\text{-}700^\circ\text{C}$ . To study the morphology and particle size of complex, an energy-filtering transmission electron microscopy (TEM) [EF-TEM, EM 912 OMEGA (ZEISS, S-4700), 120 kV] was used. For TEM observation, the 1% complex solutions in double distilled water was drop casted on 400 mesh carbon-coated copper grids and annealed at  $100^\circ\text{C}$  for 12 hours before measurement. Particle size was also measured by static light scattering technique with Ga-As semiconductor laser (mini Dawn Tristar, Wyatt). For the molecular modeling studies, the software ChemOffice 2004 (Chem 3D Ultra 8.0 version) was used.

### 5.2.2.3 Synthesis of the [60]fullerene-disaccharide complex

The complex between [60]fullerene and disaccharides were prepared by using mixed homogeneous solvent system to bring water-insoluble [60]fullerene and water-soluble disaccharide into one homogeneous phase. Thus, disaccharide (lactose monohydrated) 1000 mg (0.28 mmol) was dissolved in polar solvent DMSO and 10 mg [60]fullerene (0.014 mmol) in non-polar solvent toluene, these two solutions were mixed together and stirred for 36 hrs in nitrogen atmosphere at room temperature, during which the deep purple homogeneous solution turned deep brown. The progress of the reaction was determined by taking an aliquot of the reaction mixture after every 4hrs and absorbance measured. After the completion of the reaction the highly water-soluble complex was isolated by removing solvent by vacuum on a rotary evaporator and dissolving the brown solid into excess of water. This aqueous solution was stirred for 30 min and insoluble uncomplexed material was removed by filtration through 0.45  $\mu\text{m}$  syringe-filter. The filtrate aqueous solution of the complex was purified by ultrafiltration over a polymer membrane (MWCO = 1K) to remove excess of disaccharide. The resulting purified concentrated aqueous solution was subjected to freeze-drying to get brown color highly water-soluble [60]fullerene-disaccharide complex. The reaction between lactose and  $\text{C}_{60}$  is shown in Scheme 5.2.1.



**Scheme 5.2.1** Complexation of lactose- $\text{C}_{60}$  in mixed solvent system.

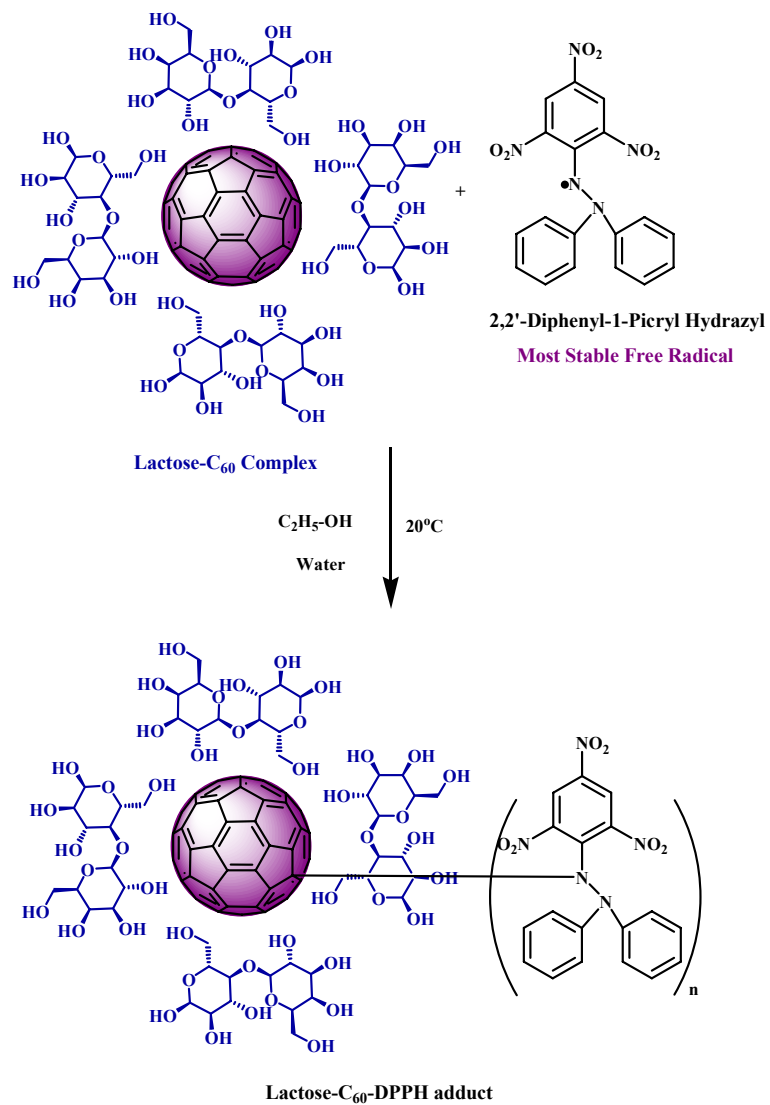
#### **5.2.2.4 Determination of Aqueous Solubility of Complex and Quantification of [60]Fullerene**

The aqueous solubility of the prepared complex with different disaccharides was determined in terms of weight by dissolving 50 mg of complex sample in the minimum amount of distilled water with the help of  $\mu\text{L}$  pipette; ensure the solution reaching saturation at room temperature ( $30^{\circ}\text{C}$ ). The solubility measured in triplicate and average value was reported.

Concentration of [60]fullerene per mg of the complex was determined by extracting [60]fullerene with toluene from the solid [60]fullerene-disaccharide complex and evaluated from the [60]fullerene standard absorbance in toluene.

#### **5.2.2.5 Radical scavenging**

A solution of lactose- $\text{C}_{60}$  complex was prepared in water (1%, w/v), and its UV-Vis absorbance spectrum was recorded. The solution of the free radical DPPH was prepared in ethanol ( $1.7 \times 10^{-4}$  M), and its UV-Vis absorbance spectrum also recorded. Both solutions were kept in a temperature bath at  $20^{\circ}\text{C}$ . In a 20-mL reaction vial, 5 mL of each of the above solutions were mixed, and the UV-Vis absorbance spectrum of the solution mixture was recorded. The reaction temperature was maintained at  $20^{\circ}\text{C}$ , and the contents were constantly stirred. At regular intervals the absorption spectra of the solution mixture were recorded. The reaction of lactose- $\text{C}_{60}$  complex and 2,2'-diphenyl-1-picrylhydrazyl (DPPH) is shown in Scheme 5.2.2. Similarly, radical scavenging of DPPH with other prepared water-soluble fullerenes has been also carried out.



**Scheme 5.2.2** Reaction scheme for radical scavenging of most-stable free radical DPPH with lactose-C<sub>60</sub> complex.

### 5.2.3 Results and Discussion

[60]Fullerene is an extremely water-insoluble molecule. Solubilizing the [60]fullerene in polar solvents is difficult and its solubility in non-polar organic solvents is also limited. The lack of genuine water-solubility and availability of macroquantities of [60]fullerene and disaccharides inspired us to prepare water-soluble [60]fullerene-disaccharides complex for the requirement of biological applications. Highly water-soluble [60]fullerene-disaccharides complex was prepared by simple complexation of reactants in homogeneous solvent system. Similarly disaccharides also solublize [70]fullerene. Among the commercially available disaccharides, the complex of [60]fullerene with lactose was fully characterized.

To see the visible evidence for the stability of the lactose-C<sub>60</sub> complex in polar and non-polar solvents, the extraction experiment was conducted in vials. [60]Fullerene in toluene shows the deep purple color (Figure 5.2.1 [A]) and it is completely insoluble in polar solvents. Lactose is completely soluble in polar DMSO (Figure 5.2.1 [B]). These two solutions when mixed together in inert atmosphere and after evaporation of organic solvents resulted in a water-soluble slightly yellowish brown color lactose-C<sub>60</sub> complex (Figure 5.2.1 [C]). When toluene was added to the solid lactose-C<sub>60</sub> complex (Figure 5.2.1 [D]), it was observed that [60]fullerene easily go into the toluene layer and lactose was settled down at the bottom of the vial. When toluene was added to the aqueous solution of lactose-C<sub>60</sub> complex (Figure 5.2.1 [E]), it was observed that aqueous solution of lactose-C<sub>60</sub> complex was stable enough and [60]fullerene does not go into the toluene layer. Thus, the aqueous solution of lactose-C<sub>60</sub> complex was stable enough and [60]fullerene was not extractable. Whereas, this is completely inverted in the case of 2:1 inclusion complex of  $\beta$ -CD with [60]fullerene as shown in earlier section.

Similar observations made for the lactose-C<sub>70</sub> complex and are shown in Figure 5.2.2. [70]Fullerene in toluene shows the reddish wine color (Figure 5.2.2 [A]) and it is completely insoluble in polar solvents. Lactose is completely soluble in polar DMSO (Figure 5.2.2 [B]). These two solutions when mixed together in inert atmosphere and after evaporation of organic solvents resulted in a water-soluble slightly reddish brown color lactose-C<sub>60</sub> complex (Figure 5.2.2 [C]). When toluene was added to the solid lactose-C<sub>70</sub> complex (Figure 5.2.2 [D]), it was observed that

[70]fullerene easily go into the toluene layer and lactose settled down at the bottom of the vial. When toluene was added to the aqueous solution of lactose-C<sub>70</sub> complex (Figure 5.2.2 [E]), it was observed that aqueous solution of lactose-C<sub>70</sub> complex was stable enough and [60]fullerene does not go into the toluene layer. Thus, the aqueous solution of lactose-C<sub>70</sub> complex was stable enough and [70]fullerene was not extractable.

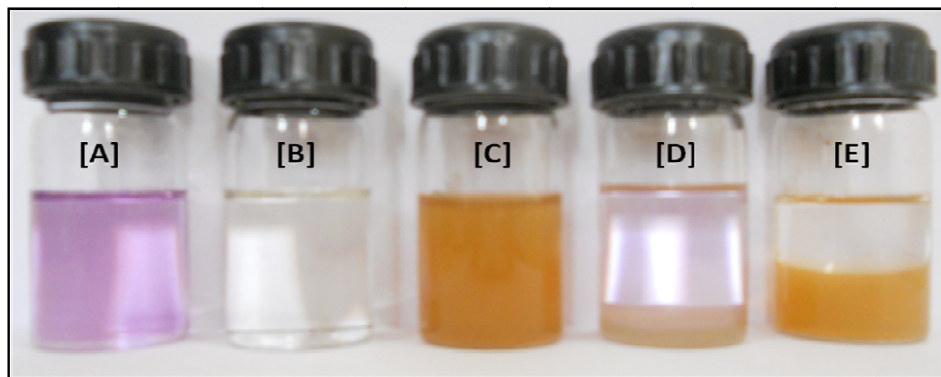


**Figure 5.2.1** Photograph of [A] C<sub>60</sub> in toluene, [B] lactose in DMSO, [C] lactose-C<sub>60</sub> complex in water, [D] lactose-C<sub>60</sub> complex in toluene and [E] lactose-C<sub>60</sub> complex in water + toluene.

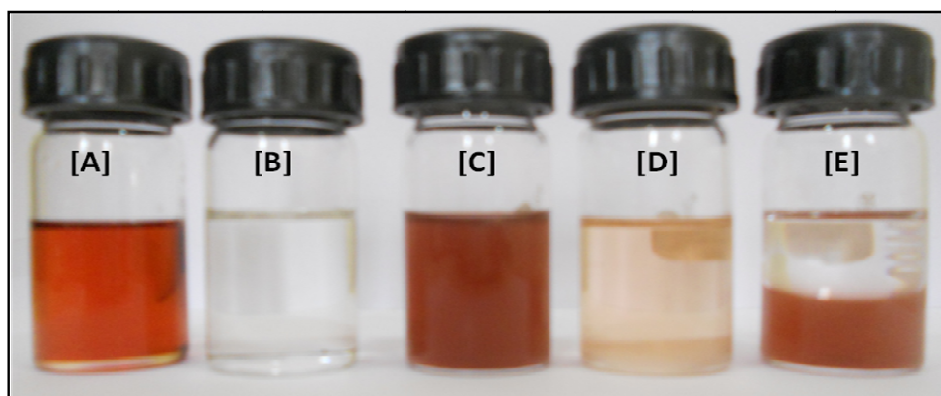


**Figure 5.2.2** Photograph of [A] C<sub>70</sub> in toluene, [B] lactose in DMSO, [C] lactose-C<sub>70</sub> complex in water, [D] lactose-C<sub>70</sub> complex in toluene and [E] lactose-C<sub>70</sub> complex in water + toluene.

### 5.2.3.1 Aqueous Solubility of Complexes

As expected, after complexation of [60]fullerene with different disaccharides, the aqueous solubility of [60]fullerene increased significantly as shown in Table 5.2.1. The complex of maltose with [60]fullerene has high water-solubility due to the maltose has highest water-solubility than other disaccharides. The complex of maltose-C<sub>60</sub> has more [60]fullerene concentration due to the higher solubilizing power of maltose. Moreover, it was found that aqueous solution of the complex was stable for the several months and does not aggregate like  $\beta$ -cyclodextrin-[60]fullerene complex. The amount of [60]fullerene/mg of the complex was determined by UV-Vis after extraction with toluene. It was observed that the amount of [60]fullerene in complex was found to be less than 10%.

**Table 5.2.1** Aqueous solubility of corresponding complex at 25°C and concentration of C<sub>60</sub> per mg of complex

Sample	Solubility (mg/mL)	Solubility of Corresponding Complex (mg/mL)	Concentration of C <sub>60</sub> /mg of Complex ( $\mu$ g)
Lactose	160.0	55.5	77.40
Maltose	1080.0	71.4	90.02
Sucrose	100.0	42.3	51.20
$\beta$ -cyclodextrin	18.5	4.0	77.30

### 5.2.3.2 Fourier Transform Infrared Spectroscopy (FTIR)

FTIR spectroscopy is an effective tool to characterize the non-covalent interactions between molecules. The FTIR absorption spectra of C<sub>60</sub>, lactose and C<sub>60</sub>-lactose are shown in Figure 5.2.3. The spectrum of pristine C<sub>60</sub> (Figure 5.2.3 a) showed four characteristic absorption bands at 1429 cm<sup>-1</sup>, 1183 cm<sup>-1</sup>, 578 cm<sup>-1</sup> and 527 cm<sup>-1</sup>. The spectrum of lactose (Figure 5.2.3 b) showed the absorption band at 3335 cm<sup>-1</sup>, 1653 cm<sup>-1</sup>, 1038 cm<sup>-1</sup> and 779 cm<sup>-1</sup>. The spectrum of C<sub>60</sub>-lactose complex

(Figure 5.2.3 c) showed  $3334\text{ cm}^{-1}$ ,  $1653\text{ cm}^{-1}$ ,  $1035\text{ cm}^{-1}$  and  $777\text{ cm}^{-1}$  of lactose and also showed distinct IR absorption bands of  $\text{C}_{60}$  at  $578\text{ cm}^{-1}$  and  $527\text{ cm}^{-1}$ . The lactose peaks remains strong in the spectrum, the positions and relative intensities of a few bands are affected by the formation of non-covalent complex between lactose and  $\text{C}_{60}$ . These results indicate the modification of environment of lactose due to the formation of lactose/ $\text{C}_{60}$  complex. If it were not so then the spectra would resemble that of a physical mixture of  $\text{C}_{60}$  and the lactose with no shift in the characteristic bands.

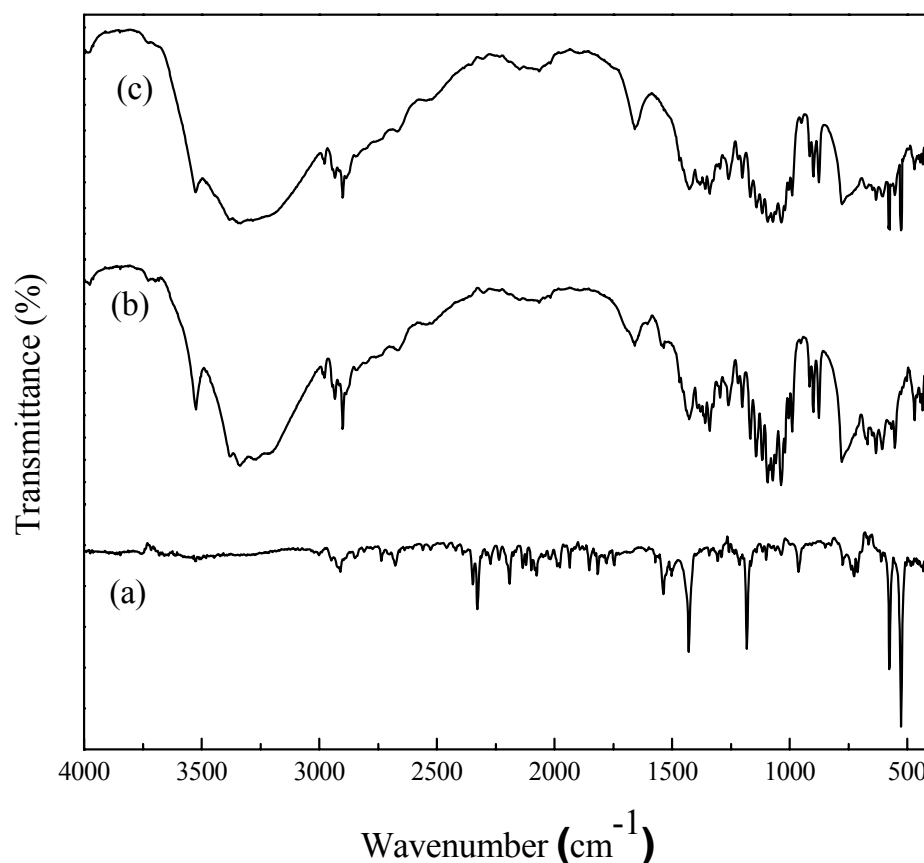


**Figure 5.2.3** FTIR absorption spectra of (a)  $\text{C}_{60}$ , (b) lactose and (c) lactose- $\text{C}_{60}$  complex.

### 5.2.3.3 UV-Visible Spectroscopy (UV-Vis)

The UV-Vis absorbance spectra of lactose in water,  $\text{C}_{60}$  in toluene and lactose- $\text{C}_{60}$  complex in water is shown in Figure 5.2.4. The UV-Vis absorbance spectrum of  $\text{C}_{60}$  in toluene shows maximum absorbance at 334 nm which is completely insoluble

in water, whereas lactose in water does not show any absorbance in this region. However, the UV-Vis absorbance spectrum of lactose- $C_{60}$  complex in water showed a maximum absorbance at 348 nm and widening of absorbance band after 400 nm as compared to typical absorbance at 334 nm and 406 nm for the pristine fullerene in toluene. Another interesting observation was that fullerene could be extracted from the dry powder of the complex by shaking it with toluene. The UV-Vis spectrum (Figure 5.2.4, Inset) showed absorbance similar to that of pristine [60]fullerene in toluene, whereas this was not possible in the aqueous solution, unlike the  $\beta$ -cyclodextrin-[60]fullerene complex (toluene can penetrate into the nonpolar cavity of  $\beta$ -cyclodextrin and kick out the [60]fullerene from the cavity), thus giving an indication that toluene is unable to penetrate into the complex as toluene does not dissolve the disaccharides<sup>52</sup>.

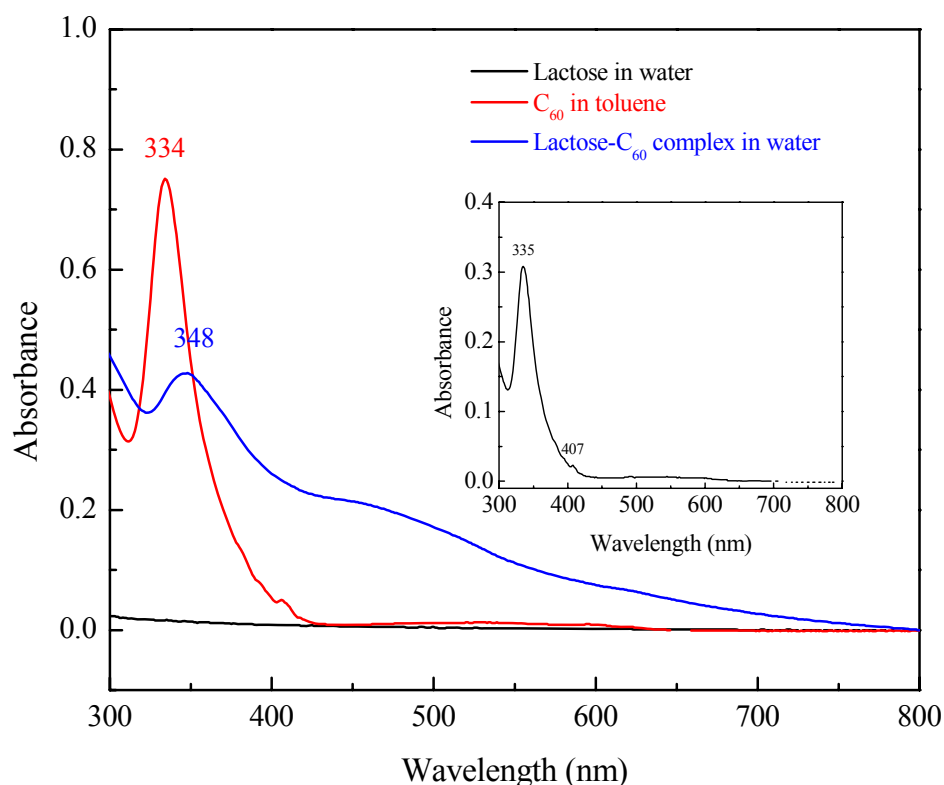


**Figure 5.2.4** UV-Vis spectra of lactose,  $C_{60}$ , lactose- $C_{60}$  complex and inset  $C_{60}$  extracted from complex by toluene.

### 5.2.3.4 Thermogravimetric Analysis (TGA)

The stoichiometry of the lactose- $C_{60}$  complex was evaluated from the thermogravimetric analysis as shown in Figure. 5.2.5. A small mass loss due to the loss of structural water molecules at the beginning was found in the lactose and lactose- $C_{60}$  complex followed by a larger mass loss corresponding to the decomposition of the glucose units of the lactose. The second mass loss for the lactose- $C_{60}$  complex was observed to be at lower temperature compared to pristine lactose, due to the modification of glucose units environment after formation of complex with [60]fullerene. Generally, lactose can form complexes with [60]fullerene in the ratio of (1:1, 2:1, 3:1, 4:1,...) with possible ratio of (1:2, 2:2, 3:2, 4:2,...). The theoretical, calculated mass content of lactose in the complex for these ratio could be (32.20%, 48.71%, 58.76%, 65.52%,...) and also possibility of (19.19%, 32.20%, 41.60%, 48.57%,...). The TG data of the lactose- $C_{60}$  complex show that the total mass loss at 375°C is 65.18%<sup>54-55</sup>. This value indicates that the ratio between lactose and  $C_{60}$  complex is 4:1.

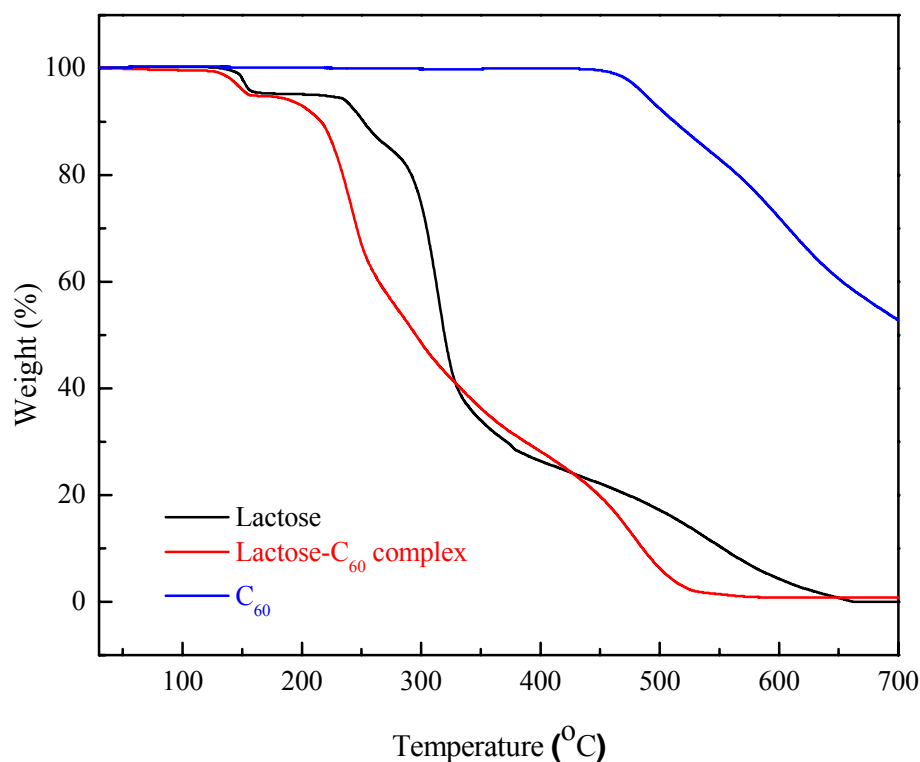


**Figure 5.2.5** TGA curves of lactose,  $C_{60}$  and lactose- $C_{60}$  complex.

### 5.2.3.5 Nuclear Magnetic Resonance Spectroscopy (NMR)

Further corroboration for the formation of non-covalent complex was obtained through NMR spectroscopy. Proton nuclear magnetic resonance provided direct evidence of supramolecular non-covalent interactions and this was confirmed by upfield or downfield shifts of the proton signals<sup>34,35</sup>. The  $^1\text{H}$  NMR spectra (Figure 5.2.6) of the complex showed a considerable upfield shift of the parent protons of lactose due the formation of complex and  $^{13}\text{C}$  NMR spectra (Figure 5.2.7) of the lactose- $\text{C}_{60}$  complex shows all the carbon chemical shift of the parent lactose along with the chemical shift at 165.27 ppm which is due to the presence of  $\text{C}_{60}$  with some chemical shift of the lactose carbon skeleton<sup>36</sup>.

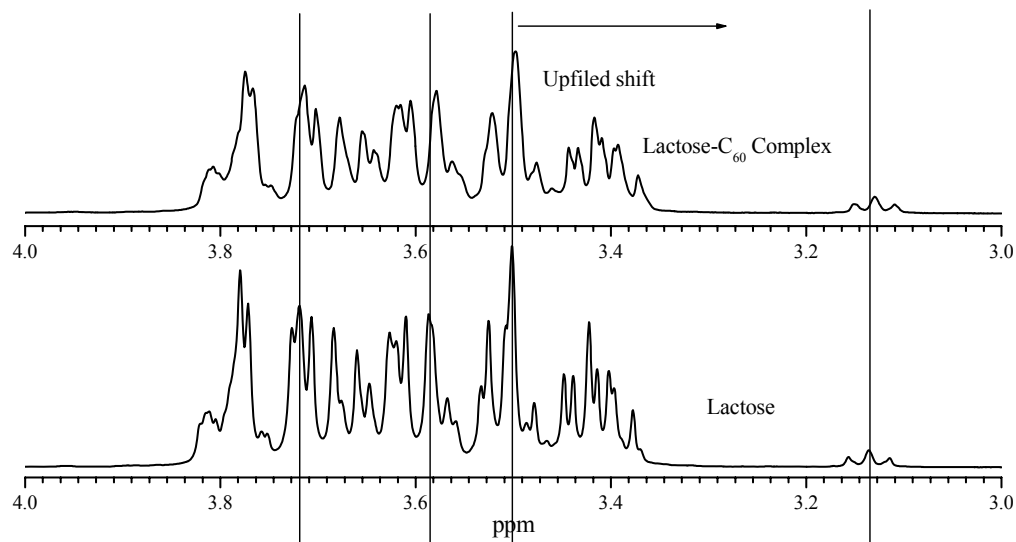


**Figure 5.2.6**  $^1\text{H}$  NMR spectra of lactose and lactose- $\text{C}_{60}$  complex in  $\text{D}_2\text{O}$ .

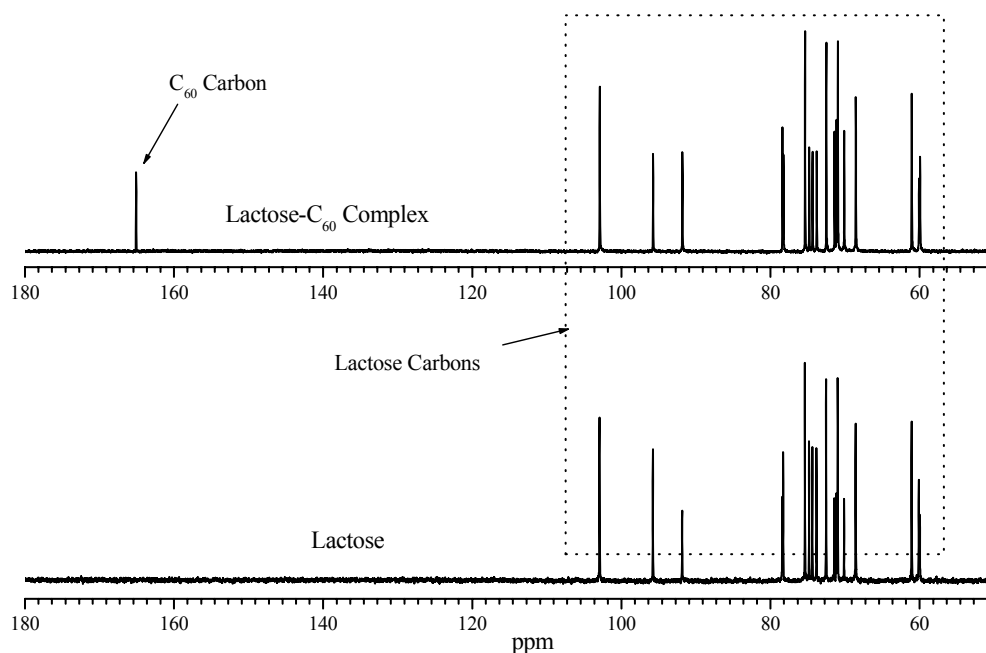


**Figure 5.2.7**  $^{13}\text{C}$  NMR spectra of lactose and lactose- $\text{C}_{60}$  complex in  $\text{D}_2\text{O}$ .

### 5.2.3.6 X-ray Diffraction (XRD)

All the complexes were subjected to XRD investigation and surprising result was that the complexes were highly crystalline. Figure 5.2.8 depicts the X-ray diffraction pattern of the  $\text{C}_{60}$ , lactose and freeze-dried lactose- $\text{C}_{60}$  complex. The signals were observed at ( $2\theta=12.44, 16.32, 19.10, 19.52, 19.92, 20.78, 21.16, 22.72, 23.66, 25.52, 27.40, 36.20, 37.88^\circ$ ) and the product isolated has nearly similar peaks corresponding to lactose with some decrease in the intensity and little peak shift. It can be seen that the complex has a similar crystalline structure to the parent lactose ( $2\theta=12.36, 16.12, 18.82, 19.28, 19.7, 20.56, 21.02, 22.54, 23.56, 25.34, 27.24, 35.88, 37.28^\circ$ ) and [60]fullerene ( $2\theta=10.68, 17.58, 20.68, 21.60, 27.34, 28.04, 30.74, 32.70^\circ$ ), with the retention of the crystalline structure of lactose<sup>52,53</sup>. This type of behaviour is completely different from the inclusion complex of [60]fullerene with any crystalline host where the host loses its crystalline nature and becomes amorphous<sup>55,58</sup>. Thus, it was obvious that the crystalline complexes were formed due to the self-assembly of the disaccharide and the fullerene molecules led to arrangement of molecules in directional order.

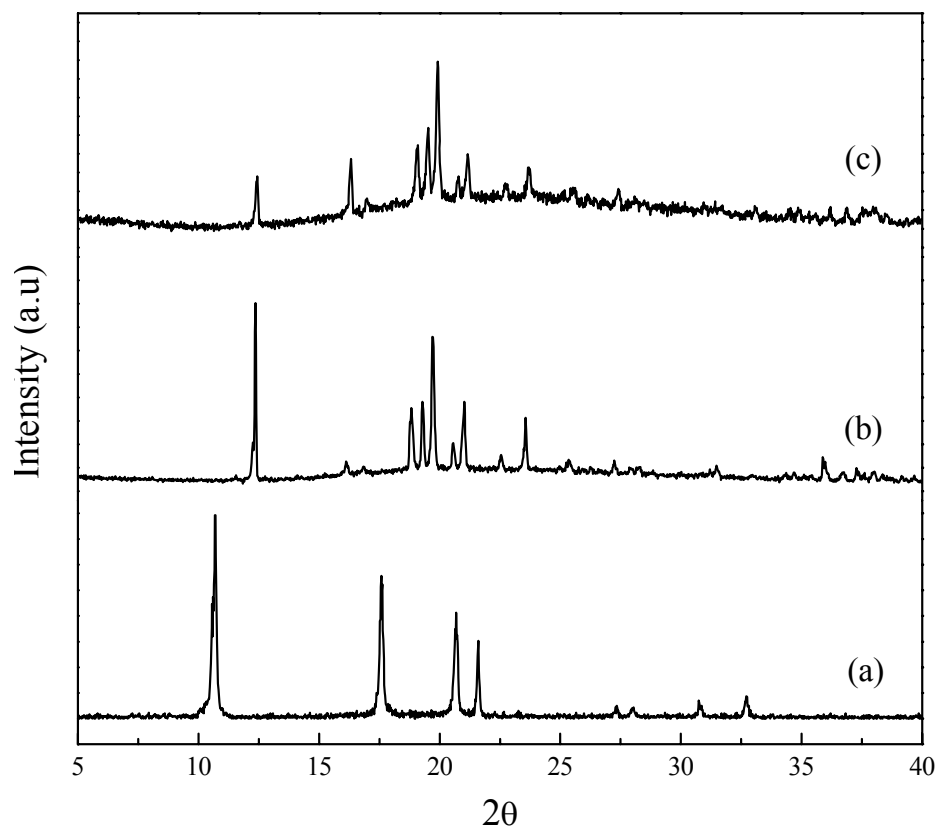


**Figure 5.2.8** X-ray diffractogram of (a) C<sub>60</sub>, (b) lactose and (c) lactose-C<sub>60</sub> complex.

### 5.2.3.7 Transmission Electron Micrograph (TEM) and Static Light Scattering (SLS)

The unique self-assembly and retention of the crystalline nature of the lactose-C<sub>60</sub> complex was further confirmed by the transmission electron micrographs (TEM) as shown in Figure 5.2.9 (a). The lactose-C<sub>60</sub> complex was found spherical in shape with uniform crystalline aggregates of about 60±5 nm. The particles size obtained from static light scattering (SLS) measurements as shown in Figure 5.2.10 also support the prior inference drawn from the TEM micrographs. Even though the concentration of complex in aqueous solution was increased, the particle size does not change and was found to be 60±5 nm. High resolution TEM (HRTEM) shows a regular array of the [60]fullerenes with lactose with the lattice spacing between the fullerene molecules of the order of 0.34 nm (Figure 5.2.9 (a), Inset). This is similar to the lattice spacing between the [60]fullerene crystal planes in the solid state<sup>59-61</sup>. Moreover, the lactose-C<sub>60</sub> complex shows self-assembly as shown in Figure 5.2.9 (b) due the strong non-covalent integrations such as van der Waals forces, hydrogen-

bonding, hydrophilic/hydrophobic interactions,  $\pi$ - $\pi$  stacking interaction, electrostatic interactions, donor and acceptor interactions, etc

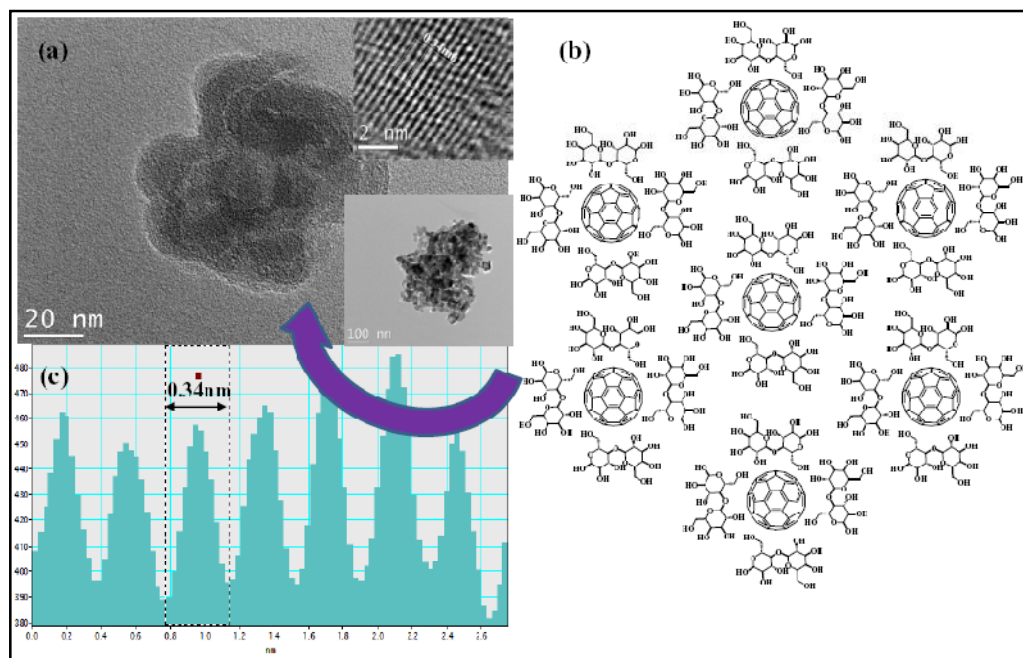


**Figure 5.2.9** (a) TEM micrograph of lactose-C<sub>60</sub> complex; inset: HRTEM image of C<sub>60</sub> lattice (b) spherical self-assembly of lactose-C<sub>60</sub> complex (c) histogram of lattice spacing.

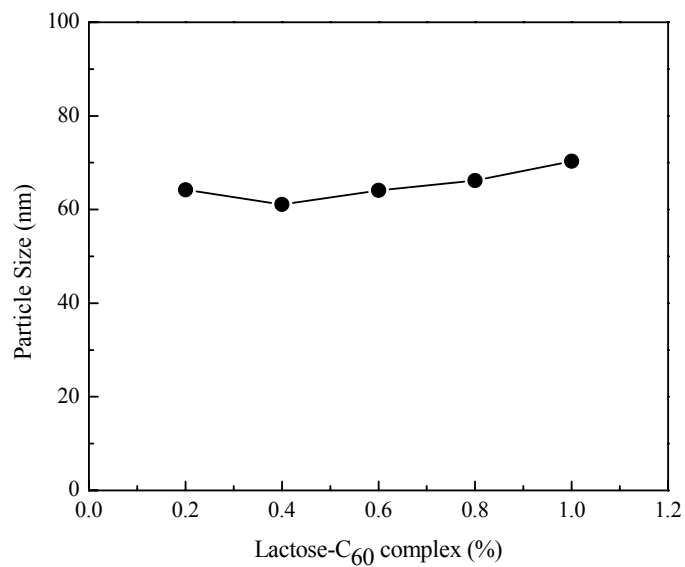


**Figure 5.2.10** Particle size of lactose-C<sub>60</sub> complex by static light scattering.

### 5.2.3.8 Molecular Modeling

Different views of space-filling molecular models of the three-dimensional conformation of the lactose- $C_{60}$  complex are shown in Figure 5.2.11. The host and guest molecules were independently built up, and their geometry was optimized. The overall structure of these possible models of complex was again subjected to energy-minimization. The final energy-minimized molecular model indicates that  $C_{60}$  was surrounded by four lactose molecules in a spherical form. This model also supported from the results obtained by TEM analysis as shown in Figure 5.2.9, lactose molecules are arranged spherically around the [60]fullerene. Furthermore, such units are coming together to form self-assembly about 60 nm and then these self-assembly coming together to form 500 nm cluster.

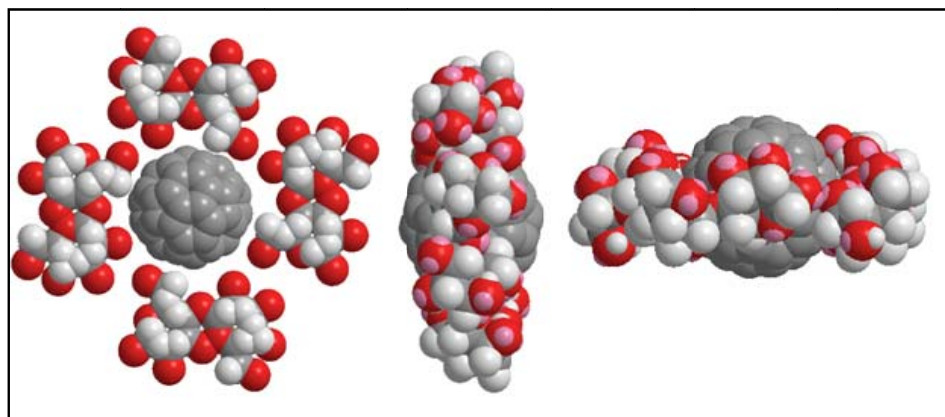


**Figure 5.2.11** Space-filling energy-minimized (MM2) molecular models showing different views of lactose- $C_{60}$  complex.

### 5.2.3.9 Radical Scavenging

The stable free radical has been used to study the antioxidant activities of phenols and catechol. In these reactions, the antioxidant transfers a hydrogen atom to the radical, which leads to a decrease of the characteristic UV-Vis absorption intensity in the spectrum of DPPH. To demonstrate the radical scavenging property of water-soluble [60]fullerene we utilized the DPPH reaction with lactose- $C_{60}$  complex. The progress of the radical scavenging reaction of lactose- $C_{60}$  complex was measured by taking UV-Vis absorbance at definite interval of time as shown Figure 5.2.12. It was observed that pristine DPPH in ethanol shows maximum UV-Vis absorbance at 517

nm, while lactose-C<sub>60</sub> complex in water shows maximum UV-Vis absorbance at 348 nm. When these two solutions were mixed together the maximum UV-Vis absorbance of DPPH shifted to 527 nm from 517 nm. It could be further seen that the absorbance of this maximum decreased steadily with time and we can observe that the pink colour of the radical being bleached gradually. The reaction of DPPH with water-soluble lactose-C<sub>60</sub> complex proceeded at a comparatively slower rate, the pink color of the radical being bleached gradually. Nevertheless, the decrease in absorbance is detectable within minutes of the reaction. To observe the solvent effect on DPPH scavenging blank experiment was conducted without lactose-C<sub>60</sub> complex by mixing DPPH solution and water. However, there was no considerable change in absorbance at the characteristic peak maximum was observed even after several hours of contact.

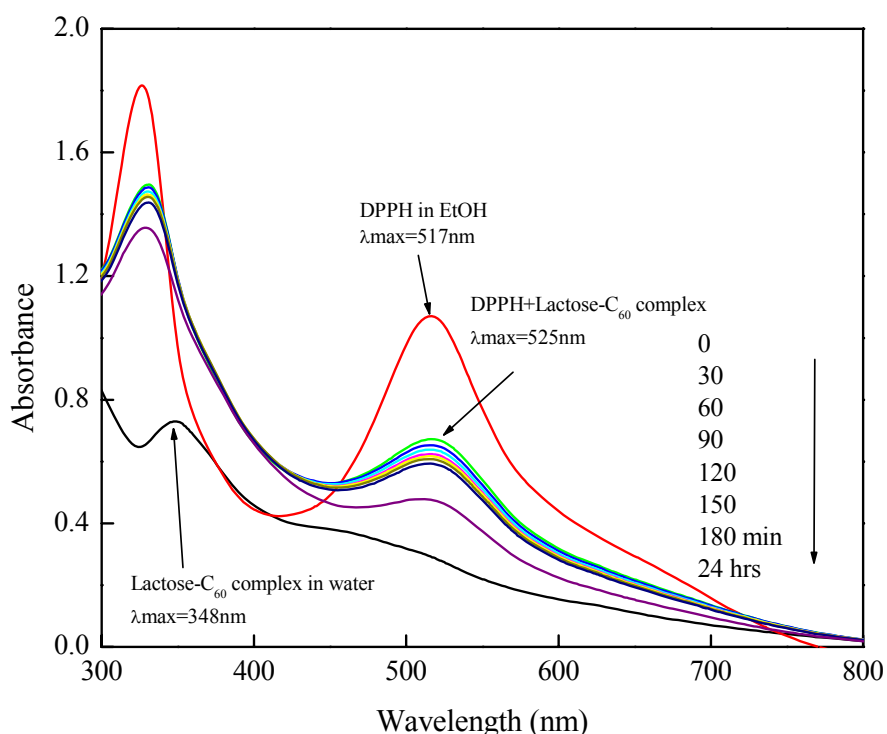


**Figure 5.2.12** Color bleaching UV-Vis spectra of radical scavenging of most stable free radical DPPH with lactose-C<sub>60</sub> complex.

### 5.2.3.10 Kinetics of Radical Scavenging Reaction

The lactose-C<sub>60</sub> complex has a large number of reaction sites on its  $\pi$ -surface of C<sub>60</sub>; each C<sub>60</sub> molecule is capable of reacting with a number of DPPH radicals.

Hence, in terms of molar equivalents, the concentration of  $C_{60}$  in effect is very high compared to that of DPPH during the initial stages of the reaction, while the concentration of DPPH would decrease steadily with time, the concentration of lactose- $C_{60}$  complex would practically remain constant. The reaction between lactose- $C_{60}$  complex and DPPH follows the first-order reaction rate law  $\{\ln [a(a - x)^{-1}] = kt\}$ . The plot of the term  $\ln [a(a - x)^{-1}]$  vs. reaction time ( $t$ , min) is shown in Figure 5.2.13, where  $a$  denotes the initial DPPH concentration and  $(a - x)$  the concentration of DPPH at different reaction times, evaluated from the DPPH standard curve, led to a straight line with a satisfactory correlation of 0.9814. The pseudo-first-order rate constant ( $k$ ) was evaluated to be  $1.05 \times 10^{-3} \text{ min}^{-1}$ . However, there was a deviation from linearity beyond 120 min, indicating that the pseudo-first-order reaction condition no longer remains valid beyond this stage i.e., the concentration of lactose- $C_{60}$  complex begins to perceptively decrease beyond a certain stage of the reaction. The pseudo-first-order reaction of DPPH observed in the early stages of the reaction further indicates that multiple sites of each  $C_{60}$  molecule reacted with DPPH.

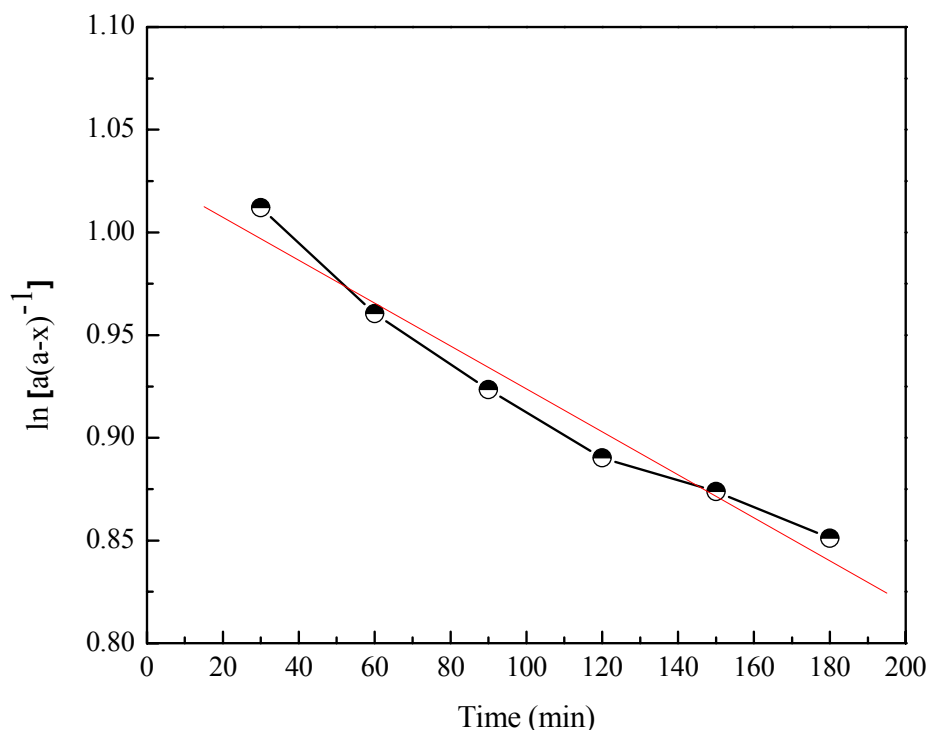


**Figure 5.2.13** Pseudo-first-order rate correlations for DPPH in of reaction between DPPH and lactose- $C_{60}$  complex.

#### **5.2.4 Conclusions**

The present study demonstrated an eco-friendly and low cost protocol for the aqueous solubilization of fullerenes by self-assembly with disaccharides. The identification of lactose complex with [60]fullerene suggested that one [60]fullerene ball was surrounded by four lactose molecule in a spherical nanostructure with retention of crystalline nature of the parent compounds. The self-assembly was formed due to the van der Waals force, charge transfer complex and hydrogen bonding. The solubility and stability of [60]fullerene-disaccharide complex was found to be higher than the traditional [60]fullerene-cyclodextrins inclusion complex. The similar observation has been observed for the [70]fullerene-disaccharides. The preliminary radical scavenging studies with most stable free radical DPPH in aqueous system suggest that the complex has potential bio-medical application.

## References

1. H. W. Kroto, J. E. Fischer, D. E. Cox, Eds., *The Fullerenes* (Pergamon, Oxford, **1993**); W. E. Billups and M. A. Ciufolini, Eds., *Buckminsterfullerenes* (VCH, New York, **1993**).
2. Z. Gaun, Y. Wang, Y. Chen, L. Zhang and Y. Zhang, *Tetrahedron*, **2009**, 65, 1125-1129.
3. A. Quaranta, Y. Zhang, Y. Wang, R. Edge, S. Navaratnam, E. J. Land, and R. V. Bensasson, *Chemical Physics*, **2008**, 354, 174-179.
4. F. Giacalone and N. Martin, *Chem. Rev.*, **2006**, 106, 5136-5190.
5. D. Wang, L. Sun, W. Liu, W. Chang, X. Gao and Z. Wang, *Enviro. Sci. Technol.*, **2009**, 43, 5825-5829.
6. X. Zhang and A. V. Teplyakov, *Langmuir*, **2008**, 24, 810-820.
7. A. Bogdanski, D. Wistuba, K. L. Larsen, U. Hartnagel, A. Hirsche and V. Schurig, *New J. Chem.*, **2010**, 43, 693-698.
8. Y. Liu, H. Wang, P. Liang, and H.-Y. Zhang, *Angew. Chem.*, **2004**, 116, 2744-2748.
9. P. Lubomir, H. Magdalena, G. Miroslav, B. Jana, S. Romana, F. Salvatore, Y. Juan, G., Zhu, R. Andre, Z. Yongmin, *Carbon*, **2010**, 48, 153-162.
10. S. Samal and K. E. Geckeler, *Macromol. Biosci.*, **2001**, 1, 329.
11. G. L. Marcorin, T. D. Ros, S. Castellano, G. Stefancich, I. Bonin, S. Miertus, and M. Prato, *Org. Lett.*, **2000**, 2(25), 3955-3958.
12. S. Kato, H. Aoshima, Y. Saitoh and N. Miwa, *Bioorg. Med. Chem. Lett.*, **2009**, 19, 5293-5296.
13. Z. Zhu, D. I. Schuster and M. E. Tuckerman, *Biochemistry*, **2003**, 42, 1326-1333.
14. T. Andersson, K. Nilsson, M. Sundahl, G. Westman and O. Wennerström, *J. Chem. Soc., Chem. Commun.*, **1992**, 604.
15. C. N. Murthy and K. E. Geckeler, *Chem. Commun.*, **2001**, 1194.
16. J. L. Atwood, G. A. Koutsantonis and C. L. Raston, *Nature*, **1994**, 368, 229.
17. K. Komatsu, K. Fujiwara, Y. Murata and T. Braun, *J. Chem. Soc., Perkin Trans.*, **1999**, 1, 2963.
18. L. S. Litvinova and V. N. Zgonnik, *Abstracts of IWFAC'99*, St. Petersburg, **1999**, October 4-8, p. 294.

19. E. Yu. Melenevskaya, V. A. Reznikov, L. S. Litvinova, L. V. Vinogradova and V. N. Zgonnik, *Vysokomol. Soedin, Ser. A*, **1999**, 41, 864 (*Polym. Sci., Ser. A*, **1999**, 41, 578).
20. E. Tarabukina, Z. Zoolshoev, E. Melenevskaya and T. Budtova, *Int. J. Pharm.*, **2010**, 384, 9-14.
21. E. Nakamura and H. Isobe, *Acc. Chem. Res.*, **2003**, 36 (11), 807–815.
22. D. Q. Yuan, K. Koga, Y. Kouroggi and K. Fujita, *Tetrahedron Lett.*, **2001**, 42, 6727-6729.
23. S. H. Friedman, D. L. DeCamp, R. P. Sijbesma, G. Srdanov, F. Wudl, and G. L. Kenyon, *J. Am. Chem. Soc.*, **1993**, 115, 6506-6509.
24. A. W. Jensen, S. R. Wilson and D. I. Schuster, *Bioorg. Med. Chem.*, **1996**, 4, 767-779;
25. T. Da Ros and M. Prato, *Chem. Commun.*, **1999**, 663-669.
26. T. Mashino, K. Okuda, T. Hirota, M. Hirobe, T. Nagano and M. Mochizuchi, *Bioorg. Med. Chem. Lett.*, **1999**, 9, 2959-2962.
27. S. R. Wilson, in: K. Kadish and R. Ruoff (Eds.), *The Fullerene Handbook*, Wiley, New York, **2000**, pp. 437- 465.
28. S. Bosi, T. Da Ros, S. Castellano, E. Banfi, and M. Prato, *Bioorg. Med. Chem. Lett.*, **2000**, 10, 1043-1045.
29. Z. Markovic and V. Trajkovi, *Biomaterials*, **2008**, 29, 3561-3553.
30. R. Partha and J. L. Conyers, *Int. J. Nanomedicine*, **2009**, 4, 261-275.
31. N. F. Steinmetz, V. Hong, E. D. Spoerke, P. Lu, K. Breitenkamp, M. G. Finn and M. Manchester, *J. Am. Chem. Soc.*, **2009**, 131, 17093-17095.
32. F. Diederich and C. Thilger, *Science*, **1996**, 271, 317-323.
33. S. Samal and K. E. Geckeler, *Chem. Commun.*, **2000**, 1101-1102.
34. V. I. Bhoi and C. N. Murthy, *Fullerenes, Nanotubes, and Carbon Nanostructures*, **2011**, 19, 668-676.
35. A. Beeby, J. Eastoe and R. K. Heenan, *J. Chem. Soc., Chem. Commun.*, **1994**, 173-175.
36. C. N. Murthy, R. R. Patel, R. Murali and A. K. Rakshit, *J. Chem. Eng. Data*, **2010**, 55, 4479-4484.
37. A. Ikeda, Y. Kawai, J. Kikuchi and M. Akiyama, *Chem. Commun.*, **2010**, 46, 2847-2849.

38. H. Wu, L. Lin, P. Wang, S. Jiang, Z. Dai and X. Zou, *Chem. Commun.*, **2011**, 47, 10659-10661.
39. T. Andersson, M. Sundahl, G. Westman and O. Wennerstrom, *Tetrahedron Letters*, **1994**, 35, 7103-7106.
40. K. I. Priyadarsini, H. Mohan, A. K. Tyagi and J. P. Mittal, *J. Phys. Chem.*, **1994**, 98, 4756-4759.
41. A. Buvári-Barcza, J. Rohonczy, N. Rozlosnik, T. Gilanyi, B. Szabo, G. Lovas, T. Braun, J. Samu and L. Barcza, *J. Chem. Soc., Perkin Trans.*, **2001**, 2, 191-196.
42. C. N. Murthy and K. E. Geckeler, *Korean patent no*, 10-0479331, **2005**.
43. C. N. Murthy and K. E. Geckeler, *Korean patent no*, 10-20020047438, **2004**.
44. Y. Yu, Z. Shi, Y. Zhao, Y. Ma, M. Xue and J. Ge, *Supramol. Chem.*, **2008**, 20, 295-299.
45. C. N. Murthy and K. E. Geckeler, *Fullerenes, Nanotubes, and Carbon Nanostructures*, **2002**, 10, 91-98.
46. Lu, H. Wang, P. Liang, and H. Y. Zhang, *Angew. Chem.*, **2004**, 116, 2744-2748.
47. S. Samal and K. E. Geckeler, *Chem. Commun.*, **2001**, 2224-2225.
48. J. Szejtli, *Cyclodextrin Technology*, Kluwer Academic, Dordrecht, Netherlands, **1988**.
49. L. S. Litvinova, V. G. Ivanov, M. V. Mokeev and V. N. Zgonnik, *Mendeleev Commun.*, **2001**, 11, 193-194.
50. L. S. Litvinova, A. V. Griбанov, M. V. Mokeev and V. N. Zgonnik, *Russ. J. Appl. Chem.*, **2004**, 77, 438-440.
51. P. P. Yakutseni, L. S. Denisova, N. I. Povarov, D. E. Sivokon and S. V. Kozyrev, *Fullerenes, Nanotubes and Carbon Nanostructures*, **2006**, 14, 537-540.
52. C. N. Murthy, *Hyperfine Interactions*, **2005**, 160, 189-192.
53. D. C. Fries, S. T. Rao and M. Sundaralingam, *Acta Cryst.*, **1971**, B27, 994-1005.
54. K. P. Guiry, S. J. Coles, H. A. Moynihan and S. E. Lawrence, *Cystal Growth & Design*, **2008**, 8, 3927-3934.
55. F. Constable and K. E. Geckeler, *Fullerenes, Nanotubes and Carbon Nanostructures*, **2004**, 12, 811-814.
56. S. Crouzy, F. Fauvelle, J. C. Debouzy, M. Goschl and Y. Chapron, *Carbohydr. Res.*, **1996**, 287, 21.
57. C. Fronza, A. Mele, E. Redenti and P. Ventura, *J. Org. Chem.*, **1996**, 61, 909.

58. T. Furuishi, Y. Ohmachi, T. Fukami, H. Nagase, T. Suzuki, T. Endo, H. Ueda and K. Tomono, *J. Incl Phenom. Macrocycl. Chem.*, **2010**, 67, 233-239.
59. P. A. Heiney, J. E. Fisher, A. R. McGhie, W. J. Romanow, A. M. Denendtein, J. P. MaCauley, A. B. Smith and D. E. Cox, *Phys. Rev. Lett.*, **1991**, 66, 2911-2914.
60. A. Smontara, A. M. Tonejc, S. Gradecak, A. Tonejc, A. Bilusic, J. C. Lasjaunias, *Mater. Sci. Eng. C*, **2002**, 19, 21-25.
61. Y. Chen, Z. E. Huang and R. F. Cai, *J. Polym. Sci.: Part B: Polym. Phys.*, **1996**, 34, 631-640.

***Chapter 6***  
***Surface Immobilization of Carbon Nanotubes by  $\beta$ -Cyclodextrins and  
Their Inclusion Ability***

## Chapter 6

### Surface Immobilization of Carbon Nanotubes by $\beta$ -Cyclodextrins and Their Inclusion Ability

#### 6.1 Introduction

The rich chemistry of carbon allotropes and methods for their commercial mass-production has attracted and inspired scientists of all over the world to evaluate them for a wide range of applications<sup>1-3</sup>. Among the commercially available carbon allotropes, carbon nanotubes (CNTs) show exceptional applications in materials science, nanotechnologies and medicinal chemistry owing to their unique electrical, mechanical, ultra-light weight and thermal properties<sup>4-6</sup>. The excellent electron affinity and charge transfer capability make CNTs attractive for a number of various applications such as adsorbent, catalyst, bio-sensing electrode, solar cell, photo sensitizer, super conducting material, gas sensor, transistor, hydrogen storage and so on<sup>7-12</sup>. However, the vital biomedical applications of CNTs are still under developed due to major barriers i.e. limited reactivity and water-insolubility owing to their strong  $\pi$ - $\pi$  stacking interactions and high aspect ratio<sup>13-16</sup>. Thus, the extensive research is being undertaken to develop new dispersion techniques, which allows using the properties of CNTs in water and other polar solvents<sup>17-20</sup>. Several covalent and non-covalent strategies have been attempted for the dispersion of CNTs in water and other organic solvents<sup>21</sup>. In covalent approaches, carboxylic acid, halogenated and azide functionalized CNTs have been effectively attached to the solubilizing agents<sup>22</sup>. In non-covalent approaches, CNTs were effectively wrapped by aromatic molecules, polymers and surfactants<sup>23-25</sup>. However, the demerit of using non-covalent interactions to make CNTs hybrids is that in a competitive reaction medium the adsorbed molecule could be easily displaced from the CNTs surface<sup>26</sup>. In general, for pursuing the practical applications of CNTs, the dispersion of CNTs in different solvents continues to be a challenge.

Recently, the considerable interest has been devoted for the dispersion of CNTs<sup>27,28</sup>. Despite the several methods described for the preparation of water-dispersible CNTs in literature; efforts are continuing to find simpler, biocompatible and more inexpensive routes for functionalization of CNTs in order to elevate their

dispersibility. The surface modification of CNTs through covalent-noncovalent functionalization with supramolecular molecules is crucial for developing high performance materials based on CNTs and supramolecular materials<sup>29</sup>. The controlled covalent-non covalent functionalization of CNTs with cyclodextrins improves their dispersibility with the simultaneous retention of their unique characteristic properties<sup>30,31</sup>. Cyclodextrins has been effectively used for the soft cutting of CNTs<sup>32</sup>.

Cyclodextrins are well known to serve as good host molecules for the aqueous solubilization of carbon allotropes<sup>33,34</sup>. The covalent attachment of cyclodextrin molecules on the surface of CNTs is an effective option of bringing the guest molecule closer to the CNTs surface and thus enhancing the interaction between the guest and CNTs<sup>35</sup>. Recently, it was realized that combination of cyclodextrins and carbon materials by covalent functionalization generates a new class of materials with more advanced properties and applications than the pristine precursors and non-covalent interaction<sup>36</sup>. The covalent attachment of molecules to CNTs broadens the range of potential applications of CNTs systems and allows one to tailor the properties of modified CNTs<sup>7</sup>. The  $\beta$ -cyclodextrin is most common, cheapest and widely used among the commercial available cyclodextrins. Selective replacement of hydroxyl groups with other functional groups have been shown to remarkably improve the reactivity and solubility of the native  $\beta$ -cyclodextrin. However, presence of similar hydroxyl groups makes selective modification of  $\beta$ -cyclodextrin extremely difficult, although regioselective modification of  $\beta$ -cyclodextrin was achieved by using geometry of reagents, which can result in a selectively difunctionalized  $\beta$ -cyclodextrin to improve water-solubility, moderate inclusion ability and reactive functionality<sup>37</sup>.

Investigations of the photophysical properties of photosensitive molecules on CNTs are of interest as they provide the scientific basis for hybrid materials with potential applications as optical sensors<sup>38,39</sup> and light harvesting devices<sup>40</sup>. Cho *et al* developed a CNT-chromophore based pH sensor in which a fluorescent dye (pyrene) was attached to the surface of CNT by a pH sensitive polymeric linker that coils up at low pH and causes quenching of the dyes<sup>38</sup>. CNTs have been used as substrates in immunoassays. CNT-electrodes were decorated with antibodies that can bind antigens, allowing an electrochemiluminescence-active second antibody to bind,

thereby enabling detection of the antigen<sup>41</sup>. CNT-polymer hybrids and CNT-phthalocyanine hybrids have been developed as lightharvesting devices<sup>42</sup>.

This chapter describes the surface immobilization of CNTs with  $\beta$ -cyclodextrins along the wall of CNTs using covalent amide linkages. For this purpose, both  $\beta$ -cyclodextrin and CNTs were functionalized. Thus,  $\beta$ -cyclodextrin was modified with reactive amino functional groups and CNTs were functionalized to generate carboxylic groups on the surface. The amine functionality on the primary side of the  $\beta$ -cyclodextrin was effectively used, as it can react with carboxylic group of CNTs via amide linkage. The presence of  $\beta$ -cyclodextrin on the surface of CNTs can provide not only excellent water-dispersibility to the CNTs but also site for inclusion of guest molecules or ions for interaction with the nanotube surface.

## 6.2 Experimental

### 6.2.1 Materials

Selectively diamino-functionalized  $\beta$ -cyclodextrin was synthesized in Chapter 2 used as reagent. MWCNTs were purchased from Wako Pure Chemical Industries, Ltd. and purified by refluxing in concentrated (69 %)  $\text{HNO}_3$  for 2 days, followed by washing with concentrated hydrochloric acid and then water on a Millipore VC membrane (pore size = 0.1  $\mu\text{m}$ ). 1-ethyl-3-(3-dimethylamino propyl) carbodiimide hydrochloride (EDC) and phosphotungstic acid was purchased from Sigma-Aldrich Chemical Co. Rhodamine 6G was a product of Acros Chemical Co. All other chemicals were commercial products of reagent grade and used without further purification. Water was purified by distillation and deionized using a Millipore Milli-Q Laboratory purification system (resistance greater than 18.2  $\text{M}\Omega$ ) and used throughout the experiments.

### 6.2.2 Measurements

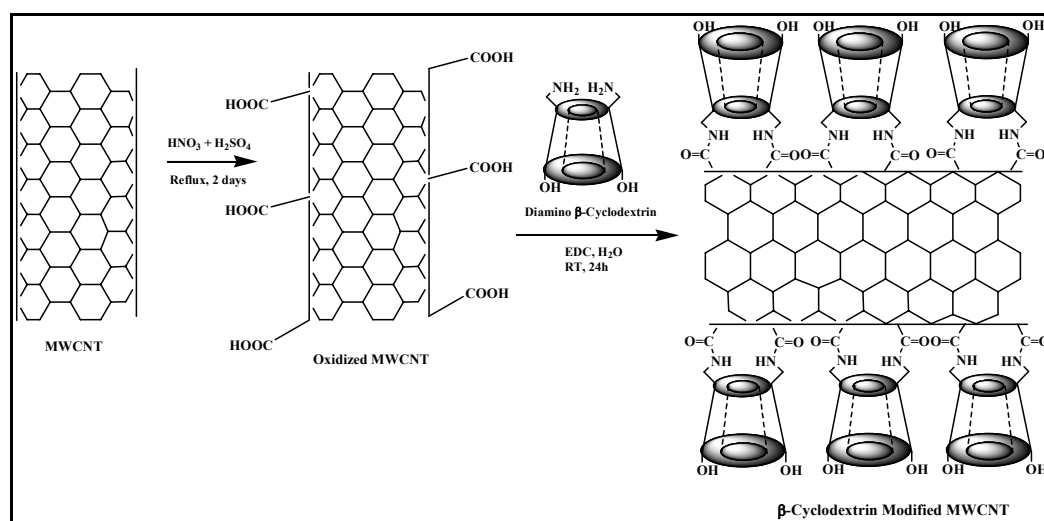
FTIR spectroscopic measurements were recorded on a Nicolet-6700 spectrometer at  $10^{-4}$  resolution and 32 scans using a KBr pellet method. Thermogravimetric analyses (TGA) were done on a TGA Q500 instrument with a heating rate of  $10^\circ\text{C}/\text{min}$  in the mixed atmosphere of nitrogen and oxygen in the ratio 60/40. The thermobalance was calibrated with an alumel alloy and nickel for temperature settings and with a 100 mg standard for weight accuracy. Sample ( $5.5 \pm 0.5$  mg) was placed on a tarred aluminum balance pan and transferred to the furnace at room temperature, where the exact sample weight was determined. The measurements of energy-dispersion X-ray spectrometry (EDS) of powders on the carbon tape after gold-coating were performed on a JEOL JSM-6500F at an operation voltage of 20 kV. Transmission Electron Microscopic (TEM) images were obtained on a Hitachi H-700 equipped with a charge-coupled device camera, operating at an accelerating voltage of 100 kV. The specimens for TEM were prepared by directly dropping the dispersion of corresponding products onto the carbon-coated copper grids and dried under bulb. Fluorescence spectra were recorded on a HITACHI F-3010 fluorometer with a 10 mm path cell.

### 6.2.3 Carboxylic acid Functionalization of MWCNTs

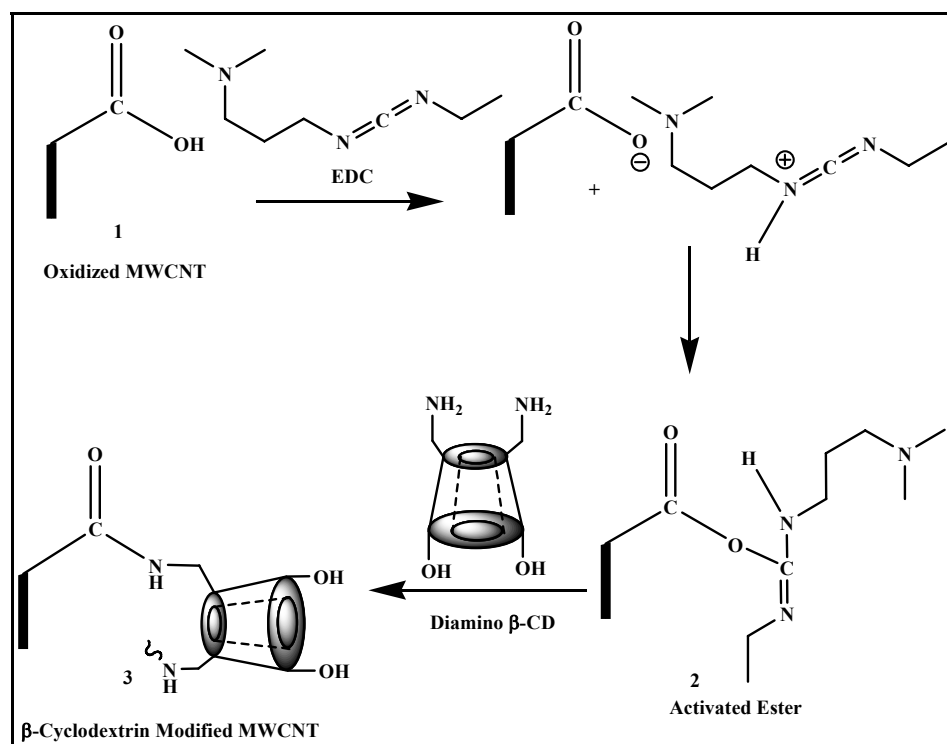
Carboxylic acid-functionalized MWCNTs (CNTs-COOH's) were obtained by refluxing 20 mg of purified MWCNTs in 20 cm<sup>3</sup> concentrated HNO<sub>3</sub>/H<sub>2</sub>SO<sub>4</sub> (3:1, v/v) for 24h after 2h sonication. After centrifugation, washing several times with water and drying overnight in vacuum oven at 60°C, the solid obtained was subjected to FTIR analysis to check the effective surface functionalization of MWCNTs with carboxylic groups.

### 6.2.4 Surface Immobilization of MWCNTs with $\beta$ -Cyclodextrins

The carboxylic acid functionalized MWCNTs were immersed into 30 cm<sup>3</sup> of a freshly prepared 10 mM EDC solution to convert the carboxylic groups of MWCNTs into active ester (2 in Scheme 6.2). After activation for 30 min, 100 mg of diamino  $\beta$ -cyclodextrin was added and the reaction mixture was allowed to stir for 24h at room temperature. The excess of diamino  $\beta$ -cyclodextrin and byproducts obtained during the progress of reaction were removed by washing with water and dialyzing with a polymer membrane (MWCO 2K) for 24h. The product, denoted as  $\beta$ -cyclodextrin-modified MWCNTs, was obtained by centrifugation and drying at 60°C for 24h. The reaction and mechanism is shown in Scheme 6.1 and Scheme 6.2, respectively.



**Scheme 6.1** Synthetic reaction scheme of chemical immobilization of  $\beta$ -cyclodextrins on MWCNTs.



**Scheme 6.2** Mechanism for the reaction of diamino  $\beta$ -cyclodextrin with oxidized MWCNT by an activated ester intermediate.

### 6.2.5 Sample Preparation for Fluorescence Measurement

A  $5.0 \times 10^{-5}$  M rhodamine 6G solution and a 25  $\mu\text{g/mL}$   $\beta$ -cyclodextrin-modified MWCNTs solution were prepared in water. The rhodamine 6G solution (1 mL) was added to the different volumes (1-9 mL) of a  $\beta$ -cyclodextrin-modified MWCNTs solution and then adjusted to a total volume of 10 mL by adding water. The mixtures were stirred and then allowed to equilibrate for 8h before fluorescence measurements. Thus, the final concentration of rhodamine 6G was constant ( $5.0 \times 10^{-6}$  M) and the concentration of  $\beta$ -cyclodextrin-modified MWCNTs was varied between 0-22.5  $\mu\text{g/mL}$ .

## 6.3 Results and Discussion

### 6.3.1 Characterization of $\beta$ -Cyclodextrins Immobilized on MWCNTs

#### 6.3.1.1 Fourier Transform Infrared Spectroscopy (FTIR)

$\beta$ -cyclodextrin-modified MWCNTs was synthesized by covalent attachment of oxidized MWCNTs with diamino  $\beta$ -cyclodextrin (Scheme 6.1) through amide linkages using water-soluble condensation agent EDC. Figure 6.1a shows a FTIR absorption spectrum of oxidized MWCNTs. The spectrum exhibited bands at 1720 and 1560  $\text{cm}^{-1}$  due to  $\text{-C=O}$  stretching and  $\text{-COO}^-$  antisymmetric stretching vibration modes, respectively, indicating the presence of carboxylic acid and carboxylate groups on the surface of MWCNTs after treatment with acid mixture<sup>43,44</sup>. The bands at 3440 and 1640  $\text{cm}^{-1}$  come from traces of water. The covalent amide linkages between MWCNTs and modified  $\beta$ -cyclodextrin were confirmed from the FTIR spectra shown in Figure 6.1b and 6.1c. In the spectrum of diamino  $\beta$ -cyclodextrin (Figure 6.1b), the absorption bands were found at 3368, 2920, 1660, 1155, and 1029  $\text{cm}^{-1}$ , which could be assigned to the typical hydrogen bonded  $\text{-OH}$  stretching,  $\text{-C-H}$  stretching,  $\text{-OH}$  bending band,  $\text{-C-O}$  stretching and  $\text{-C-O-C}$  stretching absorption bands of  $\beta$ -cyclodextrin. Incidentally, the FTIR absorption spectrum of  $\beta$ -cyclodextrin-modified MWCNTs exhibited similar absorption bands to  $\beta$ -cyclodextrin, indicating the binding of  $\beta$ -cyclodextrin on MWCNTs and the retaining of the pristine structure of  $\beta$ -cyclodextrin after the modification with MWCNTs. Besides, there was disappearance of absorption bands at 1720 and 1560  $\text{cm}^{-1}$  of oxidized MWCNTs was observed. Moreover, the typical peak of amide band at 1674  $\text{cm}^{-1}$  was hindered over the typical broad peak of  $\beta$ -CD. These results clearly suggest that carboxylic groups of MWCNTs were completely exhausted by chemical reaction with diamino  $\beta$ -cyclodextrin, confirming the successful attachment of diamino  $\beta$ -cyclodextrin onto the surface of CNTs through covalent amide linkages.

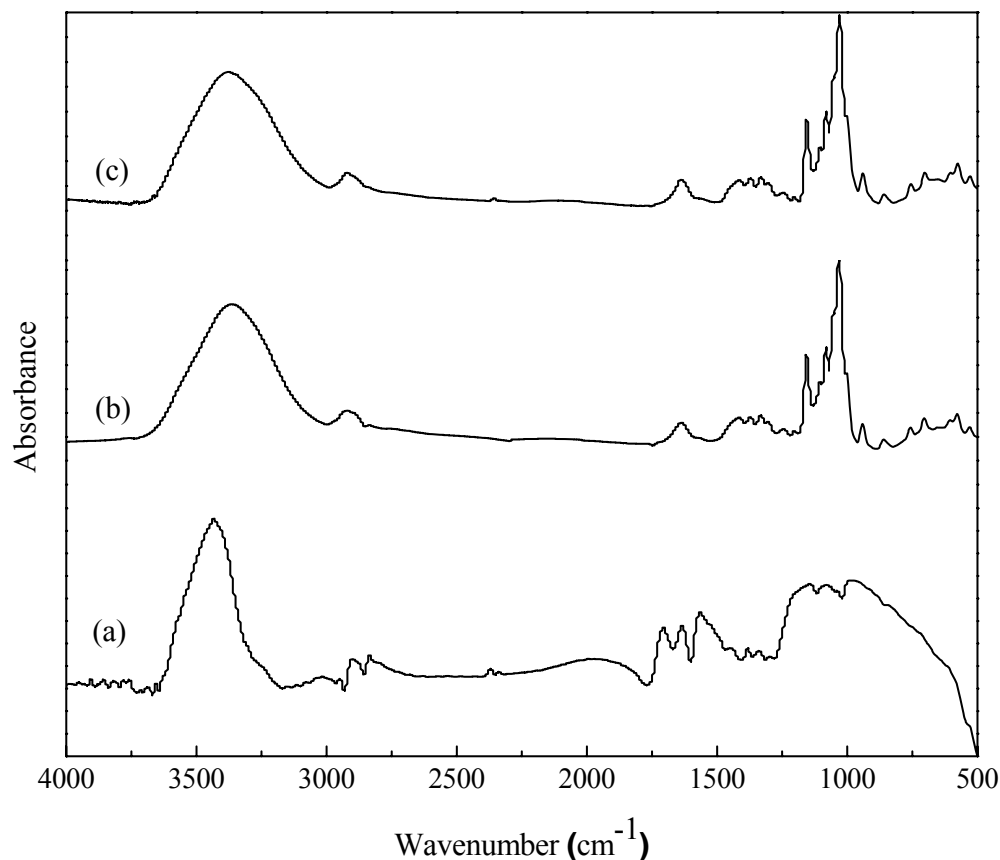


**Figure 6.1** FTIR spectra of (a) oxidized MWCNTs, (b) diamino  $\beta$ -cyclodextrin and (c)  $\beta$ -cyclodextrin-modified MWCNTs.

### 6.3.1.2 Dispersibility

One of the very convincing and visible evidence of surface modification of MWCNTs with  $\beta$ -cyclodextrins was the water-dispersibility of these nanotubes. A comparison of the dispersibility is shown in Figure 6.2. Same quantities of all the three samples of (a) pristine MWCNTs, (b) oxidized MWCNTs and (c)  $\beta$ -cyclodextrin-modified MWCNTs were suspended in equal volume of water and stirred for half an hour and left as it is. Within few minutes the pristine MWCNTs settled down to the bottom of the petri dish, whereas the oxidized MWCNTs did not precipitate at short time like one hour but settled down after 5h. In the case of  $\beta$ -cyclodextrin-modified MWCNTs, the MWCNTs were stable with no visible precipitation in the aqueous system and product was not settled down even after several months.

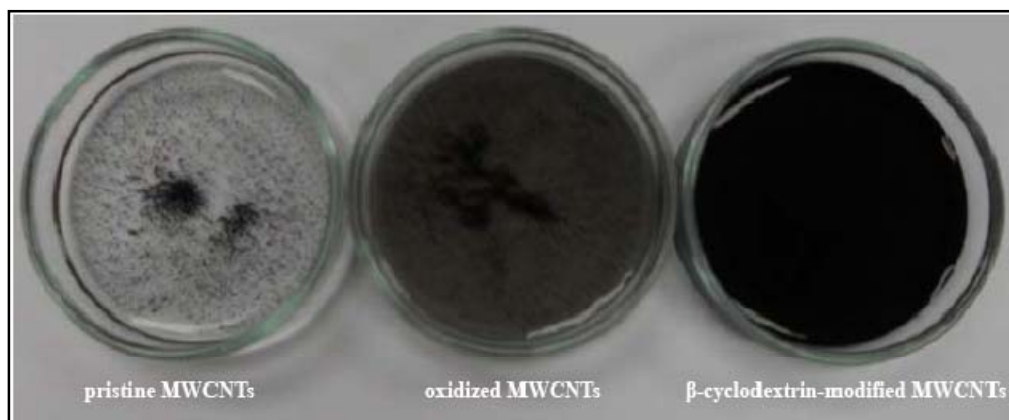


**Figure 6.2** Dispersibility of (a) pristine MWCNTs, (b) oxidized MWCNTs and (c)  $\beta$ -cyclodextrin-modified MWCNTs.

### 6.3.1.3 Thermogravimetric Analysis (TGA)

To further confirm the surface modification of MWCNTs, the obtained product was analyzed by TGA and compared to the starting materials i.e. diamino  $\beta$ -cyclodextrin and oxidized MWCNTs. Figure 6.3 shows the TGA curves of oxidized MWCNTs, diamino  $\beta$ -cyclodextrin and  $\beta$ -cyclodextrin-modified MWCNTs. As shown in Figure 6.3a, the oxidized MWCNTs showed weight loss at the temperature range of 500-700°C. On the other hand, diamino  $\beta$ -cyclodextrin (Figure 6.3b) displayed weight loss in three steps including the weight loss of contaminants (and/or water) and was completely decomposed up to 500°C. On a TGA curve of the  $\beta$ -cyclodextrin-modified MWCNTs (Figure 6.3c), the weight loss happened through some steps up to 630°C. Then weight content of  $\beta$ -cyclodextrin in  $\beta$ -cyclodextrin-modified MWCNTs was determined by weight comparison in the TGA curves at 500°C, and evaluated to be about 69 wt%. Therefore, the weight content of covalently bonded diamino  $\beta$ -cyclodextrin was estimated to be ~69 wt%.

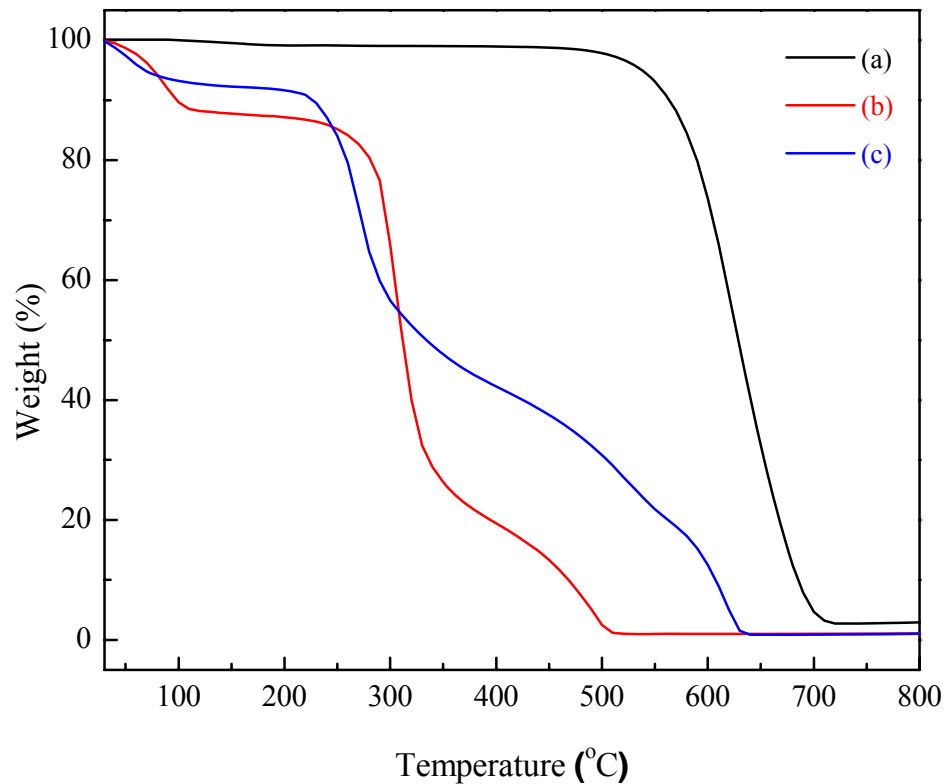


**Figure 6.3** TGA curves of (a) oxidized MWCNTs, (b) diamino  $\beta$ -cyclodextrin and (c)  $\beta$ -cyclodextrin-modified MWCNTs.

#### 6.3.1.4 Energy Dispersive Spectroscopy (EDS)

EDS analysis was also carried out on the pristine MWCNTs, oxidized MWCNTs and  $\beta$ -cyclodextrin-modified MWCNTs and the results are given in Figure 6.4. The EDS results are quite convincing in the sense that the carbon content is reducing from the pristine MWCNTs to the oxidized MWCNTs and the  $\beta$ -cyclodextrin-modified MWCNTs with a corresponding increase in the elemental content of oxygen owing to effective oxidation of MWCTNs and surface immobilization of diamino  $\beta$ -cyclodextrins on MWCTNs.

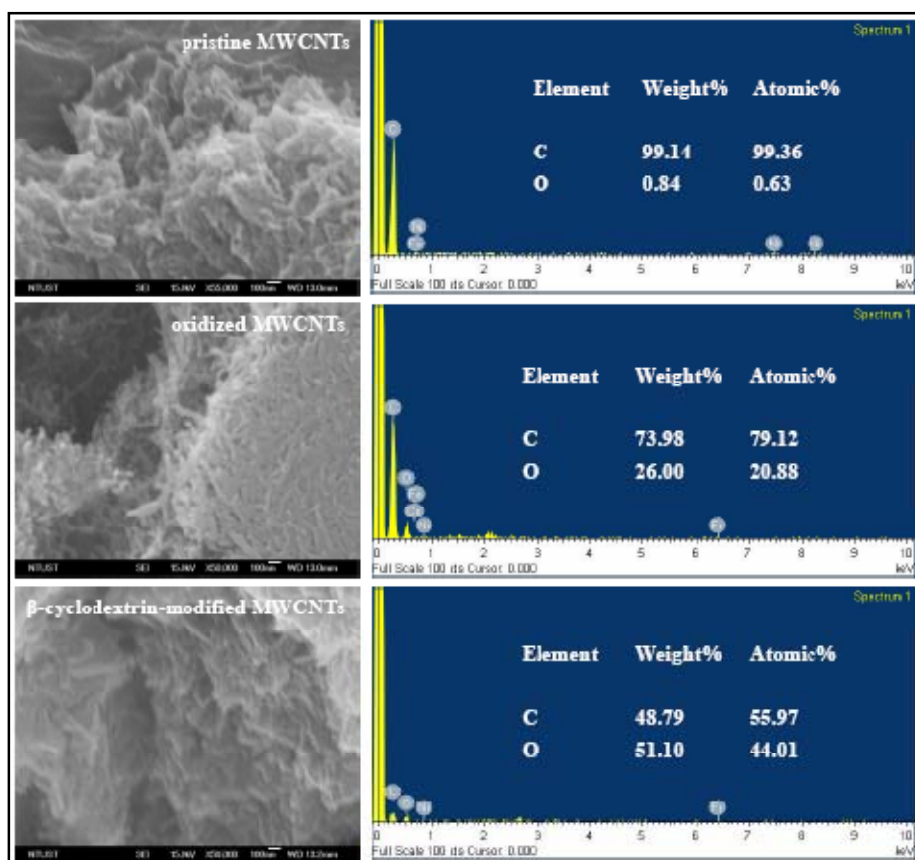


**Figure 6.4** FE-SEM combined EDS of (a) pristine MWCNTs, (b) oxidized MWCNTs and (c)  $\beta$ -cyclodextrin-modified MWCNTs.

### 6.3.1.5 Transmission Electron Micrograph (TEM)

The visible and direct confirmation of successful surface immobilization of diamino  $\beta$ -cyclodextrins on the surface of MWCNTs comes from the Transmission Electron Microscopic images. Figure 6.5 shows the TEM images of pristine MWCNTs, oxidized MWCNTs,  $\beta$ -cyclodextrin modified MWCNTs without staining and  $\beta$ -cyclodextrin modified MWCNTs staining with phosphotungstic acid. From the TEM images of pristine MWCNTs (Figure 6.5a) and oxidized MWCNTs (Figure 6.5b), we can observe the surface cleaning after treatment with acid mixture at reflux temperature; acid treatment process can remove extra metal catalyst, amorphous carbon and carbon nanoparticles which were formed during the course of production of MWCNTs. In the case of  $\beta$ -cyclodextrin-modified MWCNTs without staining (Figure 6.5c) it was difficult to see the surface immobilization of MWCNTs with  $\beta$ -

cyclodextrins although some haziness can be observed on the surface of MWCNTs ascribed the surface functionalization of MWCNTs with diamino  $\beta$ -cyclodextrin. In the case of  $\beta$ -cyclodextrin-modified MWCNTs staining with phosphotungstic acid (Figure 6.5d), results in black stains (high contrast spots) on the surface of MWCNTs. This is due to the adsorption of phosphotungstic acid on the amide linkages. From the TEM images it can be seen that the acid treatment and surface immobilization of MWCNTs with  $\beta$ -cyclodextrins does not damage the surface of MWCNTs.

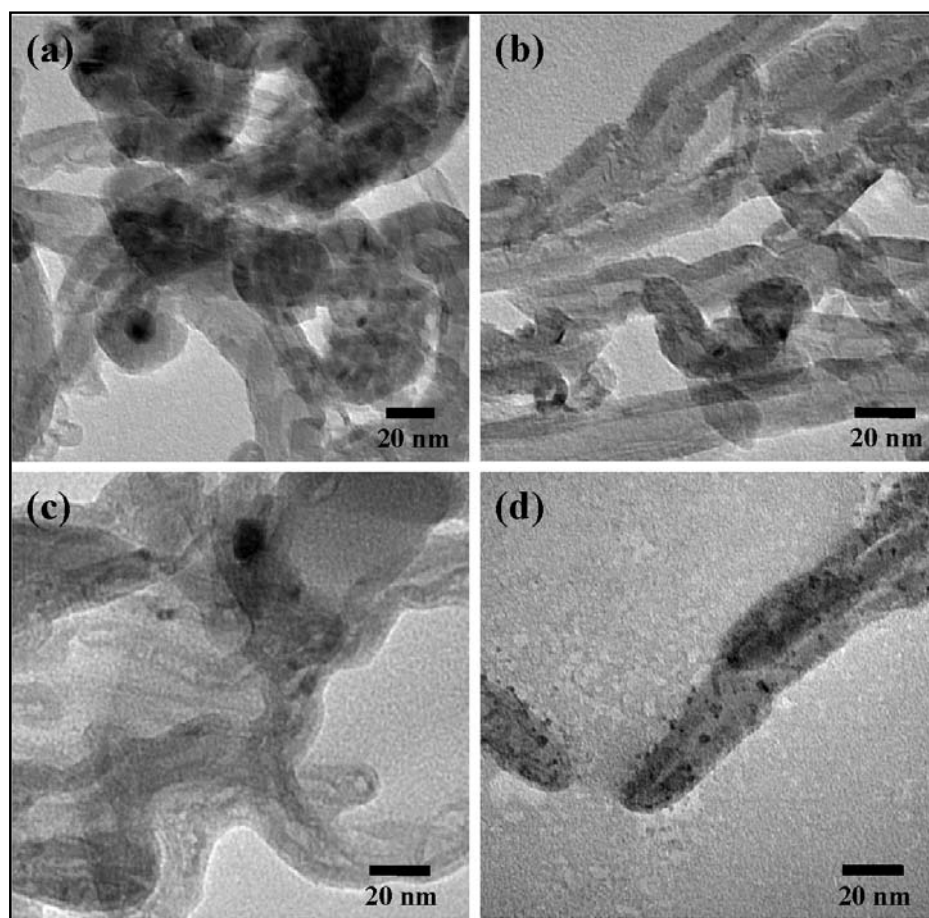


**Figure 6.5** TEM images of (a) pristine MWCNTs, (b) oxidized MWCNTs, (c)  $\beta$ -cyclodextrin-modified MWCNTs without staining and (d)  $\beta$ -cyclodextrin-modified MWCNTs staining with phosphotungstic acid.

## 6.3.2 Inclusion Ability of $\beta$ -Cyclodextrins Immobilized on MWCNTs

### 6.3.2.1 Fluorescence Spectroscopy

One of the efficient methods to confirm the functionality (especially inclusion ability) of  $\beta$ -cyclodextrin on the CNTs surface is to see if any organic molecule can be included into the  $\beta$ -cyclodextrin cavity and probed with a suitable technique. Thus, the fluorescence emission of rhodamine 6G excited at 480 nm in aqueous solutions containing various concentrations of diamino  $\beta$ -cyclodextrin, oxidized MWCNTs and  $\beta$ -cyclodextrin-modified MWCNTs, respectively, was recorded. The results of these measurements are shown in Figure 6.6. The maximum emission intensity was observed at 554 nm for all systems.

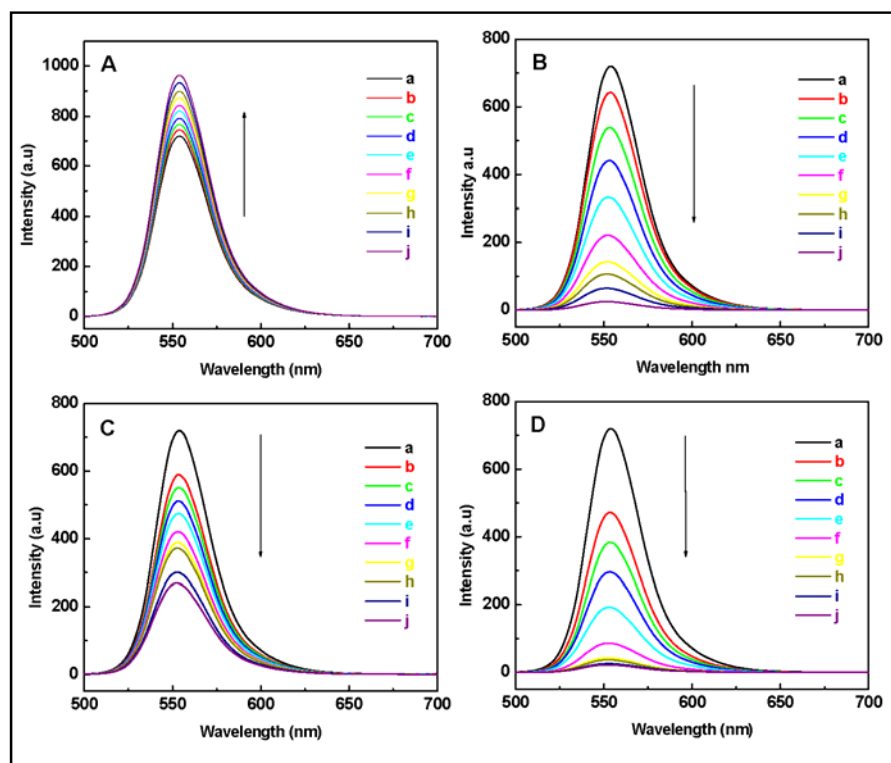
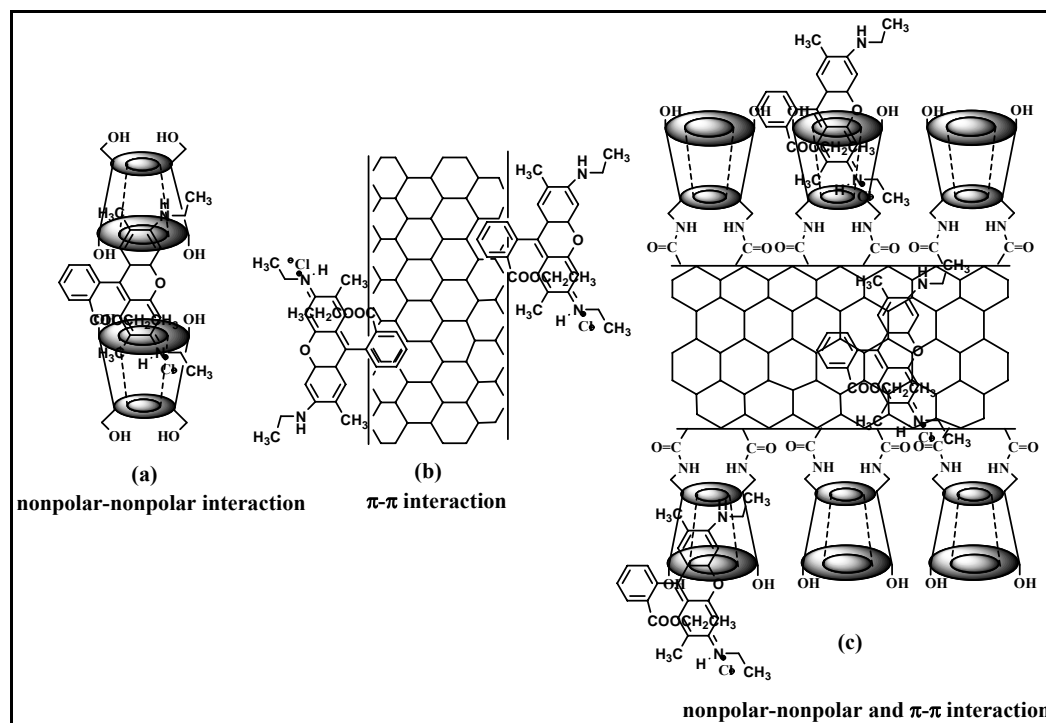


**Figure 6.6** Fluorescence spectra (excited at 480 nm) of rhodamine 6G ( $5 \times 10^{-6}$  M) in aqueous solutions of (A) diamino  $\beta$ -cyclodextrin, (B) pristine MWCNTs, (C) oxidized MWCNTs and (D)  $\beta$ -cyclodextrin-modified MWCNTs at different concentrations: (a) 0, (b) 2.5, (c) 5.0, (d) 7.5, (e) 10.0, (f) 12.5, (g) 15.0, (h) 17.5, (i) 20.0 and (j) 22.5  $\mu\text{g/mL}$ .

In the presence of pristine diamino  $\beta$ -cyclodextrin, the fluorescence intensity of rhodamine 6G increased with increasing concentration of diamino  $\beta$ -cyclodextrin as expected (Figure 6.6A). This phenomenon was observed due to the formation of inclusion complex which due to the rotation of the rhodamine 6G molecule is hindered, and the relaxation of the solvent molecules is considerably decreased. Both of these effects can result in a decrease in the vibrational deactivation. The non-polar cavity of  $\beta$ -CD protects the quenching of the rhodamine 6G emission by water molecule. The CDs cavity behaves similarly to the organic solvent which gives non-polar surrounding for the included molecule. This altered microenvironment can provide favorable polarity for enhanced quantum efficiencies and hence the intensities of fluorescence increase. Though rhodamine 6G is not a small molecule to include into a single  $\beta$ -cyclodextrin unit, it can be included into two  $\beta$ -cyclodextrin units (Scheme 6.3a), thus forming a 2:1 complex with  $\beta$ -cyclodextrin and leading to the increase in the fluorescence intensity. Meanwhile, the fluorescence intensity was reduced in the presence of pristine MWCNTs, oxidized MWCNTs and  $\beta$ -cyclodextrin-modified MWCNTs (Figure 6.6B, 6.6C, 6.6D). The mechanism of fluorescence hypochromic effect of rhodamine 6G by the pristine nanotubes (Scheme 6.3b) can be explained by the wrapping of the rhodamine 6G on six-ringed structure of the nanotubes surface. This is expected for pristine CNTs in the aqueous solution, since the strong  $\pi$ - $\pi$  stacking interaction between the rhodamine 6G and the surface of the CNTs results in the fluorescence quenching. The similar fluorescence reduction of rhodamine 6G on oxidized MWCNTs and  $\beta$ -cyclodextrin-modified MWCNTs is the indication to the fact that though covalent functionalization of the CNTs has taken place and the modification of the  $\pi$  structure on the surface, the CNTs still retains the essential property of the nanotubes, as the inner tubes are still intact.

Especially, the reduction of the fluorescence intensity of rhodamine 6G in the presence of the  $\beta$ -cyclodextrin-modified CNT is a surprising result, because apparently the rhodamine 6G molecule is not included into the cavities of two  $\beta$ -cyclodextrins or in other words the 2:1 inclusion complex is not formed in this case (Scheme 6.3c). This could be derived from the reason that the  $\beta$ -cyclodextrins are now tethered on the nanotubes surface and are not as mobile or 'free' as in the case of the pristine diamino  $\beta$ -cyclodextrin. Therefore, rhodamine 6G molecule is partially

included into non-polar cavity of  $\beta$ -cyclodextrin and also adsorbed on the surface of MWCNTs.



**Scheme 6.3** Schematic illustrations of the formation of  $\beta$ -cyclodextrin-dye inclusion complex and the adsorption of dyes on MWCNTs.

Additional insights were obtained from the analysis of the fluorescence intensity depending on concentration of rhodamine 6G. It can be seen from Figure 6.7 that the emission intensity at 554 nm of rhodamine 6G decreases for all the three (a) pristine MWCNTs, (c) oxidized MWCNTs and (d)  $\beta$ -cyclodextrin-modified MWCNTs. However, the profile of the decrease varies for all three. While the intensity decreases linearly with concentration of pristine MWCNTs, at the concentration beyond 2.5  $\mu\text{g/mL}$  for the cyclodextrin-modified MWCNTs, it shows a linear decrease with a similar slope to that for pristine MWCNTs. However, the initial decrease with a steeper slope exists at the concentration below 2.5  $\mu\text{g/mL}$  for the  $\beta$ -cyclodextrin-modified MWCNTs. This indicates that the mechanism of the initial fluorescence hypochromism results from a different origin. The possible mechanism of the fluorescence hypochromism at the initial concentration is strong  $\pi$ - $\pi$  stacking interaction of rhodamine 6G with well dispersed  $\beta$ -cyclodextrin-modified MWCNTs.

The schematic illustration of the complexes between rhodamine 6G and  $\beta$ -cyclodextrin-modified MWCNTs is given in Scheme 6.3.

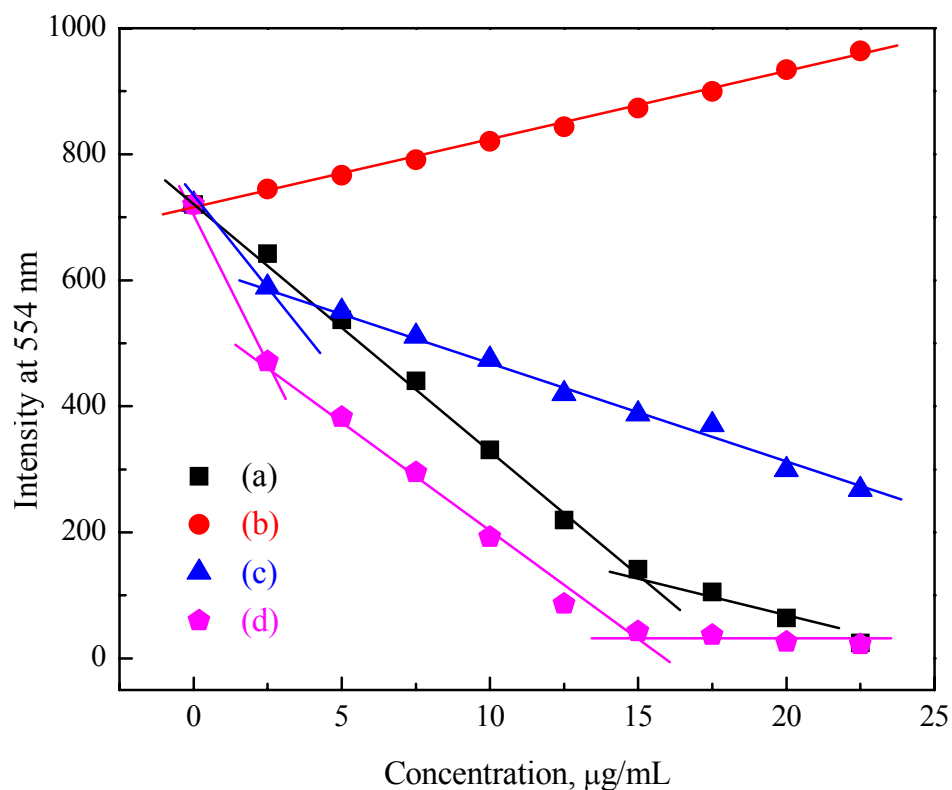


**Figure 6.7** Change in fluorescence intensity at 554 nm of rhodamine 6G ( $5 \times 10^{-6}$  M) as a function of concentration of (a) pristine MWCNTs, (b) diamino  $\beta$ -cyclodextrin, (c) oxidized MWCNTs and (d)  $\beta$ -cyclodextrin-modified MWCNTs in water.

The fluorescence hypochromism of oxidized MWCNTs also shows two steps but the slopes are different from those of  $\beta$ -cyclodextrin-modified MWCNTs. Since the oxidized MWCNTs has many carboxylic acids on MWCNTs surface, cationic rhodamine 6G can electrostatically bind with carboxylic acids on MWCNTs in the initial stage and sequentially may give rise to the  $\pi$ - $\pi$  stacking interaction with the surface of the CNT, although the latter interaction should be affected by the coexisting electrostatic interaction and/or carboxylic acid.

The hypochromism efficiency can be estimated from the Stern-Volmer constants which were evaluated from the Stern-Volmer equation given below and plots given in Figure 6.8.

*Stern-Volmer equation*

$$\frac{I_0}{I} = 1 + K_{sv}[Q] \quad (6.1)$$

Where,  $I_0$  and  $I$  are the fluorescence intensity of Rhodamine 6G in absence and presence of quencher  $[Q]$ ,  $K_{sv}$  and  $[Q]$  are Stern-Volmer quenching constant and concentration of quencher, respectively. These constants are listed in Table 6.1. The constant for the  $\beta$ -cyclodextrin-modified MWCNTs was 1.6 and 23 times higher than that for the pristine MWCNTs and the oxidized MWCNTs, respectively.

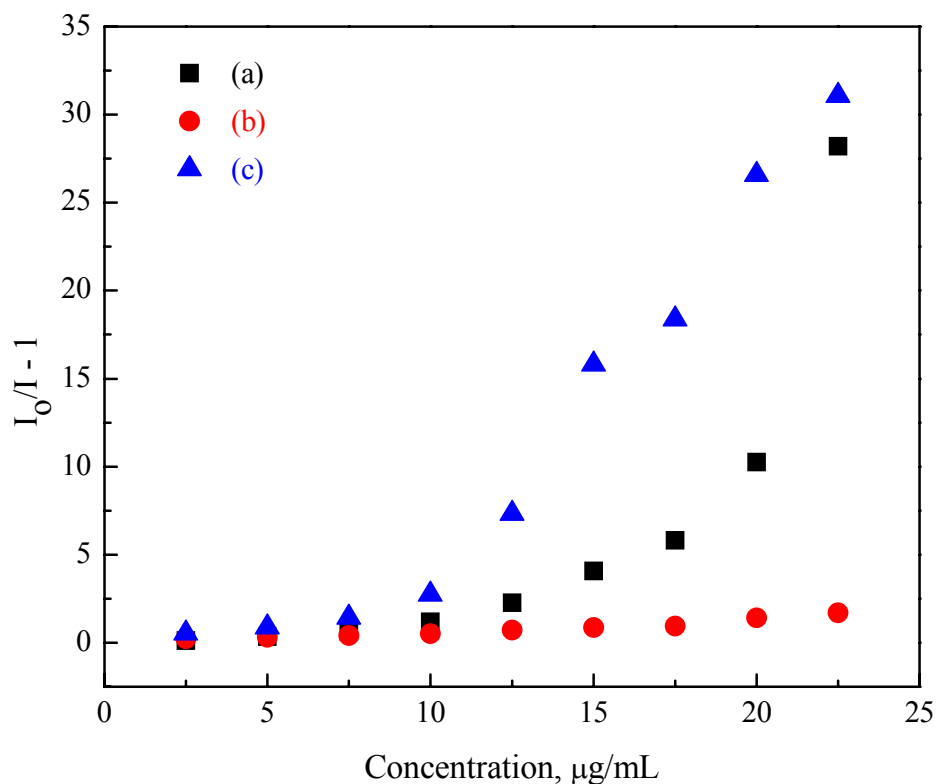


**Figure 6.8** Stern-Volmer plots for (a) pristine MWCNTs, (b) oxidized MWCNTs and (c)  $\beta$ -cyclodextrin-modified MWCNTs.

**Table 6.1** Hypochromism constants for pristine and modified MWCNTs calculated from fluorescence intensities

<b>Sample</b>	<b>Stern-Volmer Constant , (<math>K_{sv}</math>) (<math>M^{-1}</math>)</b>
pristine MWCNTs	1036
oxidized MWCNTs	71
$\beta$ -cyclodextrin-modified MWCNTs	1641

## 6.4 Conclusions

The water-dispersible hybrid material denoted as  $\beta$ -cyclodextrin-modified MWCNTs was achieved by simple conventional covalent bond formation technique. The successful attachment of  $\beta$ -cyclodextrin on the surface of MWCNTs was effectively characterized by conventional techniques like FTIR, TGA, EDS and TEM analyses. This synthetic method provided enough number of  $\beta$ -cyclodextrin units on the surface of MWCNTs. On one hand the procedure affords easy dispersion of CNTs in water, and on the other it serves as nanocavities on the surface of the MWCNT for interaction with the CNT. Then the nanocavities can include either metal ions or organic molecules, which are sufficiently small to 'fit' into the  $\beta$ -cyclodextrin cavity, as exemplified by the inclusion of rhodamine 6G and support the potential for using this material for targeting specific sensors.

## References

1. K. Tvrđy and M. S. Strano, *Nature Nanotechnology*, **2012**, 7, 8-9.
2. P. M. Ajayan and S. Iijima, *Nature*, **1993**, 361, 333.
3. T. W. Ebbesen and P. M. Ajayan, *Nature*, **1992**, 358, 220.
4. N. Hamada, S. Sawada and S. Oshiyama, *Phys. Rev. Lett.*, **1992**, 68, 1579.
5. D. H. Robertson, D. W. Brenner and J. W. Mintmire, *Phys. Rev.*, **1992**, B, 45, 12592.
6. M. S. Arnold, J. D. Zimmerman, C. K. Renshaw, X. Xu, R. R. Lunt, C. M. Austin, and S. R. Forrest, *Nano Lett.*, **2009**, 9, 3354.
7. R. H. Baughman, A. A. Zakhidov, and W. A. de Heer, *Science*, **2002**, 297, 787.
8. H. Hyung, J. D. Fortner, J. B. Hughes and J. H. Kim, *Environ. Sci. Technol.*, **2007**, 41, 179.
9. H. H. Cho, B. A. Smith, J. D. Wnuk, D. H. Fairbrother and W. P. Ball, *Environ. Sci. Technol.*, **2008**, 42, 2899.
10. B. Yoon and C. J. Wai, *J. Am. Chem. Soc.*, **2005**, 127, 17174.
11. S. Zhang, Y. Shao, G. Yin, and Y. Lin, *J. Mater. Chem.*, **2010**, 20, 2826.
12. B. K. Price, J. L. Hudson and J. M. Tour, *J. Am. Chem. Soc.*, **2005**, 127, 127, 14867.
13. A. Thess, R. Lee, P. Nikolaev, H. Dai, P. Petit, J. Robert, C. Xu, Y. H. Lee, S. G. Kim, A. G. Rinzler, D. T. Colbert, G. E. Scuseria, D. Tomanek, J. E. Fischer and R. E. Smalley, *Science*, **1996**, 273, 5274.
14. C. Journet, W. K. Maser, P. Bernier, A. Loiseau, M. L. Chapelle and S. Lefrant, P. Deniard, R. Lee, and J. E. Fisher, *Nature*, **1997**, 388, 756.
15. W. Yang, P. Thordarson, J. J. Gooding, S. P. Ringer and F. Braet, *Nanotechnology*, **2007**, 18, 412001.
16. O. Akhavan, M. Abdollahad, Y. Abdi and S. Mohajerzadeh, *J. Mater. Chem.*, **2011**, 21, 387.
17. S. Niyogi, M. A. Hamon, H. Hu, B. Zhao, P. Bhowmik, R. Sen, M. E. Itkis and R. C. Haddon, *Acc. Chem. Res.*, **2002**, 35, 1105.
18. S. Rana, N. Karak, J. W. Cho, Y. H. Kim, *Nanotechnology*, **2008**, 19, 495707.

19. S. H. Liao, C. Y. Yen, C. H. Hung, C. C. Weng, M. C. Tsai, Y. F. Lin, C. C. M. Ma, C. Pan and A. Su, *J. Mater. Chem.*, **2008**, 18, 3993.
20. X. Lu and T. Imae, *J. Phys. Chem. C*, **2007**, 111, 8459.
21. K. E. Geckeler and T. Premkumar, *Nanoscale Res. Lett.*, **2011**, 6, 136-138.
22. K. Balasubramanian and M. Burghard, *Small*, **2005**, 1, 180.
23. M. Holzinger, J. Baur, R. Haddad, X. Wang and S. Cosnier, *Chem. Commun.*, **2011**, 47, 2450.
24. L. Vaisman, H. D. Wagner and G. Marom, *Adv. Colloid Int. Sci.*, **2006**, 128-130, 37.
25. M. S. Strano, *Nature Materials*, **2006**, 5, 433.
26. J. P. McNamara, R. Sharma, M. A. Vincent, I. H. Hillier and C. A. Morgado, *Phys. Chem. Chem. Phys.*, **2008**, 10, 128.
27. H. Nie, H. Wang, A. Cao, Z. Shi, S. T. Yang, Y. Yuan and Y. Liu, *Nanoscale*, **2011**, 3, 970.
28. F. A. Lemasson, T. Strunk, P. Gerstel, F. Hennrich, S. Lebedkin, C. B. Kowollik, W. Wenzel, M. M. Kappes and M. Mayor, *J. Am. Chem. Soc.*, **2011**, 133, 652.
29. F. Meyer, J. M. Raquez, P. Verge, I. M. de Arenaza, B. Coto, P. V. D. Voort, E. Meaurio, B. Dervaux, J. M. Sarasua, F. D. Prez and P. Dubois, *Biomacromolecules*, **2011**, 12, 4086.
30. B. Leger, S. Menuel, D. Landy, J. F. Blach, E. Monflier, and A. Ponchel, *Chem. Commun.*, **2010**, 46, 7382.
31. J. G. Yu, K. L. Huang, S. Q. Liu and J. C. Tang, *Physica E*, **2008**, 40, 689.
32. J. Chen, M. J. Dyer, and M. F. Yu, *J. Am. Chem. Soc.*, **2001**, 123, 6201.
33. E. S. Shibu, and T. Pradeep, *Chem. Mater.*, **2011**, 23, 989.
34. Y. Bai, G. Y. Xu, H. Y. Sun, A. Y. Hao, H. Z. Mao, S. L. Dong, X. F. Shi, X. Xin, M. Q. Ao, J. Y. Pang and X. D. Yang, *J. Despr. Sci. Techno.*, **2010**, 31, 353-358.
35. D. I. Schuster, and J. D. Megiatto, *Nature Chemistry*, **2009**, 1, 182.
36. Y. Guo, S. Guo, J. Ren, Y. Zhai, S. Dong and E. Wang, *ACS Nano.*, **2010**, 4, 4001.
37. A. R. Khan, P. Forgo, P.; K. J. Stine, V. T. D'Souza, *Chem. Rev.*, **1998**, 98, 1977.
38. E. S. Cho, S. W. Hong, W. H. Jo, *Macromol. Rapid Commun.*, **2008**, 29(22), 1798-1803.

39. L. B. Zhang, H. Wei, J. Li, T. Li, D. Li, Y. H. Li, E. K. Wang, *Biosens. Bioelectron.* **2010**, 25(8), 1897-1901.
40. C. Y. Yen, Y. F. Lin, S. H. Liao, C. C. Weng, C. C. Huang, Y. H. Hsiao, C. C. M. Ma, M. C. Chang, H. Shao, M. C. Tsai, C. K. Hsieh, C. H. Tsai and F. B. Weng, *Nanotechnology*, **2008**, 19, 37.
41. C. B. Jacobs, M. J. Peairs and B. J. Venton, *Anal. Chim. Acta* **2010**, 662(2), 105-127.
42. E. Kymakis, G. A. J. Amaratunga, *Appl. Phys. Lett.* **2002**, 80(1), 112-114.
43. X. Lu and T. Imae, *J. Phys. Chem. C*, **2007**, 111, 2416.
44. M. Ito and T. Imae, *J. Nanosci. Nanotechnol.*, **2006**, 6, 1667.

## Summary of the Thesis

This thesis describes the synthesis of the selectively modified difunctional  $\beta$ -cyclodextrin without protection and deprotection of the other primary hydroxyl groups by oxidoreductive reaction. The selectively modified cyclodextrin derivatives used as monomers for the synthesis of linear highly water-soluble polymers consisting  $\beta$ -cyclodextrin as a part of the main-chain of the polymers. Water-soluble cyclodextrin and polyethylene glycols based polymers were also synthesized by polycondensation reaction with cyanuric chloride as a linking agent using the temperature dependent reactivity of three chlorine atoms of cyanuric chloride. The synthesized cyclodextrin based polymers were effectively used for the aqueous solubilization of hydrophobic antiepileptic drug carbamazepine using phase solubility and dissolution studies. Moreover, the fluorescence properties of pyrene in presence of cyclodextrin and cyclodextrin based polymers were also studied. The selectively modified difunctional cyclodextrin derivatives have been effectively used for the solubilization of the two hydrophobic carbon allotropes fullerenes and carbon nanotubes. The process involves covalent functionalization of carbon allotropes with reactive cyclodextrin derivatives.

Chapter 1 gives an introduction to the focus of the thesis and the review of existing literature on the scientific problems.

Chapter 2 describes the synthesis and characterization of three important water-soluble  $\beta$ -cyclodextrin based monomers by oxidoreductive substitution reaction without protection and deprotection steps. The  $\beta$ -cyclodextrin has 14 secondary hydroxyl groups on the wider rim and 7 primary hydroxyl groups on the narrow rim. Selective modification of cyclodextrins without protection is an extremely difficult task because of similar functionalities compete for the same reagent and result in multi functional cyclodextrins, though geometry of reagents has been attempted for the selective modification of cyclodextrins. The three major substitutions (iodo, azido and amino) on the primary side of the cyclodextrin was successfully introduced using bulky disubstituted reagent biphenyl 4,4'-disulphonyl chloride which can react only two specific primary hydroxyl groups of  $\beta$ -cyclodextrin. The synthesized water-soluble  $\beta$ -cyclodextrin based monomers were characterized by conventional spectroscopic techniques. These three major cyclodextrin monomers which have

reactive functional groups, enhanced inclusion ability and good water-solubility are further used for the preparation of water-soluble main-chain polymers and also used for the aqueous solubilization of two major carbon allotropes fullerenes and carbon nanotubes.

Chapter 3 describes the synthesis of linear highly water-soluble  $\beta$ -cyclodextrin based polymers using short linkers (cyanuric chloride, polyethylene glycols, urea and thiourea) to connect the  $\beta$ -cyclodextrins and selectively modified  $\beta$ -cyclodextrins. The water-soluble polymers had  $\beta$ -cyclodextrins in the main-chain. The controlled conditions were used to prevent the crosslinking of monomers. The synthesized polymers were purified by ultrafiltration using MWCO=1K membrane and solid polymers were isolated by freeze-drying. The physico-chemical properties of the synthesized polymers were characterized by FTIR, NMR spectroscopy, XRD and Thermogravimetric analysis (TGA). As expected the synthesized  $\beta$ -cyclodextrin based polymers have more aqueous solubility as compared to parent  $\beta$ -cyclodextrin. Thus, such types of polymers are quite useful for the drug delivery applications.

Chapter 4 describes the inclusion complexation (ICs) of water-insoluble drug (carbamazepine) and pyrene with parent  $\beta$ -cyclodextrin and synthesized  $\beta$ -cyclodextrin based polymers. The inclusion formation of carbamazepine with  $\beta$ -cyclodextrin and  $\beta$ -cyclodextrin based polymers were characterized by UV-Vis, FTIR and NMR spectroscopic techniques. The formation of 1:1 inclusion complex of carbamazepine was found from phase solubility diagram. The aqueous solubilization of carbamazepine achieved was 0.7 mg/mL as compared to 0.1 mg/mL. The formation of 1:1 inclusion complex of pyrene with  $\beta$ -cyclodextrin and  $\beta$ -cyclodextrin based polymers were characterized by fluorescence analysis using Benesi-Hildebrand equation and plots. Furthermore, the dynamic process of inclusion complex of pyrene was estimated using a competitive guest molecule adamantol.

The Chapter 5 is divided into two parts. The first part of the Chapter 5 describes the aqueous solubilization of [60]fullerene by covalent as well non-covalent functionalization of [60]fullerene with the selectively diazido functionalized  $\beta$ -cyclodextrin. This is the time that covalent as well as non-covalent interactions of [60]fullerene with the modified  $\beta$ -cyclodextrin has been attempted for the solubilization of [60]fullerene in aqueous media. The solubility of the  $\beta$ -CD-

[60]fullerene adduct in water was measured and it was found to be  $6.5 \text{ mg mL}^{-1}$ , which is greater than that of conventional 2:1 inclusion complex of  $\beta$ -cyclodextrin. The previously described methods only deal with the non-polar interaction of the [60]fullerene molecule with cyclodextrins. However, a competitive guest molecule in the biological media can displace [60]fullerene from the cyclodextrin cavity. Tethering the [60]fullerene molecule to the cyclodextrin molecule is an effective option of overcoming this problem and also the advantage of more [60]fullerene surface area. The  $\beta$ -CD-[60]fullerene adduct was stable enough from that fullerene was not extractable which have been characterized by simple comparison of extraction of [60]fullerene from 2:1 inclusion complex of  $\beta$ -CD inclusion complex. The evidence for the both covalent and non-covalent interactions between selectively modified  $\beta$ -cyclodextrin and [60]fullerene comes from the FTIR, UV-Vis, NMR and thermogravimetric analysis of the  $\beta$ -CD-fullerene adduct. Supramolecular self-assembly and morphology behavior of adduct was investigated by SEM, TEM, XRD and AFM characterizations.

The second part of the Chapter 5 describes the aqueous solubilization of [60]fullerene/[70]fullerene which was also achieved by self-assembly with disaccharides in mixed homogeneous solvent system. The complexation of extremely water-insoluble [60]fullerene/[70]fullerene dissolved in non-polar solvent and extremely water-soluble disaccharides dissolved in polar solvent resulted in a highly water-soluble [60]fullerene/[70]fullerene-disaccharide self-assembled complex. The interaction between [60]fullerene/[70]fullerene and disaccharides were found to be non-covalent, characterized by FTIR, UV-Vis, NMR, XRD and TGA analysis. This study demonstrated a low cost protocol for the aqueous solubilization of [60]fullerene/[70]fullerene self-assembly by disaccharides as optional to the use of cyclodextrins that are many times more expensive. The identification of the complex suggested that [60]fullerene/[70]fullerene molecule was surrounded by four lactose molecules. The morphology and particles size (self-assembly behavior) of the complex was determined by Transmission Electron Micrograph (TEM) and Static Light Scattering (SLS).

Preliminary studies of radical scavenging on the most stable free radical 2,2'-diphenyl-1-picrylhydrazyl (DPPH) suggested that the prepared water-soluble [60]fullerene/[70]fullerene has potential biological applications.

Chapter 6 describes the aqueous dispersion of multiwall carbon nanotubes by covalent immobilization of selectively functionalized  $\beta$ -cyclodextrin. The diamino-functionalized  $\beta$ -cyclodextrin and carboxylic acid-functionalized CNTs were used to covalently bind them via amide linkages using 1-ethyl-3-(3-dimethylamino propyl) carbodiimide hydrochloride as a water-soluble condensation agent at room temperature. The obtained highly dispersible product denoted as  $\beta$ -cyclodextrin-modified MWCNTs was characterized by FTIR and energy dispersive X-ray spectrometry. The thermogravimetric analyses indicated that 69 wt%  $\beta$ -cyclodextrin was attached on the surface of CNTs. Moreover, the fluorescence sensitizing of rhodamine 6G suggested that the  $\beta$ -cyclodextrin-modified CNTs have potential medicinal use.

## List of Publications

1. Aqueous solubilization of [60]fullerene by selectively modified  $\beta$ -cyclodextrin  
Vinod I. Bhoi and C. N. Murthy  
Fullerenes Nanotubes and Carbon Nanostructures, **2011**, 19(7), 668-676.
2. Surface immobilization of carbon nanotubes by  $\beta$ -cyclodextrins and their inclusion ability  
Vinod I. Bhoi, Toyoko Imae, Masaki Ujihara and C. N. Murthy  
Journal of Nanoscience and Nanotechnology, **2012**, accepted
3. The self-assembly and aqueous solubilization of [60]fullerene with disaccharides  
Vinod I. Bhoi, S. Kumar and C. N. Murthy  
Carbohydrate Research, **2012**, 359, 120-127.
4. Studies on the pyrene- $\beta$ -cyclodextrin and  $\beta$ -cyclodextrin polymer guest-host inclusion complexes by absorbance and fluorescence spectroscopy  
Vinod I. Bhoi, K. V. R. Murthy and C. N. Murthy, International Journal of Luminescence and Its Applications, **2012**, 1(2), 82-85

## List of Presentations

1. Fluorescence studies on the pyrene/cyclodextrin based polymer guest-host complexes  
Vinod I. Bhoi, K. V. R. Murthy and C. N. Murthy  
4<sup>th</sup> International Conference on Luminescence and Its Applications, February 7-10, 2012, Indian Institute of Chemical Technology, Hyderabad
2. Studies on the pyrene-cyclodextrin based polymer guest-host complexes by fluorescence spectroscopy  
Vinod I. Bhoi, K. V. R. Murthy and C. N. Murthy  
XXVI Gujarat Science Congress, February 26, 2012, The M. S. University of Baroda, Vadodara
3. Surface immobilization of carbon nanotubes by  $\beta$ -cyclodextrins and their inclusion ability  
Vinod I. Bhoi, Totoko Imae and C. N. Murthy  
Advances in Polymers Science & Nanotechnology: Design and Structure (PSNDS-11), December 16-17, 2011, Applied Chemistry Department, The M. S. University of Baroda, Vadodara
4. Fluorescence studies on the pyrene/cyclodextrin based polymer guest-host complexes  
Vinod I. Bhoi, K. V. R. Murthy and C. N. Murthy  
Western Indian Research Scholars Meet (WIRSM-11), September 17, 2011, Department of Chemistry, The M. S. University of Baroda, Vadodara
5. Functionalization of [60]fullerene using modified  $\beta$ -cyclodexyryn  
Vinod I. Bhoi and C. N. Murthy  
XXV Gujarat Science Congress, February 26-27, 2011, Gujarat Council of Science City and Gujarat Science Academy, Ahemedabad
6. Studies on the  $\beta$ -cyclodextrin based polymers for drug delivery applications  
Vinod I. Bhoi and C. N. Murthy  
11<sup>th</sup> International Conference on Frontiers of Polymers & Advance Materials, Macro-2010, December 15-17, 2010, Indian Institute of Technology Delhi, Delhi

7. Nanoencapsulation as a tool to enhance the aqueous solubility of the poorly water-soluble drugs by cyclodextrin-based polymers

Vinod I. Bhoi and C. N. Murthy

6<sup>th</sup> All Gujarat Research Scholars Meet (AGRSM), January 31, 2010, Department of Chemistry, The M. S. University of Baroda, Vadodara  
(Awarded 2<sup>nd</sup> Prize for Oral presentation)

8. Synthesis of highly water-soluble  $\beta$ -cyclodextrin based polymers for aqueous solubilization of [60]fullerene

Vinod I. Bhoi and C. N. Murthy

Recent Advances in polymer Technology, RAPT-2009, December 28-29, 2009, North Maharashtra University, Jalgaon

9. Synthesis and characterization of a highly water-soluble polyfullerene via the cycloaddition with a selectively functionalized cyclodextrin

Vinod I. Bhoi and C. N. Murthy

And

10. Synthesis and characterization of highly water-soluble  $\beta$ -cyclodextrin based polymers for aqueous Solubilization of Carbamazepine

Vinod I. Bhoi and C. N. Murthy

National Seminar on Emerging Trends in Polymer Science and Technology, Poly-2009, October 8-10, 2009, Saurashtra University, Rajkot

11. Regioselective method for the synthesis of selective functionalized  $\beta$ -monomers

Vinod I. Bhoi and C. N. Murthy

45<sup>th</sup> Annual Convention of Chemistry 2008 and International Conference on Recent Advances in Chemistry, November 23-27, 2008, Karnataka University, Dharwad